Title

Synthetic Approaches to the Pupukeanane Natural Products and the Integration of Computer-Assisted Synthesis

Author

Hardy, Melissa A

Publication Date

2021

Peer reviewed|Thesis/dissertation

Synthetic Approaches to the Pupukeanane Natural Products and the Integration of Computer-Assisted Synthesis

by

Melissa A. Hardy

A dissertation submitted in partial satisfaction of the

requirements for the degree of

Doctor of Philosophy

in

Chemistry

in the

Graduate Division

of the

University of California, Berkeley

Committee in charge:

Professor Richmond Sarpong, Chair
Professor Thomas Maimone
Professor Nicholas Ingolia

Summer 2021

Synthetic Approaches to the Pupukeanane Natural Products and the Integration of Computer-Assisted Synthesis

Abstract

Synthetic Approaches to the Pupukeanane Natural Products and the Integration of Computer-Assisted Synthesis

by

Melissa A. Hardy

Doctor of Philosophy of Chemistry

University of California, Berkeley

Professor Richmond Sarpong, Chair

This dissertation describes our synthesis of the pupukeanane natural products and our application of emerging computer-assisted synthesis techniques to the synthesis of these compounds. In Chapter 1, I review the biosynthesis, biological activities, and previous syntheses of natural products bearing the pupukeanane and allopupukeanane skeleton. Eighteen syntheses are detailed and analyzed according to the key C–C bond forming steps that allow for the synthesis of these complex, tricyclic cores.

Chapter 2, details our efforts to develop a Pd(II)-mediated cascade to form the key bicycles that represent the core of the pupukeanane skeleton and the allopupukeanane skeleton. This approach has culminated in a 10-step formal synthesis of 2-isocyanoallopupukeanane and is the first to provide a strategy toward enantioenriched material. Additionally, a late-stage intermediate bearing the allopupukeanane skeleton is leveraged to allow unified access to the pupukeanane core.

In Chapter 3, an overview of the state-of-the-art in retrosynthetic planning programs is provided. The advent of retrosynthesis occurred nearly 50 years ago, along with the dream of realizing fully automated synthetic planning. In this review, I classify types of planners that are used and the algorithms and computational systems that underlie them. Additionally, I provide analyses of the types of compounds that these programs are equipped to analyze and the limitations in applying them more generally.

Following this review, Chapter 4 details the results of Synthia^{TM}, an expert-coded synthetic planner that I used to provide synthetic routes to the pupukeanane family. The merits of this program are explored from the lens of academic synthetic chemists and the computer-designed and computer-inspired synthetic strategies are compared and contrasted with previous syntheses of these compounds on which the program has not been explicitly trained.

Contents

Acknowledgements

Throughout my doctoral studies, I have been grateful to receive support from many professors, colleagues, and friends. These studies would not have been possible without the support of my advisor, Professor Richmond Sarpong, whose unwavering support and enthusiasm for chemistry has undoubtedly shaped my future. I'd also like to express my deepest appreciation to my qualifying examination committee and dissertation committee for their valuable feedback: Professors Thomas Maimone, Robert Bergman, Peter Vollhardt, and Nicholas Ingolia.

I am very fortunate to have had the opportunity to work on many collaborative projects, and I greatly appreciate all the co-workers who made these projects possible. Many thanks to Lynée Massey, Dr. Isabel Kerschgens, Zhitao Feng, and Professor Dean Tantillo for collaborations on the synthesis of the pupukeananes. I'm extremely grateful to Yuning Shen, Julia Borowski, Professor Timothy Cernak, and Professor Abigail Doyle for our collaboration authoring a primer on computer-assisted synthesis and automation. I'd also like to extend my gratitude to the members of the Center for Computer-Assisted Synthesis for exposing me to a broad range of new techniques and providing additional collaborative opportunities. Thank you to Brandon Wright, Robert Lusi, Dr. Hannah Haley, Dr. Taku Okada in the Sarpong group and to Rachel Knapp, Timothy Boit, Dr. Logan Bachmann, Dr. Veronica Tona and Professor Neil Garg for collaborations on the computer-assisted synthesis of global medicines.

Thank you to the many colleagues and friends who helped me revise this dissertation: Ian Bakanas, Trevor Butcher, Kristen Gardner, Justin Jurczyk, Robert Lusi, Shelby McCowen, and Melecio Perea. I am very appreciative of the Sarpong group for providing a welcoming and collaborative environment. I had the great pleasure of navigating my doctoral studies alongside Shelby McCowen, Vignesh Palani, Melecio Perea, and Hwisoo Ree. I'm also extremely grateful to the many members of 842 who filled the room with sunshine: Kristen Gardner, Dr. Taku Okada, Dr. Solène Miaskiewicz, and Dr. Alexander Rovira.

Thank you to the National Science Foundation's Graduate Research Fellowship Program, the Chancellor's Fellowship Program, the Center for Emerging and Neglected Diseases and the Make Our Planet Great Again Program for providing me with funding over the course of my doctoral studies. I gratefully acknowledge the support of the University of California Berkeley staff, including Dr. Hasan Celik, Dr. Miao Zhang, and Dr. Nicholas Settineri for all of their support. Thanks go out to Meggie Zimmerman for expertise in navigating that many challenges that come along with research.

I would also like to extend my deepest gratitude to all of my friends and family, near and far, who have provided invaluable support throughout my education.

Chapter 1. Introduction to the Pupukeanane Family of Natural Products

1.1 Introduction

Marine organisms have long been studied as a source of natural products with unique biological activity.[1] One such family of marine-derived natural products is the pupukeananes, which are marked by their caged tricyclic skeletons as well as a relatively rare isonitrile functional group.

1.1.1 Isolation of the pupukeanane natural products bearing unique skeletons

The isolation of the first marine-derived isonitrile natural products in 1973 sparked a general interest in natural products of this type given the varied biological activity that had emerged for isocyanoterpenes (ICTs).[2] A few years later, in 1975, 9-isocyanopupukeanane (**1**, Figure 1) was the first of the pupukeananes to be isolated. For this reason, the caged tricyclo[4.3.1.$0^{3,7}$]-decane isotwistane core of this molecule has become known as the pupukeanane skeleton — named after the region where the organism was collected — Pupukea.[3] Subsequent studies on the organism from which it was isolated, a sponge of the *Ciocalypta* species, led to the discovery of a related congener bearing a rearranged skeleton, which has been labelled the neopupukeanane skeleton (see **2**). Shortly after, in 1979, another sample of 9-isocyanopupukeanane (**1**) was co-isolated with a natural product bearing the related [5.2.1.$0^{4,8}$]decane scaffold, which became known as the allopupukeanane skeleton (**3**).[4] In the past decade, two additional unique pupukeanane natural products: 2-formamidoabeopupukeanane (**4**)[5] and 9-isocyanoneoallopupukeanane (**5**),[6] have been isolated from related organisms. These five natural products represent the flagship members of each of the five unique skeletons in the pupukeanane family, and several congeners have been isolated with similar functionality at different positions.

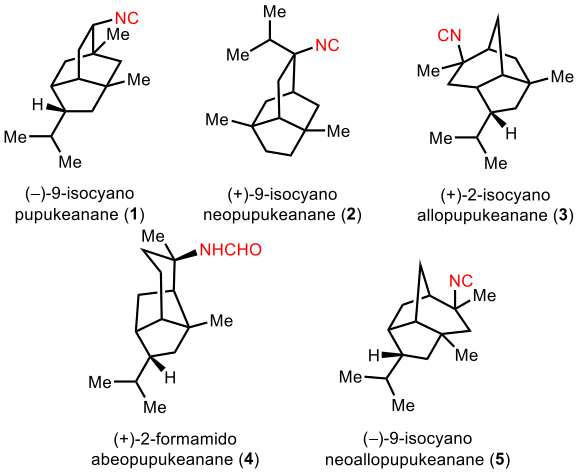

Figure 1. Flagship natural products for each unique skeleton of the pupukeanane family. The absolute configuration of **2**, **3**, **4**, and **5** have not been established and are drawn by analogy to **1**.

1.1.2 Antimalarial activity of isocyanoterpene natural products

Malaria presents a long-standing challenge for medicine and public health. While this disease has effectively been eradicated in certain areas of the world, as of 2015, there were still an estimated 212 million cases of malaria (roughly 3% of the world's population), mostly concentrated on the African continent. Malaria remains one of the leading causes of death for children in high risk areas.[7] This high mortality is mostly associated with a lack of access to proper treatment as well as increasing resistance of the *Plasmodium falciparum* parasite to available therapies such as the small molecule drugs artemisinin, chloroquine, and quinine.[8] Therefore, there has been growing interest in identifying new medications that may possess a novel mode of action.

Since the first report of their isolation in 1973, isocyanoterpenes have been regarded as promising therapeutic starting points due to their interesting and diverse biological activities.[2] In addition to cytotoxic and antibacterial activities, it has been shown that a subset of this class of natural products may serve as particularly potent antimalarials. Activity against the parasite *P. falciparum* has been observed at low nanomolar concentrations for several ICT congeners with high selectivity over human cells (Figure 2).[9] More importantly, while most prescribed drugs such as artemisinin and chloroquine are active against the blood-stage parasite through the inhibition of hemozoin crystallization,[1b] ICTs such as 7,20-diisocyanoadociane (**6**) and isocyanoamphilectene **7** have been shown to be active not only against the blood stage parasites, but also the liver-stage parasites.[10] While the mode of action for these small molecules has not yet been elucidated, this added activity suggests that a novel mechanism must be operative for these isonitrile natural products, which could prove effective at combatting drug resistant variants of the *Plasmodium* parasites.

Compared to the adociane (**6**), amphilectene (**7**), and kalihinane (**8**) isonitriles, the subclass of pupukeanane isonitriles have been less explored for their antimalarial potency, particularly against the liver-stage parasites. At the time of isolation, 9-isocyanopupukeanane (**1**) was tested for antimalarial activity and was shown to display only weak activity against the blood-stage parasite.[11] However, the correlation between blood-stage activity and liver-stage activity is unclear, and the need for antimalarial therapeutics with a novel mechanism of action has garnered renewed interest in the synthesis of isocyanoterpenes such as the pupukeananes as potential antimalarials.

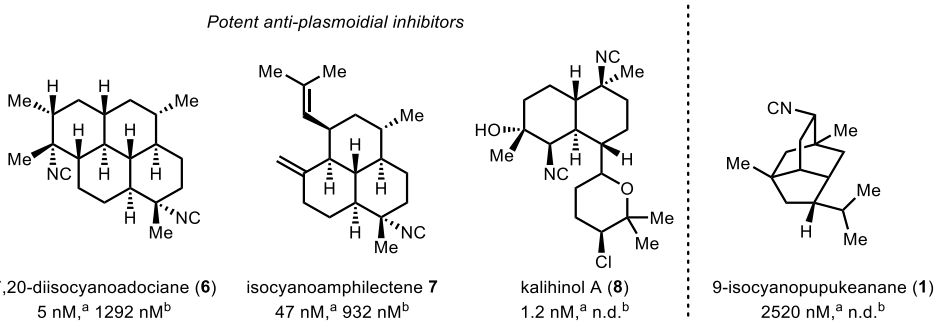

Figure 2. Isocyanoterpene natural products. [a]IC_{50} values against blood stage *P. falciparum* strain D6,[1b, 10] [b]IC_{50} values against liver stage *P. berghei*[10]

1.1.3 Proposed biosynthesis of each pupukeanane skeleton

Each of these unique congeners is proposed to arise from a common biosynthetic precursor through a series of rearrangements.[5-6, 12] These rearrangements, which are sometimes postulated to proceed through nonclassical carbocation intermediates, have been the subject of computational

studies that have shed light on the biosynthetic links that connect the skeletons. Presumably, the skeletons are forged from the α-amorphene cation (**10**, Scheme 1) which arises from farnesyl pyrophosphate (**9**) and is common to the biosynthesis of many sesquiterpenes. This carbocation is believed to undergo a cation-olefin cyclization to arrive at isotwistane **11**. At this stage, a 1,2 alkyl-shift would lead to the pupukeanane skeleton in the form of the 2-pupukeanyl cation (**12**), which can undergo additional rearrangements or be captured by inorganic cyanide.[13] A carbon shift to yield the tertiary carbocation would lead to the abeopupukeanane skeleton (**13**). Alternatively, the 9-pupukeanyl cation (**14**) is theorized to arise from this same 2-pupukeanayl intermediate (**12**) through a 1,5-hydride shift. This carbocation could be directly captured to afford natural products such as 9-isocyanopupukeanane (**1**). Alternatively, the same intermediate (**14**) could undergo a subsequent Wagner–Meerwein shift to yield either 9-neoallopupukeananyl cation (**15**) or 2-allopupukeanyl cation (**16**).

From the bridged carbocation intermediate (**11**) formed from the cation-olefin cyclization of **10**, an alternative Wagner–Meerwein shift could lead, instead, to the neopupukeanane skeleton (**17**, **18**). Natural products have been isolated that arise from both the 9- and the 2-neopupukeanyl cation. While there exist natural products that result from trapping these high energy secondary carbocation intermediates, computational studies suggest these intermediates are not minima on the potential energy surface; rather, they represent a flat region of the potential energy surface with multiple exit channels, thus accounting for the high level of diversity of the natural product skeletons.[12]

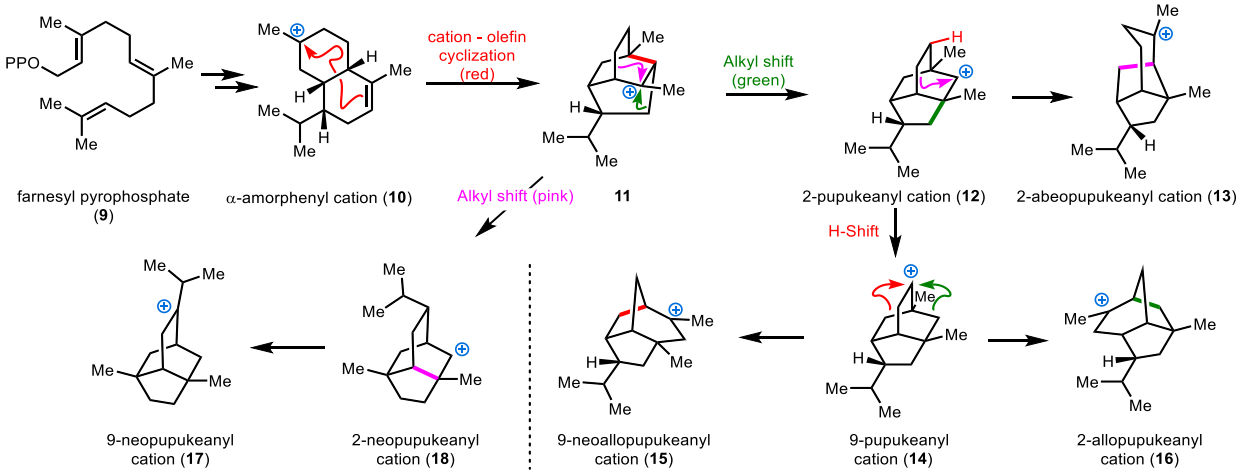

Scheme 1. Proposed biosynthesis of the pupukeanane family of natural products.

While nature has the ability to readily traverse each of these biosynthetic pathways to produce the pupukeanane congeners, these molecules have proven to be challenging to access through chemical synthesis. The pupukeananes have captured the interest of many synthetic chemists owing to their caged tricyclic structures that include multiple quaternary stereocenters as well as an isopropyl group which resides in a sterically congested location in most congeners.

1.2 Pupukeanane Natural Products

Many other molecules bearing the pupukeanane skeleton have been isolated with functionalization at the 2-[14] and 5-position[15] (**20** and **25** respectively, Figure 3) in addition to 9-isocyanopupukeanane (**1**). In total, nine natural products bearing isonitrile or related functional groups have been isolated.[3, 5, 14-16] Additionally, 9-pupukeanone (**27**) was synthesized through the degradation of a natural sample of 9-isocyanopupukeanane (**1**) and has since represented a common synthetic target in several studies.[3]

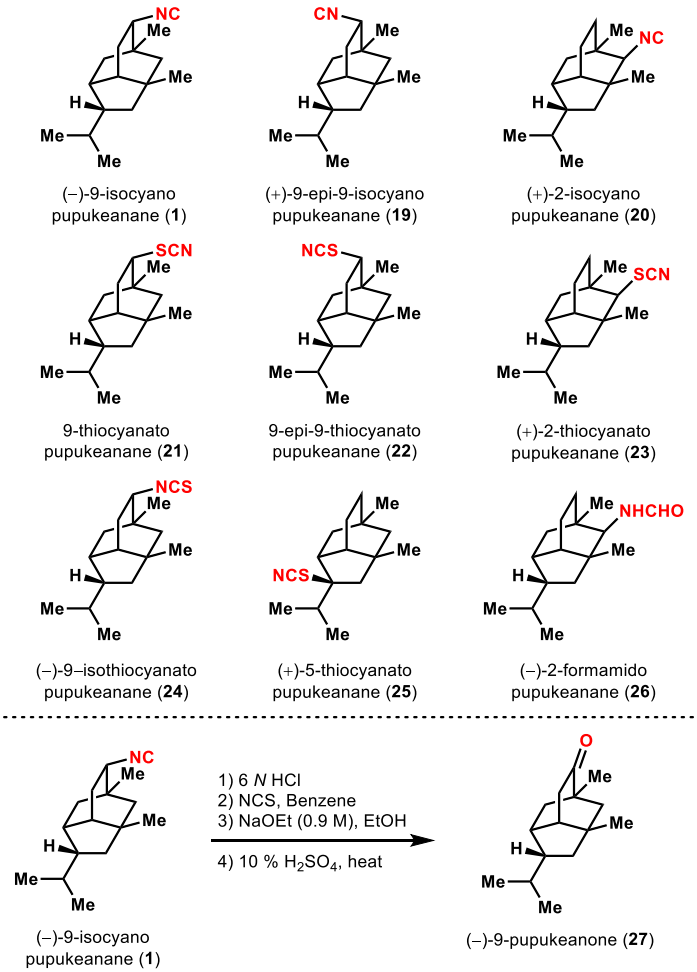

Figure 3. Natural products bearing the pupukeanane skeleton and the degradation of 9-isocyanopupukeanane (**1**) to 9-pupukeanone (**27**).

The first completed total syntheses of the pupukeanane natural products were published in back-to-back papers by Corey[17] and Yamamoto[18] in 1979. Both routes passed through 9-pupukeanone (**27**) which could be readily transformed to the corresponding isonitrile, 9-isocyanopupukeannae (**1**). While dozens of syntheses of the pupukeananes exist, they can be broadly divided into strategies that rely on the following transformations: 1) intramolecular alkylation of a functionalized bicycle, 2) Diels–Alder cycloaddition from a functionalized

monocycle, 3) Rh-carbenoid ring closure of a bridged bicycle, and 4) radical cyclization of a bridged [2.2.2]-bicycle.

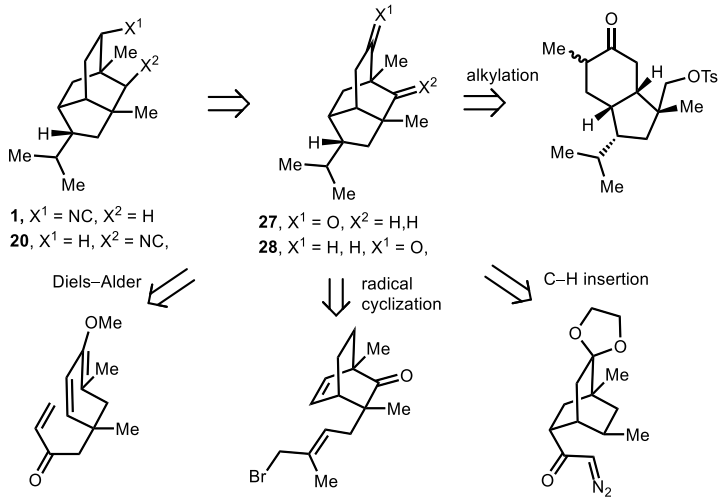

Scheme 2. Representative examples of four key retrosynthetic disconnections to build the isotwistane core of the pupukeananes.

1.2.1 Intramolecular Alkylation to build the pupukeananes

The first strategy applied to build the isotwistane core of the pupukeananes was the intramolecular enolate alkylation of a [4.3.0]-bicyclononan-2-one (Scheme 2, top left). The Corey and Chang groups have employed this disconnection to provide syntheses of both the 9-pupukeananes and the 2-pupukeananes.

Corey's synthesis of 9-isocyanopupukeanane (1979)

The first synthesis of **1** by Corey and co-workers relied on a key disconnection through a one-bond cleavage to reduce the complexity of the bridged tricycle to a fused bicyclic system (**33**, Scheme 3).[17] In the forward sense, Corey's synthesis commenced from arene **29**, which was shown to undergo facile copper-mediated conjugate addition followed by a Friedel–Crafts type cyclization to access bicycle **30**. Bicycle **30** was readily transformed to **31** using a Van Leusen reaction followed by hydrolysis, esterification and α-methylation. Subsequent cleavage of the methoxy ether and heterogeneous hydrogenation of the arene led to the spontaneous formation of lactone **32**. Reductive ring opening gave the corresponding diol, which was readily converted to bicycle **33.** This fused bicyclic intermediate was primed for an intramolecular alkylation to arrive at 9-pupukeanone (**27**). This ketone was readily converted to the natural product in four steps via oxime formation, reduction, formylation, and dehydration to give 9-isocyanopupukeanane (**1**).

In 2010, Corey and Brown developed a new method for the enantioselective synthesis of chiral bridged dienes such as **36**, which could, in turn, be used as ligands in enantioselective Rh-mediated conjugate additions (Scheme 3b).[19] Using this method, Corey developed an enantioselective route to previously employed bicycle **30**. In this way, they were able to effect the enantioselective conjugate addition of aryl boronic acid **34** into enone **35** to give **37** in 87% ee.

Transformation of the pendant methyl ketone to the acyl chloride set the stage for a Friedel–Crafts acylation to give enantioenriched *(R)*-**30**. Overall, Corey's strategy provides access to (±)-**1** in 16 steps or, formally, to enantioenriched **1** in 18 steps using the recently reported modification.

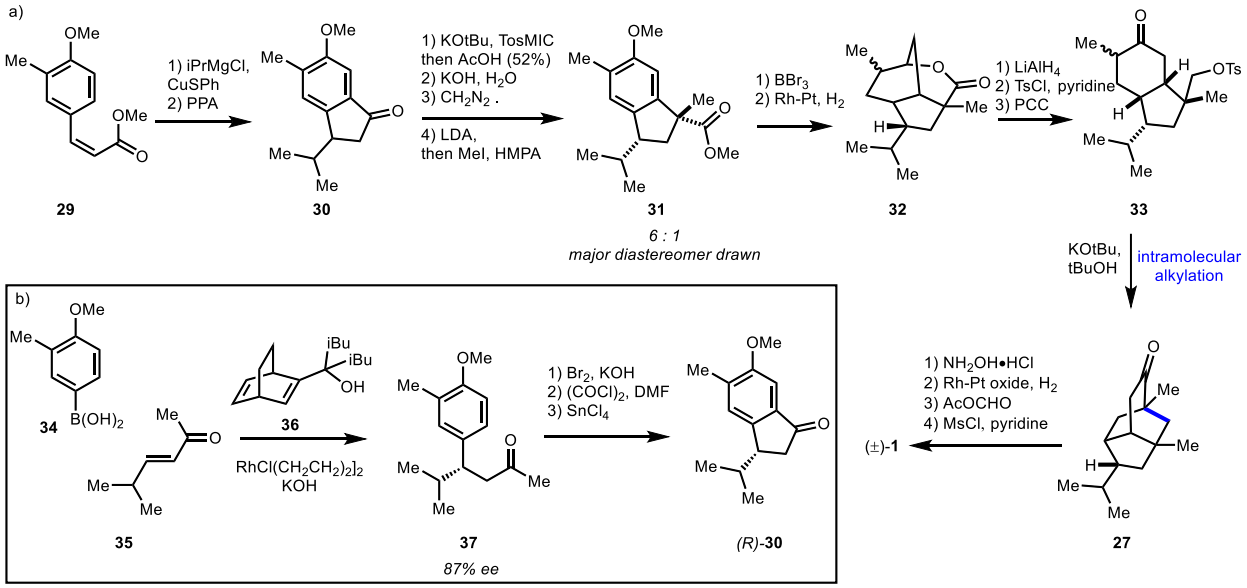

Scheme 3. Corey's a) original synthesis of (±)-9-isocyanopupukeanane (**1**) and b) modified enantioselective formal synthesis of (+)-9-isocyanopupukeanane (**1**).

Corey's synthesis of 2-isocyanopupukeanane (1979)

Later that same year, Corey and co-workers applied this same alkylation strategy to the first synthesis of 2-isocyanopupukeanane (**20**, Scheme 4).[20] From common intermediate **32**, the same reductive ring opening of the lactone led to the corresponding diol which was transformed instead to keto-aldehyde **38**, which bears close resemblance to **33** (Scheme 3a). At this stage, an intramolecular aldol reaction furnished the desired isotwistane core with functional groups placed strategically at both the C_9 and C_2 positions of the pupukeanane core. Treatment with ethanedithiol gave the corresponding mono-dithiane at the less sterically hindered position which was desulfurized using Raney®-nickel. Oxidation of the resultant secondary alcohol to the ketone gave 2-pupukeanone (**28**), which was converted to 2-isocyanopupukeanane (**20**) in a sequence analogous to that used in the synthesis of 9-isocyanopupukeanane (**1**, Scheme 3). In the case of 2-pupukeanone, this sequence furnished the corresponding amines as a 1 : 1 mixture of epimers. Gratifyingly, these epimers could be separated as the formamides. Following dehydration of these diastereomeric formamides, **20** and 2-epi-**20** were isolated. Overall, this approach constitutes an 18-step overall synthesis of (±)-2-isocyanopupukeananone (**20**) and a 14-step synthesis of (±)-2-pupukeanone (**28**).

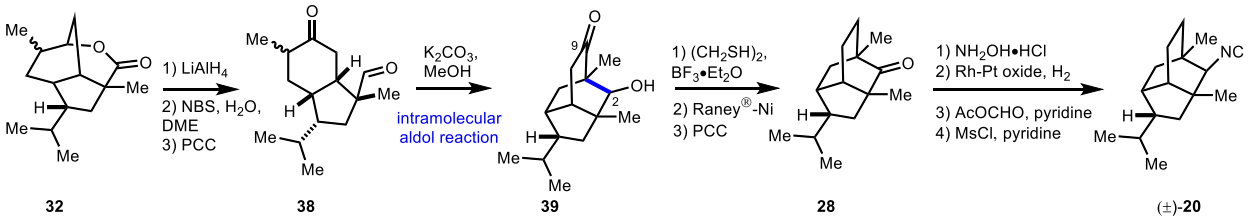

Scheme 4. Corey's synthesis of (±)-2-isocyanopupukeanane (**20**).

Chang's formal synthesis of 9-pupukeanone (1989)

Nearly a decade after the publication of the Corey synthesis, Chang and co-workers reported a related approach to the tricyclic core of **1** through the same key disconnection (Scheme 5).[21] However, in this case, the synthesis of the requisite bicycle was effected through a creative anionic oxy-Cope, which facilitated entry from a [2.2.1]-bicyclic system (**44**). Another major difference in Chang's synthesis is the late-stage introduction of the isopropyl group.

The synthesis commenced with readily available norbornene **42**, which was constructed through the Diels–Alder cycloaddition of acetoxy fulvene (**40**) and 2-chloroacrylonitrile (**41**).[22] To install the quaternary methyl group present in the natural product, the acetal group of **42** was oxidized to the carboxylic acid (presumably via the aldehyde) and esterified with diazomethane. Protection of the ketone as a ketal set the stage for α-methylation of the ester at the bridging atom to give **43**. Reduction of the methyl ester was followed by acid-catalyzed ketal cleavage, which set the stage for addition of vinyl magnesium bromide into the newly unveiled ketone to give **44**, the desired precursor for the key anionic oxy-Cope rearrangement. Upon heating, bridged bicycle **44** readily rearranged to form fused bicycle **45**. Mesylation of the pendant alcohol followed by base-mediated intramolecular alkylation led to isotwistane core **46**. Protection of the ketone group followed by hydroboration and oxidation of the southern olefin, provided a ketone that enabled the installation of the isopropenyl group. This route to mono-protected diketone **47** constitutes a formal synthesis of 9-isocyanopupukeanane through Yamamoto's approach[18] and can be transformed to the natural product in 8 steps (see Section 1.2.2). Overall, this anionic oxy-Cope/intramolecular alkylation strategy led to a formal synthesis of (±)-9-isocyanopupukeanane (**1**) in 25 steps from commercial material.

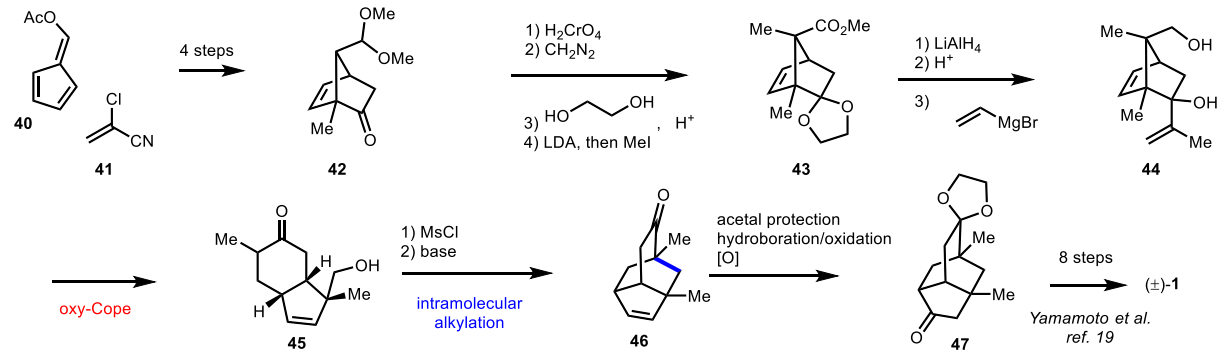

Scheme 5. Chang's synthesis of (±)-9-isocyanopupukeanane (**1**).

Chang's synthesis of 2-pupukeanone (1996)

In 1996, Chang applied a similar strategy, but a unique disconnection in an approach to 2-pupukeanone (**28**, Scheme 6). Retrosynthetically, instead of disconnecting the bridged

pupukeanane core back to an all-fused system, Chang's synthesis proposed access to the isotwistane core through the ring closure of a bridged [3.2.1]-bicycle. In this synthesis, Chang and coworkers leveraged the same norbornene **42** as in their previous synthesis; in this case, the Chang group employed a ring expansion strategy to construct the desired [3.2.1]-bicycle.

From norbornene **42**, the synthesis began with the homologation of the acetal by one carbon to give acetal **48**. At this stage, Corey–Chaykovsky epoxidation of the ketone followed by aminolysis of the epoxide with ammonium hydroxide gave the corresponding β-amino alcohol. This compound readily underwent a Tiffeneau–Demjanov ring expansion when treated with nitrous acid to furnish desired [3.2.1]-bicycle **49**. This was followed by the installation of the methyl group, which proceeded to give a single diastereomer of bicycle **50**. With the requisite methyl group installed, the northern acetal was converted into a leaving group to enable the key intramolecular alkylation of bicycle **51**. Treatment of **51** with base gave the pupukeanyl core with the only remaining challenge for the synthesis of 2-pupukeanone (**28**) being the installation of the isopropyl group. A hydroboration/oxidation sequence gave keto-alcohol **52**, which was subsequently oxidized to the diketone. Treated of this compound with cerium(III) chloride and isopropenyl magnesium bromide facilitated mono-addition to the less sterically hindered ketone (**53**). Notably, without cerium(III) chloride, only starting material was recovered, likely due to competitive α-deprotonation of the reactive ketone. From keto-alcohol **53**, elimination of the alcohol followed by sequential heterogeneous hydrogenations of the tetrasubstituted and terminal olefin groups led to the isolation of (±)-2-pupukeanone (**28**) in a total of 22 steps.

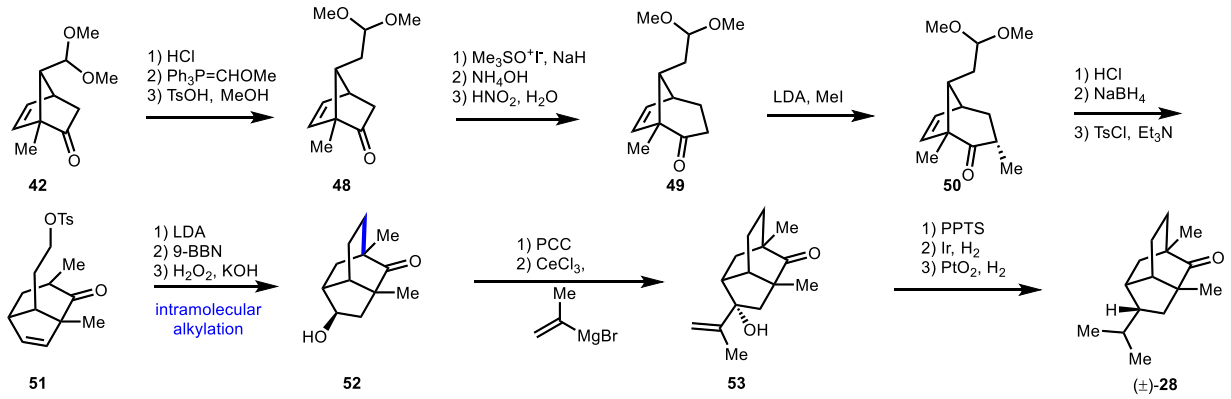

Scheme 6. Chang's synthesis of (±)-2-pupukeanone (**28**).

1.2.2 Diels–Alder cycloadditions to build the pupukeananes

Another popular strategy to build the pupukeanyl core is the implementation of a Diels–Alder cycloaddition to quickly build the tricyclic core of the pupukeananes from a monocyclic precursor. This strategy was first employed by Yamamoto in the synthesis of the 9-pupukeananes, and related syntheses were carried out by the White and Piers groups. A few years later, Frater applied this strategy to the synthesis of the 2-pupukeananes.

Yamamoto's synthesis of 9-isocyanopupukeanane (1979)

In Yamamoto's total synthesis of 9-isocyanopupukeanane, the Diels–Alder transformation was key to the synthesis of the isotwistane core (Scheme 7).[18] The Yamamoto group's synthetic

studies commenced from cyclohexenone **54**, which they envisioned could be remodeled to give the requisite monocyclic cycloaddition precursor (**56**). Reduction of ketone **56** gave the corresponding allylic alcohol, which was treated with mercuric acetate and ethyl vinyl ether to effect an *O*-vinylation of the alcohol and subsequent Claisen rearrangement to give cyclohexene **55**. At this stage, addition of vinyl magnesium bromide and subsequent protection of the resulting hydroxy group provided the tetrahydropyran ether. Allylic oxidation of the cyclohexene moiety with Collins's reagent followed by trapping of the resulting ketone as a silyl enol ether gave the corresponding diene **56** necessary for the desired Diels–Alder cycloaddition. As planned, this strategic monocyclic precursor underwent facile intramolecular cycloaddition to provide the tricyclic pupukeanane core (**57**).

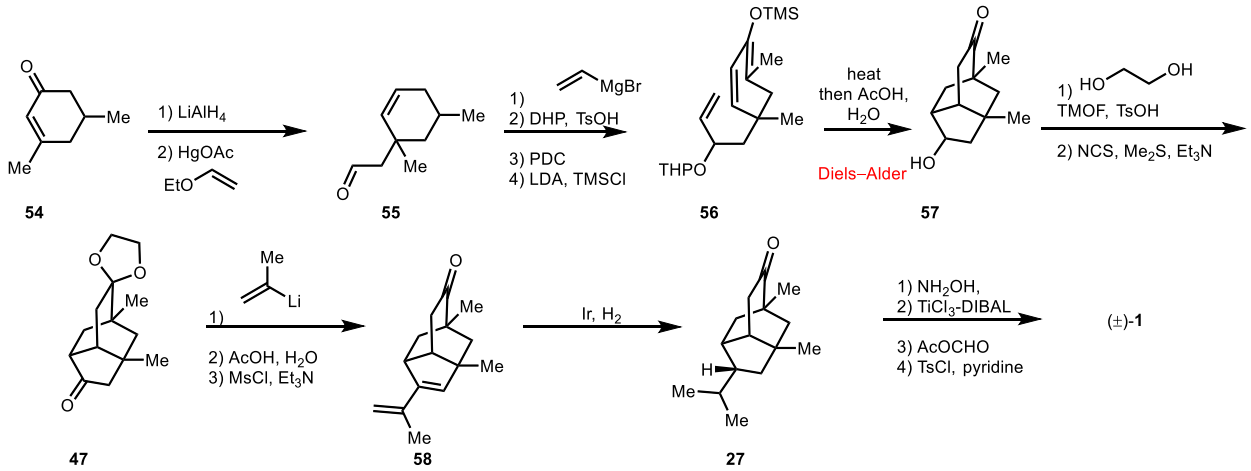

Scheme 7. Yamamoto's synthesis of (±)-9-isocyanopupukeanane (**1**).

At this stage, the next challenge they tackled was the stereoselective introduction of the isopropyl group. Following protection of the northern ketone as the ketal, treatment with Corey–Kim oxidation conditions gave mono-protected diketone **47**. From this compound, selective addition of isopropenyl lithium was possible, which furnished diene **58** after elimination of the resultant hydroxy group and cleavage of the ketal. Notably, hydrogenation of the diene in **58** with several heterogeneous catalysts (palladium on carbon, Raney®-nickel, etc.) led to non-selective formation of two epimers differing in their configuration at the secondary carbon bearing the isopropyl group. However, following hydrogenations catalyzed by iridium black, a single diastereomer of 9-pupukeanone (**27**) was observed. Yamamoto and co-workers completed the synthesis of 9-isocyanopupukeanane in a route analogous to the reports from Corey (see Section 1.2.1). Specifically, hydroxylamine was condensed onto the ketone to form the corresponding oxime, which was reduced to the amine. Formylation and dehydration completed the synthesis of (±)-9-isocyanopupukeanane (**1**) in 17 total steps. This synthesis proceeded through (±)-9-pupukeanone (**27**), which was accessed in 13 steps from **54**.

White's synthesis of 9-pupukeanone (1980)

In the route developed by White and co-workers, a monocyclic precursor similar to that used by Yamamoto (**56**, Scheme 7) was employed (**64**, Scheme 8).[23] Starting from *p*-cresyl methyl

ether (**59**), a Birch reduction led to the corresponding diene which was sequentially cyclopropanated to give **60** as a mixture of isomers. Treatment of this strained system with acid led to bis-fragmentation of the cyclopropane moieties to give **61**, a cyclohexenone with both requisite methyl groups installed. The cyclohexenone was then trapped as the methyl enol ether to provide the diene (**62**) for the proposed cycloaddition.

In order to install the necessary dienophile, reduction of the methyl ester of **62** and subsequent oxidation furnished the corresponding aldehyde (**63**). Addition of vinyl magnesium bromide followed by oxidation of the resultant allylic alcohol to the corresponding enone (**64**) set the stage for the desired cycloaddition. Notably, from **65**, the Diels–Alder cycloaddition proceeded at much lower temperature than in the case of Yamamoto's synthesis (see **56** to **57**, Scheme 7). This is likely due to the inductive electron-withdrawing effects of the enone, although the π-systems of the carbonyl and olefin are orthogonal in the transition state necessary for the cycloaddition and are not in conjugation. With the tricyclic core (**65**) constructed, the final challenge was the late-stage introduction of the isopropyl group. This was accomplished through addition of isopropenyl lithium, followed by dehydration of the resultant alcohol to give intermediate **58**, previously synthesized by Yamamoto.[18] In this case, they observed that Adams' catalyst was competent to effect the heterogeneous hydrogenation from the desired face to give (±)-9-pupukeanone (**27**) in 14 steps overall.

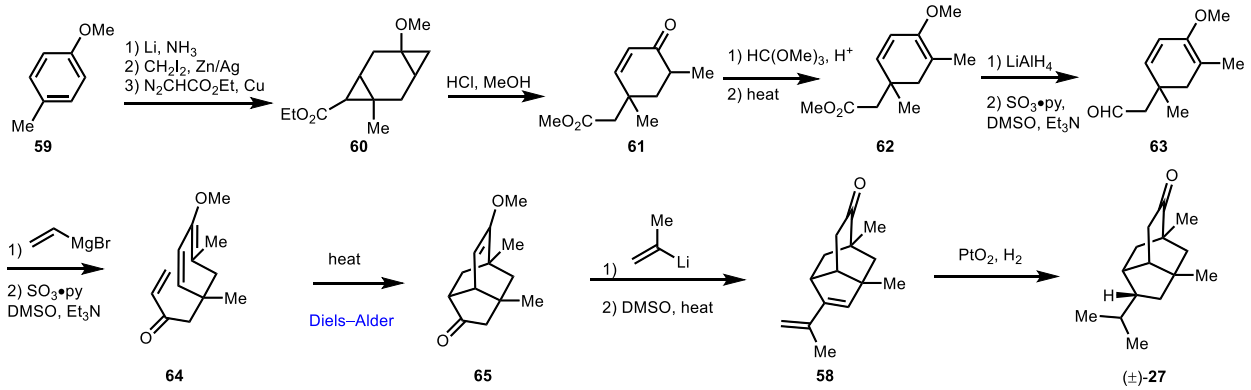

Scheme 8. White's synthesis of (±)-9-pupukeanone (**27**).

Piers' synthesis of 9-pupukeanone (1982)

Piers' synthesis of 9-pupukeanone (**27**) employed a similar intermediate (**69**) to effect the desired key cycloaddition. The Pier's synthesis began with commercially available dione **66**, which was readily tautomerized and trapped as vinyl enol ether **67** as an inconsequential mixture of epimers. Next, α-alkylation with a protected bromo-ethanol electrophile set the stage for reduction of the ketone and transposition of the alkene to give enone **68**. Treatment of the enone with LDA and trapping as a diethyl phosphate furnished the desired diene for the planned [4 + 2] cycloaddition. Subsequent cleavage of the tetrahydropyran ether group and Moffatt oxidation to the corresponding aldehyde set the stage for addition of vinyl magnesium bromide to furnish the cycloaddition precursor (**69**). Gratifyingly, **69** underwent a relatively facile Diels–Alder reaction to arrive at isotwistane core **70**. Upon treatment with ethylene glycol and acid, the phosphate group

was readily cleaved to form the corresponding ketone, which was subsequently protected as a ketal. Oxidation of the secondary alcohol set the stage for installation of the isopropenyl group followed by elimination of the corresponding alcohol in a manner similar to previous syntheses to give intermediate **58**. Using a procedure adapted from Yamamoto's synthesis,[18] it was found that treatment of **58** with heterogeneous iridium black under a hydrogen atmosphere gave (±)-9-pupukeanone (**27**) in 14 total steps from **66**.

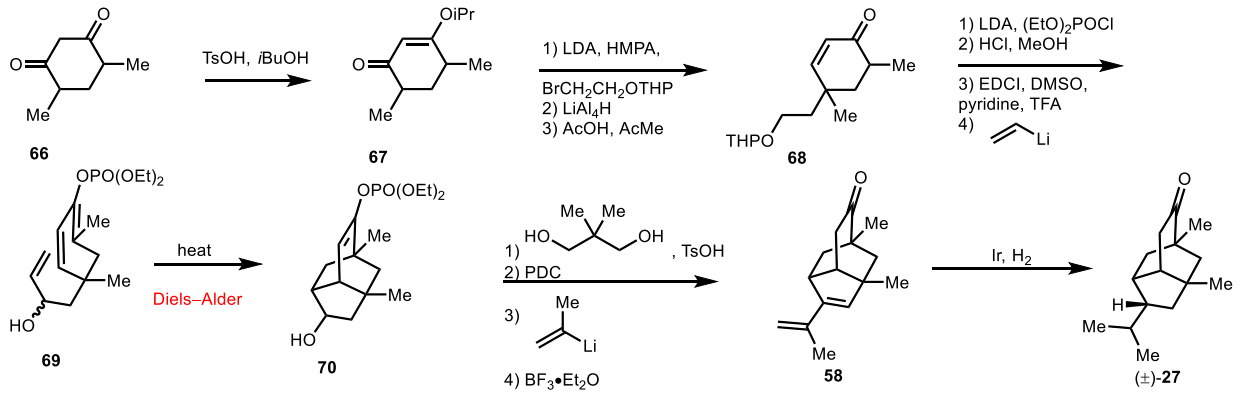

Scheme 8. Piers' synthesis of (±)-9-pupukeanone (**27**).

Frater's synthesis of 2-pupukeanone (1984)

Shortly after Yamamoto, White, and Piers had published syntheses of 9-pupukeanone (**27**), the Frater group applied a similar strategy to the synthesis of the 2-pupukeananes.[24] In this case, the Diels–Alder precursor was synthesized *in situ* by a dearomative coupling of allylic bromide (**74**) and a commercially available arene (**75**) to install all the carbons necessary for the skeleton.

In their synthesis, commercially available lactone **71** was remodeled into the necessary bromide coupling partner. Addition of phenyl selenide to open the lactone gave the corresponding carboxylic acid, which was esterified to give **72**. Oxidation of the selenide with peroxyacetic acid followed by Greico-type elimination provided diene **73**. At this stage, reduction of the ester and conversion of the resultant alcohol to the bromide yielded coupling partner **74**. Coupling of **74** with *in situ* generated sodium 2,6-dimethylphenolate from **75** led to the formation of precursor **76**, which readily underwent the desired [4 + 2] cycloaddition. Given the unbiased nature of the dienophile, two distinct isomers were observed after the Diels–Alder cycloaddition: desired isotwistane **78** and undesired twistane **77** (3:1 ratio). Gratifyingly, **77** was readily converted to the more thermodynamically stable isomer (**78**) by heating at 250 °C for five minutes. From **78**, heterogeneous hydrogenation with platinum on carbon gave the desired 2-pupukeanone (**28**). Ultimately, the Frater group's synthesis provides access to (±)-2-pupukeanone in 8-steps from commercial material. This route represents one of the shortest syntheses of **28** to date.

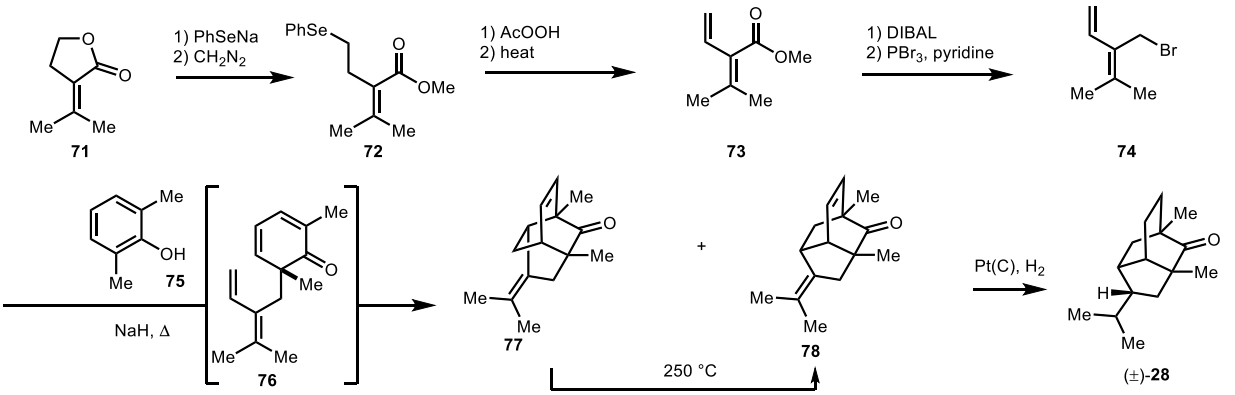

Scheme 9. Frater's synthesis of (±)-2-pupukeanone (**28**).

1.2.3 Radical cyclization to build the pupukeananes

Several years later, the Subba Rao and Srikrishna groups published a new method for the synthesis of these compounds that relied on a unique disconnection. Rather than unraveling the tricycle to a fused bicycle or monocyclic system, they proposed the use of a bridged [2.2.2]-bicycle with a pendant functional group that could engage in a radical cyclization to give the desired tricycle.

Subba Rao's synthesis of 2-pupukeanone (1997)

In Subba Rao's synthesis of the pupukeananes, a key challenge lay in building the [2.2.2]-bicycle with the methyl group attached at the bridgehead position (see **80**, Scheme 10). Notably, **80** cannot be directly accessed from methyl cyclohexadiene (**79**) through a cycloaddition with a ketene equivalent, such as **47**, due to the difficulty in preparing isomerically pure methyl diene **79**. Even if pure **79** could be obtained, one would also expect a lack of regioselectivity in the [4+2] cycloaddition. Thus, Subba Rao and co-workers developed a clever rearrangement strategy to enable the formal substitution of a methoxy group to a methyl group from known bicycle **82**.

The Subba Rao group's synthesis began with the known cycloaddition of readily available diene **81** and ketene equivalent **41** to give **82**. In order to formally substitute the methoxy ether at the bridgehead position of **82**, an acid-mediated α-ketol rearrangement was employed to give [3.2.1]-bicycle **83**. At this stage, 1,2-addition of methyl lithium into the enone moiety gave the corresponding tertiary allylic alcohol, which, under acidic conditions, underwent facile rearrangement to the desired [2.2.2]-bicycle with the methyl group installed (**80**). With **80** in hand, sequential α-alkylation of the ketone moiety gave the cyclization precursor **85** with all carbon atoms of the pupukeanane skeleton intact. Treatment of this diene (**85**) with radical generating conditions led to the desired 5-exo-trig cyclization to give the pupukeanane skeleton **86** as a mixture of diastereomers at the C_5 position. Acid-mediated isomerization of the olefin to the internal position ablated the C_5 stereocenter and this internal olefin was hydrogenated to give 2-pupukeanone (**28**) as a 4:1 mixture of epimers at the C_5 position. Overall, this synthesis provides access to (±)-2-pupukeanone (**28**) in 8 total steps from **81**. Additional studies by the Subba Rao group further explored these keto-alcohol rearrangements on the tricyclic scaffold of the pupukeananes rather than the precursor bicycle.[25]

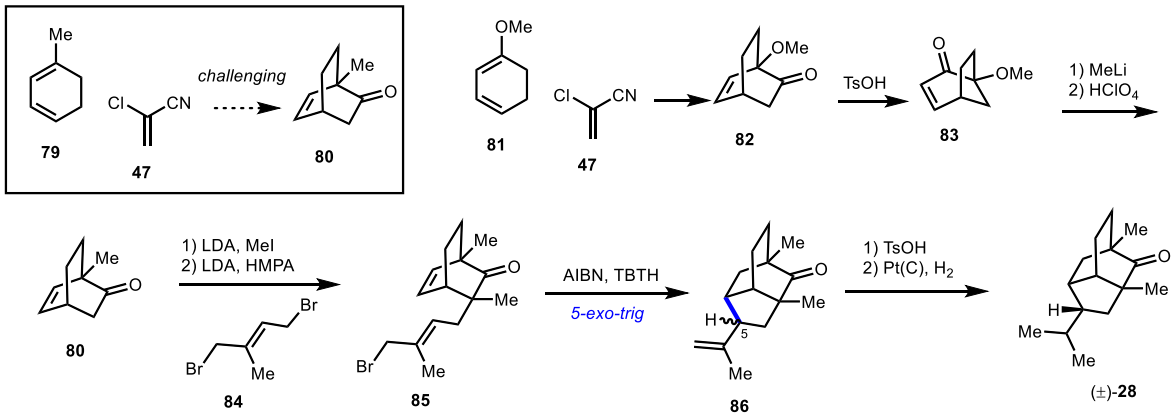

Scheme 10. Subba Rao's synthesis of (±)-2-pupukeanone (**28**).

Srikrishna's racemic synthesis of 2-pupukeanone (1997)

In Srikrishna's related approach to the pupukeananes, they directly synthesized the desired [2.2.2]-bicycle from a [4+2] cycloaddition with the methyl group intact (see **88**, Scheme 11).[26] Notably, they accessed this compound as a 1:1 mixture of the *C*-alkylation and *O*-alkylation products of arene **87**. However, treatment of this mixture with vinyl phenyl sulfone gave the desired cycloadduct (**89**), which contains both quaternary carbon atoms as well as the ketone group present in 2-pupukeanone (**28**). At this stage, treatment of **89** with radical generating conditions led to the desired 5-exo-trig cyclization to give vinyl stannane **90**. To install the requisite isopropyl group, oxidative cleavage of the vinyl tin species installed the additional ketone in **91**. Dissolving metal reduction conditions promoted desulfonylation with concomitant global reduction of both ketone moieties. Subsequent reoxidation of the resultant alcohols gave known dione **92**, which was previously employed in the Chang group's synthesis of **28** (Scheme 6).[27] In this way, Srikrishna's radical approach formally provides access to (±)-2-pupukeanone (**28**) in 10 steps from commercial materials.

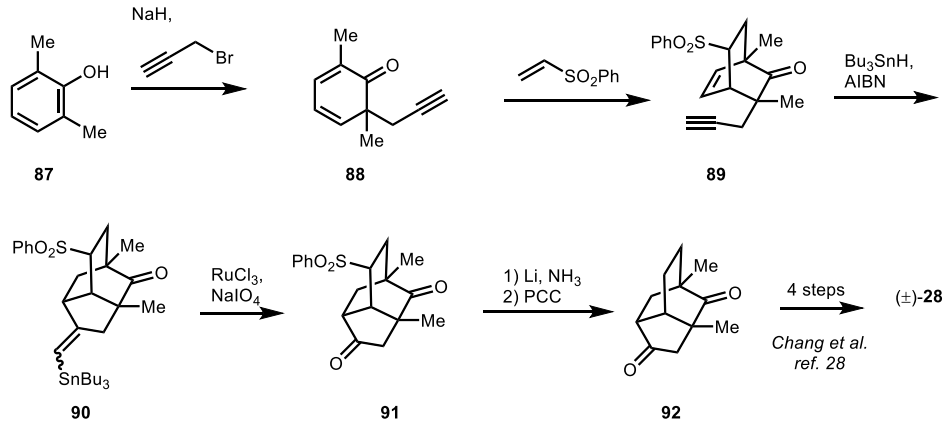

Scheme 11. Srikrishna's racemic synthesis of (±)-2-pupukeanone (**28**) by radical cyclization.

Srikrishna's enantiospecific synthesis of 2-pupukeanone (1997)

Later in the same year, the Srikrishna group reported a similar strategy that employed enantioenriched starting material to access a similar [2.2.2]-bicycle (Scheme 12).[28] From (*R*)-carvone (**93**), α-methylation followed by allylic bromination gave functionalized enone **94**. Treatment of **94** with base led to γ-deprotonation to give a dienolate. Intramolecular attack of the allylic bromide at the α-position gave [2.2.2]-bicycle **95** as an inconsequential mixture of epimers. Subsequent α-alkylation led to triene **96**, which, upon treatment with bromine, formed a trisubstituted bromonium cation. Opening of the bromonium with water gave cyclization precursor **97**. Treatment of this precursor with radical formation conditions led to the cyclization to the desired tricycle. At this stage, ozonolysis of the terminal olefin group and elimination of the tertiary alcohol group led to the formation of **98**. Wolff–Kishner reduction of the less sterically hindered ketone followed by heterogeneous reduction of the tetrasubstituted olefin led to the isolation of (+)-2-pupukeanone (**28**) along with its C_5 epimer. This sequence represents the first enantiospecific synthesis of a 2-pupukeanane. Additional reports by the Srikrishna group employed a similar approach to access analogs of the 9-pupukeanones.[29]

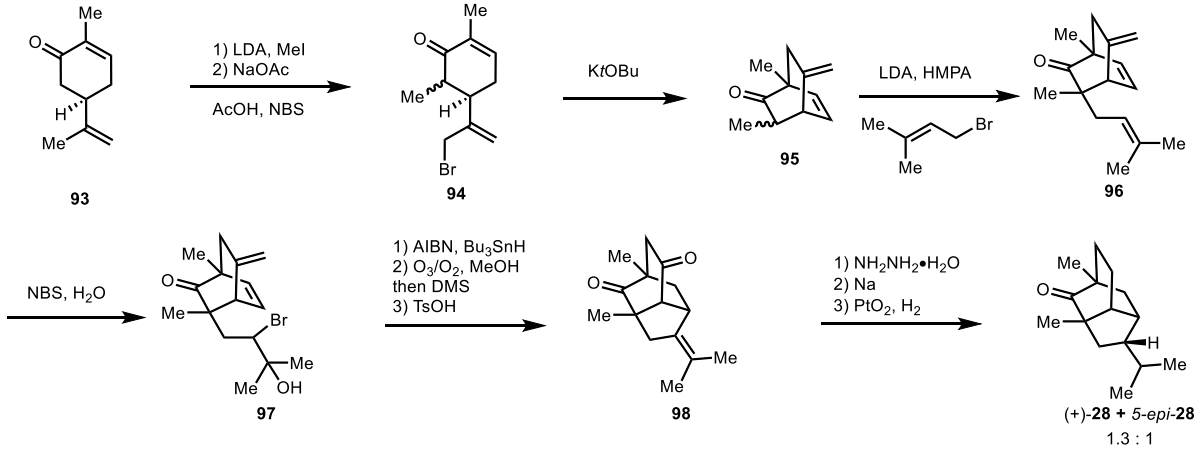

Scheme 12. Srikrishna's enantiospecific synthesis of (+)-2-pupukeanone (**28**) by radical cyclization.

1.2.4 C–H insertion to build the pupukeananes

In a similar approach, the Srikrishna group employed this same disconnection to bring the 2-pupukeananes back to a [2.2.2]-bicycle; however, in these cases, they deployed a C–H insertion reaction of a pendant diazo group to stitch together the isotwistane core.

Srikrishna's enantiospecific synthesis of 2-pupukeanone (2001)

Srikrishna and co-workers first applied this C–H insertion strategy to the enantiospecific synthesis of 2-pupukeanone (**28**, Scheme 13).[30] From (*R*)-carvone (**93**), the synthesis commenced with *α*-methylation followed by sequential inter- and intramolecular Michael additions with methyl acrylate to build the [2.2.2]-bicyclic framework (**99**). Ozonolysis of the isopropenyl group led to the corresponding hydroperoxide intermediate, which underwent a Criegee rearrangement to cleave the C–C bond and furnish **100** with only minimal amounts of the ketone, the traditional ozonolysis product of **99**. Hydrolysis of the acetate group and oxidation of the resultant alcohol

gave dione **101**. At this stage, the northern ketone was selectively reduced by treatment with ethanedithiol and desulfurization of the dithiane with Raney®-nickel to give mono-ketone **102**. In order to introduce the diazo group for the planned C–H insertion, the ester was saponified to the carboxylic acid, which, via the acid chloride, underwent a one carbon homologation with diazomethane to give α-diazo ketone **103**. At this stage, treatment of **103** with rhodium dimer effected the desired C-H insertion to give previously accessed tricycle **92**. Thus, this synthetic study represents a formal synthesis of (–)-2-pupukeanone (**28**), as Chang and co-workers had previously elaborated dione **92** to **28** in 4 steps.[27]

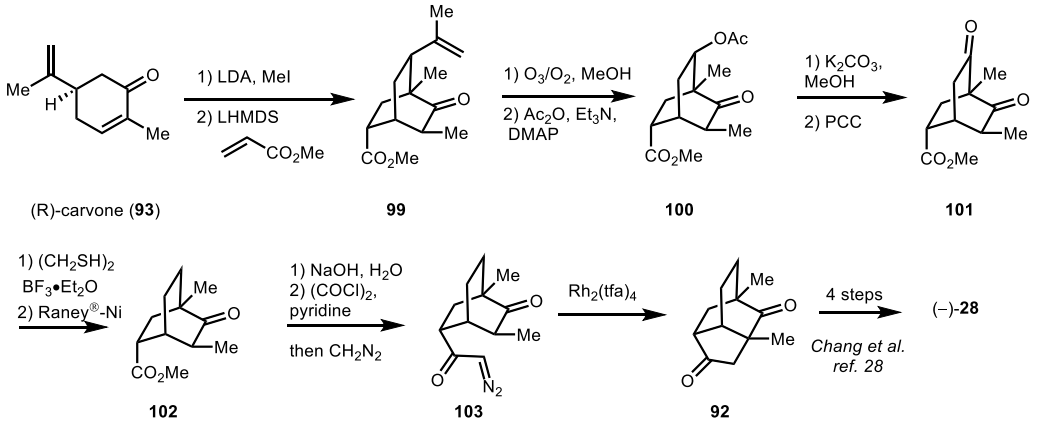

Scheme 13. Srikrishna's enantiospecific C–H insertion approach to (–)-2-pupukeanone (**28**).

Interestingly, this strategy was complementary to Srikrishna's initial enantiospecific synthesis of 2-pupukeanone (**28**), which leveraged a radical cyclization strategy (Scheme 12, Section 1.2.3). Although both strategies began from (*R*)-carvone, they furnished opposite enantiomers of 2-pupukeanone (**28**). Srikrishna's subsequent reports also included complementary synthetic routes, which indicated that the order of operations could be varied to lead to several related routes that allow access to unique intermediates.[30-31] The following year, Srikrishna reported a modified synthesis of (±)-**102** (Scheme 14), which proceeded in only two steps from 2,6-dimethylphenol (**87**), providing an alternative formal synthesis of (±)-**28**.[32]

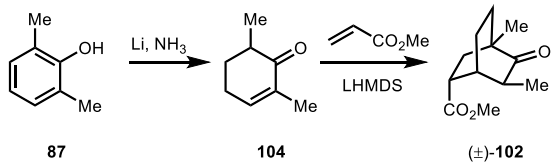

Scheme 14. Srikrishna's racemic entry into the synthesis of (–)-2-pupukeanone (**28**).

Kwon's formal's synthesis of 2-pupukeanone (2019)

In 2019, the Kwon group developed a new method for hydrodealkenylation that enabled more rapid access to bicycle **102** (Scheme 15).[33] In the hydrodealkenylation of **99**, a peroxide intermediate is generated under ozonolysis conditions which was reduced directly to the alkane. In this newly developed synthetic sequence, enantioenriched **102** was accessed in only four steps

from (*R*)-carvone, compared to Srikrishna's previous nine step synthesis from the same starting material. (Scheme 13).

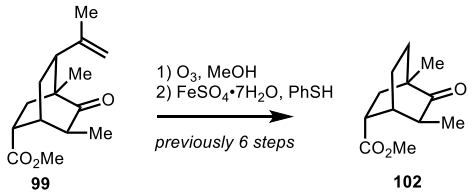

Scheme 15. Kwon's formal synthesis of (+)-2-pupukeanone (**28**).

Srikrishna's enantiospecific formal synthesis of 2-pupukeanone (2002)

Srikrishna and co-workers also leveraged this strategy to achieve the first enantiospecific formal synthesis of 9-isocyanopupukeanane (**1)** and confirm its absolute stereochemistry (**27**, Scheme 16). From previously synthesized enantioenriched **100** (see Scheme 13), treatment with ethanedithiol led to the corresponding dithiane, which was readily reduced with Raney®-nickel. Subsequently, hydrolysis of the acetate group and oxidation of the resultant hydroxy group led to ketone **105**. Unlike in their previous synthesis of 2-pupukeanane (see **102** to **103**; Scheme 13), the ketone of **105** required protection as the ketal before conversion of the ester to the α-diazo ketone. Following protection of this ketone, the same homologation sequence yielded key precursor **106**, which upon treated with rhodium furnished the desired C_9-functionalized isotwistane core (**47**). While this compound represents a formal synthesis of 9-pupukeanone and 9-isocyanopupukeanane by Yamamoto's method (Scheme 7),[18] Srikrishna employed distinct conditions to arrive at (–)-9-pupukeanone (**27**) in 14 steps overall.

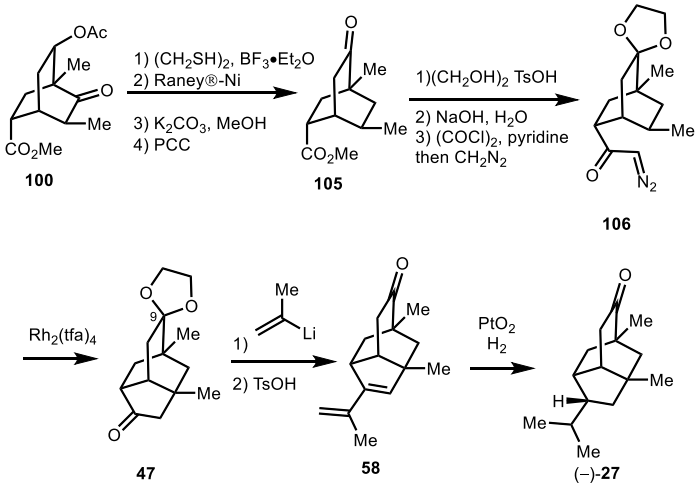

Scheme 16. Srikrishna's enantiospecific C-H insertion approach to (–)-9-pupukeanone (**27**).

1.3 Neopupukeanane natural products

In addition to these pupukeanane natural products, the related neopupukeanane skeleton also contains an isotwistane scaffold with unique substitution patterns. To date, three unique neopupukeananes have been isolated including two rare thiocyanate-containing natural products: (+)-9-isocyanoneopupukeanane (**2**),[34] (–)-4-thiocyanatoneopupukeanane (**107**)[35] and (–)-2-thiocyanatoneopupukeanane (**108**).[16b, 35] Due to the similarities between the isotwistane core of the neopupukeananes and pupukeananes (Section 1.2), the strategies that have been used for their syntheses are closely related.

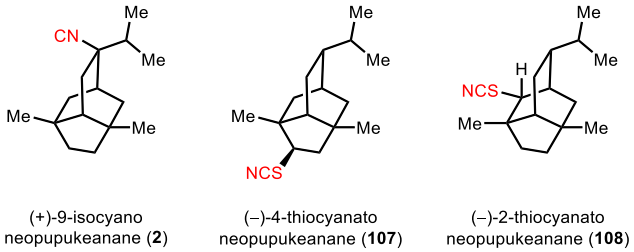

Figure 4. Natural products bearing the neopupukeanane skeleton. The absolute configuration of 9-isocyanoneopupukeanane (**2**) has not been established.

1.3.1 Cyclopropanation to build the neopupukeananes

Srikrishna's syntheses of the (–)-4-thiocyanatoneopupukeanane (1999)

The first synthesis of the neopupukeananes was accomplished by Srikrishna and co-workers using their Rh-carbenoid C–H insertion strategy. In a way, the neopupukeananes are better suited for this synthetic sequence as the isopropenyl group of carvone is readily incorporated into the neopupukeanane skeleton, whereas syntheses of 2-pupukeanone and 9-pupukeanone required the cleavage of this isopropenyl group. The first report of this method detailed a synthesis of the neopupukeanane core,[36] and this strategy was later applied to synthesize (–)-4-thiocyanatoneopupukeanane (**107**, Scheme 17).[37] Both reports predated the Srikrishna group's use of C–H insertion to furnish the 9- and 2-pupukeananes.

As in the previously discussed syntheses of the pupukeananes (Section 1.2.4), the preparation of **107** began with sequential inter- and intramolecular Michael additions of methyl acrylate across (*R*)-carvone (**93**). Given the varied substitution patterns of the neopupukeananes, methyl methacrylate was employed instead of methyl acrylate to introduce one of two quaternary stereocenters in the natural product; ultimately, this forged bicycle **109**. At this stage, heterogeneous hydrogenation of the isopropenyl group, reduction of the ketone group, and elimination of the resultant alcohol gave **110** bearing each of the peripheral alkyl groups necessary for the neopupukeananes in only five synthetic steps. Conversion of the acid to the diazo group installed all necessary carbons of the skeleton in the form of **111**. Upon irradiation of **111** in the presence of a copper salt, cyclopropanation proceeded to give strained tetracycle **112**. Gratifyingly, a dissolving metal reduction of this tetracycle led to the less strained, desired isotwistane skeleton (**113**) as opposed to the twistane product. Mesylation of the alcohol group followed by treatment with potassium thiocyanate furnished the natural enantiomer of (–)-4-thiocyanatoneopupukeanane

(**107**), thereby establishing the absolute configuration. Ultimately, this approach led to the first synthesis of **107** in 11 total steps from (*R*)-carvone (**93**).

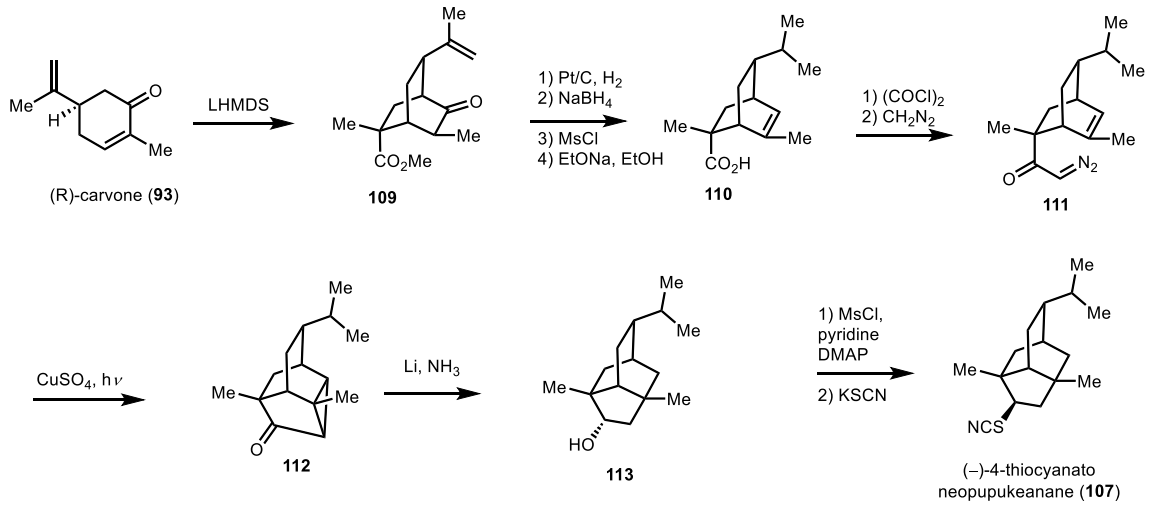

Scheme 17. Srikrishna's synthesis of (–)-4-thiocyanatoneopupukeanane (**107**).

In addition to the approaches described above, additional reports detailed modifications of these Rh-carbenoid insertion strategy that enabled related syntheses of (–)-2-thiocyanatoneopupukeanane (**108**),[38] both enantiomers of 4-thiocyanatoneopupukeanane (**107**),[39] and racemic 9-neopupukeanone (**2**)[40] using very similar methods. These syntheses, along with X-ray crystallographic analysis of these intermediates, were key to assigning the relative stereochemistry of the 2-thiocyano group of **108** as well as the absolute stereochemistry of **108**.

1.3.2 Diels–Alder reactions to forge the neopupukeananes

Ho's synthesis of (±)-9-isocyanoneopupukeanane (1999)

Around the same time as Srikrishna's studies, the Ho group employed a Diels–Alder cycloaddition to the synthesis of 9-isocyanoneopupukeanane (**2**, Scheme 18).[41] The strategy commenced with known bicycle **114**, which was accessed in three steps from commercial material. Treatment of this bicycle with perchlorous acid led to a Grob-type fragmentation to arrive at cyclohexenone **115**. Electrophilic epoxidation of the electron-rich olefin group followed by global reduction of the epoxide and the enone led to diol **116**. Global acetylation of this diol followed by thermal elimination of the diacetoxy compound led to the desired cycloaddition precursor. Under these conditions, the triene intermediate underwent the desired [4+2] cycloaddition in one-pot to give **117**. Subjecting this prochiral alkene to hydroboration/oxidation conditions led to a separable mixture of C_8 and C_9 alcohols, favoring the desired isomer (i.e., **119**). Oxidation of the hydroxy group of **119** led to 9-neopupukeanone (**120**). At this stage, the two remaining challenges were the installation of the isopropyl group and the isonitrile at the C_9 position. Toward this end, addition of an isopropyl Grignard reagent in the presence of cerium (III) chloride yielded the desired tertiary alcohol, which was transformed to the corresponding isonitrile through S_N1-type addition of hydrogen cyanide and subsequent dehydration of the resultant formamide. This strategy led to (±)-9-isocyanoneopupukeanane (**2**) in 13 total steps from **114**.

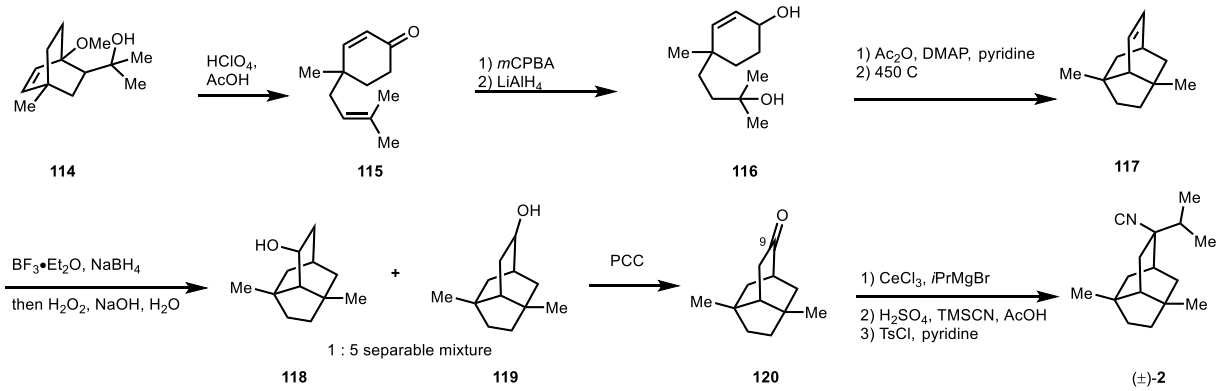

Scheme 18. Ho's synthesis of (±)-9-isocyanoneopupukeanane (**2**).

1.3.3 Intramolecular aldol reaction to build the neopupukeanane core

Uyehara's synthesis of (±)-2-thiocyanatoneopupukeanane (2001)

In a strategy conceptually akin to the one employed by Chang and co-workers in their synthesis of 2-pupukeanone (**28**, Scheme 6, Section 1.2.1)[27], the Uyehara group published a route to 2-thiocyanatoneopupukeanane (**108**) that relies on the aldol condensation of a [3.2.1]-bicycle to build the isotwistane core.[42] The requisite [3.2.1]-bicycle (e.g., **124**) is accessed from the rearrangement of a readily available [2.2.2]-bicycle (**121**).

In the forward sense, the synthesis commenced with the allylation of **121**, which occurred from the undesired face. Formation of the enolate and treatment with ethyl malonate allowed for the epimerization of the allyl group to give a mixture of epimers where the primary component was desired diastereomer **122**. Subsequent addition of a methyl Grignard reagent furnished tertiary alcohol **123**. Treatment of this alcohol with acid led to a Wagner–Meerwein rearrangement to give [3.2.1]-bicycle **124**. Wacker-type oxidation of the pendant olefin gave the corresponding diketone, which underwent a base-mediated aldol reaction followed by acid-catalyzed elimination to give the isotwistane core (**125**). At this stage, they turned their attention toward the conversion of the vinyl methyl group to the desired isopropyl group. Allylic oxidation of **125** gave the corresponding aldehyde. Methyl lithium addition to this aldehyde followed by oxidation of the resultant secondary alcohol gave dienedione **126**. At this stage, Peterson olefination of the more sterically accessible ketone installed the final carbon in the skeleton of the neopupukeanane **127**. From **127**, heterogeneous hydrogenation provided the desired stereochemistry of the isopropyl group (**128**). Conversion of **128** to the thioketone using Lawesson's reagent, followed by reduction with lithium aluminum hydride led to an epimeric mixture of the corresponding thiol. This mixture was treated with sulfuryl chloride followed by trimethylsilyl cyanide to effect conversion to the thiocyanate, also as a mixture of epimers. Following multiple rounds of column chromatography, a pure sample of (±)-2-thiocyanatoneopupukeanane (**108**) was isolated. Overall, this material was accessed in 18 total steps from **121**.

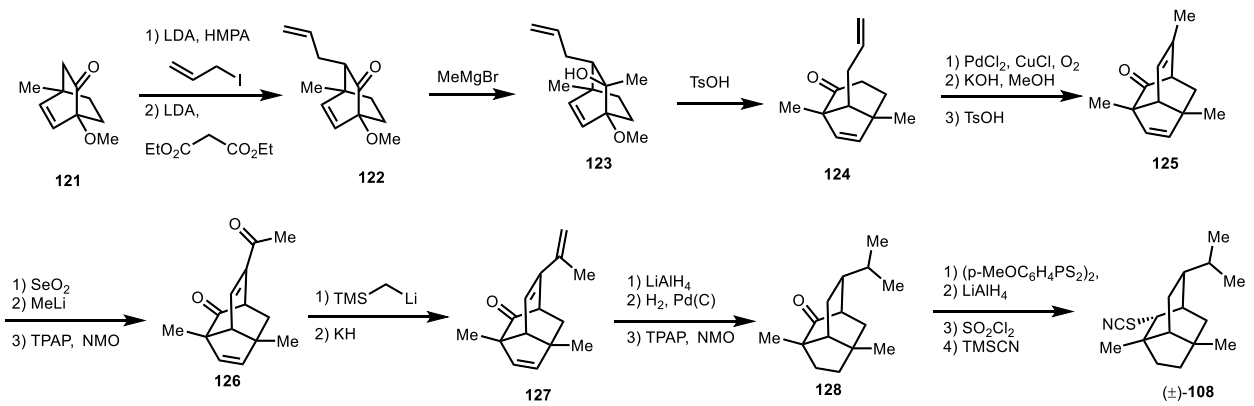

Scheme 19. Uyehara's synthesis of (±)-2-thiocyanatoneopupukeanane (**108**).

1.4 Allopupukeanane and Neoallopupukeanane Natural Products

To date, only two pupukeanane natural products bearing the [5.2.1.0^{4,8}]decane core have been isolated: 2-isocyanoallopupukeanane (**3**) and 9-isocyanoneoallopupukeanane (**5**). 2-Isocyanoallopupukeanane was isolated from the nudibranch *Phyllidia pustulosa* along with 9-isocyanopupukeanane (**1**) and other unrelated isocyanoterpene natural products of a different family.[4] The related neoallopupukeanane (**5**) was isolated in 2019 from the same organism and features the same tricyclic core with different alkyl substitution patterns.[6] A single synthesis of 2-isocyanoallopupukeanane (**3**) has been reported, while no synthetic studies toward the recently isolated neoallopupukeanane scaffold have been published to date.

Ho's synthesis of 2-isocyanoallopupukeanane (1999)

The only reported synthesis of 2-isocyanoallopupukeanane featured a ring expansion from a readily available [2.2.1]-bicyclic precursor to build the [3.2.1]-bicyclic core of the natural product (Scheme 20).[43] The natural product scaffold was completed through a hetero-Diels–Alder reaction to construct a tetracycle that was subsequently cleaved to unveil the desired tricycle.

In the forward sense, the synthesis commenced with norbornene **129** which was treated with *in situ* generated dibromocarbene. Presumably, this sequence proceeds through cyclopropanation of the alkene followed by ionization of one of the bromides to give the corresponding cyclopropyl cation. Electrocyclic ring opening coupled with capture by the saponified ester yielded the ring expanded product **130**. Copper-mediated S_N2'-type addition of a methyl nucleophile gave the desired methylation product, freeing the carboxylic acid, which was reduced and trapped as the tosylate (**131**). Displacement of the tosylate with cyanide gave the corresponding nitrile, which was reduced to the aldehyde with diisobutylaluminum hydride to arrive at diene **132**. Lithium halogen exchange of **132** and addition into the N-methoxy-N-methylacetamide gave **133**. At elevated temperatures, dienone **133** underwent a hetero-[4 + 2] cycloaddition to furnish a tetracycle containing the allopupukeanane core (**134**). In this way, the stereochemistry at the isopropyl group was set without heterogeneous hydrogenation, the most common method employed in the synthesis of the pupukeananes and neopupukeananes. Ozonolysis of tetracycle **134** led to the ring-opened product, and the resultant acetate was

eliminated via thermal pyrolysis to give **135**. At this stage, they turned their attention to the installation of the isonitrile group. The carbonyl was reduced to the corresponding alcohol, which was eliminated to give allopupukeanene **136**. This alkene was converted to (±)-2-isocyanoallopupukeanane (**3**) through a Ritter reaction with hydrogen cyanide to give a formamide followed by dehydration using tosyl chloride and pyridine. Overall, this route provided access to the natural product in 17 steps from bicycle **129** and elegantly leveraged a unique hetero-Diels–Alder reaction to establish the thermodynamically unfavorable stereochemistry of the isopropyl group.

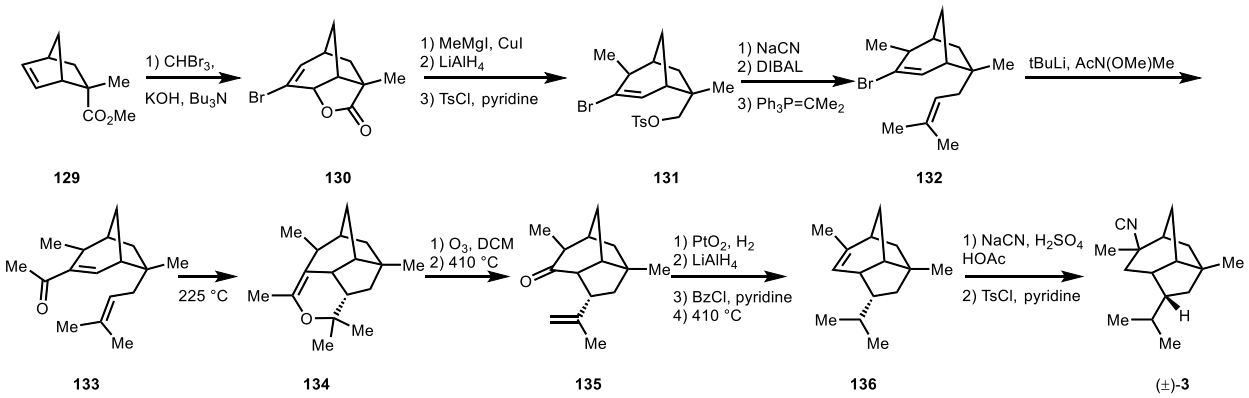

Scheme 20. Ho's synthesis of (±)-2-isocyanoallopupukeanane (**3**).

1.5 Abeopupukeanane Natural Products

To date, only a single natural product bearing the abeopupukeanane skeleton has been isolated. 4-Formamidoabeopupukeanane (**4**, Figure 1) was isolated from *P. coelestis* with 2-formamidopupukeanane (**26**, Figure 3). While this natural product bears an interesting tricyclic scaffold, there haven't been any synthetic studies toward its synthesis published to date.

1.6 Summary and Outlook

Overall, these marine-derived natural products have unique tricyclic scaffolds that bear the relatively rare isonitrile functional group. The pupukeanane family of natural products contains three unique carbon cores that comprise five different natural product skeletons, all biosynthetically connected. Additionally, the unique antimalarial activity of isocyanoterpenes has led to significant interest in the syntheses of these isonitrile-containing natural products. Indeed, synthetic interest in these molecules has led to the development of several strategies, especially to access the isotwistane core of the pupukeananes and neopupukeananes. Typically, these fall into one of four categories on the basis of the key C–C bond forming reaction: 1) alkylation, 2) cycloaddition, 3) radical cyclization, and 4) C–H insertion. However, the natural product skeletons bearing the [5.2.1.$0^{4,8}$]decane core are relatively less explored as are the abeopupukeananes.

One element common to several of these syntheses is the determination of the stereochemistry of the isopropyl group by a heterogeneous hydrogenation, which typically delivers the hydrogen from the convex face of the molecules to access the desired isomer. Additionally, while many of the detailed syntheses only provide racemic access to the compounds of interest,

several reports that access these natural products in an enantioenriched form leverage the use of the chiral, enantioenriched terpene carvone, which can be remodeled into this more complex scaffold. These elements were incorporated into our own work toward the pupukeanane family of natural products.

1.7 References

1. (a) Emsermann, J.; Kauhl, U.; Opatz, T. *Mar. Drugs* **2016**, *14*, 16; (b) Schnermann, M. J.; Shenvi, R. A. *Nat. Prod. Rep.* **2015**, *32*, 543–577; (c) Le Bideau, F.; Kousara, M.; Chen, L.; Wei, L.; Dumas, F. *Chem. Rev.* **2017**, *117*, 6110–6159.
2. Cafieri, F.; Fattorusso, E.; Magno, S.; Santacroce, C.; Sica, D. *Tetrahedron* **1973**, *29*, 4259–4262.
3. Burreson, B. J.; Scheuer, P. J.; Finer, J.; Clardy, J. *J. Org. Chem.* **1975**, *97*, 4763–4764.
4. Fusetani, N.; Wolstenholme, H. J.; Matsunaga, S.; Hirota, H. *Tetrahedron Lett.* **1991**, *32*, 7291–7294.
5. Jaisamut, S.; Prabpai, S.; Tancharoen, C.; Yuenyongsawad, S.; Hannongbua, S.; Kongsaeree, P.; Plubrukarn, A. *J. Nat. Prod.* **2013**, *76*, 2158–2161.
6. Sim, D. C. M.; Hungerford, N. L.; Krenske, E. H.; Pierens, G. K.; Andrews, K. T.; Skinner-Adams, T. S.; Garson, M. J. *Aust. J. Chem.* **2020**, *73*, 129–136.
7. *World Malaria Report 2016.* World Health Organization; Geneva, 2016. (Accessed 5 May 2017).
8. a) *Artemisinin and Artemisinin-Based Combination Therapy Resistance.* World Health Organization; Geneva, April 2017. (Accessed 5 May 2017). b) *Global Plan for Artemisinin Resitance Containment.* World Health Organization; Geneva, January 2011. (Accessed 5 May 2017).
9. (a) König, G. M.; Wright, A. D.; Angerhofer, C. K. *J. Org. Chem.* **1996**, *61*, 3259–3267; (b) Wright, A. D.; Konig, G. M.; Angerhofer, C. K.; Greenidge, P.; Linden, A.; Desqueyroux-Faundez, R. *J. Nat. Prod.* **1996**, *59*, 710–716.
10. Lu, H. H.; Pronin, S. V.; Antonova-Koch, Y.; Meister, S.; Winzeler, E. A.; Shenvi, R. A. *J. Am. Chem. Soc.* **2016**, *138*, 7268–7271.
11. Zhang, Y. H.; Shi, B. F.; Yu, J. Q. *J. Am. Chem. Soc.* **2009**, *131*, 5072–5074.
12. McCulley, C. H.; Tantillo, D. J. *J. Phys. Chem. A* **2018**, *122*, 8058–8061.
13. Garson, M. J. *J. Chem. Soc., Chem. Commun.* **1986**, 35.
14. Hagadone, M. R.; Burreson, B. J.; Scheuer, P. J.; Finer, J. S.; Clardy, J. *Helv Chim Acta* **1979**, *62*, 2484–2494.
15. Marcus, A. H.; Molinski, T. F.; Fahy, E.; Faulkner, D. J.; Xu, C.; Clardy, J. *J. Org. Chem.* **1989**, *54*, 5184–5186.
16. (a) Fusetani, N.; Wolstenholme, H. J.; Matsunaga, S. *Tetrahedron Lett.* **1990**, *31*, 5623–5624; (b) He, H. Y.; Salva, J.; Catalos, R. F.; Faulkner, D. J. *J. Org. Chem.* **1992**, *57*, 3191–3194; (c) Simpson, J. S.; Garson, M. J.; Hooper, J. N. A.; Cline, E. I.; Angerhofer, C. K. *Aust. J. Chem.* **1997**, *50*, 1123–1128; (d) Yasman, Y.; Edrada, R. A.; Wray, V.; Proksch, P. *J. Nat. Prod.* **2003**, *66*, 1512–1514; (e) Lyakhova, E. G.; Kolesnikova, S. A.; Kalinovskii, A. I.; Stonik, V. A. *Chem. Nat. Compd* **2010**, *46*, 534–538.
17. Corey, E. J.; Behforouz, M.; Ishiguro, M. *J. Am. Chem. Soc.* **1979**, *101*, 1608–1609.
18. Yamamoto, H.; Sham, H. L. *J. Am. Chem. Soc.*

1979, *101*, 1609–1611.
19. Brown, M. K.; Corey, E. J. *Org. Lett.* **2010**, *12*, 172–175.
20. Corey, E. J.; Ishiguro, M. *Tetrahedron Lett.* **1979**, *20*, 2745–2748.
21. Hsieh, S. L.; Chiu, C. T.; Chang, N. C. *J. Org. Chem.* **1989**, *54*, 3820–3823.
22. Chang, N.-C.; Lu, W.-F.; Tseng, C.-Y. *J. Chem. Soc., Chem. Commun.* **1988**, 182–183.
23. Schiehser, G. A.; White, J. D. *J. Org. Chem.* **1980**, *45*, 1864–1868.
24. Fráter, G.; Wenger, J. *Helv Chim Acta* **1984**, *67*, 1702–1706.
25. Kaliappan, K.; Subba Rao, G. S. R. *J. Chem. Soc. Perkin Trans. I* **1997**, 3393–3400.
26. (a) Srikrishna, A.; Vijaykumar, D.; Sharma, G. V. R. *Tetrahedron Lett.* **1997**, *38*, 2003–2004; (b) Srikrishna, A.; Vijaykumar, D.; Sharma, G. V. R. *Indian J. Chem., Sect. B* **1999**, *38*, 766–770.
27. Chang, N.-C.; Chang, C.-K. *J. Org. Chem.* **1996**, *61*, 4967–4970.
28. (a) Srikrishna, A.; Jagadeeswar Reddy, T. *J. Chem. Soc. Perkin Trans. I* **1997**, 3293–3294; (b) Srikrishna, A.; Reddy, T. J. *J. Chem. Soc. Perkin Trans. I* **1998**, 2137–2144.
29. Srikrishna, A.; Hemamalini, P.; Sharma, G. V. R. *J. Org. Chem.* **1993**, *58*, 2509–2516.
30. Srikrishna, A.; Ravi Kumar, P.; Gharpure, S. J. *Tetrahedron Lett.* **2001**, *42*, 3929–3931.
31. Srikrishna, A.; Kumar, P. R.; Gharpure, S. J. *Indian J. Chem., Sect. B* **2006**, *45*, 1909–1919.
32. Srikrishna, A.; Kumar, P. R. *Indian J. Chem., Sect. B* **2002**, *41*, 152–153.
33. Smaligo, A. J.; Swain, M.; Quintana, J. C.; Tan, M. F.; Kim, D. A.; Kwon, O. *Science* **2019**, *364*, 681–685.
34. Karuso, P.; Poiner, A.; Scheuer, P. J. *J. Org. Chem.* **1989**, *54*, 2095–2097.
35. Pham, A. T.; Ichiba, T.; Yoshida, W. Y.; Scheuer, P. J.; Uchida, T.; Tanaka, J.-i.; Higa, T. *Tetrahedron Lett.* **1991**, *32*, 4843–4846.
36. Srikrishna, A.; Gharpure, S. J. *ChemComm* **1998**, 1589–1590.
37. Srikrishna, A.; Gharpure, S. J. *Tetrahedron Lett.* **1999**, *40*, 1035–1038.
38. (a) Srikrishna, A.; Gharpure, S. J. *J. Chem. Soc. Perkin Trans. I* **2000**, 3191–3193; (b) Srikrishna, A.; Gharpure, S. J.; Venugopalan, P. *Indian J. Chem., Sect. B* **2003**, *42*, 129–134.
39. (a) Srikrishna, A.; Gharpure, S. J. *J. Org. Chem.* **2001**, *66*, 4379–4385; (b) Ramsden, C. A.; Srikrishna, A.; Gharpure, S. J. *Arkivoc* **2002**, *2002*, 52–62.
40. Srikrishna, A.; Satyanarayana, G. *Tetrahedron* **2005**, *61*, 8855–8859.
41. Ho, T. L.; Jana, G. H. *J. Org. Chem.* **1999**, *64*, 8965–8967.
42. Uyehara, T.; Onda, K.; Nozaki, N.; Karikomi, M.; Ueno, M.; Sato, T. *Tetrahedron Lett.* **2001**, *42*, 699–702.
43. Ho, T.-L.; Kung, L.-R. *Org. Lett.* **1999**, *1*, 1051–1052.

Chapter 2. Synthesis of 2-Isocyanopupukanane with Access to the Pupukeanyl Core

2.1 Toward a Unified Synthesis of the Pupukeanane and Allopupukeanane Frameworks

Nature has the ability to elaborate an early-stage, 'upstream', biosynthetic intermediate into a wide variety of 'downstream' secondary metabolites (natural products) through highly efficient and divergent biosynthetic pathways. Inspired by nature, chemists have continued to develop syntheses that provide unified access to families of structurally unique natural products from a common scaffold.[1] Modern computational techniques have been shown to provide a deeper understanding of the potential energy surface for myriad biosynthetic pathways,[2] which may now enable chemists to reverse the course of these pathways in order to access multiple natural products from a downstream biosynthetic intermediate.

Given their topologically complex scaffolds and underexplored biological activity (as discussed in Chapter 1), we set out to develop a bio-inspired, unified route to skeletons of the 9-isocyanopupukeananes (**1** and **2**, Scheme 1A) and 2-isocyanoallopupukeanane (**3**). While many approaches to prepare natural products with the pupukeanane core have been reported,[3] only a single total synthesis of (±)-2-isocyanoallopupukeanane (**3**) has been achieved to date.[4] Notably, we were drawn to a synthesis of **3** specifically given the low isolation yield of this biosynthetically downstream congener,[5] as well as the lack of synthetic strategies to provide this natural product in enantioenriched form. Given the proposed biosynthetic link between the 9-pupukeanyl cation (**5**, Scheme 1B) and the 2-allopupukeanyl cation (**6**) from amorphene (**4**),[6,7] we sought to develop a bio-inspired synthesis which establishes a synthetic link between these skeletons.

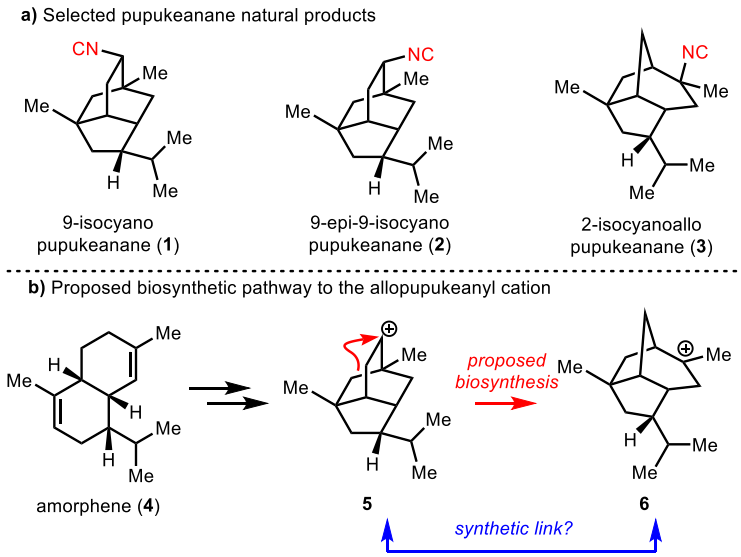

Scheme 1. a) Natural product targets; b) Biosynthetic link between the pupukeanane skeletons.

2.2 First Generation Approach

Specifically, we proposed that both 9-isocyanopupukeanane (**1**) and 2-isocyanoallopupukeanane (**3**) could be accessed from intermediate **7** (Scheme 2). In the forward sense, application of Shenvi's conditions for isocyanide installation[8] to an intermediate such as **7** should directly produce 9-isocyanopupukeanane (**1**). Under an alternative set of conditions, a biomimetic Wagner-Meerwein type rearrangement was expected to forge the allopupukeanane skeleton, yielding 2-isocyanoallopupukeanane (**3**) after isocyanide installation. We envisioned that rearrangement precursor **7** could be accessible from a carbonyl-alkene coupling of fused bicycle **8**. Key to our synthetic strategy was rapid access to the bicyclo[2.2.2] framework of **8**. Given our group's longstanding interest in the rearrangement of readily available chiral, enantioenriched terpenes to access diverse scaffolds,[9] we envisioned an approach that leverages the C–C cleavage of a strained cyclobutanol.[10] Specifically, we envisioned **9** undergoing sequential ring-opening and Heck-type cyclization. This key intermediate can be readily accessed from (*S*)-carvone (**10**), which is abundant, inexpensive, and commercially available in both enantiomeric forms. Overall, should it be successful, this proposed route would provide a unified approach to enantiopure 9-isocyanopupukeanane (**1**) and 2-isocyanoallopupukeanane (**3**) in only 10 steps.

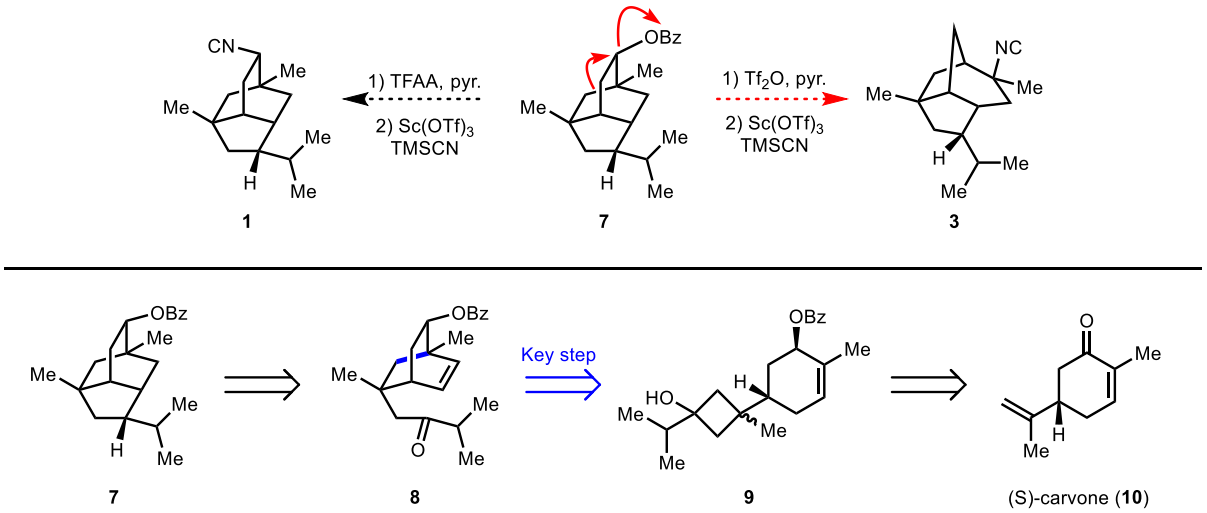

Scheme 2. Proposed retrosynthesis of **1** and **3** through a common pupukeanyl precursor (**7**).

2.2.1 Route to Key Intermediate **9**:

Thus, our synthesis route commenced with the reduction of (*S*)-carvone (**10**) with lithium aluminum hydride to give cis-carveol (**11**),[11] which was subjected to Mitsunobu-type substitution to give the corresponding benzoylated *trans*-carveol (**12**).[12] From this known compound, [2+2] cycloaddition of in situ generated dichloroketene and subsequent reductive dechlorination provided benzoyl protected cyclobutanone **14**. At this stage, we attempted addition of isopropyl magnesium bromide to **14**. Initially this reaction was sluggish, however in further studies we found that pretreatment of the cyclobutanone with cerium (III) chloride facilitated formation of the desired cyclobutanol as a separable mixture of *anti*- and *syn*- addition adducts **9a** and **9b**. Ultimately, we have shown this entire sequence to be robust on gram scale.[13]

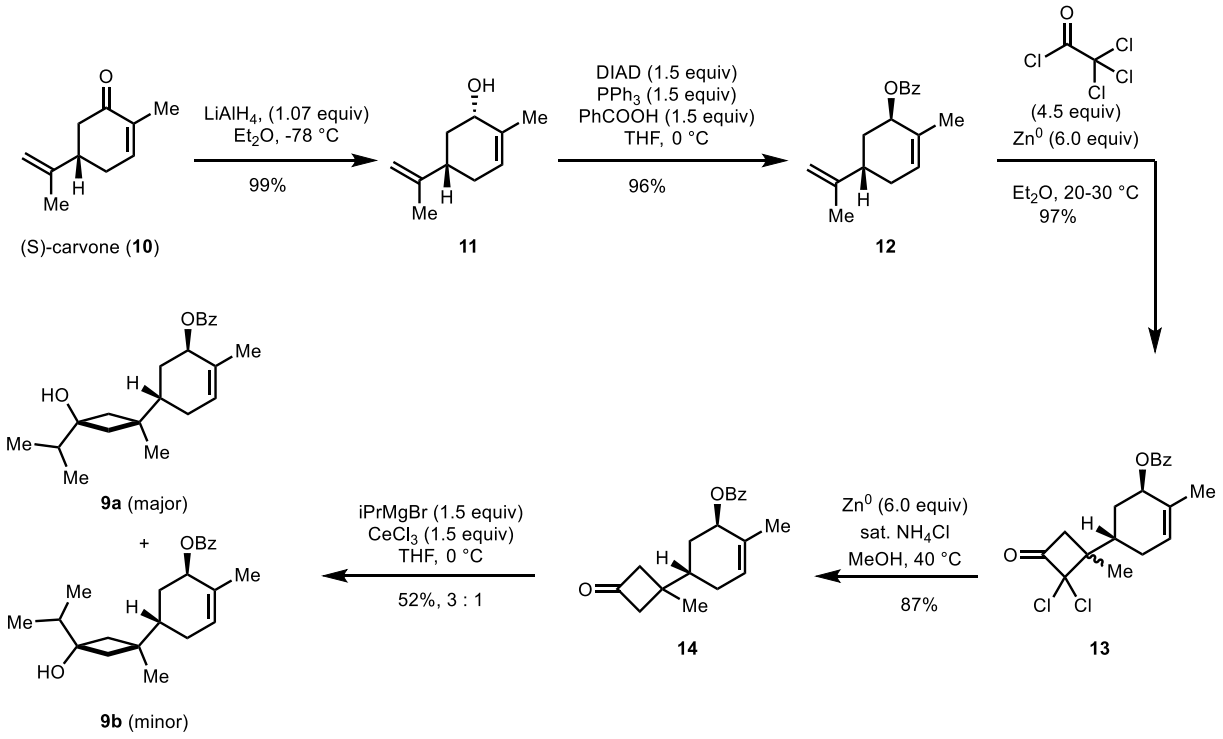

Scheme 3. Route to key step precursor **9.**[13]

2.2.2 Progress on Palladium (II)-Mediated Cascade

Since 1999, strained cyclobutanols have been successfully leveraged as substrates that undergo C–C bond cleavage.[10b, 14] These reactions have been used in accessing multiple natural product cores.[9a, 9b] For our purposes, we envisioned a novel application of selective C–C bond cleavage to initiate a tandem migratory insertion process (Scheme 4). The proposed mechanism begins with an X-type ligand substitution of cyclobutanol **9** to form Pd-alkoxide **I1**. Subsequent *β*–carbon elimination should form sp^3-palladium(II) alkyl **I2**; we anticipated that careful ligand optimization would allow us to achieve diastereoselective C–C bond cleavage in line with the precedent of Uemura and co-workers.[15] Historically, the organopalladium intermediate would undergo *β*–hydride elimination; however, given the lack of a *β*–hydrogen, we envisioned **I2** would undergo migratory insertion across the cyclohexene double bond to give **I3** followed by a *β*–H elimination to yield bicycle **8** in an oxidative Heck-type process. We expected the migratory insertion to proceed in the desired 6-*endo*-trig pathway for this protected allylic alcohol rather than the 5-*exo*-trig alternative, as this would place the metal at the less sterically hindered position.

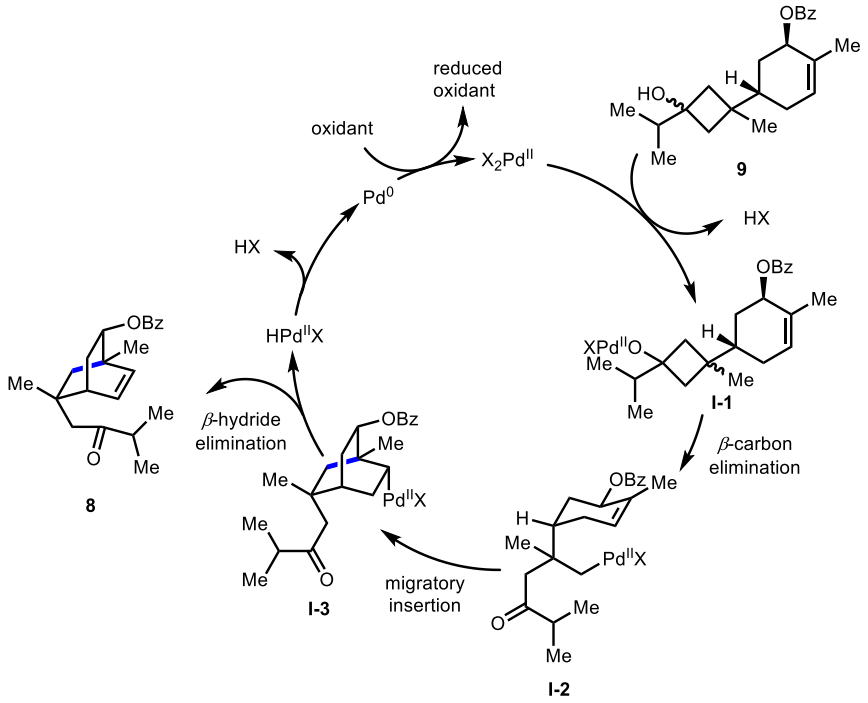

Scheme 4. Proposed catalytic cycle for key C-C bond shuffling cascade.

Interestingly, initial application of standard conditions for an oxidative cyclobutanol ring cleavage[10b] did not produce the desired bicycle (**8**), but rather led to a complex diastereomeric mixture that appeared to leave the cyclohexene moiety untouched (Scheme 5). While the mixture was not fully separable, careful characterization by NMR spectroscopy matched the formation of products consistent with reports by Uemura that 1,3,3-trisubstituted cyclobutanols (such as **9**) can undergo a ring contraction to form the corresponding cyclopropane (**15**).[14a] Cyclopropane formation is purported to proceed through **I-2** which then forms the palladium enolate (**I-4**) that undergoes reductive elimination to give the cyclopropyl ketone (**15**). Our observations indicated that at least the first steps in the catalytic cycle proceeded as planned, albeit with low conversion. As such, these conditions were used as a basis for subsequent investigations.

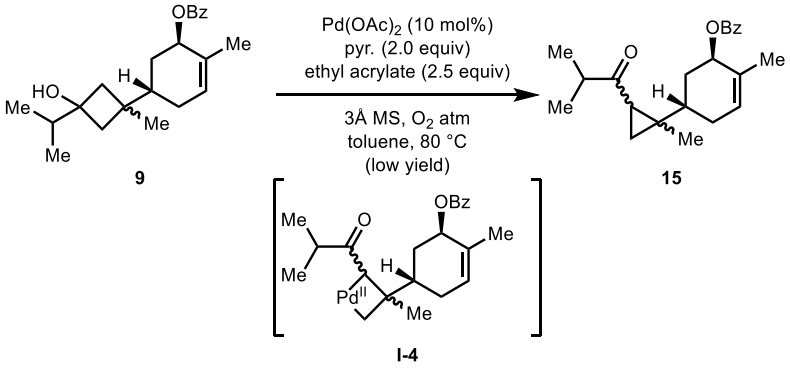

Scheme 5. Preliminary attempts for the Pd(II)-mediated cyclization.

With the goal of coaxing intermediate **I-2** into undergoing an oxidative Heck-type migratory insertion, many classes of ligands were screened. Due to the strongly oxidizing conditions required to reoxidize the generated palladium(0), we began with nitrogen-based ligands, particularly those that had been successful in related processes.[14c, 16] While these ligands demonstrated varying conversion to the cyclopropane diastereomers (**15**), we did not observe any formation of desired bicycle **8**.

Exploration of phosphine ligands led to unexpected reactivity between intermediate **I-2** and the ethyl acrylate additive using a triphenylphosphine ligand system (Scheme 6). While this compound was not completely purified and characterized, characteristic ^{1}H NMR splitting patterns of the alkene protons indicate that intermediate **I-2** underwent an intermolecular Heck-type reaction with ethyl acrylate to give ester **16** in low yield.

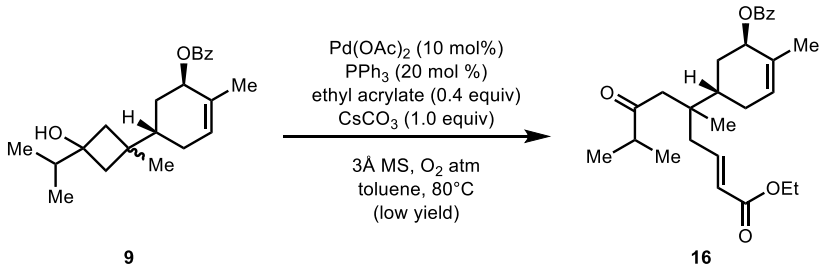

Scheme 6. Intermolecular Heck-type reaction of **9.**

The use of ethyl acrylate is important as it has previously been shown to coordinate to the organopalladium intermediate, facilitating the final step of β–H elimination.[14a] This effectively dissociates the product and allows the palladium catalyst to reenter the catalytic cycle. On the basis of this result, additional additive screenings were conducted to determine whether a more sterically hindered acrylate would enhance coordination to the organopalladium to facilitate β–H elimination but retard the intermolecular Heck-type reaction (Figure 1). Unfortunately, use of these additives resulted in only recovery of starting material. Additional screening studies have been conducted without an additive but using stoichiometric palladium (II) to increase conversion. Additional phosphine ligand screenings with both electron-poor and electron-rich triarylphosphines gave only the cyclopropane product (**15**) in small quantities.

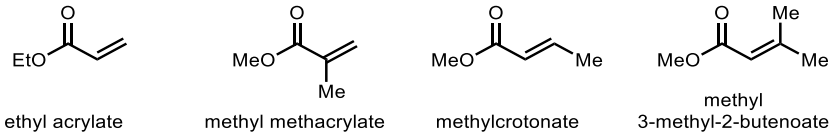

Figure 1. Acrylate additives screened.

Even after additional screening of solvents, ligands, bases, additives, and palladium sources, we have still not been able to access the desired bicycle **8**.

2.3 Second Generation Approach to the Pupukeanane Family

Given the challenges we faced in forging the [2.2.2]-bicyclic core of the pupukeanane skeleton, and the success we observed in intercepting the Pd(II)-mediated opening with a sufficiently electron poor alkene (i.e., **16**), we revised our synthetic strategy to target the [3.2.1]-bicycle present in the allopupukeanane core through the installation of an electron-deficient enone.

2.3.1 Proposed retrosynthesis of 2-isocyanoallopupukeanane

In our revised strategy, we sought to maintain the key elements of a palladium-mediated C–C bond shuffling cascade to build a bicycle related to the pupukeanane natural products from commercially available carvone. Specifically, we envisioned the Pd-cascade would enable us to access a [3.2.1]-bicycle that would map directly onto the allopupukeanyl core (Scheme 7). We envisioned late-stage diversification of the allopupukeanane skeleton could furnish the pupukeanyl core through a 'contra-biosynthetic' rearrangement.

In the retrosynthetic sense, we anticipated that carbocation **6** would lead to **3** through direct cyanide capture, whereas a late-stage 'contra-biosynthetic' rearrangement of **6** might yield 9-isocyanopupukeanane (**1**). Carbocation **6** could arise from corresponding alkene **17**, which, in turn, would be prepared from **18** through an aldol condensation in the forward sense to forge the tricyclic allopupukeanene core. Cyclobutanol **19** (notably similar to cyclobutanol **9**) was envisioned to arise in 3 steps from (*R*)-carvone (**20**).

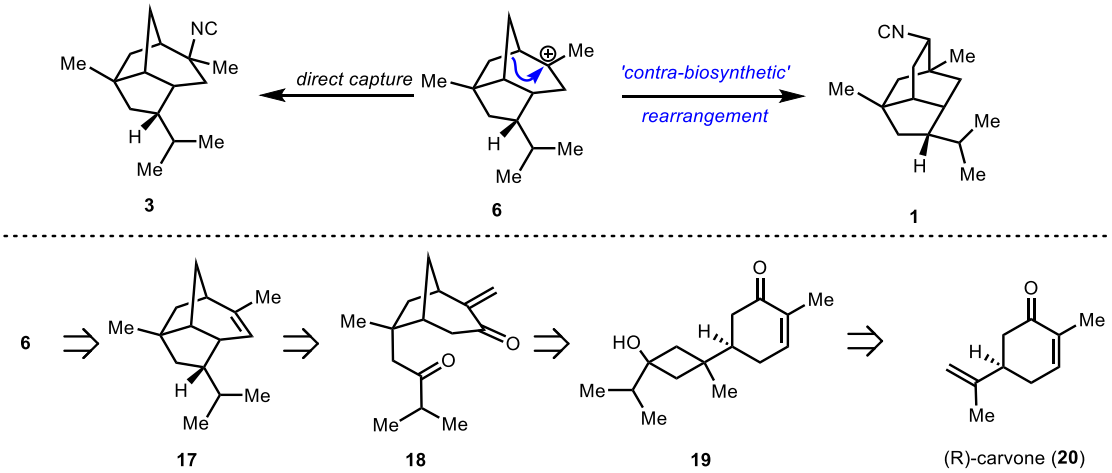

Scheme 7. Our proposed retrosynthesis of 2-isocyanoallopupukeanane (**3**) and the pupukeanane core (**1**).

2.3.2 Attempts to effect a Pd(II)-mediated cascade to forge a [3.2.1]bicycle

From an enone such as **19** (Scheme 8), we expected that the proposed Pd-mediated C–C bond cleavage/forming cascade reaction would yield [3.2.1]bicycle **18** (Table 1).[10b] We hypothesized that a palladium(II)-complex would first undergo X-type ligand exchange with the tertiary hydroxy group of cyclobutanol **19** (see **I-5**) followed by a β-carbon elimination to form alkyl palladium intermediate **I-6**. Given the absence of a β-hydrogen in **I-6**, this alkyl palladium intermediate was anticipated to undergo a Heck-type migratory insertion across the enone double bond to form the corresponding palladium enolate (**I-7**). Finally, a β-hydride elimination would yield the exocyclic enone diastereomers **18** and **21**.

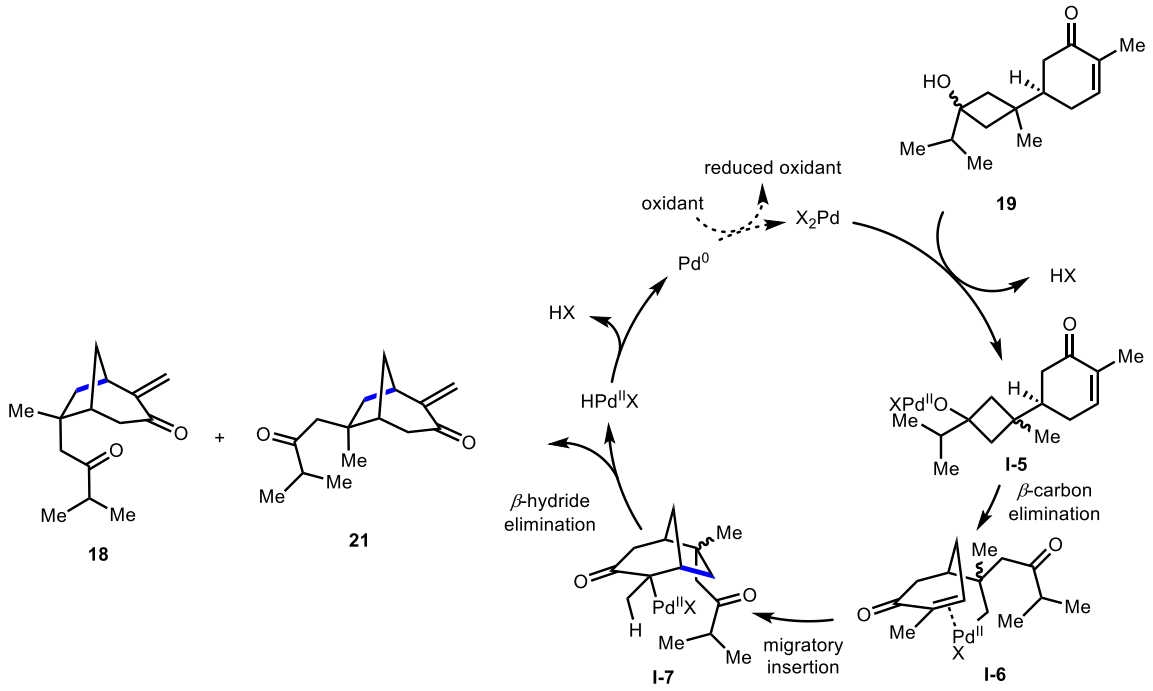

Scheme 8. Proposed Pd(II)-cascade to access [3.2.1]-bicycle **18**.

To test this proposed transformation, the enantiomer of each diastereomer of the previously synthesized cyclobutanol (*ent*-**9a** and *ent*-**9b**, obtained from (R)-carvone, Scheme 9) was treated with base to cleave the benzoyl group and the corresponding allylic alcohols were oxidized to give the enones **19a** and **19b**.

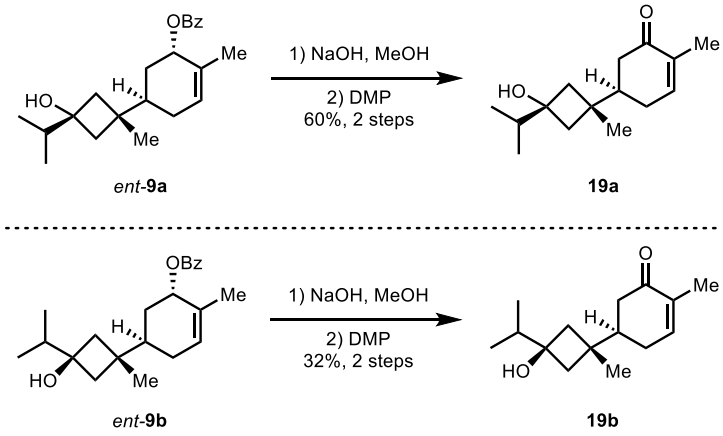

Scheme 9. Synthesis of cyclohexenones **19a** and **19b.**

With cyclobutanols **19a** and **19b** in hand, application of the conditions disclosed by Uemura in the seminal report of cyclobutanol opening through a Pd(II)/Pd(0) cycle,[10b] gave rise to small amounts of the desired bicycle (Table 1, entry 1). Using 1,2-dichloroethane as solvent led to an increase in yield (Table 1, entry 2). Of the ligands that were screened for this transformation, only nitrogen-based ligands led to the desired product. We also observed that electron-deficient pyridines were competent ligands that led to a comparable outcome (Table 1, entry 3–4). However,

we chose to proceed with pyridine as the ligand of choice due to its comparatively lower cost. The ratio of palladium to pyridine was crucial to the success of this reaction (Table 1, entries 5–7). To date, we have not been able to obtain high yields of the desired product using sub-stoichiometric amounts of Pd(II) salts (Table 1, entry 8). In many previous reports of transformations that proceed through a Pd(II)/Pd(0) catalytic cycle, an excess of the pyridine ligand was vital to maintaining Pd(0) in solution without precipitation as Pd-black.[10a, 14a] However, in our case, we observed that a 1 : 1 ratio of Pd(II) salt : ligand gave the best results and product formation was not observed in cases using a large excess of pyridine. While we would still expect the active Pd species to be bis-ligated under these conditions,[17] presumably an excess of pyridine hinders the ligand dissociation required to promote the β-carbon elimination/migratory insertion sequence. In our studies, even the introduction of external oxidants (Table 1, entry 9), did not improve conversion. However, the currently employed protocol is scalable to provide bicycle **18** in sufficient quantities (Table 1, entry 10). Despite recent progress in improving speciation in Pd(II)/(0) catalytic cycles,[18] it is well-known that reoxidation of Pd(0) intermediates is often slow and can fail due to the precipitation of Pd black.[18b, 19]

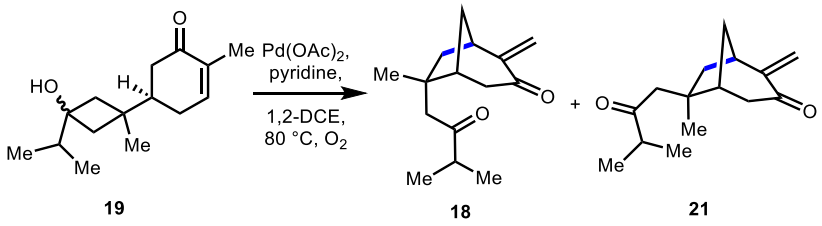

19 **18** **21**

entry	$Pd(OAc)_2$(equiv)	ligand (equiv)	deviation*	yield (%)[a] **18**	yield (%)[a] **21**
1	$Pd(OAc)_2$ (1.0)	pyridine (2.0)	toluene	trace	trace
2	$Pd(OAc)_2$ (1.0)	pyridine (2.0)	-	7	7
3	$Pd(OAc)_2$ (0.5)	pyridine (1.0)	-	10	10
4	$Pd(OAc)_2$ (0.5)	4-CF_3pyridine (1.0)	-	10	12
5	$Pd(OAc)_2$ (1.0)	pyridine (1.0)	-	27	33
6	$Pd(OAc)_2$ (1.0)	pyridine (0.5)	-	18	23
7	$Pd(OAc)_2$ (1.0)	none	-	trace	trace
8	$Pd(OAc)_2$ (0.5)	pyridine (0.5)	-	12	13
9	$Pd(OAc)_2$ (0.5)	pyridine (0.5)	$Cu(OAc)_2$	9	13
10	$Pd(OAc)_2$ (1.0)	pyridine (1.0)	50 mmol scale	22[b]	23[b]

Table 1. Selected conditions for the Pd(II)-mediated cascade.[20] [a] Determined by ^{1}H NMR analysis using 1,3,5-trimethoxybenzene as an internal standard. [b]Isolated yield

2.3.3 Forward Synthesis of 2-isocyanoallopupukanane

While the use of **9** provided access to cyclobutanols **19a** and **19b**, we sought a more elegant and direct way to prepare these compounds that would avoid the reduction/protection/hydrolysis/oxidation sequence. Ultimately, our completed synthetic route commenced with the known [2+2] cycloaddition of in situ generated dichloroketene to the isopropenyl group of (*R*)-carvone (**20**)[21] and subsequent reductive dechlorination to provide cyclobutanone **22** (Scheme 10). At this stage, we attempted addition of isopropyl magnesium bromide. As anticipated, addition of Grignard reagents to **P9** led to non-selective mono- and

double-addition products. However, treating enone **22** with PPh_3 and TESOTf effected in situ protection of the enone moiety,[22] which enabled the addition of isopropyl lithium to the cyclobutanone carbonyl. In the same pot, the enone was unmasked following addition of the nucleophile, to provide cyclohexenones **19a** and **19b** as an inseparable, but ultimately inconsequential, mixture of *anti*- and *syn*- addition adducts.

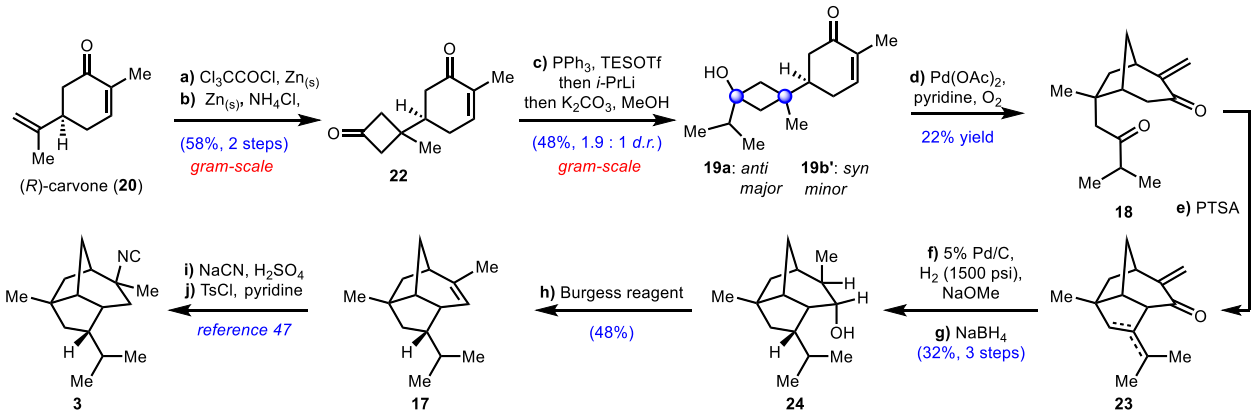

Scheme 10. Formal synthesis of 2-isocyanoallopupukeanane (**3**).

Application of our best conditions for the Pd(II)-mediated cascade led to the isolation of key bicycle **18**. At this stage, an aldol condensation forged the tricyclic core of allopupukeanane (**23**) as an inconsequential mixture of alkene isomers. Global hydrogenation, followed by sodium borohydride reduction of the resulting ketone group yielded alcohol **24**. However, this reaction was quite sluggish and mono-hydrogenation products were often isolated after extended reaction times, even under high pressure of hydrogen. We hypothesized that the reduction of the mixture of tri- or tetra-substituted alkenes was hindered by a steric clash with the α-disposed methyl group, which results from reduction of the enone, and the developing α-disposed isopropyl group on the concave face of the bridged tricycle. The addition of sodium methoxide to the hydrogenation reaction mixture overcame this challenge by epimerization to place the methyl group on the β-face. Following reduction of the resulting ketone with sodium borohydride, alcohol **24** was isolated as a single diastereomer in 32% yield over 3 steps.[23]

From this secondary alcohol, a Burgess dehydration gave the volatile allopupukeanene **17**. Ho and co-workers have previously reported the conversion of 17 to 2-isocyanoallopupukeanane (**3**) through addition of HCN across the alkene in a Ritter reaction and subsequent dehydration of the resulting formamide to yield **3**.[4a] In summary, allopupukeanene **7** was prepared in 8 steps from (*R*)-carvone and constitutes a 10-step formal synthesis of 2-isocyanoallopupukeanane (**3**) — shortened from Ho's 17-step synthesis of the racemate.[24]

2.4 Development of a 'contra'-biosynthetic rearrangement

At this stage, we turned our attention to effecting the rearrangement of the allopupukeanane framework (i.e., **17**) to the pupukeanane core. We anticipated that this transformation would be difficult to accomplish since trapping of the pupukeanane skeleton would require the formal

capture of a secondary carbocation (**5**) that is unlikely to be a minimum on the potential energy surface.[2a, 7a, 25] However, we speculated that the desired transformation might be possible through a concerted Wagner–Meerwein shift and nucleophilic capture of a kinetically generated allopupukeanyl cation (**6**).

Indeed, formation of the pupukeanane core from an allopupukeanyl precursor proved particularly challenging. Our initial attempts led only to decomposition or capture of **6** by the exogenous nucleophile. Therefore, we sought to gather further mechanistic insight through computational modeling. Calculations were conducted on the capture of **6** with a nucleophilic cyanide source, here trimethylsilyl cyanide (Scheme 12), using the Gaussian 16 software[26] at the ωB97XD(SMD)/def2-SVP level of theory (see the Experimental Section for additional information).[27] The corresponding transition state structure for TMSCN addition was located (**B-TS1**) and, as expected, the direct capture of **6** to give 2-isocyanoallopupukeanane (**3**) was calculated to be both kinetically and thermodynamically feasible. Additionally, the 9-pupukeanyl cation (**5**) was not observed to be a minimum on the potential energy surface. An alternative transition state structure for concerted attack of TMSCN and alkyl shift (see **B-TS2**) could not be located, despite the fact that 9-isocyanopupukeanane (**1**) was predicted to be thermodynamically much more stable than the 2-isocyanoallopupukeanane congener (**3**).

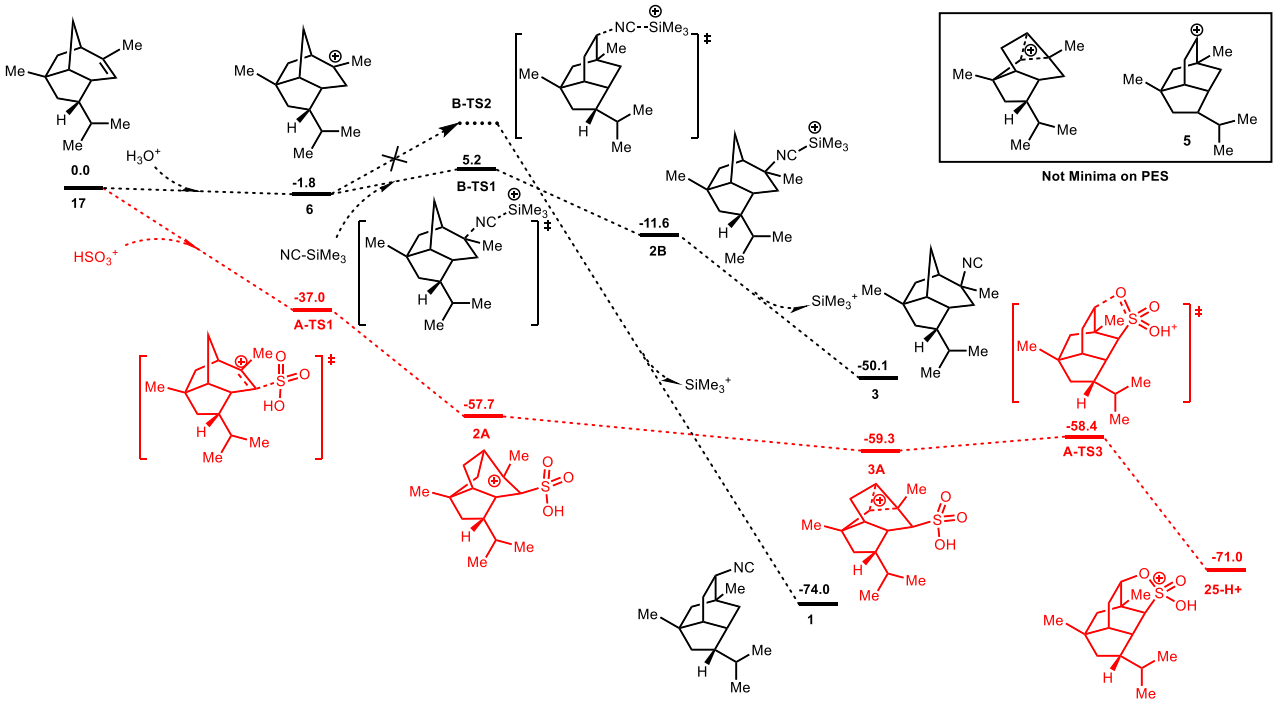

Scheme 11. Computational studies on the rearrangement of the allopupukeanane core (17).

When allopupukeanene **17** was subjected to H_2SO_4 and glacial AcOH at elevated temperatures, we observed the formation of small amounts of pupukeanyl sultone **25** (Scheme 13). The sulfonation of alkenes is known and constitutes an important step in the formation of camphor sulfonic acid.[28] Furthermore, simple sultones have been formed through the addition of electrophilic SO_3 across an alkene followed by Wagner–Meerwein type rearrangements.[29]

Ultimately, we were able to improve upon our initial observation by accessing sultone **25** directly from alcohol **24**, which avoided the isolation of volatile allopupukeanene **7**. Presumably **24** → **25** proceeds through an acid-mediated elimination of the hydroxy group to give allopupukeanene **7** followed by an electrophilic sulfonation and subsequent Wagner–Meerwein rearrangement. The structure of **15** was unambiguously confirmed by single crystal x-ray crystallography.

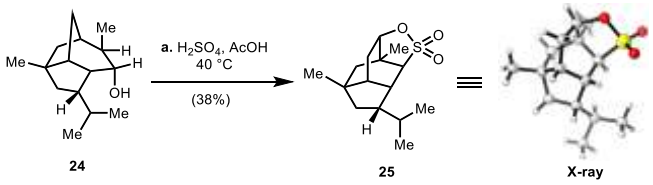

Scheme 12. Rearrangement to the pupukeanane core (**25**).

On the basis of these empirical findings, we modeled the reaction coordinate for the sulfonation of **17** with an activated sulfur electrophile to form intermediate **2A**. From this intermediate, the rearrangement is nearly barrierless, proceeding through a nonclassical carbocation (**3A**)[30] on a flat region of the potential energy surface to reach protonated pupukeanyl sultone **25-H**$^+$ as an energy minimum. Thus, it would appear that while a direct capture of the 9-pupukeanyl cation (**5**) is not feasible, by coupling the generation of **5** with a sulfonation process, we are able to trap the allopupukeanane skeleton in the form of pupukeanyl sultone **25**. This transformation effectively reverses the proposed biosynthetic pathway to access the pupukeanane core from a downstream biosynthetic intermediate.

2.5 Summary and Outlook

In conclusion, we have developed a short enantiospecific synthesis of 2-isocyanoallopupukeanane, formally, in only 10 steps from (*R*)-carvone. Key features of the synthesis include a Pd-mediated cascade to form a [3.2.1] bicycle followed by an aldol condensation/cyclization to build the carbon skeleton of allopupukeanane in two steps from a strategic monocyclic precursor. The short synthetic sequence has enabled us to explore the proposed biosynthetic pathway to these architecturally fascinating molecules and the corresponding potential energy surface. These efforts culminated in the development of a bioinspired rearrangement from a downstream biosynthetic intermediate to access the pupukeanane skeleton in the form of a sultone. The short synthetic sequence should prove useful in accessing the 9-pupukeanane, the 9-epi-9-pupukeanane, and the 2-allopupukeanane natural products and their analogs for testing as potential antimalarial compounds.

2.6 Experimental Contributors

This chapter includes content reproduced with permission from Hardy, M. A.; Feng, Z.; Kerschgens, I.; Massey, L. A.; Tantillo, D. J.; and Sarpong, R. "Unifying synthesis of 2-isocyanoallopupukeanane and the pupukeanane core through a bio-inspired rearrangement", *unpublished*, **2021**. Development of the first-generation route was conducted in tandem with a postdoctoral fellow in our laboratory, Dr. Isabel Kerschgens. Visiting undergraduate researcher Lynée A. Massey assisted in scale up and the investigation of an alternative coupling strategy for

the Pd-mediated cascade that is not discussed. The computational studies were carried out entirely by Zhitao Feng with Prof. Dean J. Tantillo at the University of California, Davis.

2.7 Experimental Details

2.7.1 General Procedures

Solvents and reagents

Unless otherwise stated, all commercial reagents were purchased from Sigma Aldrich, Acros Organics, Advanced Combi-blocks, TCI, Fisher Scientific and/or Alfa Aesar and used without further purification. Solvents were purchased from Fisher Scientific. Tetrahydrofuran (THF), ether (Et_2O), toluene (PhMe), benzene (PhH), acetonitrile (MeCN), and methanol (MeOH) were sparged with argon and dried by passing through a column of activated alumina in a Glass Contour solvent purification system. Dichloromethane (DCM) was distilled over calcium hydride prior to each use. All other solvents used were purchased from Acros Organics and used without further purification.

Reaction setup, monitoring, and purification

Unless noted below, all reactions were carried out in flame-dried glassware under an atmosphere of N_2 and stirred with Teflon-coated magnetic stir bars. Reaction temperatures above room temperature (20–23 ºC) were modulated by an IKA® temperature controller. Reaction progress was monitored by a combination of LC/MS analysis [Shimadzu LCMS-2020 (UFLC) equipped with the LC-20AD solvent delivery system, a SPD-20AV prominence UV/Vis detector (SPD-M20A Photo Diode Array), and a Thermo Scientific Hypersil GOLD HPLC column (5 μm particle size, 4.6 × 50 mm)] and thin-layer chromatography (Silicycle Siliaplate™, glass backed, extra hard layer, 60 Å, 250 μm thickness, indicator F254). Visualization of the developed plates was performed using UV irradiation (254 nm) and staining with potassium permanganate ($KMnO_4$), *p*-anisaldehyde, or ceric ammonium molybdate (CAM). Purification and isolation of products were performed with silica gel chromatography (preparative thin-layer chromatography and flash column chromatography). Manual flash column chromatography was conducted with Sorbent Technologies 60 Å silica gel of particle size 40–63 μm in glass columns. Automated flash column chromatography was performed on a Yamazen® Smart Flash EPCLC W-Prep 2XY automated flash chromatography system, with prefilled Universal Premium Columns (60 Å silica gel of particle size 30 μm). Volatile solvents were evaporated under reduced pressure using a Büchi temperature-controlled rotary evaporator.

NMR Spectroscopy

NMR spectra were recorded on Bruker spectrometers at the UC Berkeley College of Chemistry NMR Facility, operating at 300, 400, 500, 600, or 700 MHz for ^{1}H NMR, and at 75, 100, 125, 150, or 175 MHz for ^{13}C NMR. Chemical shifts are reported relative to the residual solvent peak of $CDCl_3$ (δ = 7.260 ppm for ^{1}H NMR, δ = 77.16 ppm for ^{13}C NMR). ^{1}H NMR data are reported as follows: chemical shift, multiplicity (s = singlet, br s = broad singlet, d = doublet, t = triplet, q = quartet, p = pentet, se = sextet, hept = heptet, m = multiplet, and app = apparent multiplicity), coupling constant (Hz), number of protons. ^{13}C NMR data are reported using chemical shift. In addition to 1D NMR experiments, 2D NMR techniques such as homonuclear correlation spectroscopy (COSY), heteronuclear single quantum coherence (HSQC),

heteronuclear multiple bond coherence (HMBC), and nuclear Overhauser effect spectroscopy (1D NOE and NOESY) were used to assist structure elucidation.

IR Spectroscopy

IR spectra were recorded on a Bruker Alpha FT-IR spectrophotometer using a diamond attenuated total reflectance (ATR) accessory. Samples were applied as a solution in a volatile solvent and the data were acquired after the solvent had evaporated. Only select transmission signals are reported and are given by frequency of absorption (cm^{-1}).

Mass Spectrometry

High resolution mass spectra were recorded on an LTQ-FT instrument at the QB3/Chemistry Mass Spectrometry Facility at UC Berkeley.

Optical Rotation

Optical rotation values were recorded on a Perkin-Elmer 241 polarimeter using the Na D-line (path length = 1 dm, cell volume = 1 mL). The specific rotation is calculated according to the following equation where α represents the observed optical rotation, c represents the concentration of the analyte (10 mg/mL) and d represents the length of the cuvette (dm):

$$[\alpha]_D^T = \frac{\alpha \; x \; 100}{c \; x \; d}$$

Thus, the specific rotation is given in 10^{-1}·deg·cm^2·g^{-1}.

Computational Details

Geometry optimizations were carried out with the Gaussian 16 software[26] and the ωB97XD(SMD, solvent=acetic acid)/def2-SVP level of theory.[27] Potential energy surface (PES) minima and transition state structures (TSS) were identified by the number of imaginary frequencies obtained in frequency calculations conducted at the same level, with 0 for minima and 1 for TSSs. The Cartesian coordinates for each structure are listed in Appendix 2C.

2.7.2 Synthetic Procedures and Product Characterization

Initial route to key step precursor 19b

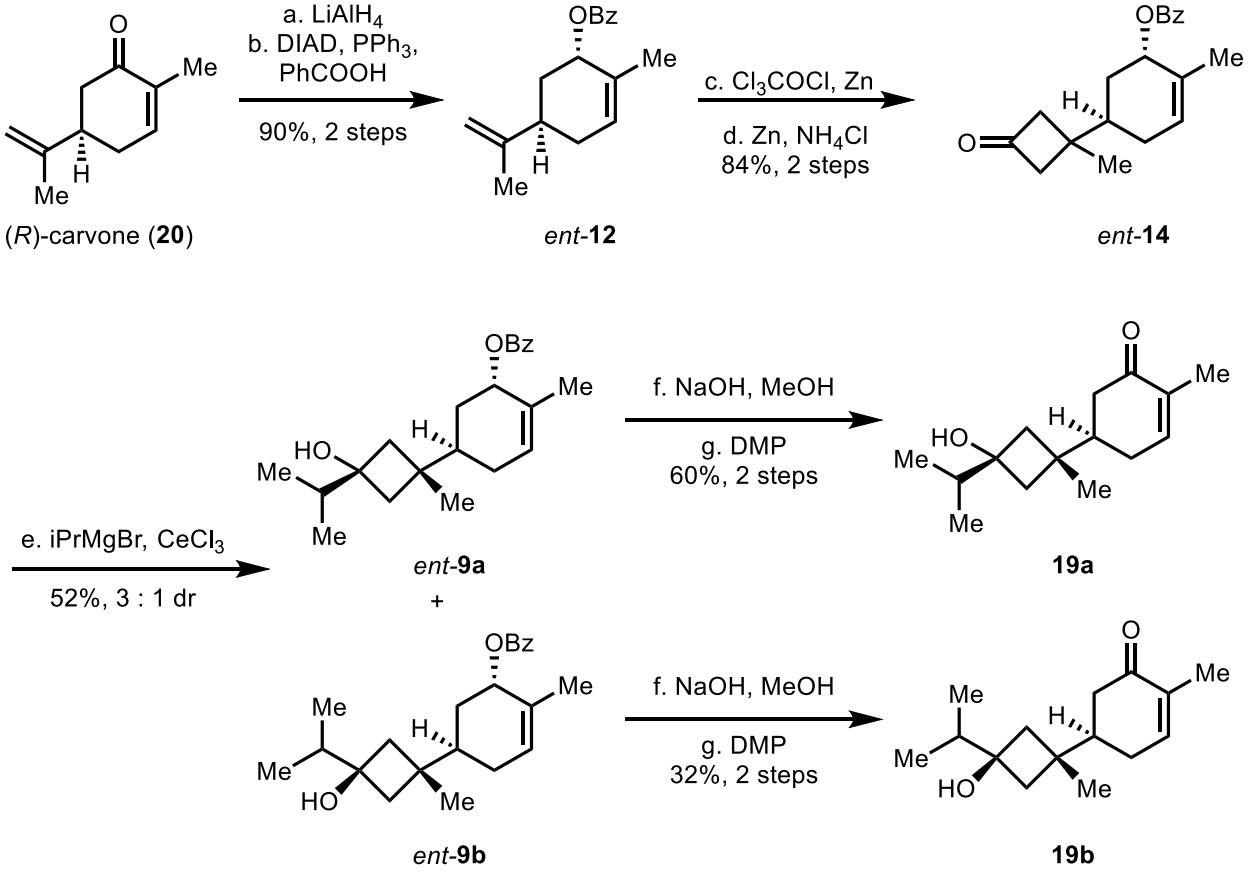

*Synthesis of cis-carveol (ent-**11**)*

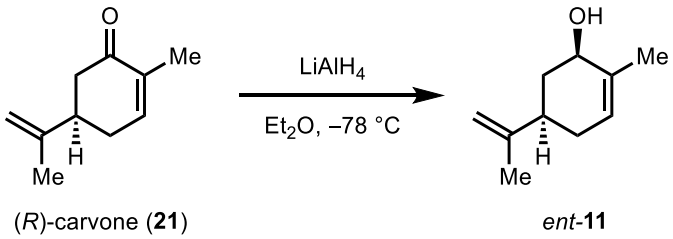

This procedure was adapted from a literature procedure by Labadie et al.[11] A three-necked 500 mL round-bottomed flask with an internal temperature monitor was charged with a solution of (*R*)-carvone (13.5 g, 90.0 mmol, 1.0 equiv) in Et_2O (240 mL, 0.38M) and cooled to –78 ºC. Lithium aluminum hydride (3.76 g, 99.1 mmol, 1.1 equiv) was subsequently added in six portions at –78 ºC. After continued stirring at –78 ºC for two h, the reaction mixture was warmed to 0 ºC and sequentially diluted with H_2O (3.8 mL), 15% $NaOH_{(aq)}$ (7.8 mL), and H_2O (11 mL) under Fieser–Fieser work-up conditions,[31] thereby quenching excess lithium aluminum hydride. After 15 minutes, the reaction mixture was dried over $MgSO_4$. After an additional 15 minutes of stirring, the crude mixture was filtered over cotton and the resulting filtrate was concentrated *in vacuo* to

give cis-carveol (*ent*-**11**) (13.5 g, 88.7 mmol, 99%) as a clear oil. The characterization data for *ent*-**11** were in full agreement with values previously reported.[11]

*Synthesis of trans-benzoylcarveol (ent-**12**)*

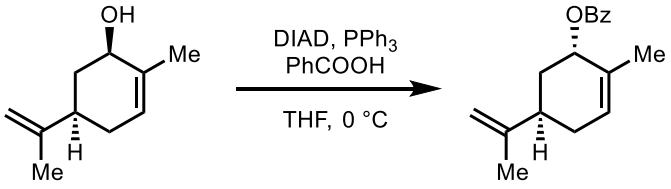

ent-**11** *ent*-**12**

This preparation was adapted from a literature procedure by Genet et al.[12] Cis-carveol (*ent*-**11**) (13.5 g, 88.7 mmol, 1.0 equiv), triphenylphosphine (34.9 g, 133 mmol, 1.5 equiv), and benzoic acid (16.2 g, 133 mmol, 1.5 equiv) were dissolved in THF (0.3 M, 300 mL) and the resulting solution was cooled to 0 ºC. Diisopropyl azodicarboxylate (26.2 mL, 133 mmol, 1.5 equiv) was added dropwise over 15 minutes and the solution was allowed to continue to stir at 0 ºC until TLC analysis indicated complete consumption of **11** (typically overnight). The mixture was concentrated *in vacuo* to give a yellow oil, which was dissolved in EtOAc (16 mL). Hexanes (140 mL) were added and the mixture was sonicated (VWR™ International, model 75D) for 5 minutes to precipitate by-product triphenylphosphine oxide. The suspension was filtered over a pad of celite and the filtrate was concentrated *in vacuo* and the resulting residue was purified by flash column chromatography (9% EtOAc in hexanes) to give *ent*-**12** as a yellow oil (21.0 g, 82.1 mmol, 91%). The characterization data for *ent*-**12** were in full agreement with values previously reported.[12]

*Synthesis of dichlorocyclobutanone ent-**13***

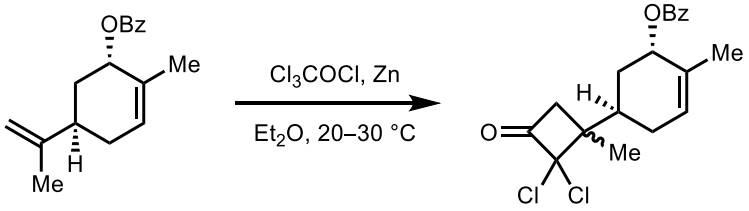

ent-**12** *ent*-**13**

A round-bottomed flask was charged with benzoylcarveol *ent*-**12** (21.0 g, 82.1 mmol, 1.0 equiv) and zinc dust (32.2 g, 493 mmol, 6.0 equiv), which were suspended in Et_2O (200 mL, 0.2 M) at room temperature. A solution of trichloroacetyl chloride (41.2 mL, 369 mmol, 4.5 equiv) in Et_2O (160 mL, 2.25 M with respect to trichloroacetyl chloride) was added dropwise over 2 h (by syringe pump) to the suspension. Throughout the addition, the reaction mixture was sonicated (Bransonic® model 2510R-DTH, Output: 42 kHz) with overhead stirring while the bath temperature was maintained between 20 and 30 ºC. The heterogeneous solution was sonicated with continued stirring for an additional 3 h after addition was complete. The crude mixture was filtered

over a pad of celite and the resulting organic filtrate was sequentially washed with H_2O (500 mL), saturated solution of $NaHCO_{3(aq)}$ (300 mL), and brine (300 mL). The washed organic layer was dried over $MgSO_4$. The dried solution was filtered and the resulting filtrate was concentrated *in vacuo* to give a brown residue. The residue was purified by flash column chromatography (9% EtOAc in hexanes) to give dichlorocyclobutanone **13** (29.3 g, 79.8 mmol, 97%, 1.2:1 dr) as a yellow oil. Non-quantitative chromatography was used to obtain an analytical sample as a 4:1 mixture of diastereomers.

Note: Pursuing the same reaction under sonication with 35 kHz output resulted in significantly lower yield (67%, 20.0 mmol scale).

In cases where the proton or carbon resonances show a distinct double set of signals, the signal of the second diastereomer is marked with an asterisk.

TLC (9% EtOAc in hexanes): R_f = 0.30 (UV/*p*-anisaldehyde)

^{1}H NMR (600 MHz, $CDCl_3$) δ 8.09 – 8.03 (m, 2H), 7.58* (dd, *J* = 7.5, 7.5 Hz, 1H), 7.54 (dd, *J* = 7.4, 7.4 Hz, 1H), 7.46* (dd, *J* = 7.6, 7.6 Hz, 2H), 7.42 (dd, *J* = 7.7, 7.7 Hz, 2H), 5.83 – 5.79 (m, 1H), 5.55 – 5.51 (m, 1H), 3.30 (d, *J* = 16.6 Hz, 1H), 3.15* (d, *J* = 16.5 Hz, 1H), 2.76 – 2.69 (m, 2H), 2.72 – 2.66* (m, 2H), 2.56* (dddd, *J* = 11.9, 11.9, 4.1, 4.1 Hz, 1H), 2.36* (ddd, *J* = 17.4, 4.9, 4.9 Hz, 1H), 2.19 – 2.13 (m, 1H), 2.08 – 2.02* (m, 1H), 2.02 – 1.96 (m, 2H), 1.81 – 1.75 (m, 3H), 1.75 – 1.67 (m, 1H), 1.25 (s, 3H), 1.23* (s, 3H).

IR (ATR, thin film): 2968, 2937, 1805, 1710, 1265, 762 cm^{-1}.

HRMS (EI+) m/z calc'd for $C_{19}H_{20}O_3Cl_2$ $[M]^+$: 366.0790, found: 366.0787.

*Note: Full characterization data reported above for dichlorocyclobutanone **13** were obtained from a sample synthesized from (S)-carvone. ^{1}H NMR spectra were identical to the enantiomer synthesized from (R)-carvone and no further characterization data were obtained.*

*Synthesis of cyclobutanone ent-**14***

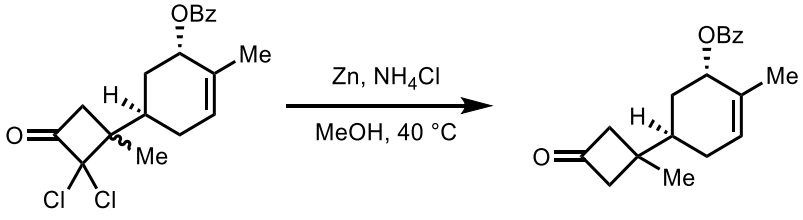

ent-**13** *ent*-**14**

Dichlorocyclobutanone *ent*-**13** (9.00 g, 24.5 mmol, 1.0 equiv) and zinc dust (6.40 g, 98.0 mmol, 4.0 equiv) were suspended in a solution of saturated NH_4Cl in MeOH (190 mL, 0.13 M). The resulting suspension was heated to 40 ºC and held at this temperature with continued stirring until TLC analysis indicated complete consumption of *ent*-**13** (typically overnight). The crude mixture was filtered over a pad of celite and the resulting filtrate was concentrated *in vacuo.* The resulting yellow solid was dissolved in EtOAc (750 mL) and H_2O (750 mL), and the separated aqueous

layer was extracted with EtOAc (3 x 300 mL). The combined organic extracts were washed sequentially with saturated solution of $NaHCO_{3(aq)}$ (300 mL) and brine (300 mL). The washed organic layer was dried over $MgSO_4$. The dried solution was filtered and the resulting filtrate was concentrated *in vacuo* to give cyclobutanone *ent*-**14** (6.38 g, 21.4 mmol 87%) as a clear oil.

TLC (33% EtOAc in hexanes): R_f = 0.55 (UV/*p*-anisaldehyde)

^{1}H NMR (600 MHz, $CDCl_3$) δ 8.04 (d, dd, *J* = 8.2 Hz 2H), 7.56 (dd, *J* = 7.4, 7.4 Hz, 1H), 7.44 (dd, *J* = 7.8, 7.8 Hz, 2H), 5.83 – 5.79 (m, 1H), 5.55 – 5.52 (m, 1H), 2.95 – 2.89 (m, 1H), 2.81 – 2.75 (m, 1H), 2.70 – 2.63 (m, 2H), 2.19 – 2.12 (m, 1H), 1.99 – 1.87 (m, 3H), 1.75 (s, 3H), 1.69 – 1.62 (m, 1H), 1.20 (s, 3H).

^{13}C NMR (150 MHz, $CDCl_3$) δ 207.7, 166.5, 133.1, 131.5, 130.6, 129.7, 128.6, 127.8, 127.8, 71.3, 57.8, 57.2, 38.4, 31.6, 31.1, 27.2, 21.6, 20.9.

IR (ATR, thin film): = 2962, 1780, 1713, 1267, 1109, 714 cm^{-1}.

HRMS (EI+) m/z calc'd for $C_{19}H_{22}O_3$ $[M]^+$: 298.1563, found: 298.1565.

$[\alpha]_D^{20}$ = –104° (c = 0.65, $CHCl_3$)

Synthesis of cyclobutanol 19a and 19b

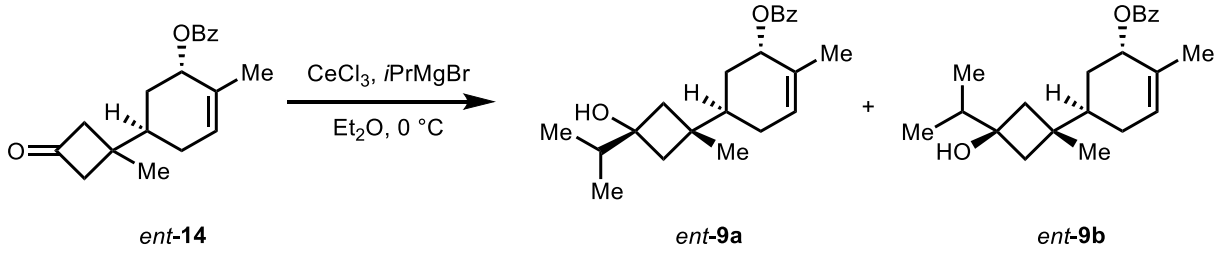

ent-**14** *ent*-**9a** *ent*-**9b**

A flame-dried flask was charged with anhydrous cerium (III) chloride (5.78 g, 23.5 mmol, 1.75 equiv) and cyclobutanone *ent*-**14** (3.90 g, 13.4 mmol, 1.0 equiv) in THF (24 mL, 0.2 M) and the resulting mixture was stirred at room temperature. After 1 h, the suspension was cooled to 0 ºC and isopropyl magnesium bromide (23.5 mL, 1.0 M in THF, 23.5 mmol, 1.75 equiv) was added dropwise over 30 minutes. The reaction mixture was stirred at 0 °C until TLC analysis indicated full consumption of cyclobutanone *ent*-**14** (typically 1–2 h). Excess Grignard reagent was carefully quenched with the addition of saturated $NH_4Cl_{(aq)}$ (20 mL) at 0 °C. The resulting mixture was diluted with Et_2O (50 mL) and water (50 mL), and allowed to stir at room temperature. After 15 minutes, the layers were separated and the aqueous layer was extracted with Et_2O (2 x 50 mL). The combined organic extracts were sequentially washed with a saturated solution of $NaHCO_{3(aq)}$ (30 mL) and brine (30 mL). The washed organic layer was dried over $MgSO_4$. The dried solution was filtered and the resulting filtrate was concentrated *in vacuo* to give a clear oil. The crude residue was purified by flash column chromatography (9% EtOAc in hexanes) to give, in order of elution, cyclobutanol **19b** (605 mg, 1.77 mmol, 13%) as a white solid and cyclobutanol **19a** (1.79 g, 5.23 mmol, 39%) as a clear oil. The relative stereochemistry was determined by 2D NOESY

experiments of cyclohexenones **19a** and **19b** (elaborated from cyclobutanols *ent*-**9a** and *ent*-**9b** respectively).

Characterization data for cyclobutanol *ent*-**9a**

TLC (9% EtOAc in hexanes): R_f = 0.18 (UV/*p*-anisaldehyde)

^{1}H NMR (400 MHz, $CDCl_3$) δ 8.06 (d, *J* = 7.0 Hz, 2H), 7.57 (dd, *J* = 7.4, 7.4 Hz, 1H), 7.45 (dd, *J* = 7.7, 7.7 Hz, 2H), 5.82 – 5.78 (m, 1H), 5.52 – 5.48 (m, 1H), 2.09 – 2.00 (m, 1H), 1.98 – 1.92 (m, 1H), 1.87 – 1.81 (m, 1H), 1.81 – 1.76 (m, 1H), 1.74 – 1.72 (m, 5H), 1.68 – 1.60 (m, 2H), 1.60 – 1.52 (m, 1H), 1.52 – 1.41 (m, 1H), 1.32 (br s, 1H), 1.15 (s, 3H), 0.82 (d, *J* = 6.8 Hz, 3H), 0.75 (d, *J* = 6.8 Hz, 3H).

^{13}C NMR (175 MHz, $CDCl_3$) δ 166.6, 133.0, 131.3, 130.9, 129.7, 128.7, 128.5, 73.8, 71.9, 45.0, 44.3, 39.5, 38.5, 31.5, 30.2, 26.2, 22.8, 20.9, 15.3, 15.2.

IR (ATR, thin film): 3517 (br.), 2958, 2927, 1714, 1267, 711 cm^{-1}.

HRMS (EI+) m/z calc'd for $C_{22}H_{30}O_3$ $[M]^+$: 342.2195, found: 342.2196.

$[\alpha]_D^{20}$ = +97° (c = 1.04, $CHCl_3$)

Characterization data for cyclobutanol *ent*-**9b**

TLC (9% EtOAc in hexanes): R_f = 0.37 (UV/*p*-anisaldehyde)

^{1}H NMR (600 MHz, $CDCl_3$) δ 8.07 (d, *J* = 7.7 Hz, 2H), 7.55 (dd, *J* = 7.4, 7.4 Hz, 1H), 7.44 (dd, *J* = 7.7, 7.7 Hz, 2H), 5.84 – 5.77 (m, 1H), 5.53 – 5.48 (m, 1H), 2.17 – 2.09 (m, 1H), 2.07 – 1.99 (m, 1H), 1.96 – 1.92 (m, 1H), 1.92 – 1.89 (m, 1H), 1.88 – 1.82 (m, 2H), 1.78 – 1.70 (m, 5H), 1.69 (hept, *J* = 6.8 Hz, 1H), 1.48 (ddd, *J* = 13.8, 13.7, 4.0 Hz, 1H), 0.95 (s, 3H), 0.85 (d, *J* = 6.8 Hz, 3H), 0.82 (d, *J* = 6.8 Hz, 3H).

^{13}C NMR (150 MHz, $CDCl_3$) δ 166.7, 132.9, 131.2, 130.9, 129.8, 128.7, 128.5, 72.9, 71.9, 45.6, 44.6, 39.4, 38.1, 30.1, 30.0, 26.1, 22.9, 20.9, 15.2, 15.1.

IR (ATR, thin film): 2967, 2917, 1714, 1269, 712 cm^{-1}.

HRMS (ESI+) m/z calc'd for $C_{22}H_{30}O_3Na$ $[M+Na]^+$: 365.2087, found: 365.2091.

$[\alpha]_D^{20}$ = +118° (c = 0.51, $CHCl_3$)

*Note: Full characterization data reported above for **9a** and **9b** were obtained from samples synthesized from (S)-carvone, ^{1}H NMR spectra were identical when starting from (R)-carvone and no further characterization data were obtained.*

Synthesis of cyclohexenone 19a

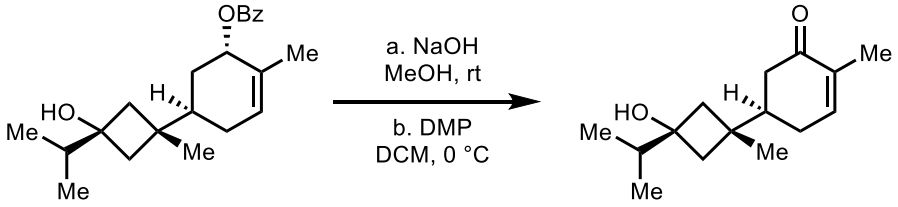

ent-**9a** **19a**

Cyclobutanol *ent*-**9a** (1.30 g, 3.80 mmol, 1.0 equiv) was dissolved in a solution of NaOH (1.52 g, 38.0 mmol, 10 equiv) in MeOH (38 mL, 0.1 M) and the resulting mixture was stirred at room temperature. After 14 h, the mixture was concentrated *in vacuo* and the resulting white solid was dissolved in EtOAc (100 mL) and H_2O (100 mL). The layers were separated and the aqueous layer was extracted with EtOAc (2 x 100 mL). The combined organic extracts were dried over $MgSO_4$. The dried solution was filtered and the resulting filtrate was concentrated *in vacuo*.

The resulting crude allyl alcohol (presumed 3.80 mmol) was dissolved in DCM (10 mL, 0.30 M) and the resulting solution was cooled to 0 °C. The solution was charged with Dess–Martin Periodinane (2.42 g, 5.69 mmol, 1.5 equiv) and the resulting mixture was stirred and held at 0 °C. After 2 h, the reaction mixture was diluted with DCM (10 mL), saturated solution of $Na_2S_2O_{3(aq)}$ (5 mL), and saturated solution of $NaHCO_{3(aq)}$ (5 mL) and warmed to room temperature. After stirring at room temperature for 20 minutes, the layers were separated and the aqueous layer was extracted with DCM (3 x 50 mL). The combined organic extracts were sequentially washed with H_2O (50 mL) and brine (50 mL). The washed organic layer was dried over $MgSO_4$. The dried solution was filtered and the resulting filtrate was concentrated *in vacuo* to give an off-white solid, which was purified by flash column chromatography (10% to 30 % EtOAc in hexanes) to give cyclohexenone **19a** (535 mg, 2.26 mmol, 60%) as a white crystalline solid. The relative configuration of the cyclobutanol was assigned by 2D NOESY experiments.

TLC (20% EtOAc in hexanes): R_f = 0.29 (UV/*p*-anisaldehyde)

^{1}H NMR (700 MHz, $CDCl_3$) δ 6.79 – 6.73 (m, 1H), 2.39 – 2.33 (m, 1H), 2.26 – 2.18 (m, 1H), 2.13 – 2.07 (m, 1H), 2.07 – 2.02 (m, 1H), 1.97 – 1.91 (m, 1H), 1.93 – 1.86 (m, 2H), 1.77 (s, 3H), 1.74 – 1.66 (m, 2H), 1.54 (d, *J* = 6.8 Hz, 1H), 1.35 (s, 1H), 1.21 (s, 3H), 0.82 (d, *J* = 6.6 Hz, 6H).

^{13}C NMR (150 MHz, $CDCl_3$) δ 200.7, 145.3, 135.5, 73.7, 46.5, 44.5, 44.1, 39.6, 38.7, 31.8, 27.1, 22.7, 15.8, 15.1, 15.1.

IR (ATR, thin film): 3477 (br.), 2957, 2922, 1671, 1451, 1246 cm^{-1}.

HRMS (EI+) m/z calc'd for $C_{15}H_{24}O_2$ $[M]^+$: 236.1771, found: 236.1774.

$[\alpha]_D^{20}$ = +8.2° (c = 0.64, $CHCl_3$)

mp: 61 – 70 °C

Synthesis of cyclohexenone 19b

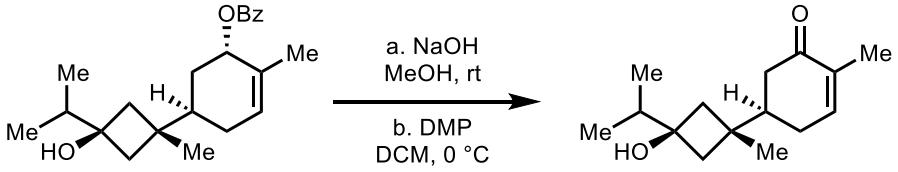

ent-**9b** **19b**

Following the procedure for the synthesis of cyclohexanone **19a** (Section 2.1.6)**,** cyclohexenone **19b** (epimer of **19a**) was obtained (219 mg, 0.927 mmol, 32%) as a white crystalline solid from cyclobutanol *ent*-**9b** (999 mg, 2.92 mmol). The relative configuration of the cyclobutanol was assigned by 2D NOESY experiments.

TLC (20% EtOAc in hexanes): R_f = 0.29 (UV/*p*-anisaldehyde)

^{1}H NMR (600 MHz, $CDCl_3$) δ 6.77 (m, 1H), 2.44 (m, 1H), 2.36 – 2.28 (m, 2H), 2.12 – 2.01 (m, 2H), 1.91 – 1.81 (m, 4H), 1.76 (s, 3H), 1.69 (hept, *J* = 6.8 Hz, 1H), 1.63 – 1.36 (br s, 1H), 0.99 (s, 3H), 0.85 (d, *J* = 6.8 Hz, 6H).

^{13}C NMR (150 MHz, $CDCl_3$) δ 200.7, 145.4, 135.5, 73.0, 45.7, 44.7, 44.2, 39.4, 38.2, 30.7, 27.0, 23.0, 15.8, 15.2, 15.1.

IR (ATR, thin film): 3487 (br.), 2959, 2923, 1665, 1366 cm^{-1}.

HRMS (EI+) m/z calc'd for $C_{15}H_{24}O_2$ $[M]^+$: 236.1771, found: 236.1772

$[\alpha]_D^{20}$ = +8.6° (c = 0.44, $CHCl_3$)

mp: 98 – 101 °C

Shortened synthesis of key step precursor 9 and 9'

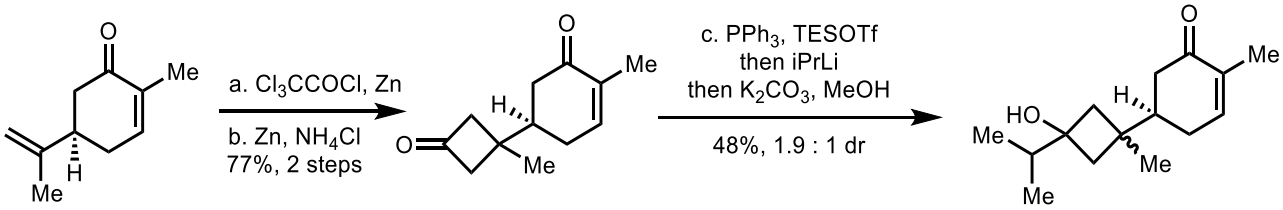

(*R*)-carvone (**20**) **22** **19a** and **19b**

Synthesis of dichlorocyclobutanone SI-1

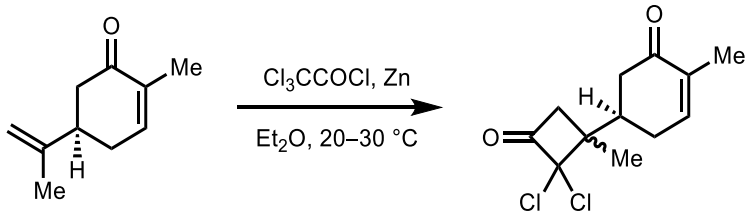

(*R*)-carvone (**20**) **SI-1**

This preparation was adapted from a procedure by Dowd et al.[21a] A round-bottomed flask was charged with (*R*)-carvone (6.31 mL, 40.0 mmol, 1.0 equiv) and zinc dust (15.7 g, 240 mmol, 6.0 equiv) which were suspended in Et_2O (200 mL, 0.2 M) at room temperature. A solution of trichloroacetyl chloride (20.1 mL, 180 mmol, 4.5 equiv) in Et_2O (80 mL, 2.25 M with respect to trichloroacetyl chloride) was added via cannula to the suspension over 1 h. Throughout the addition, the reaction mixture was sonicated (Bransonic® model 2510R-DTH, Output: 42 kHz) with overhead stirring while the bath temperature was maintained between 20 and 30 ºC. After addition of trichloroacetyl chloride, the heterogeneous solution was sonicated with continued stirring for an additional 3 h. The crude mixture was filtered over a pad of celite and the resulting organic filtrate was sequentially washed with H_2O (500 mL), saturated solution of $NaHCO_{3(aq)}$ (300 mL), and brine (300 mL). The washed organic layer was dried over $MgSO_4$. The dried solution was filtered and the resulting filtrate was concentrated *in vacuo* to give a brown residue. The residue was purified by flash column chromatography (11% to 20% EtOAc in hexanes) to give dichlorocyclobutanone **SI-1** (7.70 g, 29.5 mmol, 74%, 1.7:1) as a yellow solid. The characterization data for **SI-1** were in full agreement with values previously reported.[21a]

Note: Pursuing the same reaction using a sonicator with a 35 kHz output resulted in significantly lower yield (56%, 7.0 mmol scale).

Note: Depending on the source of the Zn dust, we found some batches required activation with HCl immediately prior to use.

Synthesis of cyclobutanone 11

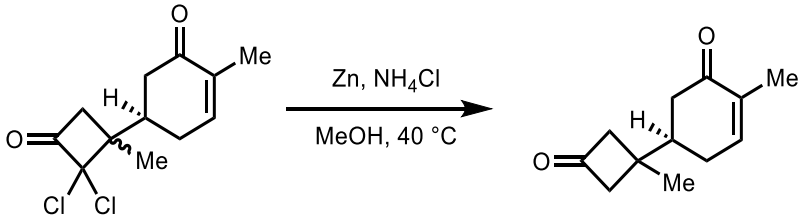

SI-1 **22**

Dichlorocyclobutanone **SI-1** (7.70 g, 29.5 mmol, 1.0 equiv) and zinc dust (7.72 g, 118 mmol, 4.0 equiv) were suspended in a solution of saturated NH_4Cl in MeOH (225 mL, 0.13 M). The resulting suspension was heated to 40 ºC and held at this temperature with continued stirring until ^1H NMR analysis indicated full consumption of **SI-1** and the monochlorinated intermediate (typically 3–4

h). The crude mixture was filtered over a pad of celite and the resulting filtrate was concentrated *in vacuo*. The resulting yellow solid was dissolved in EtOAc (1 L) and H_2O (400 mL). The resulting heterogeneous mixture was filtered over a pad of celite (rinsed with 2 x 200 mL EtOAc) and the layers were separated. The aqueous layer was extracted with EtOAc (2 x 300 mL) and the combined organic extracts were washed sequentially with saturated solution of $NaHCO_{3(aq)}$ (300 mL) and brine (300 mL). The washed organic layer was dried over $MgSO_4$. The dried solution was filtered and the resulting filtrate was concentrated *in vacuo*. The resulting yellow solid was purified by flash column chromatography (20% EtOAc in hexanes) to give cyclobutanone **22** (4.58 g, 23.8 mmol, 78%) as an off-white amorphous solid.

TLC (33% EtOAc in hexanes): R_f = 0.45 (UV/*p*-anisaldehyde)

^{1}H NMR (500 MHz, $CDCl_3$) δ 6.79 – 6.76 (m, 1H), 2.94 – 2.85 (m, 2H), 2.73 – 2.65 (m, 2H), 2.50 – 2.43 (m, 1H), 2.38 – 2.16 (m, 4H), 1.77 (s, 3H), 1.24 (s, 3H).

^{13}C NMR (125 MHz, $CDCl_3$) δ 206.3, 199.4, 144.4, 135.7, 57.3, 57.0, 44.9, 40.3, 31.7, 27.9, 21.7, 15.8.

IR (ATR, thin film): 2955, 2922, 1775, 1666, 1367, 1105 cm^{-1}.

HRMS (EI+) m/z calc'd for $C_{12}H_{16}O_2^+$ $[M]^+$: 192.1145, found: 192.1145.

$[\alpha]_D^{20}$ = –1.4° (c = 0.98, $CHCl_3$)

Synthesis of cyclobutanol 9 and 9'

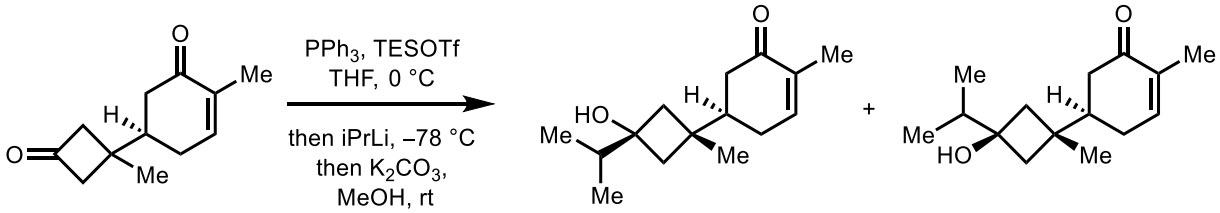

22 **19a** **19b**

This procedure was adapted from a similar literature preparation by Fujioka and co-workers.[22] Cyclobutanone **11** (1.12 g, 5.83 mmol, 1 equiv) and PPh_3 (2.30 g, 8.74 mmol, 1.5 equiv) were dissolved in THF (25 mL, 0.2 M) and the mixture was cooled to 0 ºC. Triethylsilyl triflate (1.98 mL, 8.74 mmol, 1.5 equiv) was added dropwise to the cooled solution and the reaction mixture was allowed to stir at 0 ºC. After 90 minutes, the reaction mixture was cooled to –78 ºC and isopropyl lithium (25 mL, 0.7 M in pentane, 17.5 mmol, 3.0 equiv) was added via cannula to the solution over 1 h with continued stirring at –78 ºC. After 4 h, MeOH (6 mL) was slowly added to the dark brown mixture (turned clear orange in appearance upon addition) and the resulting solution was gradually warmed to room temperature. A saturated solution of K_2CO_3 in MeOH (6 mL) was added and the reaction mixture was allowed to stir at room temperature. After 14 h, the cloudy orange mixture was diluted with EtOAc (200 mL) and H_2O (100 mL). The layers were separated and the aqueous layer was extracted with EtOAc (3 x 100 mL). The combined organic extracts were washed with brine (100 mL). The washed organic layer was dried over $MgSO_4$. The

dried solution was filtered and the resulting filtrate was concentrated *in vacuo* to give a crude yellow residue, which was purified by flash column chromatography (0 to 15% EtOAc in DCM) to give a mixture of cyclobutanols **19a** and **19b** (653 mg, 2.76 mmol, 48%, 1.9 : 1 **19a** : **19b**) as an off-white solid. Isolated samples of **19a** and **19b** could be obtained through non-quantitative chromatography and matched exactly with data collected from samples obtained through the initial route to these compounds.

Note: Pursuing the same reaction on larger scale (3.10 g, 16.0 mmol, 1 equiv) was effective although the product was obtained in lower yield (1.43 g, 6.05 mmol, 38%, 1.6 : 1 ***19a : 19b****).*

Optimization of the Pd-mediated cascade:

General procedure for screening of the Pd-mediated cascade reaction

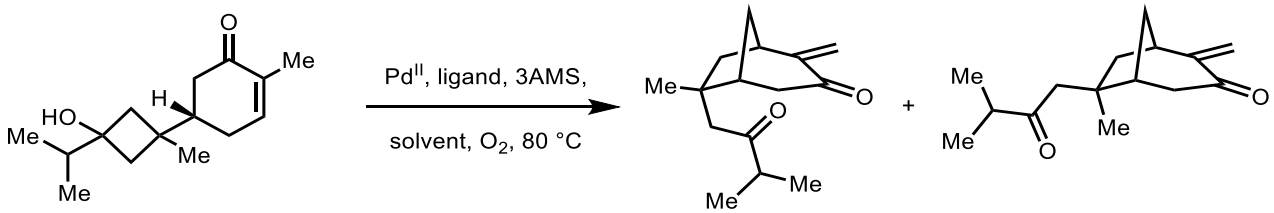

19a + 19b **18** **21**

Pre-activated 3ÅMS (2.6 mg, 300 mg/mmol) and the indicated additive (1.0 equiv) were massed into oven-dried 4 mL vials. To each vial was added a stock solution of Pd(II) (0.0042 mmol, 0.5 equiv) and ligand (0.0085 mmol, 1.0 equiv) in the chosen solvent (80 µL, 0.05 M) and the headspace of each vial was subsequently flushed with O_2. Cyclobutanol **9/9'** (2.0 mg, 0.0085 mmol, 1.0 equiv) was added to each vial as a solution in the indicated solvent (40 µL, 0.2 M) and the vials were placed in a heating block that had been preheated to the indicated reaction temperature. After 24 h (or the indicated reaction time), the individual reaction mixtures were filtered over a small pad of celite and the filtrate was concentrated *in vacuo*. NMR yield was determined by comparison to an internal standard of 1,3,5-trimethoxybenzene (0.47 mg, 0.0028 mmol, 0.33 equiv) added as a stock solution in $CDCl_3$. A selection of the variations and the results of these experiments are summarized below:

Note: Screening was an iterative process. On small scale some variability was observed within the error of the NMR yield. In all cases, a control reaction with the best previous result was run for a direct comparison in order to correct for any systematic variance from run to run.

Table 1. Selected conditions varying solvents and palladium sources for the Pd-mediated cascade reaction. Optimal conditions are highlighted in red. 1,2-DCE = 1,2-dichloroethane, DMF = N,N-dimethylformamide, DMSO = dimethylsulfoxide. Mesitylene was used as the internal standard for these runs.

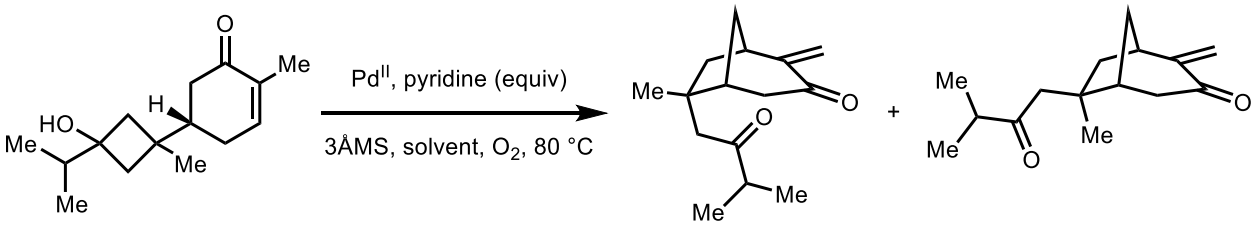

19a and **19b** **18** **21**

Pd (equiv)	pyridine (equiv)	solvent	NMR yield (%) 18	21
$Pd(OAc)_2$ (1.0)	2.0	toluene	1	1
$Pd(OAc)_2$ (1.0)	2.0	MeCN	1	2
$Pd(OAc)_2$ (1.0)	2.0	1,2-DCE	6	8
$Pd(OAc)_2$ (1.0)	2.0	PhH	3	3
$Pd(OAc)_2$ (1.0)	2.0	THF	1	1
$Pd(OAc)_2$ (1.0)	2.0	dioxane	3	3
$Pd(OAc)_2$ (0.5)	0.5	DMF	3	3
$Pd(OAc)_2$ (0.5)	0.5	DMSO	0	0
$Pd(OAc)_2$ (0.5)	0.5	*o*-dichlorobenzene	4	4
$Pd(OAc)_2$ (1.0)	2.0	1,2-DCE	6	8
$PdCl_2$ (1.0)	2.0	1,2-DCE	0	0
$PdBr_2$ (1.0)	2.0	1,2-DCE	0	0
PdI_2 (1.0)	2.0	1,2-DCE	0	0
$Pd(CN)_2$ (1.0)	2.0	1,2-DCE	0	0
$Pd(SO_4)_2$ (1.0)	2.0	1,2-DCE	0	0
Pd(dba) (1.0)	2.0	1,2-DCE	0	0
$Pd(acac)_2$ (1.0)	2.0	1,2-DCE	0	0
$Pd(MeCN)_4(BF_4)_2$ (1.0)	2.0	1,2-DCE	4	2

Note: In early screening, cyclobutanol **9** and cyclobutanol **9'** were found to give similar reactivity (**9** led to 48% combined yield while **9'** led to 46% without significant difference in diastereoselectivity**)**. In subsequent studies, a mixture of diastereomers **9** and **9'** was used in screening.

Table 2. Selected conditions varying ligands in the Pd-mediated cascade reaction. Optimal conditions are highlighted in red. *This reaction was conducted on larger scale (0.04 mmol).

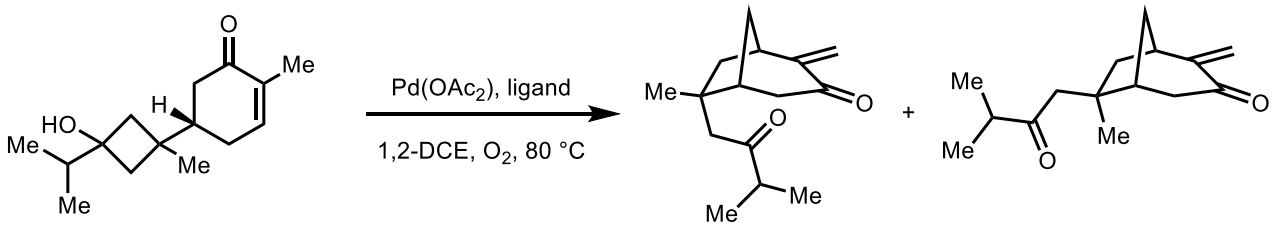

19a + 19b **18** **21**

$Pd(OAc)_2$ (equiv)	ligand (equiv)	NMR yield (%) 18	21
1.0	DMAP (2.0)	3	3
1.0	p-tBu pyridine (2.0)	1	1
1.0	pyridine (2.0)	9	13
1.0	p-CO_2Me pyridine (2.0)	8	9
1.0	2-picoline (2.0)	3	3
1.0	2,6-lutidine (2.0)	1	1
1.0	m-CO_2Me pyridine (2.0)	6	7
1.0	bipyridine (2.0)	0	0
1.0	p-OMe bipyridine (2.0)	0	0
1.0	phenanthroline (2.0)	0	0
1.0	4,5-diazafluoren-9-one (2.0)	2	2
1.0	PPh_3 (2.0)**	0	0
0.5	pyridine (1.0)	10	10
0.5	p-CF_3 pyridine (1.0)	10	12
0.5	p-CN pyridine (1.0)	6	7
0.5	m-CO_2Me pyridine (1.0)	9	10
0.5	o-CO_2Me pyridine (1.0)	4	5
0.5	DMAP (1.0)	2	2
0.5	2-Me pyridine (1.0)	5	6
0.5	2-Et pyridine (1.0)	3	4
0.5	2-pentyl pyridine (1.0)	4	5
0.5	2-benzyl pyridine (1.0)	0	0
0.5	2,6 lutidine (1.0)	5	7
0.5	2-Me, 6-OMe pyridine (1.0)	8	10
0.5	2,6-OMe pyridine (1.0)	0	0
0.5	quinoline (1.0)	6	6
0.5	3-CN quinoline (1.0)	7	8
0.5	5-NO_2 quinoline (1.0)	4	6
0.5	2-Me quinoline (1.0)	4	5
0.5	2-Me tetrahydroquinoline (1.0)	5	6
0.5	3-CO_2Me isoquinoline (1.0)	3	5
0.5	benzoquinoline (1.0)	0	0
0.5	phenanthridine (1.0)	4	4
0.5	acridine (1.0)	5	6

Table 3. Selected conditions varying equivalents of palladium and pyridine, reaction temperature, and reaction time for the Pd-mediated cascade reaction. Optimal conditions are highlighted in red. For entries where equivalents are indicated as 0.5 x *X*, the palladium/pyridine mixture was added in *X* aliquots every 60 minutes.

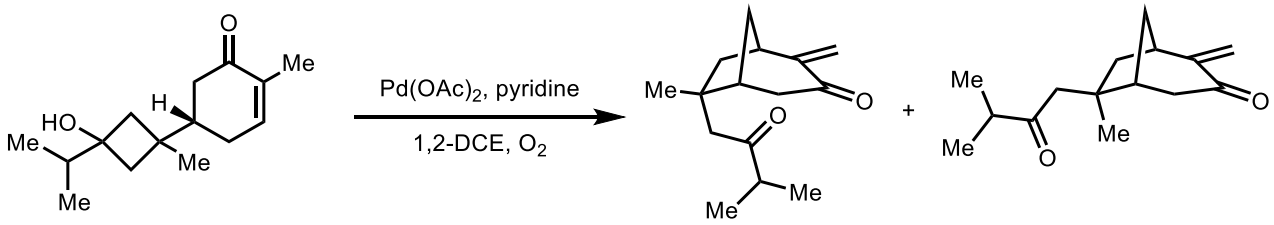

19a + 19b **18** **21**

$Pd(OAc)_2$ (equiv)	pyridine (equiv)	temperature (°C)	time	NMR yield (%) 18	21
1.0	0	80	2 hr	1	1
1.0	0.25	80	2 hr	21	29
1.0	0.5	80	2 hr	18	23
1.0	1.0	80	2 hr	27	33
1.0	2.0	80	2 hr	7	7
1.0	10	80	2 hr	0	0
1.0	20	80	2 hr	0	0
0.2	0.2	80	1 hr	5	6
0.5 x 2	0.5 x 2	80	2 hr	23	25
0.5 x 3	0.5 x 3	80	3 hr	22	26
0.5 x 4	0.5 x 4	80	4 hr	23	29
0.5 x 5	0.5 x 5	80	5 hr	19	21
0.5 x 6	0.5 x 6	80	6 hr	16	19
0.5	0.5	80	5 min	6	6
0.5	0.5	80	10 min	8	8
0.5	0.5	80	25 min	7	7
0.5	0.5	80	1 hr	13	12
0.5	0.5	80	2 hr	10	11
0.5	0.5	80	4 hr	11	12
0.5	0.5	rt	2 hr	0	0
0.5	0.5	65	2 hr	6	6
0.5	0.5	80	2 hr	13	13
0.5	0.5	100	2 hr	11	10

Table 4. Selected conditions varying additives in the Pd-mediated cascade reaction. Optimal conditions are highlighted in red. *denotes that the reaction was conducted without molecular sieves

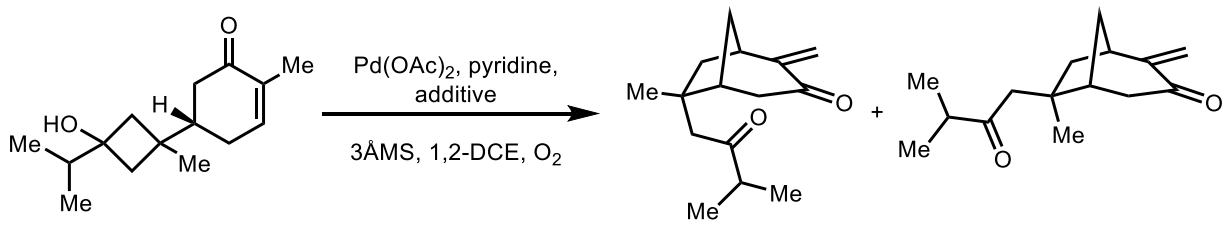

19a + 19b **18** **21**

$Pd(OAc)_2$ (equiv)	pyridine (equiv)	additive (1.0 equiv)	NMR yield (%) 18	21
1.0	1.0	none	23	25
1.0	1.0	Ag_2CO_3	24	27
1.0	1.0	$Na_2S_2O_8$	21	23
1.0	1.0	AcOH*	12	15
0.5	0.5	$CuCl_2$	0	0
0.5	0.5	$Cu(OTf)_2$	3	5
0.5	0.5	$Cu(OAc)_2$	9	13
0.5	0.5	CuCN	0	0
0.5	0.5	$CuBr_2$	0	0
0.5	0.5	ethyl acrylate	7	7
0.5	0.5	ethyl methacrylate	11	11
0.5	0.5	ethyl crotonate	11	10
0.5	0.5	Li_2CO_3	12	12
0.5	0.5	$NaCO_3$	8	8
0.5	0.5	Ag_2CO_3	12	12
0.5	0.5	Ac_2O	6	6
0.5	0.5	Ag(OAc)	7	8
0.5	0.5	Ag(OBz)	5	5
0.5	0.5	tBuOOH	9	9
0.5	0.5	dimethylbenzoquinone, Ag_2CO_3	7	7
1.0	none	$CsCO_3$	1	1
1.0	none	K_2CO_3	0	0
1.0	none	HOAc	1	1
1.0	none	Ac_2O	1	1
1.0	none	NaOAc	1	2
none	none	none	0	0

Scaled preparation and characterization of bicycle 18 and undesired epimer 21

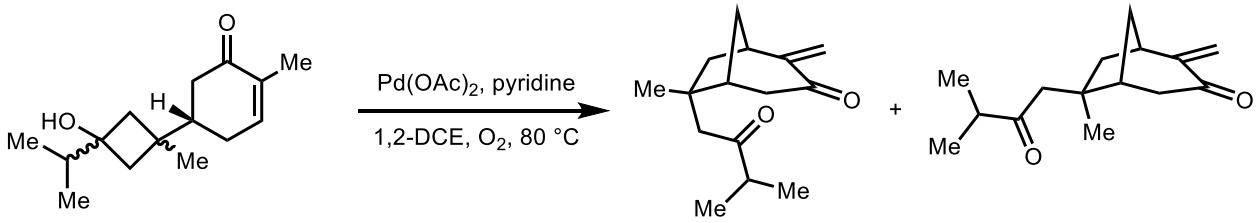

19a + 19b **18** **21**

$Pd(OAc)_2$ (1.33 g, 6.05 mmol, 1.0 equiv) and pyridine (0.47 mL, 6.1 mmol, 1.0 equiv) were suspended in 1,2-dichloromethane (20 mL, 0.3 M) under an O_2 atmosphere. In a separate flask, cyclobutanol **19a** and **19b** (1.43 g, 6.05 mmol, 1.0 equiv, 1.6 : 1 mixture of diastereomers) was dissolved in 1,2-dichloroethane (40 mL, 0.15 M) under an O_2 atmosphere and the resulting mixture was treated with the premixed Pd solution (10 mL). After addition, the reaction mixture was lowered into a preheated oil bath at 80 °C and stirred at that temperature. After 2 h, the reaction mixture was treated with the remaining Pd solution and continued to stir at 80 °C. After an additional 2 h, the reaction mixture was cooled to room temperature and filtered over a pad of celite. The resulting filtrate was concentrated *in vacuo* to give a brown oil which was purified by flash column chromatography (3% to 11% to 20% EtOAc in hexanes) to give, in order of elution, the desired bicycle 1**8** (311 mg, 1.33 mmol, 22%) as a clear oil, epimer **21** (322 mg, 1.37 mmol, 23%) as a clear oil, and recovered cyclobutanols 1**9a** and 1**9b** (226 mg, 0.956 mmol, 16%). The relative stereochemistry of the two epimers (**18** and **21**) was characterized by 2D NOESY experiments.

Characterization data for desired bicycle **18**

TLC (20% EtOAc in hexanes): R_f = 0.58 (UV/*p*-anisaldehyde)

^{1}H NMR (700 MHz, $CDCl_3$) δ 5.66 (d, *J* = 1.7 Hz, 1H), 4.99 (d, *J* = 1.6 Hz, 1H), 3.05 – 2.99 (m, 1H), 2.60 – 2.45 (m, 5H), 2.39 – 2.35 (m, 1H), 2.19 – 2.14 (m, 1H), 1.89 (dd, *J* = 14.0, 7.1 Hz, 1H), 1.80 – 1.75 (m, 1H), 1.45 (dd, *J* = 14.0, 1.7 Hz, 1H), 1.11 (s, 3H), 1.06 (d, *J* = 6.9 Hz, 3H), 1.05 (d, *J* = 6.9 Hz, 3H).

^{13}C NMR (150 MHz, $CDCl_3$) δ 213.9, 202.4, 151.9, 116.7, 49.6, 47.6, 45.7, 44.1, 42.9, 41.9, 41.5, 36.3, 29.0, 18.3, 18.2.

IR (ATR, thin film): 2960, 2936, 1707, 1693, 1048, 933 cm^{-1}.

HRMS (EI+) m/z calc'd for $C_{15}H_{22}O_2^+$ $[M]^+$: 234.1614, found: 234.1617.

$[\alpha]_D^{20}$ = +64° (c = 0.25, $CHCl_3$)

Characterization data for undesired bicycle **21**

TLC (20% EtOAc in hexanes): R_f = 0.46 (UV/*p*-anisaldehyde)

^{1}H NMR (600 MHz, $CDCl_3$) δ 5.74 (d, *J* = 1.8 Hz, 1H), 5.03 (d, *J* = 1.8 Hz, 1H), 3.04 – 2.97 (m, 1H), 2.73 (ddd, *J* = 18.5, 2.6, 2.6 Hz, 1H), 2.58 – 2.49 (m, 3H), 2.42 – 2.37 (m, 1H), 2.33 (dd, *J* = 18.5, 4.8 Hz, 1H), 2.06 – 2.01 (m, 1H), 1.98 (dd, *J* = 14.0, 7.0 Hz, 1H), 1.80 – 1.76 (m, 1H), 1.47 (dd, *J* = 14.0, 2.2 Hz, 1H), 1.09 (s, 3H), 1.05 (d, *J* = 6.9 Hz, 3H), 1.04 (d, *J* = 6.9 Hz, 3H).

^{13}C NMR (150 MHz, $CDCl_3$) δ 214.1, 201.7, 151.3, 117.8, 53.1, 47.9, 45.0, 43.3, 43.1, 42.1, 42.0, 36.8, 24.6, 18.2, 18.2.

IR (ATR, thin film): 2961, 2936, 1693, 1612, 1040, 938 cm^{-1}

HRMS (EI+) m/z calc'd for $C_{15}H_{22}O_2^+$ $[M]^+$: 234.1614, found: 234.1617.

$[\alpha]_D^{20}$ = +48° (c = 0.79, $CHCl_3$)

Building the tricyclic cores of allopupukeanane and pupukeanane

Synthesis of tricycle 12

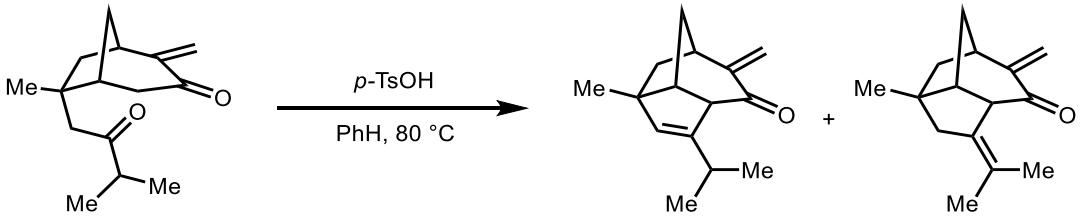

18 **23** **23'**

Bicyclic diketone **18** (280 mg, 1.19 mmol, 1 equiv) and *p*-toluenesulfonic acid monohydrate (227 mg, 1.19 mmol, 1 equiv) were suspended in PhH (12 mL, 0.1 M) in a 25 mL round-bottomed flask that was lowered into a preheated oil bath at 80 ºC and stirred at the same temperature. The reaction progress was monitored by TLC which first indicated the consumption of the bicyclic diketone **18** to give a mixture of compounds: TLC (5% EtOAc in hexanes): R_f = 0.13, 0.20. After approximately 15 minutes, the mixture converged to a single product as indicated by TLC analysis. The reaction mixture was cooled to room temperature and was diluted with a saturated solution of $NaHCO_{3(aq)}$ (5 mL), EtOAc (30 mL) and H_2O (30 mL). The layers were separated, and the aqueous layer was extracted with EtOAc (3 x 20 mL). The combined organic extracts were washed with brine (30 mL). The washed organic layer was dried over $MgSO_4$. The dried solution was filtered and the resulting filtrate was concentrated *in vacuo* to give an inseparable mixture of tricycles **23** and **23'** (260 mg, 1.8:1 **23**:**23'**) as a yellow oil. The compounds were used directly, without further purification.

In cases where the proton or carbon resonances show a double set of signals, the signal of the minor isomer is marked with an asterisk.

TLC (5% EtOAc in hexanes): R_f = 0.48 (UV/p-anisaldehyde)

^{1}H NMR (600 MHz, $CDCl_3$) δ 5.86 (d, J = 1.7 Hz, 1H), 5.78* (d, J = 1.8 Hz, 1H), 5.48 (s, 1H), 5.14 (d, J = 1.4 Hz, 1H), 5.02* (d, J = 1.6 Hz, 1H), 3.63 – 3.60* (m, 1H), 3.44 – 3.40 (m, 1H), 3.08 – 3.02 (m, 1H), 3.01 – 2.96* (m, 1H), 2.60 – 2.55 (m, 1H), 2.52 – 2.32 (m, 2H), 2.13 (hept, J = 6.0 Hz, 1H), 2.05 – 1.99* (m, 1H), 1.93 – 1.87* (m, 1H), 1.84* (s, 3H), 1.84 – 1.81* (m, 1H), 1.76 – 1.69 (m, 1H), 1.60 – 1.58* (m, 4H), 1.59* (m, 3H), 1.56 – 1.51 (m, 1H), 1.18* (s, 3H), 1.16 (s, 3H), 1.02 (t, J = 7.0 Hz, 3H), 1.00 (d, J = 6.8 Hz, 3H).

^{13}C NMR (150 MHz, $CDCl_3$) δ 200.4,* 199.7, 151.6,* 150.9, 146.1, 136.5, 132.4,* 128.5,* 120.2, 118.6,* 62.2, 58.2,* 53.6, 53.2,* 52.6,* 49.8,* 48.8, 48.0,* 47.2, 44.6, 42.4,* 32.6,* 31.8, 29.6,* 27.6, 27.1, 22.2,* 22.0,* 21.8, 20.9.

IR (ATR, thin film): 3489, 2948, 2867, 1706, 1461, 1375, 732 cm^{-1}

HRMS (EI+) m/z calc'd for $C_{15}H_{20}O^+$ $[M]^+$: 216.1509, found: 216.1514.

Synthesis of alcohol 13

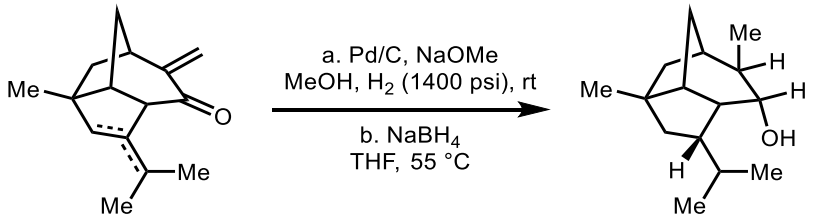

23 **24**

Tricycles **23** and **23'** (260 mg, 1.19 mmol, 1.0 equiv), NaOMe (2.38 mL, 0.5 M in MeOH, 1.19 mmol, 1.0 equiv), and 5% Pd/C (260 mg, 100 wt%) were suspended in MeOH (24 mL, 0.05 M) in a round-bottomed flask. The flask was placed in a high-pressure vessel which was subsequently pressurized to 1400 psi with H_2, and stirred at room temperature.

Note: Attempts to isolate the aliphatic ketone proceeded in extremely low yield, and the compound was observed to be quite volatile. For this reason, a procedure was developed to reduce the ketone to the corresponding alcohol directly without isolation or evaporation.

After 48 h, the reaction mixture was filtered over a pad of celite and rinsed with dry THF (24 mL, 0.05M) directly into a round-bottomed flask. The filtrate was treated with $NaBH_4$ (226 mg, 5.97 mmol, 5.0 equiv) and the resulting reaction mixture was lowered into an oil bath preheated to 55 °C and stirred at that temperature. After 2 h, additional $NaBH_4$ (226 mg, 5.97 mmol, 5.0 equiv) was added to the suspension and the reaction mixture was allowed to stir at 55 °C (repeated 3x, a total of 5 aliquots added every 2 h). After 14 h post final addition of $NaBH_4$, the reaction mixture was cooled to room temperature and diluted with EtOAc (50 mL) and H_2O (50 mL). The layers were separated, and the aqueous layer was washed with EtOAc (3 x 40 mL). The combined organic extracts were washed with brine (30 mL). The washed organic layer was dried over $MgSO_4$. The dried solution was filtered and the resulting filtrate was concentrated *in vacuo*. The resulting oil was purified by flash column chromatography (0 to 11% EtOAc in hexanes) to give alcohol **13** (86

mg, 0.39 mmol, 32%) as a clear oil. A mixture of other compounds assumed to be diastereomers of alcohol **24** based on preliminary ^{1}H NMR analysis were also isolated as an inseparable mixture (<10% combined). The ^{13}C NMR spectrum matches the previously reported spectrum by Ho et al.[4a] While no image of an ^{1}H NMR spectrum has been published, the ^{1}H NMR spectra that we obtained are in good agreement with the tabulated data.

TLC (5% EtOAc in hexanes): R_f = 0.48 (CAM)

^{1}H NMR (600 MHz, $CDCl_3$) δ 3.53 (dd, *J* = 10.4, 8.0 Hz, 1H), 2.63 – 2.57 (m, 1H), 2.04 (dh, *J* = 10.7, 6.4 Hz, 1H), 1.94 – 1.90 (m, 1H), 1.86 – 1.81 (m, 1H), 1.81 – 1.78 (m, 1H), 1.72 – 1.67 (m, 1H), 1.59 – 1.42 (m, 4H), 1.32 (s, 1H), 1.28 (dd, *J* = 12.0, 5.1 Hz, 1H), 1.12 – 1.08 (m, 1H), 1.07 (s, 3H), 1.05 (d, *J* = 6.4 Hz, 3H), 1.00 (d, *J* = 6.7 Hz, 3H), 0.83 (d, *J* = 6.5 Hz, 3H).

^{13}C NMR (150 MHz, $CDCl_3$) δ 77.0, 54.0, 53.3, 51.1, 47.5, 46.3, 45.9, 43.6, 42.9, 30.8, 30.6, 28.0, 23.7, 23.5, 22.3.

IR (ATR, thin film): 3494, 2917, 2865, 1463, 1035 cm^{-1}

HRMS (EI+) m/z calc'd for $C_{15}H_{26}O^{+}$ $[M]^{+}$: 222.1978, found: 222.1980.

$[\alpha]_D^{20}$ = – 22° (c = 0.51, $CHCl_3$)

Synthesis of allopupukeanene 17

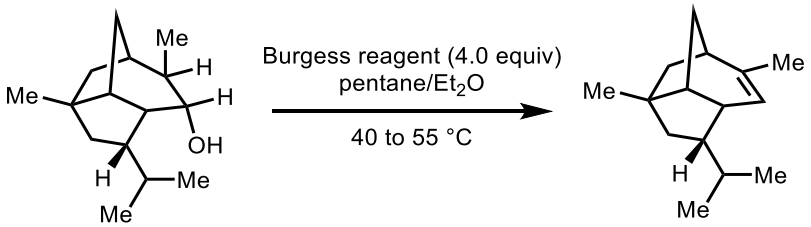

24 **17**

Alcohol **24** (29 mg, 0.13 mmol, 1.0 equiv) and Burgess reagent (124 mg, 0.52 mmol, 4.0 equiv) were suspended in a 1:1 mixture of pentane:ether (0.1 M) in a crimp-top sealed 20 mL vial which was heated to 55 °C with stirring. After 8 h, the reaction mixture was cooled to 40 °C, and stirred at this temperature overnight. After 14 h, the reaction vessel was cooled to room temperature, and a second portion of Burgess reagent (62 mg, 0.26 mmol, 2.0 equiv) were added. The vial was resealed and heated to 55 °C with stirring. After 6 h, the crude reaction mixture was loaded onto a plug of silica and eluted with 90 : 10 pentane ether. The organic filtrate was concentrated *in vacuo* at 0 °C to give allopupukeanene 1**7** as a clear oil (13 mg, 0.06 mmol, 48%) without further purification.

Note: The product was quite volatile and could not be recovered efficiently from $CDCl_3$. A small aliquot was used for HRMS, ^{1}H NMR, and ^{13}C NMR analysis to confirm the identity of the product, which matched the previously reported spectrum by Ho et al. No further characterization data was obtained.

^{1}H NMR (600 MHz, $CDCl_3$) δ 5.05 – 5.02 (m, 1H), 2.68 – 2.62 (m, 1H), 2.13 – 2.09 (m, 1H), 1.93 – 1.88 (m, 1H), 1.73 – 1.67 (m, 2H), 1.67 (dd, *J* = 1.7 Hz, 3H), 1.63 – 1.60 (m, 1H), 1.57 – 1.55 (m, 1H), 1.52 – 1.48 (m, 2H), 1.49 – 1.39 (m, 2H), 1.07 (s, 3H), 0.94 (d, *J* = 6.1 Hz, 3H), 0.80 (d, *J* = 6.1 Hz, 3H).

^{13}C NMR (150 MHz, $CDCl_3$) δ 143.8, 117.6, 53.4, 52.4, 52.3, 47.6, 46.6, 45.9, 42.0, 33.7, 30.7, 29.9, 23.3, 22.4, 22.2.

HRMS (EI+) m/z calc'd for $C_{15}H_{24}^{+}$ $[M]^{+}$: 204.1873, found: 204.1877.

Rearrangement to pupukeanyl sultone 15

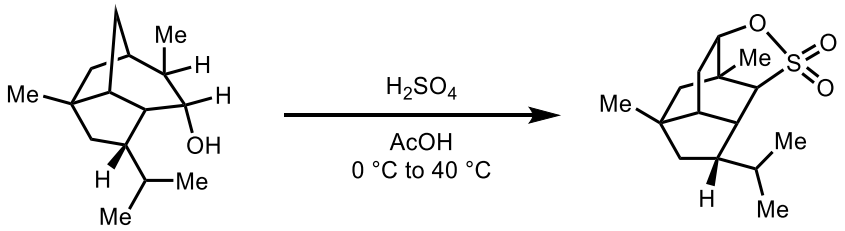

17 **25**

Alcohol **13** (16 mg, 0.070 mmol, 1.0 equiv) was dissolved in glacial AcOH (470 µL, 0.15M) and the mixture was cooled to 0 °C. Concentrated H_2SO_4 (30 µL, 0.56mmol, 8.0 equiv) was added and the mixture was warmed to room temperature then lowered into to a preheated oil bath at 40 °C and stirred at the same temperature. After 22 h, the light brown reaction mixture was cooled to 0 °C and diluted with several drops of cold H_2O. The mixture was then neutralized with a saturated solution of $NaHCO_{3(aq)}$ (3 mL) and extracted with EtOAc (4 x 3 mL). The combined organic extracts were washed with brine (5 mL). The washed organic layer was dried over $MgSO_4$. The dried solution was filtered and the resulting filtrate was concentrated *in vacuo*. The resulting oil was purified by flash column chromatography (5 to 20% EtOAc in hexanes) to give sultone **15** (7.5 mg, 0.030 mmol, 38%) as an off-white solid.

^{1}H NMR (700 MHz, $CDCl_3$) δ 4.43 – 4.38 (m, 1H), 3.07 – 3.02 (m, 1H), 2.98 (s, 1H), 2.04 – 1.96 (m, 2H), 1.96 – 1.89 (m, 1H), 1.78 – 1.71 (m, 1H), 1.57 – 1.55 (m, 1H), 1.49 – 1.45 (m, 1H), 1.39 (s, 3H), 1.38 – 1.33 (m, 2H), 1.18 – 1.11 (m, 1H), 1.01 (s, 3H), 0.95 (d, *J* = 6.4 Hz, 3H), 0.92 (d, *J* = 6.4 Hz, 3H).

^{13}C NMR (150 MHz, $CDCl_3$) δ 88.6, 59.1, 48.1, 48.0, 47.3, 41.8, 41.4, 39.4, 38.8, 30.6, 27.5, 26.1, 24.1, 21.8, 21.4.

IR (ATR, thin film): 2956, 2868, 1462, 1325, 1191, 1170 cm^{-1}

HRMS (EI+) m/z calc'd for $C_{15}H_{24}O_3S^{+}$ $[M]^{+}$: 284.1441, found: 284.1440.

$[\alpha]_D^{20}$ = – 6.1° (c = 0.34, $CHCl_3$)

2.8 References

1. (a) Palani, V.; Hugelshofer, C. L.; Sarpong, R. *J. Am. Chem. Soc.* **2019**, *141*, 14421–14432; (b) Zhou, S.; Xia, K.; Leng, X.; Li, A. *J. Am. Chem. Soc.* **2019**, *141*, 13718–13723.
2. (a) Tantillo, D. J. *Nat. Prod. Rep.* **2011**, *28*, 1035–1053; (b) Tantillo, D. J. *Chem. Soc. Rev.* **2018**, *47*, 7845–7850; (c) Sato, H.; Saito, K.; Yamazaki, M. *Front. Plant. Sci.* **2019**, *10*, 802; (d) Major, D. T.; Freud, Y.; Weitman, M. *Curr. Opin. Chem. Biol.* **2014**, *21*, 25–33; (e) Tantillo, D. J. *Nat. Prod. Rep.* **2013**, *30*, 1079–1086; (f) Tantillo, D. J. *Wiley Interdiscip. Rev. Comput. Mol. Sci.* **2019**, *10*; (g) Tantillo, D. J. *Angew. Chem. Int. Ed.* **2017**, *56*, 10040–10045.
3. (a) Brown, M. K.; Corey, E. J. *Org. Lett.* **2010**, *12*, 172–175; (b) Corey, E. J.; Behforouz, M.; Ishiguro, M. *J. Am. Chem. Soc.* **1979**, *101*, 1608–1609; (c) Yamamoto, H.; Sham, H. L. *J. Am. Chem. Soc.* **1979**, *101*, 1609–1611; (d) Srikrishna, A.; Ravi Kumar, P. *Tetrahedron Lett.* **2002**, *43*, 1109–1111; (e) Schiehser, G. A.; White, J. D. *J. Org. Chem.* **1980**, *45*, 1864–1868; (f) Piers, E.; Winter, M. *Liebigs Ann. Chem.* **1982**, *1982*, 973–984; (g) Hsieh, S. L.; Chiu, C. T.; Chang, N. C. *J. Org. Chem.* **1989**, *54*, 3820–3823; (h) Chang, N.-C.; Chang, C.-K. *J. Org. Chem.* **1996**, *61*, 4967–4970; (i) Corey, E. J.; Ishiguro, M. *Tetrahedron Lett.* **1979**, *20*, 2745–2748; (j) Fráter, G.; Wenger, J. *Helv Chim Acta* **1984**, *67*, 1702–1706; (k) Kaliappan, K.; Rao, G. S. R. S. *Tetrahedron Lett.* **1997**, *38*, 2185–2186; (l) Smaligo, A. J.; Swain, M.; Quintana, J. C.; Tan, M. F.; Kim, D. A.; Kwon, O. *Science* **2019**, *364*, 681–685; (m) Srikrishna, A.; Danieldoss, S. *J. Org. Chem.* **1997**, *62*, 7863–7865; (n) Srikrishna, A.; Ravi Kumar, P.; Gharpure, S. J. *Tetrahedron Lett.* **2001**, *42*, 3929–3931.
4. (a) Ho, T. L.; Kung, L. R.; Chein, R. J. *J. Org. Chem.* **2000**, *65*, 5774–5779; (b) Srikrishna, A.; Satyanarayana, G.; Ravi Kumar, P. *Tetrahedron Lett.* **2006**, *47*, 363–366.
5. 2-isocyanoallopupukeanane was isolated as a colorless gum (1.5 mg) from two 3-4cm nudibranchs.
6. Karuso, P.; Poiner, A.; Scheuer, P. J. *J. Org. Chem.* **1989**, *54*, 2095–2097.
7. (a) McCulley, C. H.; Tantillo, D. J. *J. Phys. Chem. A* **2018**, *122*, 8058–8061; (b) Sim, D. C. M.; Hungerford, N. L.; Krenske, E. H.; Pierens, G. K.; Andrews, K. T.; Skinner-Adams, T. S.; Garson, M. J. *Aust. J. Chem.* **2020**, *73*, 129–136.
8. Pronin, S. V.; Reiher, C. A.; Shenvi, R. A. *Nature* **2013**, *501*, 195–199.
9. (a) Masarwa, A.; Weber, M.; Sarpong, R. *J. Am. Chem. Soc.* **2015**, *137*, 6327–6334; (b) Weber, M.; Owens, K.; Masarwa, A.; Sarpong, R. *Org. Lett.* **2015**, *17*, 5432–5435; (c) Kuroda, Y.; Nicacio, K. J.; da Silva-Jr, I. A.; Leger, P. R.; Chang, S.; Gubiani, J. R.; Deflon, V. M.; Nagashima, N.; Rode, A.; Blackford, K.; Ferreira, A. G.; Sette, L. D.; Williams, D. E.; Andersen, R. J.; Jancar, S.; Berlinck, R. G. S.; Sarpong, R. *Nat. Chem.* **2018**, *10*, 938–945; (d) Kerschgens, I.; Rovira, A. R.; Sarpong, R. *J. Am. Chem. Soc.* **2018**, *140*, 9810–9813.
10. (a) Uemura, S.; Nishimura, T. *Synlett.* **2004**, *2004*, 201–216; (b) Nishimura, T.; Ohe, K.; Uemura, S. *J. Am. Chem. Soc.* **1999**, *121*, 2645–2646; (c) Yada, A.; Fujita, S.; Murakami, M. *J. Am. Chem. Soc.* **2014**, *136*, 7217–7220; (d) Seiser, T.; Roth, O. A.; Cramer, N. *Angew. Chem. Int. Ed.* **2009**, *48*, 6320–6323.
11. Cravero, R. M.; Gonzalez-Sierra, M.; Labadie, G. R. *HeIv. Chim. Acta* **2003**, *86*, 2741–2753.
12. Genet, J. P.; Juge, S.; Achi, S.; Mallart, S.; Ruiz Montes, J.; Levif, G. *Tetrahedron* **1988**, *44*, 5263–5275.

13. Although we began our studies with (*S*)-carvone, the optimized yields and procedures reported were performed from samples synthesized from (*R*)-carvone after modification of our approach in the second generation.
14. (a) Nishimura, T.; Ohe, K.; Uemura, S. *J. Org. Chem.* **2001**, *66*, 1455–1465; (b) Seiser, T.; Cramer, N. *J. Am. Chem. Soc.* **2010**, *132*, 5340–5341; (c) Ziadi, A.; Martin, R. *Org. Lett.* **2012**, *14*, 1266–1269.
15. Matsumura, S.; Maeda, Y.; Nishimura, T.; Uemura, S. *J. Am. Chem. Soc.* **2003**, *125*, 8862–8869.
16. (a) Ferreira, E. M.; Stoltz, B. M. *J. Am. Chem. Soc.* **2001**, *123*, 7725–7726; (b) Jensen, D. R.; Pugsley, J. S.; Sigman, M. S. *J. Am. Chem. Soc.* **2001**, *123*, 7475–7476.
17. (a) Steinhoff, B. A.; Stahl, S. S. *Org. Lett.* **2002**, *4*, 4179–4181; (b) Schultz, M. J.; Adler, R. S.; Zierkiewicz, W.; Privalov, T.; Sigman, M. S. *J. Am. Chem. Soc.* **2005**, *127*, 8499–8507.
18. (a) Salazar, C. A.; Flesch, K. N.; Haines, B. E.; Zhou, P. S.; Musaev, D. G.; Stahl, S. S. *Science* **2020**, *370*, 1454; (b) Wang, D.; Weinstein, A. B.; White, P. B.; Stahl, S. S. *Chem. Rev.* **2018**, *118*, 2636–2679.
19. (a) Campbell, A. N.; Stahl, S. S. *Acc. Chem. Res.* **2012**, *45*, 851–863; (b) Shi, Z.; Zhang, C.; Tang, C.; Jiao, N. *Chem. Soc. Rev.* **2012**, *41*, 3381–3430; (c) Gligorich, K. M.; Sigman, M. S. *ChemComm* **2009**, 3854–3867.
20. For a detailed listing of conditions we explored, see section 1.7.2.
21. (a) Dowd, P.; Zhang, W.; Geib, S. J. *Tetrahedron* **1995**, *51*, 3435–3454; (b) Zhang, W.; Dowd, P. *Tetrahedron Lett.* **1994**, *35*, 5161–5164.
22. (a) Yahata, K.; Minami, M.; Watanabe, K.; Fujioka, H. *Org. Lett.* **2014**, *16*, 3680–3683; (b) Watanabe, K.; Ohta, R.; Morita, K.; Yahata, K.; Minami, M.; Fujioka, H. *Tetrahedron* **2016**, *72*, 2420–2428.
23. A small amount (<10%) of a mixture of other side products, presumed to be epimers of **24** were also isolated.
24. Ho, T.-L.; Kung, L.-R. *Org. Lett.* **1999**, *1*, 1051–1052.
25. Tantillo, D. J. *Chem. Soc. Rev* **2010**, *39*, 2847–2854.
26. Frisch, M. J.; Trucks, G. W.; Schlegel, H. B.; Scuseria, G. E.; Robb, M. A.; Cheeseman, J. R.; Scalmani, G.; Barone, V.; Petersson, G. A.; Nakatsuji, H.; Li, X.; Caricato, M.; Marenich, A. V.; Bloino, J.; Janesko, B. G.; Gomperts, R.; Mennucci, B.; Hratchian, H. P.; Ortiz, J. V.; Izmaylov, A. F.; Sonnenberg, J. L.; Williams; Ding, F.; Lipparini, F.; Egidi, F.; Goings, J.; Peng, B.; Petrone, A.; Henderson, T.; Ranasinghe, D.; Zakrzewski, V. G.; Gao, J.; Rega, N.; Zheng, G.; Liang, W.; Hada, M.; Ehara, M.; Toyota, K.; Fukuda, R.; Hasegawa, J.; Ishida, M.; Nakajima, T.; Honda, Y.; Kitao, O.; Nakai, H.; Vreven, T.; Throssell, K.; Montgomery Jr., J. A.; Peralta, J. E.; Ogliaro, F.; Bearpark, M. J.; Heyd, J. J.; Brothers, E. N.; Kudin, K. N.; Staroverov, V. N.; Keith, T. A.; Kobayashi, R.; Normand, J.; Raghavachari, K.; Rendell, A. P.; Burant, J. C.; Iyengar, S. S.; Tomasi, J.; Cossi, M.; Millam, J. M.; Klene, M.; Adamo, C.; Cammi, R.; Ochterski, J. W.; Martin, R. L.; Morokuma, K.; Farkas, O.; Foresman, J. B.; Fox, D. J. *Gaussian 16 Rev. C.01*, Wallingford, CT, 2016.
27. (a) Sengupta, A.; Raghavachari, K. *Org. Lett.* **2017**, *19*, 2576–2579; (b) Marenich, A. V.; Cramer, C. J.; Truhlar, D. G. *J. Phys. Chem. B* **2009**, *113*, 6378–6396; (c) Weigend, F.; Ahlrichs, R. *Phys. Chem. Chem. Phys.* **2005**, *7*, 3297–305.

28. (a) Knox, P. D. B. a. L. H. *Org. Synth.* **1965**, *45*, 12–14; (b) Piątek, A.; Chapuis, C. *Tetrahedron Lett.* **2013**, *54*, 4247–4249.
29. (a) Dimmel, D. R.; Fu, W. Y. *J. Org. Chem.* **1973**, *38*, 3778–3782; (b) Mustafa, A. *Chem. Rev.* **1954**, *54*, 195–223; (c) Roberts, D. W.; Williams, D. L. *Tetrahedron* **1987**, *43*, 1027–1062.
30. (a) Brown, H. C. *Acc. Chem. Res.* **2002**, *16*, 432–440; (b) Grob, C. A. *Acc. Chem. Res.* **1983**, *16*, 426–431; (c) Olah, G. A.; Prakash, G. K. S.; Saunders, M. *Acc. Chem. Res.* **1983**, *16*, 440–448; (d) Walling, C. *Acc. Chem. Res.* **1983**, *16*, 448–454; (e) Brown, H. C., *The Nonclassical Ion Problem*. Plenum: New York, 1977.
31. Smith, P. A. S. *J. Polym. Sci* **1969**, *7*, 795–796.
32. CYLview20; Legault, C. Y., Université de Sherbrooke, 2020 (http://www.cylview.org)

Appendix 2A. NMR Spectral Data for Chapter 2

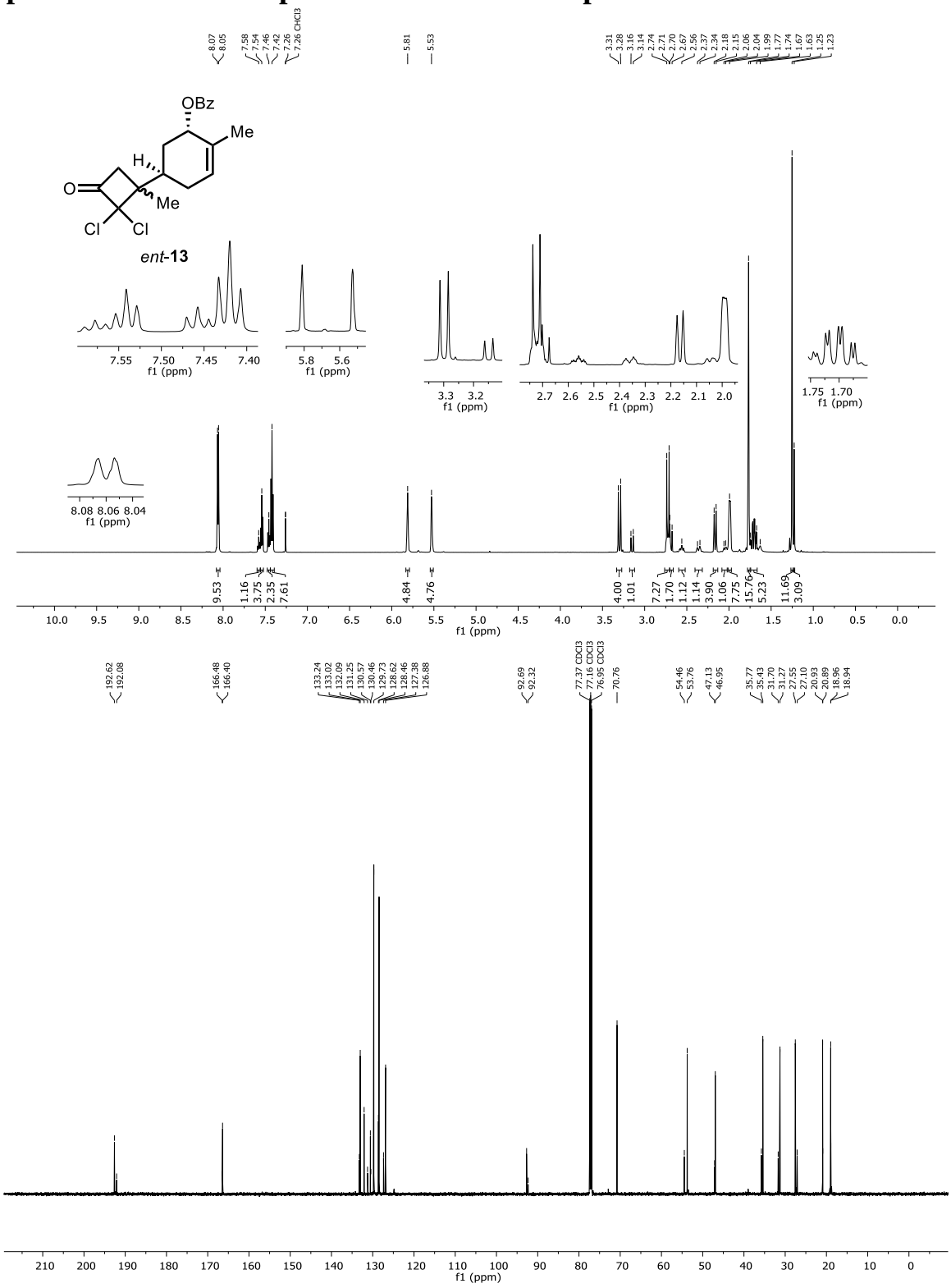

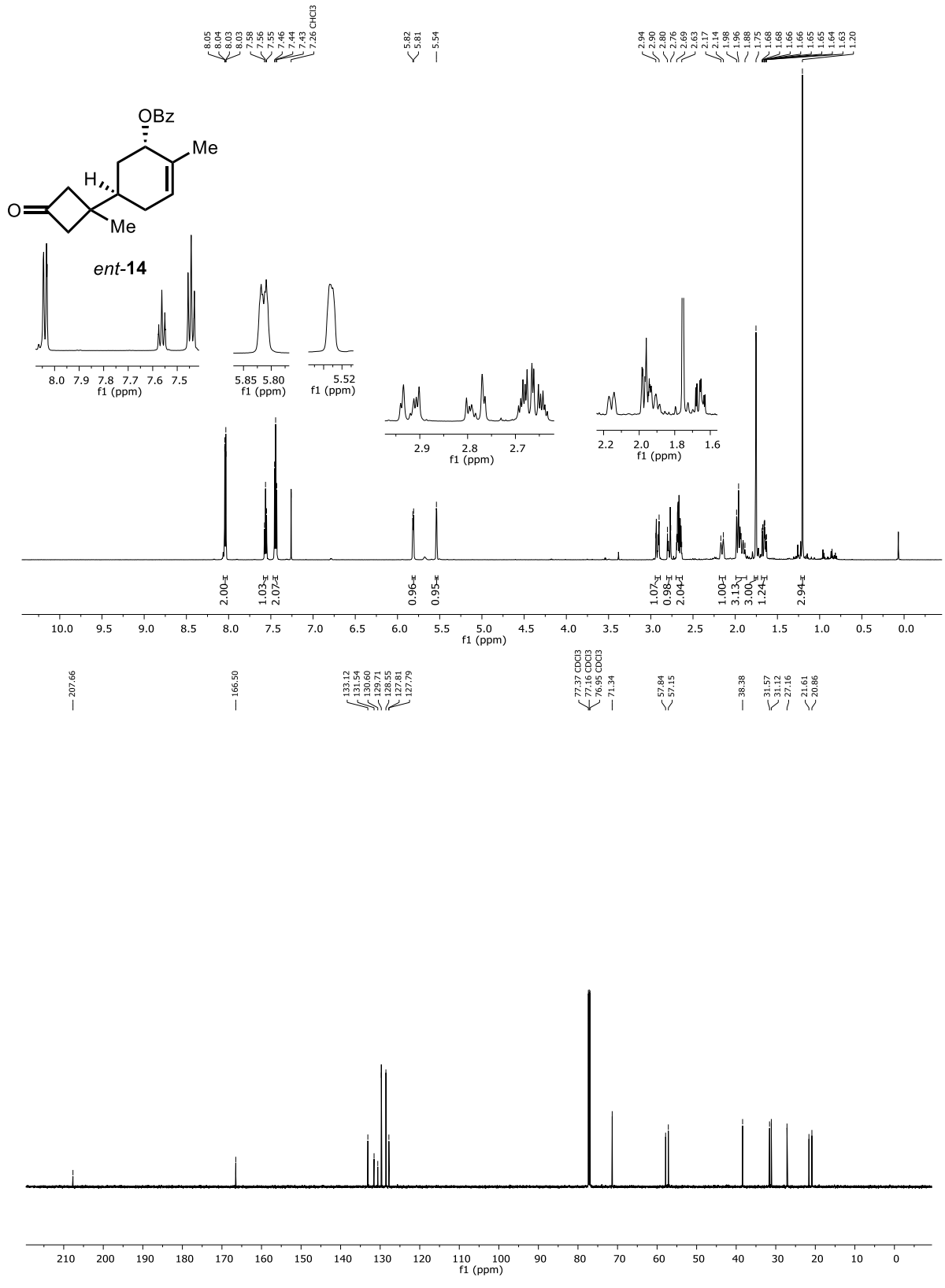
OBz
Me
H
O
Me
ent-14
8.05
8.04
8.03
8.03
7.58
7.56
7.55
7.46
7.44
7.43
7.26 CHCl3
5.82
5.81
5.54
2.94
2.90
2.80
2.76
2.69
2.63
2.17
2.14
1.98
1.96
1.88
1.75
1.68
1.68
1.66
1.66
1.65
1.65
1.64
1.63
1.20
f1 (ppm)
2.00
1.03
2.07
0.96
0.95
1.07
0.98
2.04
1.00
3.13
3.00
1.24
2.94
207.66
166.50
133.12
131.54
130.60
129.71
128.55
127.81
127.79
77.37 CDCl3
77.16 CDCl3
76.95 CDCl3
71.34
57.84
57.15
38.38
31.57
31.12
27.16
21.61
20.86

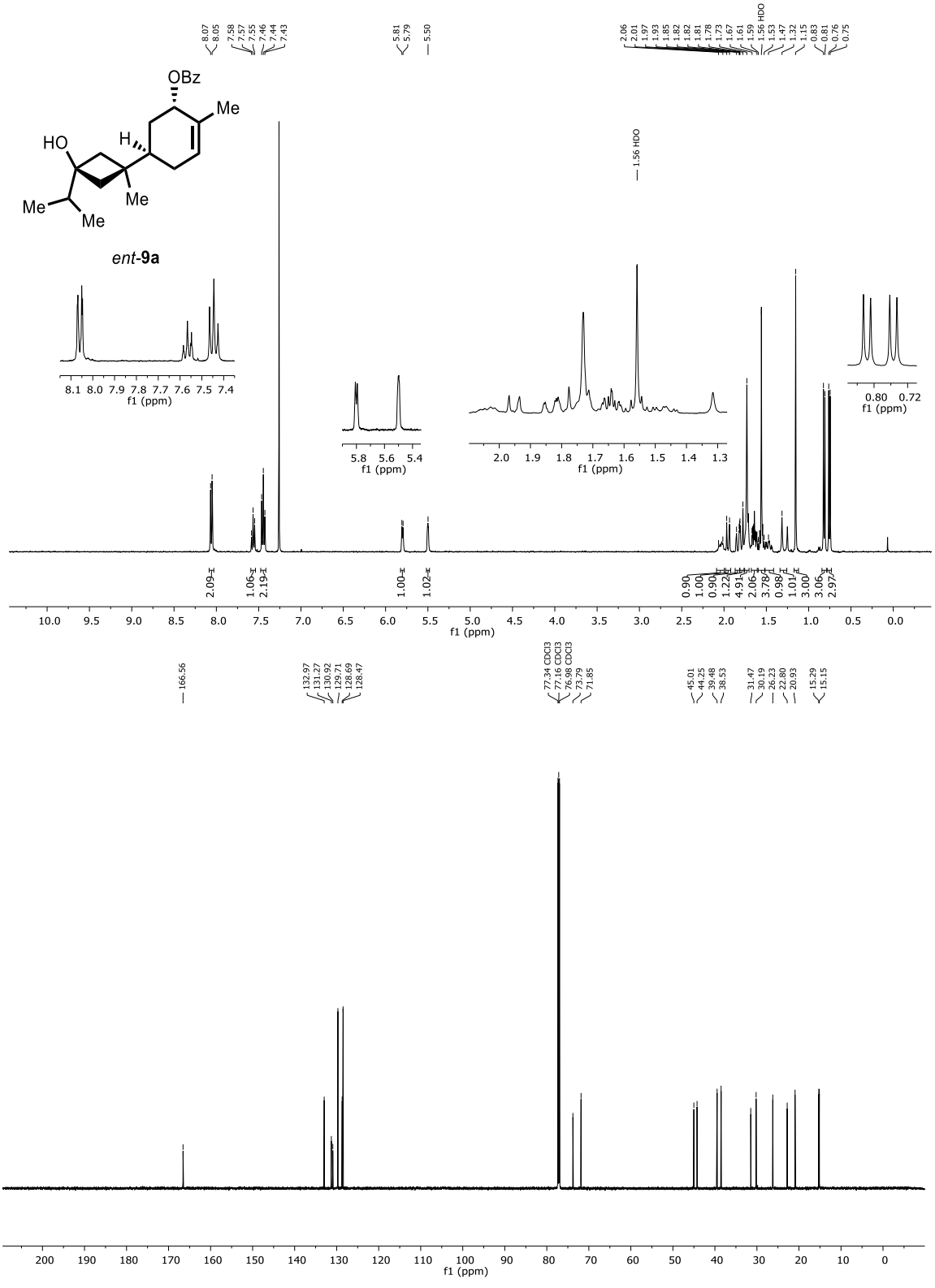
OBz
Me
HO
H
Me
Me
Me
ent-9a
f1 (ppm)

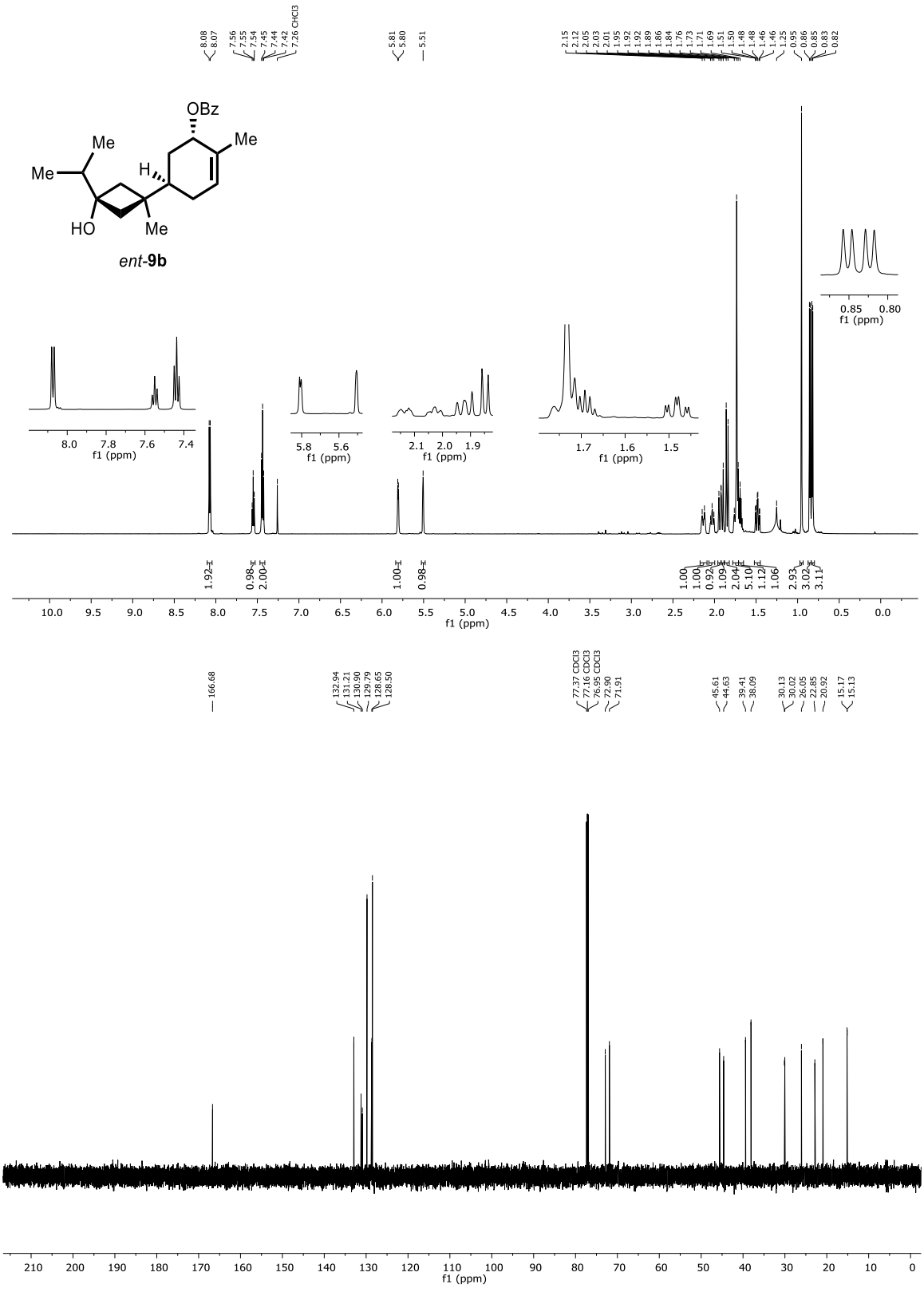
OBz
Me
Me
H
HO
Me
Me
ent-9b
f1 (ppm)

^{1}H NMR, 700 MHz, $CDCl_3$

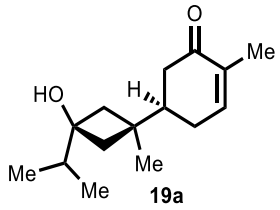

19a

^{13}C NMR, 150 MHz, $CDCl_3$

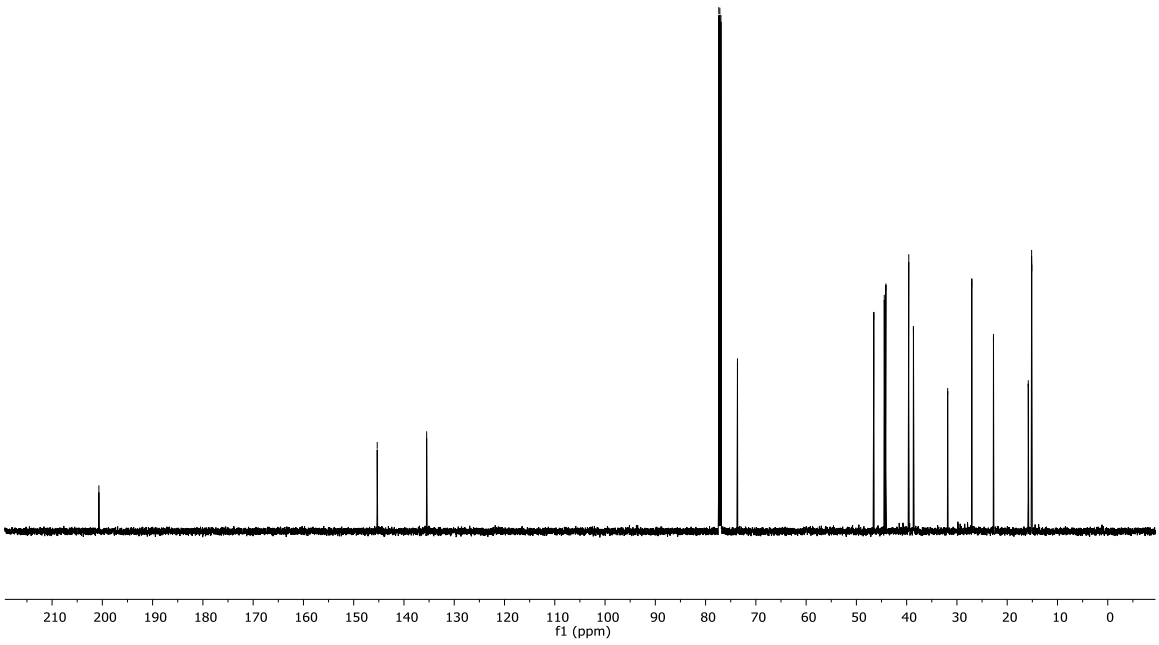

^{1}H NMR, 600 MHz, $CDCl_3$

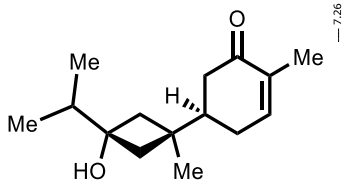

19b

^{13}C NMR, 150 MHz, $CDCl_3$

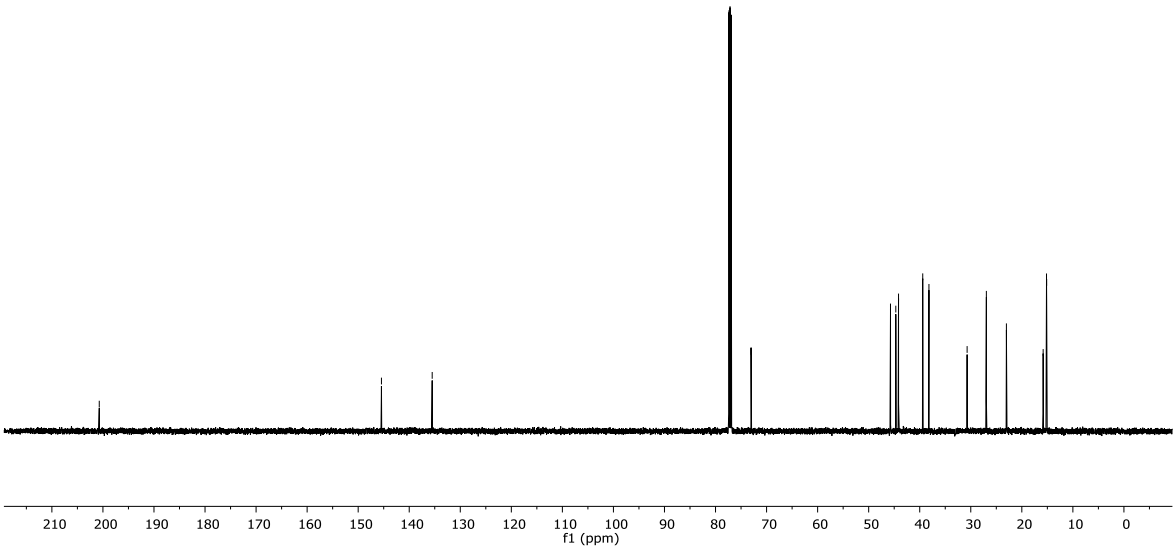

^{1}H NMR, 700 MHz, $CDCl_3$

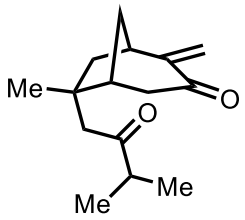

18

^{13}C NMR, 150 MHz, $CDCl_3$

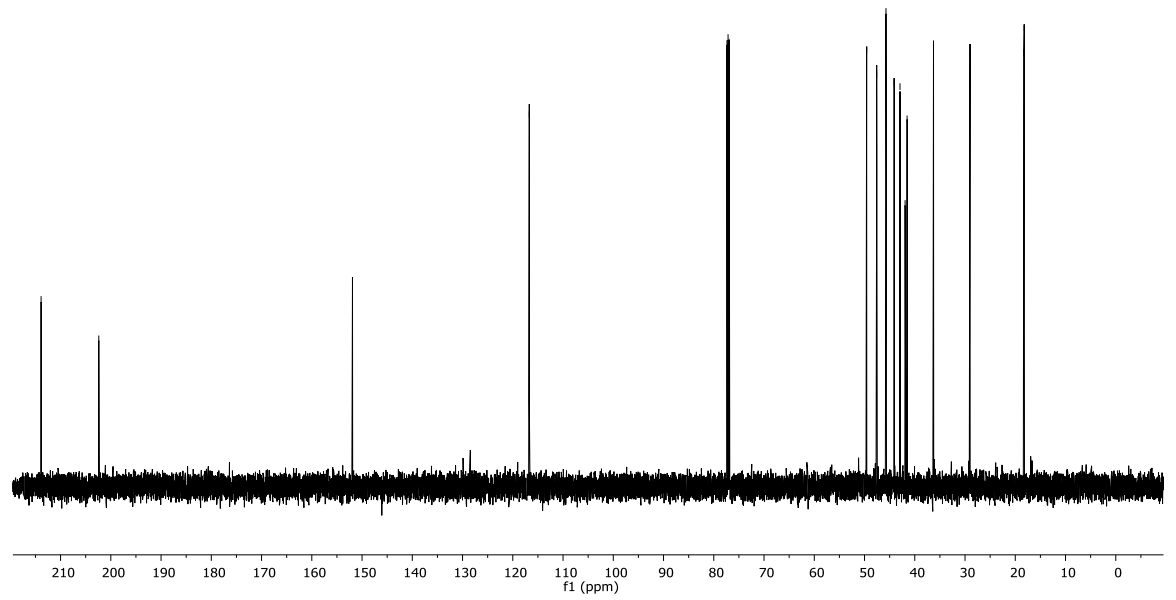

^{1}H NMR, 600 MHz, $CDCl_3$

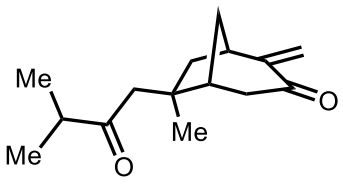

21

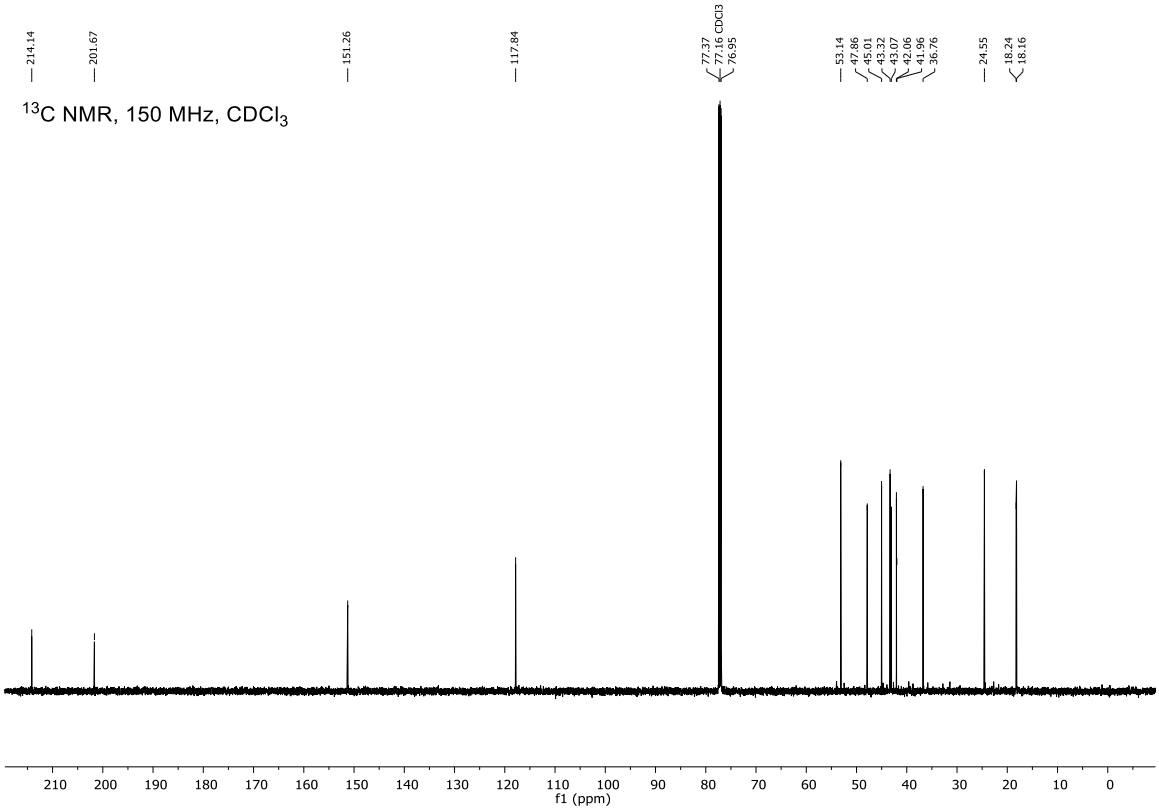

^{13}C NMR, 150 MHz, $CDCl_3$

^{1}H NMR, 500 MHz, $CDCl_3$

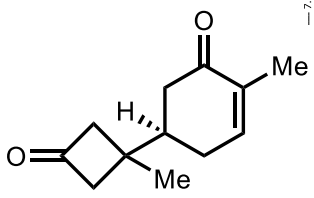

22

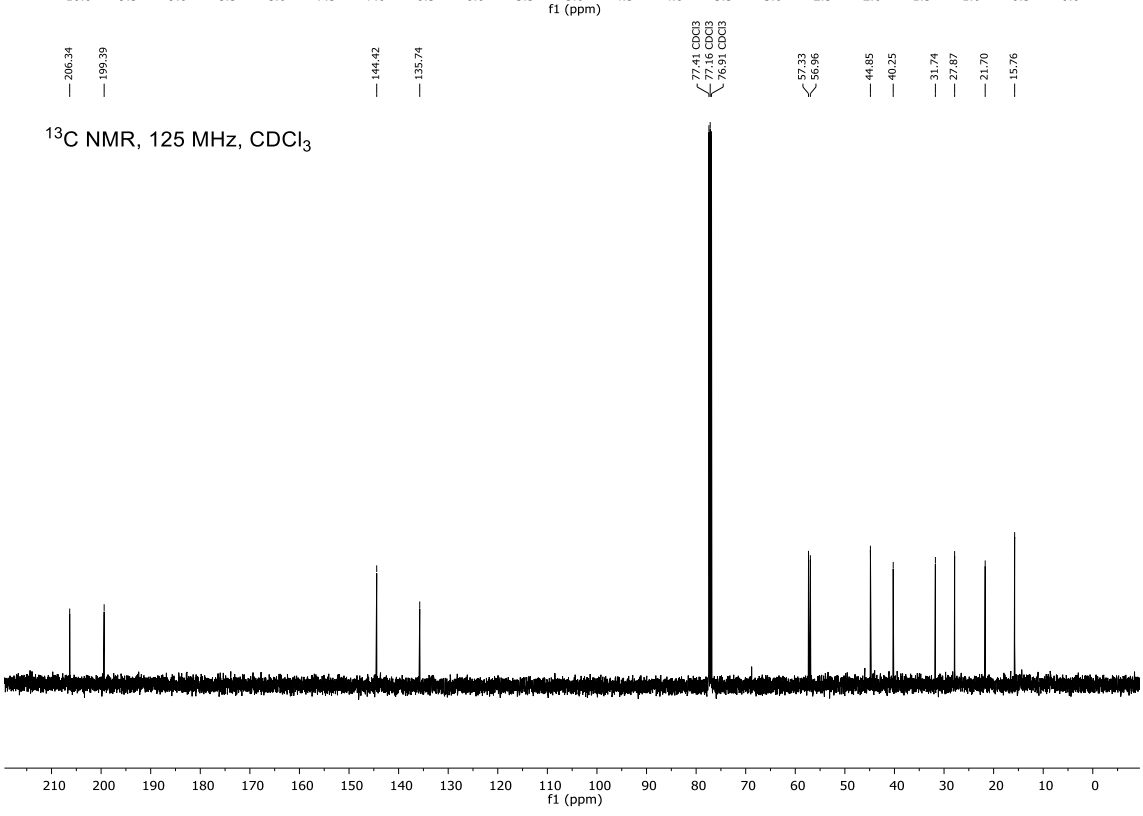

^{13}C NMR, 125 MHz, $CDCl_3$

^{1}H NMR, 600 MHz, $CDCl_3$

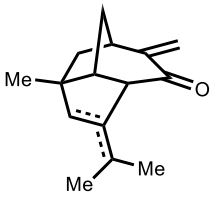

23

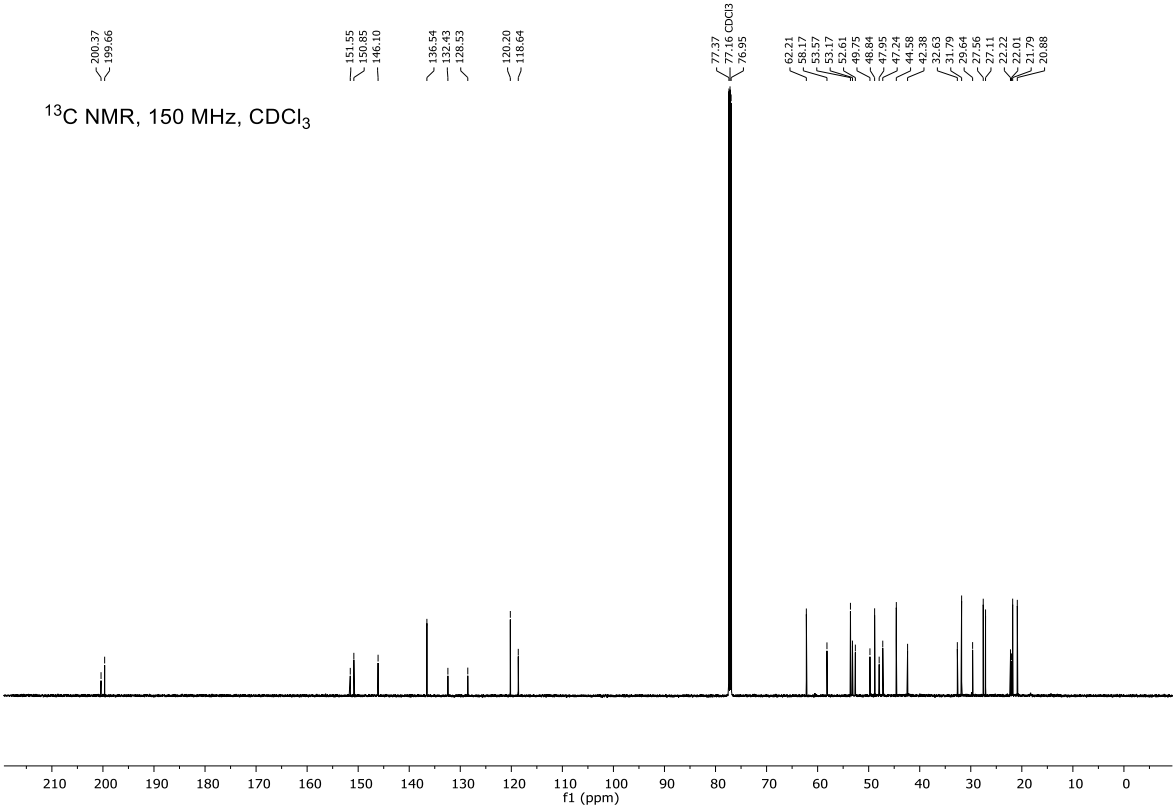

^{13}C NMR, 150 MHz, $CDCl_3$

^{1}H NMR, 600 MHz, $CDCl_3$

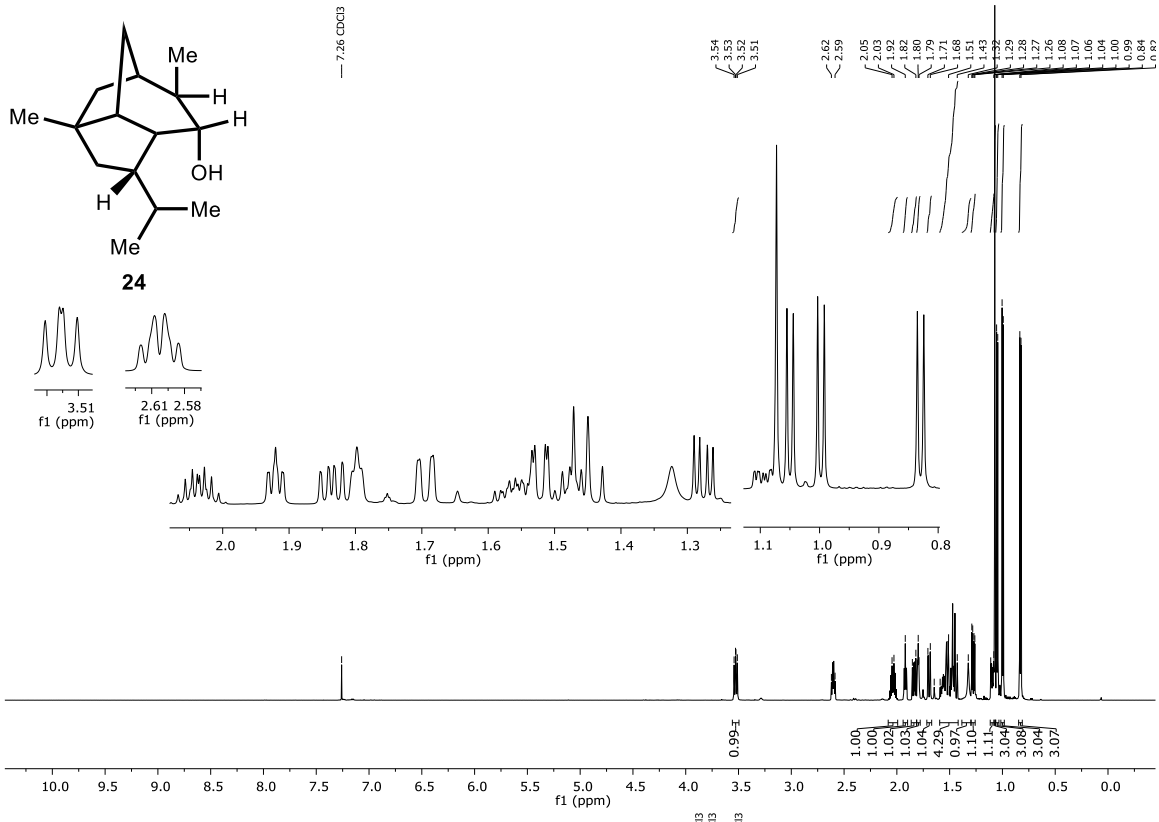

^{13}C NMR, 150 MHz, $CDCl_3$

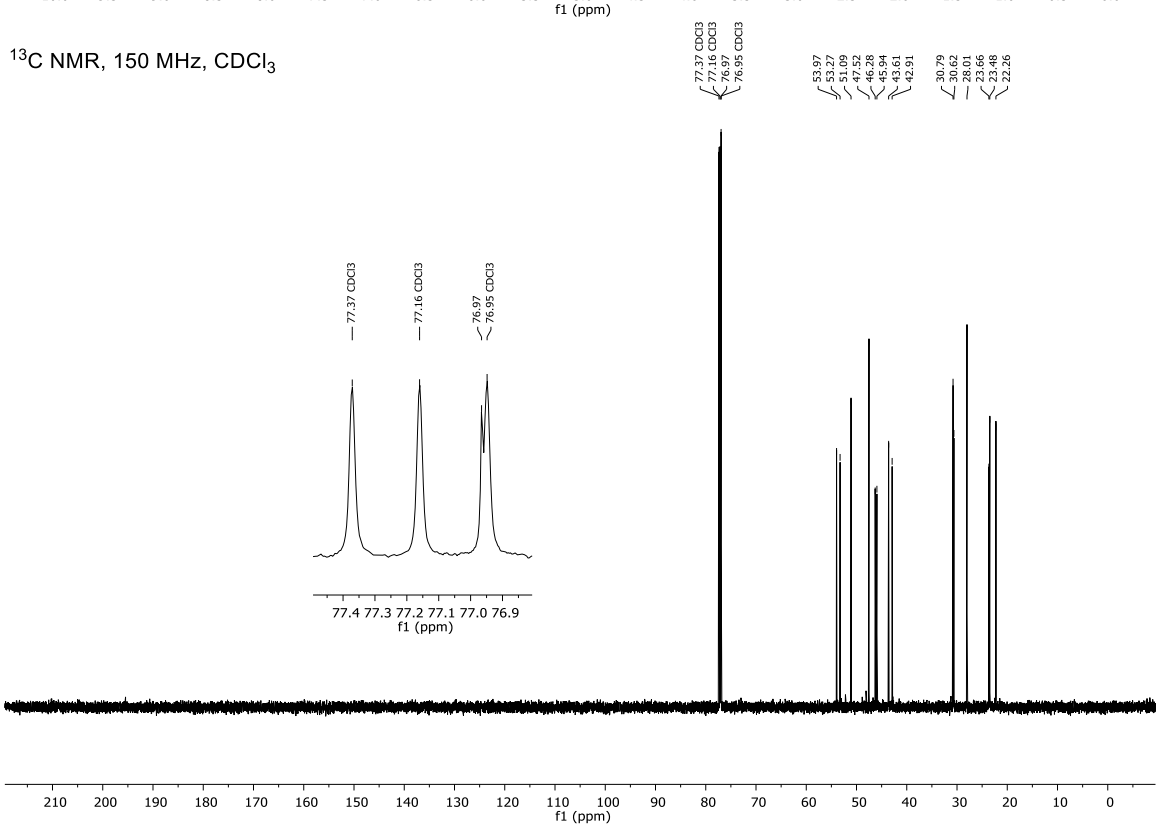

^{1}H NMR, 600 MHz, $CDCl_3$

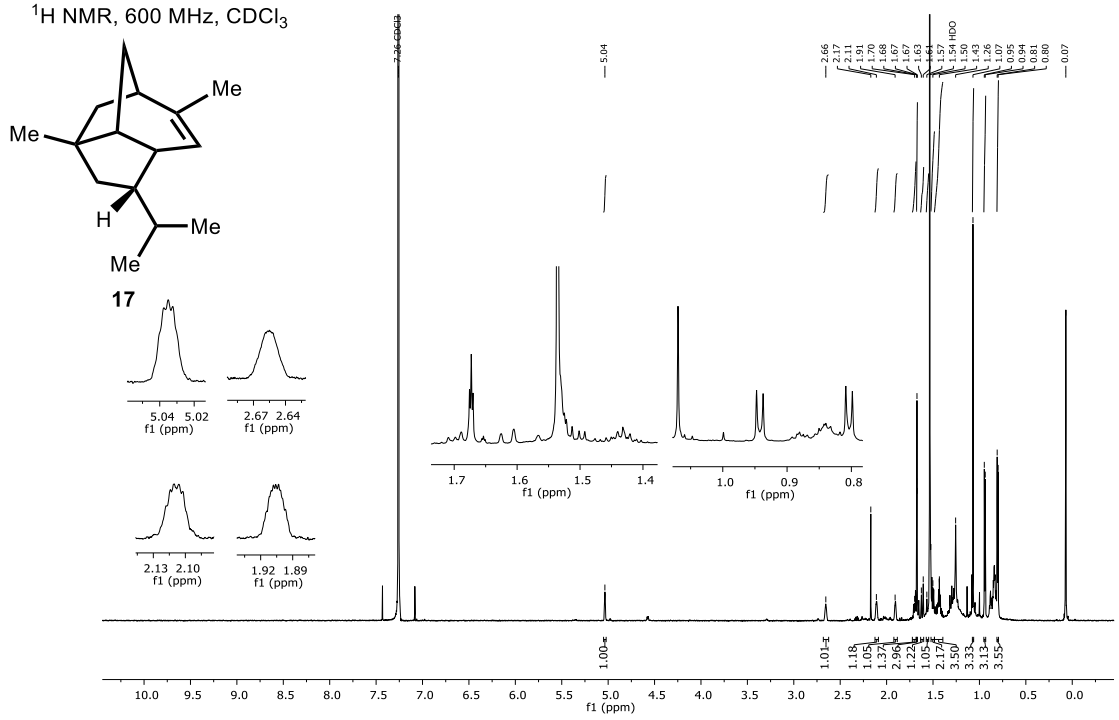

^{13}C NMR, 150 MHz, $CDCl_3$

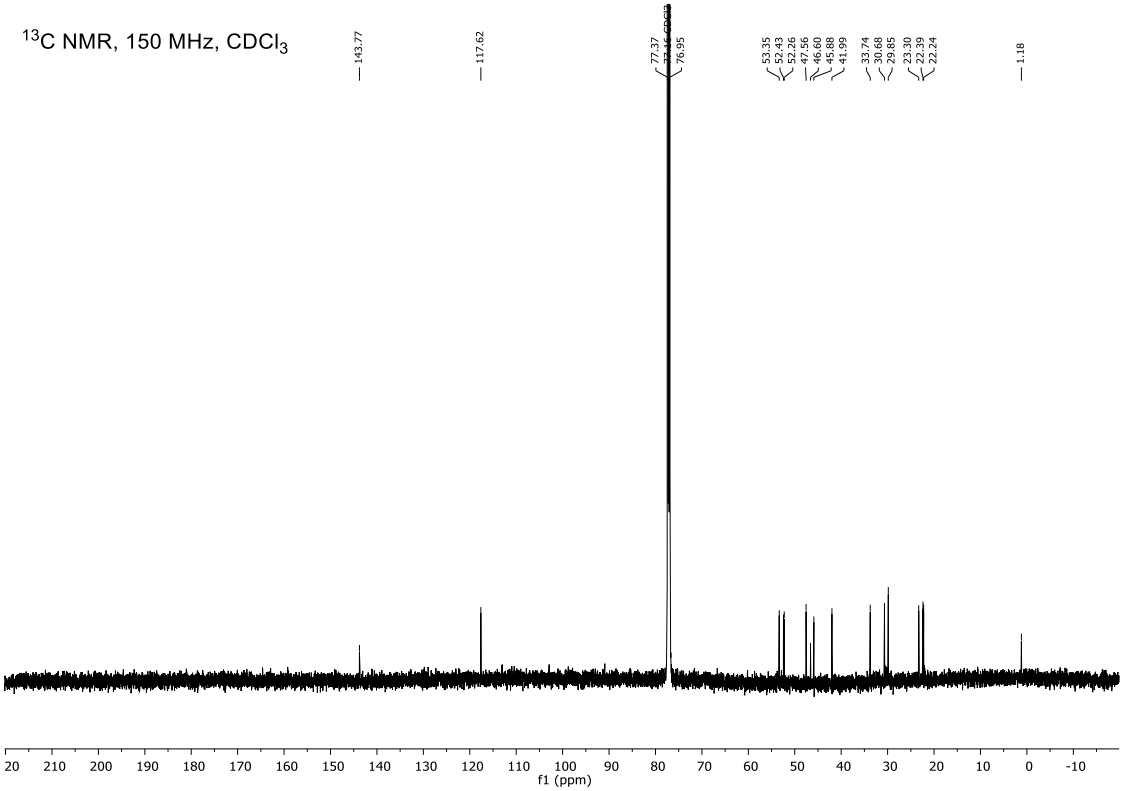

^{1}H NMR, 700 MHz, $CDCl_3$

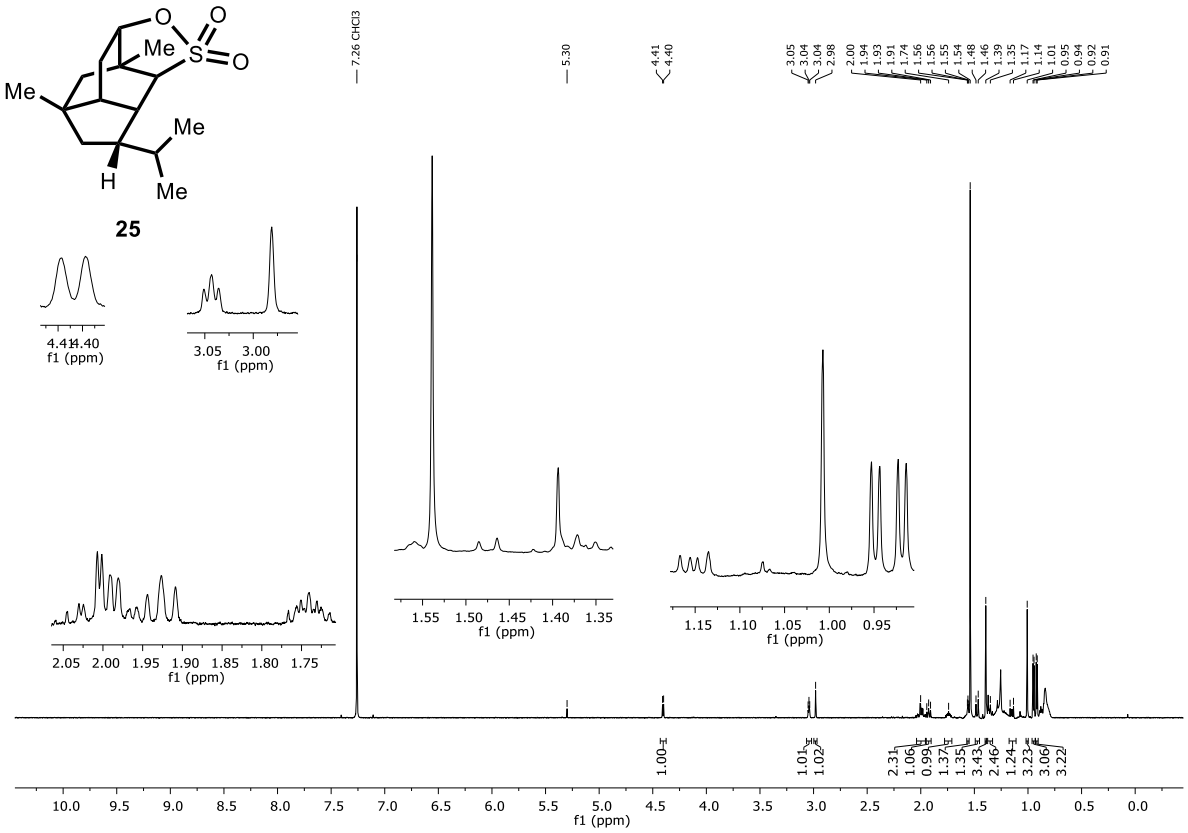

^{13}C NMR, 150 MHz, $CDCl_3$

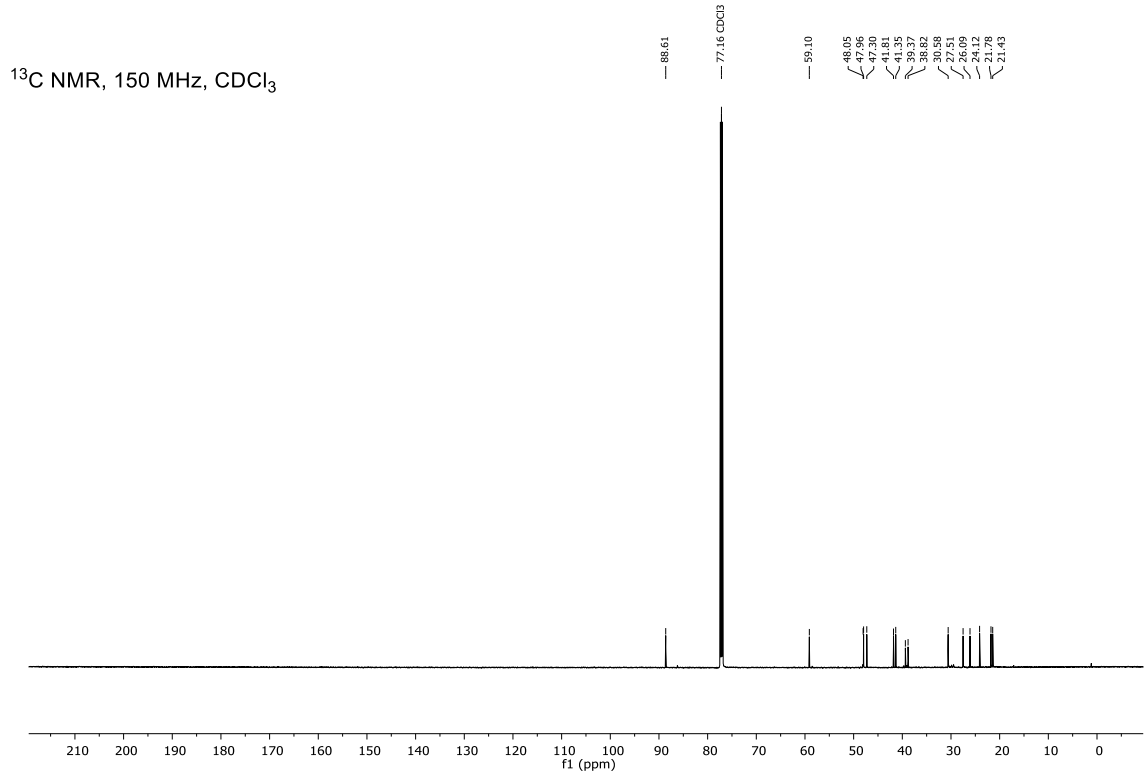

Appendix 2B. X-Ray Crystallography Data for Chapter 2

Single crystal X-ray diffraction experiments were performed at the UC Berkeley CHEXRAY crystallographic facility. Data were collected in a nitrogen gas stream at 100(2) K using omega scans. Crystal-to-detector distance was 30.23 mm and exposure time was 0.50 seconds per frame at low angles and 2.00 seconds at high angles, using a scan width of 0.5°. Data collection was 100% complete to 74.000° in θ. A total of 43809 reflections were collected covering the indices -11<=h<=11, -20<=k<=20, -12<=l<=12. 6078 reflections were found to be symmetry independent, with an R_{int} of 0.0710. Indexing and unit cell refinement indicated a primitive, monoclinic lattice. The space group was found to be P 21 (No. 4). The data were integrated using the CrysAlis^{Pro} 1.171.40.54a software program and scaled using the SCALE3 ABSPACK scaling algorithm. Solution by intrinsic phasing (SHELXT-2015) produced a heavy-atom phasing model consistent with the proposed structure. All non-hydrogen atoms were refined anisotropically by full-matrix least-squares (SHELXL-2014). All hydrogen atoms were placed using a riding model. Their positions were constrained relative to their parent atom using the appropriate HFIX command in SHELXL-2014. The X-ray structures in the main chapter and shown below were visualized using CYLView.[32]

Table 1. Crystal data and structure refinement for MHardy001_Sarpong (CCDC 2073700).

Identification code	MHardy001_Sarpong	
Empirical formula	C15 H24 O3 S	
Formula weight	284.40	
Temperature	100(2) K	
Wavelength	1.54184 Å	
Crystal system	Monoclinic	
Space group	P 21	
Unit cell dimensions	a = 9.36640(10) Å	a= 90°.
	b = 16.5555(2) Å	b= 93.5710(10)°.
	c = 9.64630(10) Å	g = 90°.
Volume	1492.90(3) Å^3	
Z	4	
Density (calculated)	1.265 Mg/m^3	
Absorption coefficient	1.942 mm^{-1}	
F(000)	616	

Crystal size	0.240 x 0.120 x 0.080 mm^3
Theta range for data collection	4.593 to 74.497°.
Index ranges	-11<=h<=11, -20<=k<=20, -12<=l<=12
Reflections collected	43809
Independent reflections	6078 [R(int) = 0.0710]
Completeness to theta = 74.000°	99.9 %
Absorption correction	Semi-empirical from equivalents
Max. and min. transmission	1.00000 and 0.85875
Refinement method	Full-matrix least-squares on F^2
Data / restraints / parameters	6078 / 1 / 352
Goodness-of-fit on F^2	1.141
Final R indices [I>2sigma(I)]	R1 = 0.0452, wR2 = 0.1265
R indices (all data)	R1 = 0.0471, wR2 = 0.1333
Absolute structure parameter	-0.006(14)
Extinction coefficient	0.0024(6)
Largest diff. peak and hole	0.245 and -0.492 e.$Å^{-3}$

Table 2. Atomic coordinates (x 10^4) and equivalent isotropic displacement parameters ($Å^2$x 10^3) for mhardy001_sarpong. U(eq) is defined as one third of the trace of the orthogonalized U^{ij} tensor.

	x	y	z	U(eq)
C(1)	3977(4)	5930(2)	1799(4)	29(1)
C(2)	4652(4)	5246(2)	2723(4)	30(1)
C(3)	4150(4)	5510(3)	4133(4)	32(1)
C(4)	4135(5)	4402(2)	2303(5)	38(1)
C(5)	6297(4)	5274(2)	2773(4)	33(1)
C(6)	6919(4)	6131(2)	2968(4)	29(1)
C(7)	8243(4)	6113(3)	3968(5)	37(1)
C(8)	5688(4)	6664(2)	3437(4)	30(1)
C(9)	4912(5)	6286(3)	4626(4)	33(1)
C(10)	4753(4)	6746(2)	2070(4)	27(1)
C(11)	5873(4)	6947(2)	1008(4)	29(1)
C(12)	5461(4)	6799(3)	-527(4)	32(1)
C(13)	4037(5)	7183(3)	-1005(4)	37(1)
C(14)	6634(5)	7121(3)	-1420(4)	39(1)
C(15)	7243(4)	6500(2)	1553(4)	32(1)
C(16)	8703(4)	3880(2)	7394(4)	24(1)
C(17)	9485(4)	4027(2)	8840(4)	26(1)
C(18)	8994(4)	4884(3)	9135(4)	30(1)
C(19)	9065(4)	3431(3)	9952(4)	35(1)
C(20)	11122(4)	4030(2)	8767(4)	30(1)
C(21)	11621(4)	4503(2)	7510(4)	29(1)
C(22)	12973(4)	4984(3)	7921(5)	39(1)
C(23)	10345(4)	5038(2)	6985(4)	28(1)
C(24)	9676(4)	5487(2)	8171(4)	33(1)
C(25)	9356(4)	4406(2)	6266(4)	25(1)
C(26)	10396(4)	3946(2)	5368(4)	28(1)
C(27)	9893(4)	3136(3)	4776(4)	33(1)
C(28)	8405(5)	3186(3)	4034(5)	48(1)

C(29)	10966(5)	2815(3)	3773(5)	42(1)
C(30)	11817(4)	3930(3)	6269(4)	32(1)
O(1)	2588(3)	5649(2)	3915(3)	38(1)
O(2)	1659(3)	6788(2)	2511(3)	42(1)
O(3)	1253(3)	5415(2)	1688(3)	43(1)
O(4)	7418(3)	4886(2)	8862(3)	36(1)
O(5)	6306(3)	4693(2)	6519(3)	38(1)
O(6)	6061(3)	3663(2)	8278(3)	34(1)
S(1)	2182(1)	5987(1)	2402(1)	31(1)
S(2)	6929(1)	4257(1)	7685(1)	28(1)

—

Table 3. Bond lengths [Å] and angles [°] for mhardy001_sarpong.

C(1)-C(10)	1.549(5)
C(1)-C(2)	1.550(5)
C(1)-S(1)	1.815(4)
C(1)-H(1)	1.0000
C(2)-C(4)	1.527(5)
C(2)-C(3)	1.530(5)
C(2)-C(5)	1.539(5)
C(3)-O(1)	1.483(5)
C(3)-C(9)	1.530(6)
C(3)-H(3)	1.0000
C(4)-H(4A)	0.9800
C(4)-H(4B)	0.9800
C(4)-H(4C)	0.9800
C(5)-C(6)	1.540(5)
C(5)-H(5A)	0.9900
C(5)-H(5B)	0.9900
C(6)-C(7)	1.523(5)
C(6)-C(8)	1.542(5)
C(6)-C(15)	1.543(5)
C(7)-H(7A)	0.9800
C(7)-H(7B)	0.9800
C(7)-H(7C)	0.9800
C(8)-C(9)	1.530(5)
C(8)-C(10)	1.543(5)
C(8)-H(8)	1.0000
C(9)-H(9A)	0.9900
C(9)-H(9B)	0.9900
C(10)-C(11)	1.548(5)
C(10)-H(10)	1.0000
C(11)-C(12)	1.526(5)
C(11)-C(15)	1.545(5)
C(11)-H(11)	1.0000
C(12)-C(13)	1.523(5)
C(12)-C(14)	1.534(6)

C(12)-H(12)	1.0000
C(13)-H(13A)	0.9800
C(13)-H(13B)	0.9800
C(13)-H(13C)	0.9800
C(14)-H(14A)	0.9800
C(14)-H(14B)	0.9800
C(14)-H(14C)	0.9800
C(15)-H(15A)	0.9900
C(15)-H(15B)	0.9900
C(16)-C(25)	1.549(5)
C(16)-C(17)	1.553(5)
C(16)-S(2)	1.813(4)
C(16)-H(16)	1.0000
C(17)-C(18)	1.524(5)
C(17)-C(19)	1.527(5)
C(17)-C(20)	1.540(5)
C(18)-O(4)	1.483(4)
C(18)-C(24)	1.530(6)
C(18)-H(18)	1.0000
C(19)-H(19A)	0.9800
C(19)-H(19B)	0.9800
C(19)-H(19C)	0.9800
C(20)-C(21)	1.541(5)
C(20)-H(20A)	0.9900
C(20)-H(20B)	0.9900
C(21)-C(22)	1.527(5)
C(21)-C(23)	1.547(5)
C(21)-C(30)	1.547(5)
C(22)-H(22A)	0.9800
C(22)-H(22B)	0.9800
C(22)-H(22C)	0.9800
C(23)-C(24)	1.531(5)
C(23)-C(25)	1.534(5)
C(23)-H(23)	1.0000
C(24)-H(24A)	0.9900
C(24)-H(24B)	0.9900

C(25)-C(26)	1.544(5)
C(25)-H(25)	1.0000
C(26)-C(27)	1.521(5)
C(26)-C(30)	1.544(5)
C(26)-H(26)	1.0000
C(27)-C(28)	1.528(6)
C(27)-C(29)	1.532(6)
C(27)-H(27)	1.0000
C(28)-H(28A)	0.9800
C(28)-H(28B)	0.9800
C(28)-H(28C)	0.9800
C(29)-H(29A)	0.9800
C(29)-H(29B)	0.9800
C(29)-H(29C)	0.9800
C(30)-H(30A)	0.9900
C(30)-H(30B)	0.9900
O(1)-S(1)	1.588(3)
O(2)-S(1)	1.421(3)
O(3)-S(1)	1.433(3)
O(4)-S(2)	1.588(3)
O(5)-S(2)	1.429(3)
O(6)-S(2)	1.419(3)

C(10)-C(1)-C(2)	111.7(3)
C(10)-C(1)-S(1)	109.6(3)
C(2)-C(1)-S(1)	101.9(2)
C(10)-C(1)-H(1)	111.1
C(2)-C(1)-H(1)	111.1
S(1)-C(1)-H(1)	111.1
C(4)-C(2)-C(3)	112.8(3)
C(4)-C(2)-C(5)	109.6(3)
C(3)-C(2)-C(5)	109.0(3)
C(4)-C(2)-C(1)	113.9(3)
C(3)-C(2)-C(1)	99.5(3)
C(5)-C(2)-C(1)	111.6(3)
O(1)-C(3)-C(9)	110.5(3)

O(1)-C(3)-C(2)	105.9(3)
C(9)-C(3)-C(2)	110.7(3)
O(1)-C(3)-H(3)	109.9
C(9)-C(3)-H(3)	109.9
C(2)-C(3)-H(3)	109.9
C(2)-C(4)-H(4A)	109.5
C(2)-C(4)-H(4B)	109.5
H(4A)-C(4)-H(4B)	109.5
C(2)-C(4)-H(4C)	109.5
H(4A)-C(4)-H(4C)	109.5
H(4B)-C(4)-H(4C)	109.5
C(2)-C(5)-C(6)	113.7(3)
C(2)-C(5)-H(5A)	108.8
C(6)-C(5)-H(5A)	108.8
C(2)-C(5)-H(5B)	108.8
C(6)-C(5)-H(5B)	108.8
H(5A)-C(5)-H(5B)	107.7
C(7)-C(6)-C(5)	110.3(3)
C(7)-C(6)-C(8)	114.8(3)
C(5)-C(6)-C(8)	106.2(3)
C(7)-C(6)-C(15)	111.7(3)
C(5)-C(6)-C(15)	110.5(3)
C(8)-C(6)-C(15)	102.9(3)
C(6)-C(7)-H(7A)	109.5
C(6)-C(7)-H(7B)	109.5
H(7A)-C(7)-H(7B)	109.5
C(6)-C(7)-H(7C)	109.5
H(7A)-C(7)-H(7C)	109.5
H(7B)-C(7)-H(7C)	109.5
C(9)-C(8)-C(6)	112.6(3)
C(9)-C(8)-C(10)	114.0(3)
C(6)-C(8)-C(10)	101.3(3)
C(9)-C(8)-H(8)	109.6
C(6)-C(8)-H(8)	109.6
C(10)-C(8)-H(8)	109.6
C(3)-C(9)-C(8)	110.1(3)

C(3)-C(9)-H(9A)	109.6
C(8)-C(9)-H(9A)	109.6
C(3)-C(9)-H(9B)	109.6
C(8)-C(9)-H(9B)	109.6
H(9A)-C(9)-H(9B)	108.2
C(8)-C(10)-C(11)	102.3(3)
C(8)-C(10)-C(1)	107.6(3)
C(11)-C(10)-C(1)	114.0(3)
C(8)-C(10)-H(10)	110.9
C(11)-C(10)-H(10)	110.9
C(1)-C(10)-H(10)	110.9
C(12)-C(11)-C(15)	114.0(3)
C(12)-C(11)-C(10)	117.8(3)
C(15)-C(11)-C(10)	104.7(3)
C(12)-C(11)-H(11)	106.5
C(15)-C(11)-H(11)	106.5
C(10)-C(11)-H(11)	106.5
C(13)-C(12)-C(11)	113.0(3)
C(13)-C(12)-C(14)	109.2(3)
C(11)-C(12)-C(14)	110.0(3)
C(13)-C(12)-H(12)	108.2
C(11)-C(12)-H(12)	108.2
C(14)-C(12)-H(12)	108.2
C(12)-C(13)-H(13A)	109.5
C(12)-C(13)-H(13B)	109.5
H(13A)-C(13)-H(13B)	109.5
C(12)-C(13)-H(13C)	109.5
H(13A)-C(13)-H(13C)	109.5
H(13B)-C(13)-H(13C)	109.5
C(12)-C(14)-H(14A)	109.5
C(12)-C(14)-H(14B)	109.5
H(14A)-C(14)-H(14B)	109.5
C(12)-C(14)-H(14C)	109.5
H(14A)-C(14)-H(14C)	109.5
H(14B)-C(14)-H(14C)	109.5
C(6)-C(15)-C(11)	106.6(3)

C(6)-C(15)-H(15A)	110.4
C(11)-C(15)-H(15A)	110.4
C(6)-C(15)-H(15B)	110.4
C(11)-C(15)-H(15B)	110.4
H(15A)-C(15)-H(15B)	108.6
C(25)-C(16)-C(17)	111.0(3)
C(25)-C(16)-S(2)	108.7(2)
C(17)-C(16)-S(2)	101.1(2)
C(25)-C(16)-H(16)	111.9
C(17)-C(16)-H(16)	111.9
S(2)-C(16)-H(16)	111.9
C(18)-C(17)-C(19)	112.2(3)
C(18)-C(17)-C(20)	108.6(3)
C(19)-C(17)-C(20)	109.6(3)
C(18)-C(17)-C(16)	100.5(3)
C(19)-C(17)-C(16)	113.7(3)
C(20)-C(17)-C(16)	112.0(3)
O(4)-C(18)-C(17)	106.1(3)
O(4)-C(18)-C(24)	109.8(3)
C(17)-C(18)-C(24)	110.6(3)
O(4)-C(18)-H(18)	110.1
C(17)-C(18)-H(18)	110.1
C(24)-C(18)-H(18)	110.1
C(17)-C(19)-H(19A)	109.5
C(17)-C(19)-H(19B)	109.5
H(19A)-C(19)-H(19B)	109.5
C(17)-C(19)-H(19C)	109.5
H(19A)-C(19)-H(19C)	109.5
H(19B)-C(19)-H(19C)	109.5
C(17)-C(20)-C(21)	113.0(3)
C(17)-C(20)-H(20A)	109.0
C(21)-C(20)-H(20A)	109.0
C(17)-C(20)-H(20B)	109.0
C(21)-C(20)-H(20B)	109.0
H(20A)-C(20)-H(20B)	107.8
C(22)-C(21)-C(20)	110.4(3)

C(22)-C(21)-C(23)	113.5(3)
C(20)-C(21)-C(23)	106.4(3)
C(22)-C(21)-C(30)	112.6(3)
C(20)-C(21)-C(30)	110.7(3)
C(23)-C(21)-C(30)	102.9(3)
C(21)-C(22)-H(22A)	109.5
C(21)-C(22)-H(22B)	109.5
H(22A)-C(22)-H(22B)	109.5
C(21)-C(22)-H(22C)	109.5
H(22A)-C(22)-H(22C)	109.5
H(22B)-C(22)-H(22C)	109.5
C(24)-C(23)-C(25)	113.9(3)
C(24)-C(23)-C(21)	112.1(3)
C(25)-C(23)-C(21)	101.0(3)
C(24)-C(23)-H(23)	109.8
C(25)-C(23)-H(23)	109.8
C(21)-C(23)-H(23)	109.8
C(18)-C(24)-C(23)	110.1(3)
C(18)-C(24)-H(24A)	109.6
C(23)-C(24)-H(24A)	109.6
C(18)-C(24)-H(24B)	109.6
C(23)-C(24)-H(24B)	109.6
H(24A)-C(24)-H(24B)	108.2
C(23)-C(25)-C(26)	101.9(3)
C(23)-C(25)-C(16)	108.6(3)
C(26)-C(25)-C(16)	114.0(3)
C(23)-C(25)-H(25)	110.7
C(26)-C(25)-H(25)	110.7
C(16)-C(25)-H(25)	110.7
C(27)-C(26)-C(25)	117.0(3)
C(27)-C(26)-C(30)	115.6(3)
C(25)-C(26)-C(30)	104.1(3)
C(27)-C(26)-H(26)	106.4
C(25)-C(26)-H(26)	106.4
C(30)-C(26)-H(26)	106.4
C(26)-C(27)-C(28)	112.3(3)

C(26)-C(27)-C(29)	110.0(4)
C(28)-C(27)-C(29)	109.8(4)
C(26)-C(27)-H(27)	108.2
C(28)-C(27)-H(27)	108.2
C(29)-C(27)-H(27)	108.2
C(27)-C(28)-H(28A)	109.5
C(27)-C(28)-H(28B)	109.5
H(28A)-C(28)-H(28B)	109.5
C(27)-C(28)-H(28C)	109.5
H(28A)-C(28)-H(28C)	109.5
H(28B)-C(28)-H(28C)	109.5
C(27)-C(29)-H(29A)	109.5
C(27)-C(29)-H(29B)	109.5
H(29A)-C(29)-H(29B)	109.5
C(27)-C(29)-H(29C)	109.5
H(29A)-C(29)-H(29C)	109.5
H(29B)-C(29)-H(29C)	109.5
C(26)-C(30)-C(21)	106.6(3)
C(26)-C(30)-H(30A)	110.4
C(21)-C(30)-H(30A)	110.4
C(26)-C(30)-H(30B)	110.4
C(21)-C(30)-H(30B)	110.4
H(30A)-C(30)-H(30B)	108.6
C(3)-O(1)-S(1)	111.2(2)
C(18)-O(4)-S(2)	111.4(2)
O(2)-S(1)-O(3)	116.8(2)
O(2)-S(1)-O(1)	108.96(19)
O(3)-S(1)-O(1)	108.20(19)
O(2)-S(1)-C(1)	113.73(18)
O(3)-S(1)-C(1)	111.02(18)
O(1)-S(1)-C(1)	95.88(16)
O(6)-S(2)-O(5)	116.78(17)
O(6)-S(2)-O(4)	108.24(18)
O(5)-S(2)-O(4)	108.51(19)
O(6)-S(2)-C(16)	112.18(17)
O(5)-S(2)-C(16)	112.66(17)

O(4)-S(2)-C(16)	96.34(15)

Symmetry transformations used to generate equivalent atoms:

Table 4. Anisotropic displacement parameters ($Å^2$x 10^3)for mhardy001_sarpong. The anisotropic displacement factor exponent takes the form: $-2p^2[h^2a^{*2}U^{11} + ... + 2 h k a^* b^* U^{12}]$

	U^{11}	U^{22}	U^{33}	U^{23}	U^{13}	U^{12}
C(1)	29(2)	31(2)	26(2)	-1(2)	0(1)	-4(2)
C(2)	30(2)	29(2)	32(2)	-1(2)	-1(1)	-3(2)
C(3)	27(2)	38(2)	32(2)	6(2)	2(1)	-4(2)
C(4)	37(2)	27(2)	50(2)	-2(2)	-1(2)	-5(2)
C(5)	32(2)	28(2)	38(2)	1(2)	1(2)	-1(2)
C(6)	29(2)	27(2)	32(2)	3(1)	-1(1)	-4(1)
C(7)	29(2)	40(2)	42(2)	3(2)	-7(2)	-5(2)
C(8)	30(2)	29(2)	29(2)	-2(1)	2(1)	-6(2)
C(9)	36(2)	37(2)	27(2)	-1(2)	2(2)	-5(2)
C(10)	26(2)	28(2)	28(2)	1(1)	4(1)	2(1)
C(11)	28(2)	27(2)	33(2)	0(1)	5(1)	0(1)
C(12)	33(2)	35(2)	28(2)	1(2)	7(1)	6(2)
C(13)	36(2)	43(2)	30(2)	6(2)	2(2)	9(2)
C(14)	40(2)	43(2)	34(2)	7(2)	13(2)	8(2)
C(15)	26(2)	33(2)	36(2)	6(2)	5(2)	2(2)
C(16)	24(2)	24(2)	24(2)	0(1)	1(1)	2(1)
C(17)	24(2)	31(2)	24(2)	-1(1)	2(1)	1(1)
C(18)	24(2)	36(2)	31(2)	-6(2)	4(1)	1(2)
C(19)	34(2)	45(2)	28(2)	10(2)	2(2)	0(2)
C(20)	26(2)	35(2)	30(2)	2(1)	0(1)	3(1)
C(21)	22(2)	34(2)	32(2)	-2(2)	4(1)	-1(1)
C(22)	28(2)	50(2)	39(2)	-9(2)	5(2)	-8(2)
C(23)	28(2)	27(2)	30(2)	2(1)	4(1)	-2(1)
C(24)	33(2)	27(2)	39(2)	-6(2)	5(2)	1(2)
C(25)	25(2)	26(2)	25(2)	4(1)	1(1)	3(1)
C(26)	27(2)	32(2)	24(2)	1(1)	3(1)	4(1)
C(27)	35(2)	38(2)	28(2)	-6(2)	3(2)	5(2)
C(28)	42(2)	63(3)	36(2)	-19(2)	-7(2)	6(2)
C(29)	44(2)	49(3)	32(2)	-10(2)	6(2)	10(2)
C(30)	26(2)	37(2)	32(2)	-4(2)	5(1)	3(2)

O(1)	28(1)	50(2)	35(2)	3(1)	6(1)	-4(1)
O(2)	32(1)	43(2)	51(2)	1(1)	9(1)	6(1)
O(3)	31(2)	55(2)	42(2)	-6(1)	-1(1)	-9(1)
O(4)	25(1)	41(2)	43(2)	-7(1)	7(1)	4(1)
O(5)	26(1)	46(2)	41(2)	13(1)	2(1)	8(1)
O(6)	28(1)	34(1)	42(2)	5(1)	6(1)	-2(1)
S(1)	25(1)	38(1)	31(1)	0(1)	2(1)	-4(1)
S(2)	22(1)	30(1)	31(1)	2(1)	3(1)	2(1)

Table 5. Hydrogen coordinates (x 10^4) and isotropic displacement parameters ($Å^2$x 10^3) for mhardy001_sarpong.

	x	y	z	U(eq)
H(1)	3955	5780	794	34
H(3)	4340	5071	4832	39
H(4A)	3097	4368	2374	57
H(4B)	4610	4001	2923	57
H(4C)	4366	4293	1344	57
H(5A)	6623	5045	1898	39
H(5B)	6682	4929	3546	39
H(7A)	8693	6648	3997	56
H(7B)	8921	5713	3652	56
H(7C)	7966	5968	4899	56
H(8)	6070	7206	3728	36
H(9A)	5610	6161	5410	40
H(9B)	4204	6673	4958	40
H(10)	4048	7197	2131	33
H(11)	6081	7538	1105	35
H(12)	5381	6203	-677	38
H(13A)	3282	6971	-447	55
H(13B)	3812	7055	-1986	55
H(13C)	4102	7770	-889	55
H(14A)	6715	7708	-1304	58
H(14B)	6388	6995	-2399	58
H(14C)	7549	6867	-1129	58
H(15A)	7489	6070	896	38
H(15B)	8056	6881	1665	38
H(16)	8687	3294	7139	29
H(18)	9247	5028	10127	36
H(19A)	9637	3536	10818	53
H(19B)	9242	2878	9641	53

H(19C)	8048	3496	10109	53
H(20A)	11464	3466	8715	36
H(20B)	11561	4272	9630	36
H(22A)	13722	4615	8290	59
H(22B)	12764	5382	8633	59
H(22C)	13302	5263	7103	59
H(23)	10664	5434	6285	34
H(24A)	10421	5802	8704	39
H(24B)	8940	5868	7785	39
H(25)	8585	4674	5667	30
H(26)	10559	4301	4555	33
H(27)	9851	2745	5562	40
H(28A)	7699	3314	4709	72
H(28B)	8165	2666	3592	72
H(28C)	8397	3610	3323	72
H(29A)	11026	3193	2996	63
H(29B)	10649	2286	3419	63
H(29C)	11909	2763	4264	63
H(30A)	12615	4117	5724	38
H(30B)	12030	3375	6604	38

—

Table 6. Torsion angles [°] for mhardy001_sarpong.

C(10)-C(1)-C(2)-C(4)	-168.4(3)
S(1)-C(1)-C(2)-C(4)	74.7(4)
C(10)-C(1)-C(2)-C(3)	71.3(3)
S(1)-C(1)-C(2)-C(3)	-45.6(3)
C(10)-C(1)-C(2)-C(5)	-43.6(4)
S(1)-C(1)-C(2)-C(5)	-160.5(3)
C(4)-C(2)-C(3)-O(1)	-70.5(4)
C(5)-C(2)-C(3)-O(1)	167.4(3)
C(1)-C(2)-C(3)-O(1)	50.5(4)
C(4)-C(2)-C(3)-C(9)	169.7(3)
C(5)-C(2)-C(3)-C(9)	47.6(4)
C(1)-C(2)-C(3)-C(9)	-69.3(4)
C(4)-C(2)-C(5)-C(6)	171.2(4)
C(3)-C(2)-C(5)-C(6)	-64.8(4)
C(1)-C(2)-C(5)-C(6)	44.1(4)
C(2)-C(5)-C(6)-C(7)	139.6(4)
C(2)-C(5)-C(6)-C(8)	14.6(4)
C(2)-C(5)-C(6)-C(15)	-96.4(4)
C(7)-C(6)-C(8)-C(9)	-73.5(4)
C(5)-C(6)-C(8)-C(9)	48.6(4)
C(15)-C(6)-C(8)-C(9)	164.8(3)
C(7)-C(6)-C(8)-C(10)	164.4(3)
C(5)-C(6)-C(8)-C(10)	-73.5(3)
C(15)-C(6)-C(8)-C(10)	42.7(4)
O(1)-C(3)-C(9)-C(8)	-104.5(4)
C(2)-C(3)-C(9)-C(8)	12.4(4)
C(6)-C(8)-C(9)-C(3)	-65.4(4)
C(10)-C(8)-C(9)-C(3)	49.2(5)
C(9)-C(8)-C(10)-C(11)	-167.4(3)
C(6)-C(8)-C(10)-C(11)	-46.3(3)
C(9)-C(8)-C(10)-C(1)	-47.1(4)
C(6)-C(8)-C(10)-C(1)	74.1(3)
C(2)-C(1)-C(10)-C(8)	-14.7(4)
S(1)-C(1)-C(10)-C(8)	97.5(3)

C(2)-C(1)-C(10)-C(11)	98.0(4)
S(1)-C(1)-C(10)-C(11)	-149.8(3)
C(8)-C(10)-C(11)-C(12)	159.8(3)
C(1)-C(10)-C(11)-C(12)	44.0(5)
C(8)-C(10)-C(11)-C(15)	31.9(4)
C(1)-C(10)-C(11)-C(15)	-83.9(4)
C(15)-C(11)-C(12)-C(13)	174.7(3)
C(10)-C(11)-C(12)-C(13)	51.3(5)
C(15)-C(11)-C(12)-C(14)	-63.0(4)
C(10)-C(11)-C(12)-C(14)	173.7(3)
C(7)-C(6)-C(15)-C(11)	-146.8(3)
C(5)-C(6)-C(15)-C(11)	90.0(4)
C(8)-C(6)-C(15)-C(11)	-23.1(4)
C(12)-C(11)-C(15)-C(6)	-135.7(3)
C(10)-C(11)-C(15)-C(6)	-5.5(4)
C(25)-C(16)-C(17)-C(18)	69.5(3)
S(2)-C(16)-C(17)-C(18)	-45.6(3)
C(25)-C(16)-C(17)-C(19)	-170.4(3)
S(2)-C(16)-C(17)-C(19)	74.4(3)
C(25)-C(16)-C(17)-C(20)	-45.6(4)
S(2)-C(16)-C(17)-C(20)	-160.7(3)
C(19)-C(17)-C(18)-O(4)	-72.0(4)
C(20)-C(17)-C(18)-O(4)	166.8(3)
C(16)-C(17)-C(18)-O(4)	49.1(3)
C(19)-C(17)-C(18)-C(24)	169.0(3)
C(20)-C(17)-C(18)-C(24)	47.7(4)
C(16)-C(17)-C(18)-C(24)	-69.9(3)
C(18)-C(17)-C(20)-C(21)	-67.0(4)
C(19)-C(17)-C(20)-C(21)	170.2(3)
C(16)-C(17)-C(20)-C(21)	43.1(4)
C(17)-C(20)-C(21)-C(22)	140.5(3)
C(17)-C(20)-C(21)-C(23)	17.0(4)
C(17)-C(20)-C(21)-C(30)	-94.1(4)
C(22)-C(21)-C(23)-C(24)	-74.6(4)
C(20)-C(21)-C(23)-C(24)	47.0(4)
C(30)-C(21)-C(23)-C(24)	163.4(3)

C(22)-C(21)-C(23)-C(25)	163.8(3)
C(20)-C(21)-C(23)-C(25)	-74.6(3)
C(30)-C(21)-C(23)-C(25)	41.8(3)
O(4)-C(18)-C(24)-C(23)	-103.2(4)
C(17)-C(18)-C(24)-C(23)	13.6(4)
C(25)-C(23)-C(24)-C(18)	48.2(4)
C(21)-C(23)-C(24)-C(18)	-65.7(4)
C(24)-C(23)-C(25)-C(26)	-168.7(3)
C(21)-C(23)-C(25)-C(26)	-48.3(3)
C(24)-C(23)-C(25)-C(16)	-48.0(4)
C(21)-C(23)-C(25)-C(16)	72.4(3)
C(17)-C(16)-C(25)-C(23)	-12.2(4)
S(2)-C(16)-C(25)-C(23)	98.1(3)
C(17)-C(16)-C(25)-C(26)	100.6(3)
S(2)-C(16)-C(25)-C(26)	-149.1(3)
C(23)-C(25)-C(26)-C(27)	164.9(3)
C(16)-C(25)-C(26)-C(27)	48.1(4)
C(23)-C(25)-C(26)-C(30)	36.0(4)
C(16)-C(25)-C(26)-C(30)	-80.9(4)
C(25)-C(26)-C(27)-C(28)	50.4(5)
C(30)-C(26)-C(27)-C(28)	173.7(4)
C(25)-C(26)-C(27)-C(29)	173.0(3)
C(30)-C(26)-C(27)-C(29)	-63.7(4)
C(27)-C(26)-C(30)-C(21)	-139.7(3)
C(25)-C(26)-C(30)-C(21)	-9.9(4)
C(22)-C(21)-C(30)-C(26)	-142.2(4)
C(20)-C(21)-C(30)-C(26)	93.7(4)
C(23)-C(21)-C(30)-C(26)	-19.6(4)
C(9)-C(3)-O(1)-S(1)	86.3(3)
C(2)-C(3)-O(1)-S(1)	-33.6(4)
C(17)-C(18)-O(4)-S(2)	-30.7(4)
C(24)-C(18)-O(4)-S(2)	88.8(3)
C(3)-O(1)-S(1)-O(2)	-113.9(3)
C(3)-O(1)-S(1)-O(3)	118.1(3)
C(3)-O(1)-S(1)-C(1)	3.7(3)
C(10)-C(1)-S(1)-O(2)	21.5(3)

C(2)-C(1)-S(1)-O(2)	140.0(3)
C(10)-C(1)-S(1)-O(3)	155.7(3)
C(2)-C(1)-S(1)-O(3)	-85.8(3)
C(10)-C(1)-S(1)-O(1)	-92.2(3)
C(2)-C(1)-S(1)-O(1)	26.3(3)
C(18)-O(4)-S(2)-O(6)	117.0(3)
C(18)-O(4)-S(2)-O(5)	-115.3(3)
C(18)-O(4)-S(2)-C(16)	1.1(3)
C(25)-C(16)-S(2)-O(6)	158.0(2)
C(17)-C(16)-S(2)-O(6)	-85.2(3)
C(25)-C(16)-S(2)-O(5)	23.7(3)
C(17)-C(16)-S(2)-O(5)	140.6(2)
C(25)-C(16)-S(2)-O(4)	-89.4(3)
C(17)-C(16)-S(2)-O(4)	27.5(3)

Appendix 2C. Cartesian Coordinates of Computed Structures for Chapter 2

Cartesian coordinates for 17

C 1.40302200 -1.61964800 -0.21904100

C 2.37425000 -0.46079800 -0.05906200

C 0.79719600 0.75471400 1.17554800

C -0.30911700 -0.31182800 1.06655300

H -0.69162300 -0.60120200 2.06016400

C 2.18649600 0.14712700 1.33388200

H 2.93885200 0.92986800 1.52455500

H 2.25204700 -0.59453300 2.14536700

C 0.81203800 1.44034700 -0.23195900

H 3.40127300 -0.80804300 -0.25035500

H 0.54120400 1.47027100 1.97227700

C 0.18686200 -1.53890400 0.34028000

H -0.50660900 -2.38197900 0.24260800

C -0.58094500 1.12793600 -0.84431500

H -1.07526700 2.03956100 -1.21296300

H -0.48396200 0.44911300 -1.70744900

C -1.39661200 0.43722000 0.25970000

H -1.79892400 1.21884000 0.93306300

C 1.05396100 2.94543400 -0.13521000

H 1.97455600 3.16893800 0.42885500

H 1.15890300 3.39830000 -1.13529900

H 0.21760400 3.45174900 0.37402500

C 1.87076100 -2.80132100 -1.01409000

H 1.09308300 -3.57381200 -1.10789400

H 2.16986500 -2.49147100 -2.03036100

H 2.76194200 -3.26156500 -0.55407200

C -2.58640700 -0.39319200 -0.23838200

H -2.19575500 -1.14463100 -0.94866800

C -3.58938900 0.47697400 -0.99707200

H -3.13660100 0.95869100 -1.87714900

H -4.44376700 -0.12044000 -1.35336900

H -3.99093400 1.27476200 -0.34878100

C -3.27822500 -1.13727300 0.90382500

H -2.60852900 -1.85810300 1.39724700

H -3.63573400 -0.43342000 1.67476600

H -4.15255800 -1.69940800 0.53853400

C 1.99343200 0.72921900 -0.96311400

H 1.73072500 0.42129700 -1.98703600

H 2.85627800 1.41117100 -1.04333300

Cartesian coordinates for A-TS1

C -1.00010500 0.32886700 0.91593400

C -0.92223300 1.75923900 0.43066300

C 0.66556800 1.20672300 -1.21458800

C 0.66568400 -0.29411900 -0.88603500

H 0.48179300 -0.95909300 -1.74475300

C -0.72169700 1.82475900 -1.08679500

H -0.70987000 2.87745800 -1.40218100

H -1.49775800 1.32550200 -1.68202300

C 0.41460900 2.37416800 0.92318300

H 0.31217200 3.46652800 0.84915300

H 0.64888500 2.15407300 1.97444500

C 1.50682300 1.85663600 -0.06403500

H -1.79767800 2.31148700 0.79662400

H 1.12294000 1.35817500 -2.20156900

C -0.24812000 -0.63197800 0.21259400

H -0.29927100 -1.67316000 0.55479300

C 2.36432100 0.70390000 0.52902700

H 3.42898400 0.97115800 0.56541800

H 2.06985400 0.47813600 1.56880600

C 2.13118200 -0.53024000 -0.34995500

H 2.74637700 -0.43999500 -1.26277800

C 2.37729800 3.00521900 -0.57079100

H 1.77548100 3.75582600 -1.10601800

H 2.88302200 3.51329200 0.26425700

H 3.15140300 2.63733100 -1.26115400

C -1.46001200 0.08260100 2.32703500

H -2.42330300 0.57570800 2.51651600

H -1.52616200 -0.98215200 2.58194900

H -0.71695000 0.55236000 2.99057700

C 2.44371300 -1.88676800 0.29317100

H 1.86641000 -1.96602700 1.23490200

C 3.92536000 -1.96362100 0.66673200

H 4.21061300 -1.18175900 1.38476400

H 4.15998900 -2.93499200 1.12453900

H 4.56045400 -1.85325500 -0.22688000

C 2.05279800 -3.05542900 -0.61360100

H 0.97055400 -3.09823100 -0.81816300

H 2.57127800 -2.98814300 -1.58340100

H 2.32999200 -4.01513200 -0.15524900

S -2.68036400 -0.67851900 -0.14762300

O -2.93099900 -1.89168000 0.58709000

O -3.53380300 0.47291100 -0.16452600

O -2.32455900 -1.04345600 -1.66067700

H -2.28963000 -2.01072100 -1.77094700

Cartesian coordinates for 6

C 1.29729400 -1.60056900 -0.26515300

C 2.36631500 -0.65256300 0.04416200

C 0.86087800 0.74056600 1.20223500

C -0.33335000 -0.22941800 1.15239000

H -0.75396900 -0.40609700 2.15067400

C 2.18457800 0.00628200 1.40806700

H 3.01260700 0.70776600 1.58219400

H 2.16732000 -0.71137000 2.24191000

C 0.93543600 1.34851900 -0.24351800

H 3.34825000 -1.09387000 -0.17849900

H 0.67864300 1.51505100 1.95897400

C -0.43403500 1.01730500 -0.89269100

H -0.85860300 1.88843000 -1.41124700

H -0.32667400 0.22693000 -1.65811900

C -1.33109200 0.50486500 0.23716300

H -1.67516200 1.37674900 0.82447800

C 1.21068700 2.84895000 -0.22711500

H 2.11520500 3.08307700 0.35665400

H 1.35726300 3.23754200 -1.24765100

H 0.36739100 3.39533400 0.22367900

C 1.41376200 -2.53942000 -1.37934500

H 2.39801000 -2.53726000 -1.86044800

H 1.14925500 -3.55061400 -1.02258300

H 0.62337100 -2.28840200 -2.11006200

C -2.57932800 -0.26351200 -0.21367000

H -2.25070300 -1.10783800 -0.84763800

C -3.48295800 0.61993000 -1.07459700

H -2.97525100 0.96251300 -1.98883000

H -4.38674900 0.07351200 -1.38611000

H -3.80911900 1.51409300 -0.51731400

C -3.35218100 -0.83813000 0.97288900

H -2.75753400 -1.56616300 1.54652800

H -3.66031800 -0.03875000 1.66749800

H -4.26419300 -1.35451600 0.63529000

C 2.09889700 0.57625700 -0.91155100

H 1.90151400 0.29298400 -1.95482700

H 3.03663500 1.15001400 -0.89548200

C 0.10540100 -1.59949700 0.57706800

H 0.51093300 -2.20854900 1.42189900

H -0.70993800 -2.19796700 0.15102000

Cartesian coordinates for 2A

C 0.71842100 -1.19320700 0.97960200

C 0.22055100 -2.34253600 0.27520000

C -0.97941000 -1.01100400 -1.26012100

C -0.37294400 0.32817500 -0.81224800

H 0.09819700 0.85484100 -1.65223900

C 0.02606500 -2.15533100 -1.22246700

H -0.40455000 -3.07607900 -1.64017200

H 0.96327400 -1.94994400 -1.75737700

C -1.31516700 -2.31143200 0.78168800

H -1.62290300 -3.35556500 0.62666200

H -1.43501700 -2.08838200 1.84996700

C -2.04598000 -1.33045300 -0.16142800

H 0.68512800 -3.27069000 0.63243400

H -1.43842700 -0.87946000 -2.24849800

C 0.70167600 0.13933300 0.29228100

H 0.66791900 0.94838400 1.03623900

C -2.35268500 0.03024700 0.51848500

H -3.43319400 0.22358700 0.56711100

H -1.98904100 0.04032800 1.56130300
C -1.60485700 1.09562200 -0.29188700
H -2.19583800 1.31564000 -1.19921400
C -3.29826200 -1.98186500 -0.74231900
H -3.04613800 -2.87520300 -1.33531400
H -3.99311800 -2.28894600 0.05515400
H -3.82953400 -1.27711900 -1.40023800
C 1.20561500 -1.28577200 2.35033000
H 0.77067500 -0.49160700 2.97765000
H 1.07484400 -2.28111000 2.78851600
H 2.28769100 -1.04589000 2.30599700
S 2.39770600 0.35114100 -0.39288500
O 2.98813800 -0.94094300 -0.69556100
O 2.36980400 1.38291200 -1.40384600
O 3.06773400 0.92229400 0.94374900
H 4.03640500 0.79902800 0.93029200
C -1.37206300 2.42916000 0.42878900
H -0.84283800 2.22334300 1.37879100
C -2.70405100 3.08178400 0.79978700
H -3.30741300 2.44551200 1.46480400
H -2.53915600 4.03795600 1.31991000
H -3.30470500 3.29126300 -0.10093300
C -0.51058700 3.38263400 -0.39893800
H 0.50027400 2.98774900 -0.58196300
H -0.97246000 3.57738400 -1.38105600
H -0.39671000 4.35049600 0.11306300

Cartesian coordinates for 3A

C 0.79424300 -1.22198100 0.86432500
C 0.76629000 -2.30287600 -0.02681900
C -0.90448500 -1.11197200 -1.27939400

C -0.45900300 0.28947200 -0.84412000
H -0.04145700 0.86698300 -1.67828800
C 0.23344300 -2.11668100 -1.41025700
H -0.10371600 -3.07818700 -1.81627500
H 1.05427700 -1.74937000 -2.04779200
C -0.74732800 -2.03395600 0.95853800
H -0.71833700 -3.13041100 1.09231800
H -0.87745400 -1.66856900 1.98851700
C -1.77521000 -1.54834000 -0.07278800
H 1.23544000 -3.24181800 0.27649400
H -1.49885600 -1.03878900 -2.19889400
C 0.59522200 0.17581700 0.28523300
H 0.40157200 0.88997000 1.09919100
C -2.47998200 -0.25269900 0.39340200
H -3.55229600 -0.29498100 0.16026400
H -2.39378400 -0.12391900 1.48386900
C -1.78762500 0.90570900 -0.35326600
H -2.35555500 1.10793100 -1.27761900
C -2.74249300 -2.67953900 -0.39991800
H -2.20859100 -3.56117800 -0.78463600
H -3.30216500 -2.98360000 0.49696300
H -3.46251600 -2.34627700 -1.16044700
C 1.55754000 -1.34168400 2.15602700
H 1.19538700 -0.61010400 2.88953300
H 1.45979700 -2.35621500 2.56298900
H 2.62174500 -1.15391300 1.95860400
S 2.24080500 0.68952400 -0.32938600
O 2.98574000 -0.47459600 -0.77078500
O 2.09452600 1.82485000 -1.22305600
O 2.98316300 1.18011500 0.99579000
H 2.72711700 2.09425200 1.23308400

C -1.72955500 2.21853600 0.43102400

H -1.23913400 2.02412300 1.40189600

C -3.14614700 2.70902900 0.72810700

H -3.71969000 1.97441500 1.31188500

H -3.12237200 3.64829300 1.29971600

H -3.69188500 2.89746000 -0.21049400

C -0.93527600 3.28716600 -0.31346000

H 0.11585700 2.99790200 -0.45346900

H -1.37059300 3.46562200 -1.31017800

H -0.95090400 4.23905400 0.23754700

Cartesian coordinates for A-TS3

C 0.85797800 -1.16229200 0.85464200

C 1.23651700 -2.06399300 -0.20017800

C -0.76121000 -1.19646100 -1.26494700

C -0.49922200 0.25204900 -0.83130500

H -0.14003100 0.87394200 -1.66126600

C 0.50413900 -2.01789400 -1.46264100

H 0.32640700 -3.04316700 -1.82444100

H 1.19279000 -1.57372400 -2.20897000

C -0.50276300 -2.01912100 1.03865700

H -0.25487600 -3.09681900 1.08702000

H -0.81334700 -1.76316600 2.06268400

C -1.55935600 -1.73435200 -0.04254100

H 1.94249800 -2.87709900 0.00978900

H -1.37321400 -1.20605300 -2.17627200

C 0.54436100 0.24366100 0.31334900

H 0.25690100 0.90965900 1.13850300

C -2.45793900 -0.53796400 0.36189800

H -3.50174800 -0.73057800 0.07778400

H -2.45463000 -0.39483000 1.45414400

C -1.90029400 0.70185500 -0.36722400

H -2.47056800 0.83517000 -1.30274800

C -2.35466200 -3.00045000 -0.34276100

H -1.70114100 -3.82002300 -0.68199900

H -2.89001000 -3.34922000 0.55420800

H -3.09982400 -2.81122400 -1.12980700

C 1.69596100 -1.22463200 2.12083500

H 1.27351100 -0.56281400 2.88948300

H 1.70784700 -2.25043400 2.51531900

H 2.73411000 -0.92415600 1.92959000

S 2.13000000 0.92415000 -0.29372400

O 2.92668100 -0.20132000 -0.76732600

O 1.89771100 2.06311800 -1.16206700

O 2.85632700 1.43527400 1.03399300

H 2.70679300 2.38764600 1.17770100

C -2.01917100 2.01702500 0.41188200

H -1.52250900 1.88843000 1.39237700

C -3.48872400 2.33381600 0.69322200

H -3.98337200 1.53612200 1.26808700

H -3.58566200 3.26582000 1.27108500

H -4.04891700 2.46522600 -0.24759600

C -1.34567600 3.17834300 -0.31661900

H -0.26457000 3.02335000 -0.44512200

H -1.77957800 3.31701700 -1.32100300

H -1.48226100 4.12042000 0.23662100

Cartesian coordinates for 1

C -1.48045700 -0.09267800 0.91170100

C -2.47015400 -0.05073600 -0.27841500

C -0.30149100 0.57450300 -1.36970400

C 0.43320500 -0.54300300 -0.69729000

H 0.48652800 -1.34309400 -1.46167200

C -1.77691000 0.56364700 -1.50567500

H -2.15181600 1.57580300 -1.70931500

H -1.99570900 -0.01986700 -2.41909400

C 0.13233900 1.80680400 0.12547900

H -3.33821800 0.56117500 0.00111700

H 0.24295900 1.10097100 -2.16106100

C 1.54151300 1.31973300 0.40686700

H 2.26272400 2.11004100 0.16374200

H 1.61748100 1.10449500 1.48486500

C 1.82710800 0.03089500 -0.39879600

H 2.26150000 0.32467500 -1.36916000

C -0.00712200 3.15804900 -0.47797500

H -1.02349500 3.36405200 -0.83684800

H 0.20352700 3.86730600 0.34780600

H 0.73920300 3.33918900 -1.26222300

C -2.18926500 -0.54429900 2.18064400

H -1.47825500 -0.58445100 3.01766100

H -2.99894500 0.15257100 2.44256700

H -2.62048800 -1.54694700 2.04721700

C 2.81733700 -0.91555400 0.28329100

H 2.44592400 -1.12932700 1.29987500

C 4.18140300 -0.24103200 0.41689400

H 4.12054600 0.69365300 0.99356300

H 4.89508900 -0.90413700 0.92685600

H 4.59169900 -0.00154000 -0.57727400

C 2.93299100 -2.23469500 -0.47536500

H 1.98632200 -2.79528100 -0.47020700

H 3.21873100 -2.05593100 -1.52469800

H 3.70242500 -2.87584400 -0.02089200

C -0.96152500 1.35802800 1.07397200

H -0.52314500 1.44170200 2.08298400

H -1.81149400 2.05267300 1.00482200

C -0.31615000 -1.02837100 0.56022900

H -0.70568600 -2.04668600 0.41989100

H 0.36822800 -1.06871100 1.41977700

N -2.96344800 -1.36286400 -0.55805300

C -3.32140800 -2.45736500 -0.74484500

Cartesian coordinates for 3

C 2.07338000 0.90857600 -0.18458500

C 0.17985800 1.10890800 1.17713500

C -0.38231900 -0.28358500 0.82915800

H -0.42835600 -0.90988300 1.73424700

C 1.69214000 1.18612200 1.26811400

H 2.01003200 2.19958600 1.55973100

H 2.13477300 0.48312800 1.98798800

C -0.19085600 1.96082700 -0.06765800

H 3.11828700 1.16776000 -0.41273800

H -0.32377600 1.47339300 2.08594000

C -1.47655900 1.29303500 -0.62461500

H -2.31126200 2.00743500 -0.67985900

H -1.32293800 0.91903600 -1.65067200

C -1.79276000 0.12852800 0.33554500

H -2.30455300 0.56218300 1.21549800

C -0.42723000 3.42932300 0.27895000

H 0.44588400 3.86907900 0.78809800

H -0.61805000 4.02542000 -0.62882000

H -1.29770400 3.54285800 0.94524600

C -2.73120700 -0.95231200 -0.21563200

H -2.20574400 -1.49401000 -1.02263200

C -3.98979700 -0.33716500 -0.83148800

H -3.76112700 0.29220700 -1.70457800

H -4.68654300 -1.12237100 -1.16581900

H -4.52387100 0.28894400 -0.09624700

C -3.12131700 -1.95446900 0.87186400

H -2.24622500 -2.40127000 1.36635200

H -3.72318300 -1.46079100 1.65363100

H -3.72618300 -2.77699000 0.45795700

C 1.07874000 1.79676000 -0.96625400

H 0.83593800 1.39665900 -1.96114700

H 1.54946000 2.77716700 -1.13539200

C 0.40993800 -1.05097800 -0.27400000

H -0.05492400 -0.80629800 -1.24169600

C 0.29721100 -2.56440800 -0.09170900

H -0.74700900 -2.89251900 -0.17221000

H 0.86856500 -3.11627800 -0.85315000

H 0.66744800 -2.87536700 0.89742500

C 1.89207400 -0.60211600 -0.48057700

C 2.37860800 -0.94521400 -1.89297500

H 3.43839600 -0.67382500 -2.00720600

H 2.27569100 -2.01892400 -2.10323800

H 1.79611900 -0.39158700 -2.64144300

N 2.74556000 -1.32108500 0.43253800

C 3.43041900 -1.92468900 1.16155400

Cartesian coordinates for 2B

C -0.14014600 2.01558600 -0.48844800

C -1.38804500 1.01519300 1.22308400

C -1.33458200 -0.40460000 0.62677400

H -0.81063400 -1.08763900 1.31401200

C -0.13134000 1.84284000 1.02917100

H -0.23503600 2.82301800 1.51911600

H 0.77974800 1.37519400 1.43180200

C -2.47048000 1.72258100 0.36178500

H 0.54600400 2.79823900 -0.84509300

H -1.69049900 0.93982300 2.27842700

C -3.40980800 0.57526100 -0.09714600

H -4.45043800 0.76028900 0.20608100

H -3.42161000 0.48146400 -1.19589600

C -2.85267900 -0.70742300 0.55198200

H -3.20614700 -0.72314000 1.59986400

C -3.22947400 2.79264400 1.14327100

H -2.54283700 3.53930100 1.57433900

H -3.93916500 3.32886600 0.49228800

H -3.80315600 2.34414000 1.97003900

C -3.31288000 -2.02836500 -0.07678600

H -2.87626100 -2.10694000 -1.08897000

C -4.83381700 -2.06652600 -0.23930500

H -5.19786300 -1.29579300 -0.93491600

H -5.16103900 -3.04307600 -0.62987200

H -5.33837800 -1.91090500 0.72949600

C -2.84804500 -3.22767000 0.75087300

H -1.76157900 -3.22607200 0.92452100

H -3.33760700 -3.22685500 1.73933400

H -3.10489300 -4.17711100 0.25505800

C -1.61611200 2.36764200 -0.77825300

H -1.94338800 2.05200400 -1.77915100

H -1.71523500 3.46290800 -0.75263700

C -0.66887800 -0.49943500 -0.77932900

H -1.46614300 -0.40166900 -1.53176700

C -0.00758700 -1.86019000 -1.00019100

H -0.75574900 -2.66139700 -0.95875600

H 0.48490400 -1.93201400 -1.98168400

H 0.74160700 -2.07639100 -0.22179500

C 0.27889200 0.68327500 -1.16039100

C 0.41936800 0.83460600 -2.67796100

H 1.13784800 1.63044000 -2.92126800

H 0.75478700 -0.09906100 -3.14928900

H -0.55474400 1.10525400 -3.10414200

N 1.60539300 0.37872100 -0.66864900

C 2.65011200 0.09943700 -0.27935700

Si 4.39132800 -0.41167700 0.40714800

C 4.12901800 -0.39495100 2.24533500

H 5.06949800 -0.68148800 2.74476300

H 3.84663500 0.60698100 2.60416300

H 3.35177600 -1.11335600 2.54880000

C 4.64642200 -2.09596200 -0.33334300

H 4.64370900 -2.05904500 -1.43382000

H 5.62580300 -2.48623700 -0.00984100

H 3.87279400 -2.80485600 0.00012500

C 5.52331100 0.90960000 -0.23978300

H 6.55108800 0.69697000 0.09860600

H 5.52824800 0.93438900 -1.34050000

H 5.24211400 1.90493700 0.13713300

Cartesian coordinates for 25-H$^+$

C -0.89923500 0.95036600 0.94739300

C -1.75826600 1.43996500 -0.23216400

C 0.52381000 1.21686500 -1.24535900
C 0.55038000 -0.25894200 -0.81124100
H 0.26903200 -0.94698100 -1.61977700
C -0.88134300 1.79446300 -1.42923900
H -0.82447600 2.88904900 -1.50946000
H -1.35936900 1.43221400 -2.35004300
C 1.28280000 1.87405000 -0.06489500
H -2.47067400 2.21909500 0.05618700
H 1.10665400 1.32261200 -2.17136200
C -0.41133900 -0.41943400 0.40119800
H -0.07732100 -1.12500900 1.17503700
C 2.43251700 0.87552900 0.22578600
H 3.37375500 1.24213900 -0.20762600
H 2.59622700 0.77159000 1.30979900
C 2.02343700 -0.46990100 -0.41352500
H 2.55488200 -0.57661100 -1.37407400
C 1.80272100 3.27064200 -0.37610500
H 0.98173600 3.95568900 -0.63701800
H 2.32316600 3.69044300 0.49872500
H 2.51349300 3.24263300 -1.21536400
C -1.69577700 0.85898900 2.24503300
H -1.13403600 0.28563900 2.99540200
H -1.85505400 1.87491200 2.63194800
H -2.68184500 0.39512500 2.11324900
S -1.94199400 -1.08536700 -0.26308900
O -2.64127600 0.27625600 -0.57920400
O -1.91183200 -1.97803900 -1.39039500
O -2.72876400 -1.70831100 0.93342000
H -3.30527600 -2.45855300 0.65799700
C 2.34210400 -1.71876800 0.41129900
H 1.90127800 -1.59466500 1.41687100

C 3.85271100 -1.85934700 0.58784200

H 4.28894500 -0.97207700 1.06972500

H 4.09648100 -2.73438300 1.20785900

H 4.34311100 -1.98940800 -0.39020500

C 1.75727300 -2.97458600 -0.23106600

H 0.65812200 -2.94448500 -0.29252000

H 2.14357000 -3.09693400 -1.25577800

H 2.02986300 -3.87240300 0.34260500

C 0.28336800 1.92031800 1.11418700

H 0.78485200 1.71058800 2.06954200

H -0.16121000 2.92516500 1.2022670

Chapter 3. Introduction to Computer-Assisted Retrosynthesis Planning Programs

3.1 Introduction

In this chapter, I introduce computer-assisted retrosynthetic logic, and consider both the manner by which computers disconnect a molecule and the strategic value of a given transformation. In doing so, I summarize the necessary considerations, capabilities, and limitations of modern retrosynthetic computer programs. This area of research has a long history,[1] and today enjoys a resurgence that has been enabled in part by the availability of digitized reaction data from sources like Reaxys® and SciFinder®. I define and discuss two distinct approaches, both of which aim to automate the process of applying traditional logic and heuristics to synthesis but have different levels of human-input required: a) high level logic-based programs and b) detailed retrosynthetic planners.

3.1.1 Traditional Logic

Retrosynthesis was defined by Corey in the 1960's to describe the iterative process of reducing a complex target molecule into a simple precursor by breaking bonds[1a] to arrive at a readily available compound. This recursive analysis revolutionized complex molecule synthesis and introduced rules that were codified in an express attempt to develop computer-assisted synthesis.[2] After all, understanding the logic of retrosynthesis is necessary in order to program a computer to automate the process.

The game of chess is often employed as a metaphor for organic synthesis.[3] Similarly to chess, several attempts have been made to apply computer-assisted logic to organic synthesis. However, unlike games like chess, one reason chemical synthesis cannot be easily solved is the non-trivial evaluation of whether a given retrosynthetic transformation will make the route more efficient overall, both strategically and experimentally. Therefore, rather than concrete rules for retrosynthesis, heuristics or guidelines that were first codified in the Logic and Heuristics Applied to Synthetic Analysis (LHASA) are favored.[4] Unlike chess, the value of each move, and even the overall objective of the route, are open to interpretation through a chemical lens. In any event, chess was a logical proving ground for the advancement of artificial intelligence with the Deep Blue chess program.[5] More recently, the more sophisticated game of Go has succumbed to computational planning, with the AlphaGo program able to beat the world's best Go players.[6] The logical and creative nature of organic synthesis has made it attractive as a higher computational bar to clear.

3.2 High Level Logic-Based Programs

High level logic-based retrosynthetic programs (Figure 1a) are designed to apply a particular heuristic to a given compound and are intended to be used with significant input from an experienced user. First, this requires the identification of a specific heuristic followed by the

application of an algorithm that can modify the molecular representation and present routes or key disconnections. Once the proposed solutions are generated, significant human input is required to transform the heuristic solutions into a synthetic plan to execute in the laboratory. This is distinct from a detailed retrosynthetic planner which typically produces a synthesis plan without additional human input (Figure 1b).

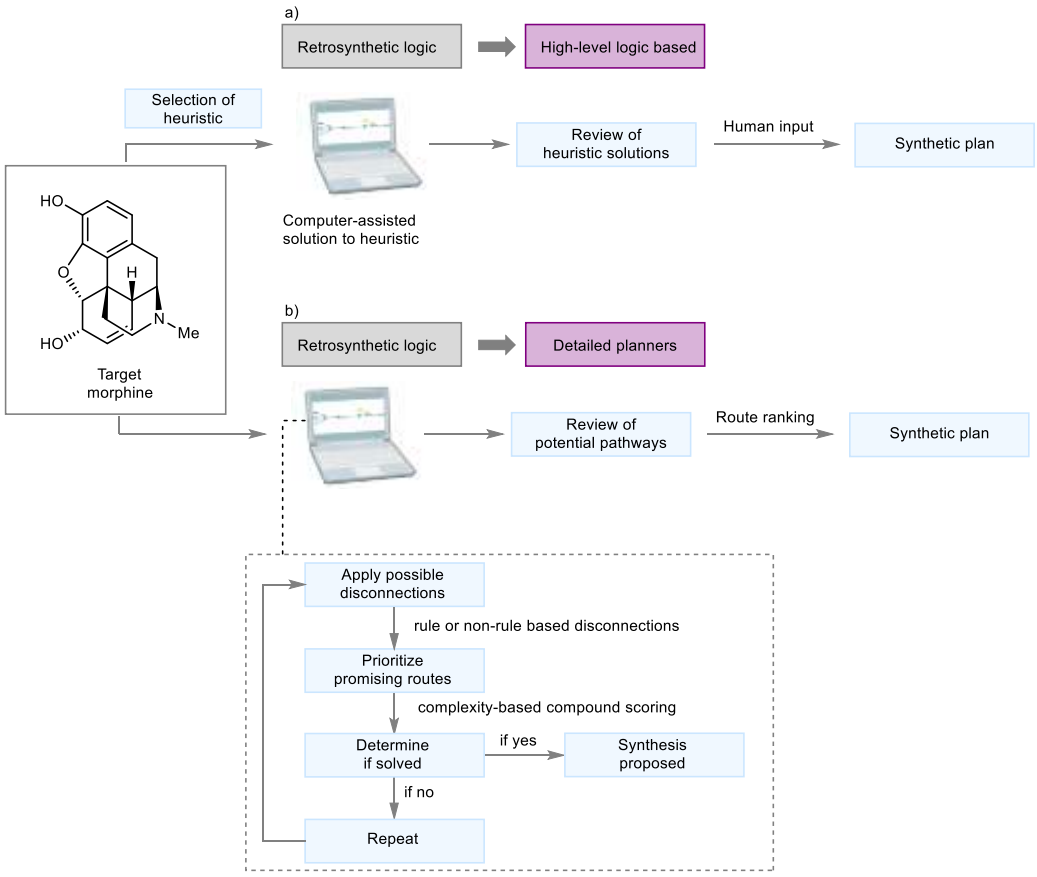

Figure 1. a) Workflow for high- level logic- based retrosynthetic planners showcasing significant human input in the planning stages. b) General workflow employed iteratively for detailed retrosynthetic planners.

3.2.1 General Considerations for Developing High Level Logic-Based Programs

For any high-level logic-based program, the algorithms used are defined by the heuristic to be applied and can be highly specialized. For example, it can be advantageous for a synthetic route toward a chiral, enantioenriched molecule to start from readily available enantioenriched precursors to obviate the need to install stereocenters using asymmetric reactions. On the basis of this guideline, many programs have been developed to map readily available enantioenriched starting materials to a particular target.[4, 7] In the case of starting material-based programs, the software is based on similarity recognition while application of bond-network analysis requires software specifically trained to analyze the molecule as a graph.

3.2.2 Results from High Level Logic-Based Programs

Given the variety of heuristics that can be applied, the results from high level logic-based programs are far from uniform. For example, some programs allow the chemist to apply a particular transform, in which case the software will output any proposed instance of, for example, the Diels–Alder cycloaddition to build the core of the molecule (Figure 2a).[4] Ultimately, in this case, the user selects the desired transform-based strategy (e.g., Robinson annulation, sigmatropic rearrangements etc.) and must select the most promising proposal manually.

Another well-recognized strategy for the synthesis of topologically complex molecules is the use of network analysis to identify the most impactful bond to disconnect in simplifying a topologically complex structure (Figure 2b).[8] In this case, the software can identify a particular bond or ring that may be advantageous to disconnect in a retrosynthetic fashion while proposals of particular transformations would be left to the chemist user.

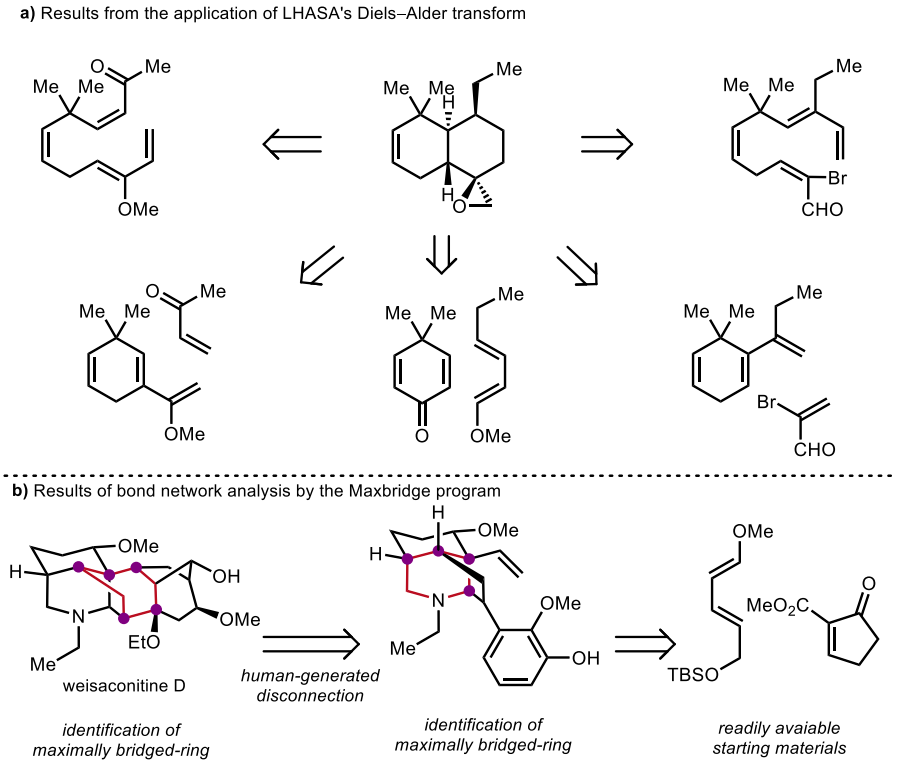

Figure 2. Example results from retrosynthetic planning programs. a. Results of a Diels-Alder transform from application of Logic and Heuristics Applied to Synthetic Analysis (LHASA) to a fused bicycle. b. Results of bond-network analysis by the program Maxbridge as applied to the synthesis of diterpenoid alkaloid weisaconitine D.

It is worth noting that a given heuristic, by definition, does not perform equally well on all molecules. For example, as an analysis that seeks to reduce structural complexity by breaking apart bridged structures, applications of bond-network analysis can only be invoked in the synthesis of bridged molecules. Therefore, evaluation and direct comparison of different programs is a challenge and each program is, by intention, applicable or advantageous only in certain cases.

3.2.3 Case Study: Logic and Heuristics Applied to Synthetic Analysis

The LHASA program is a forerunner in the field that is intimately tied to the development of retrosynthesis as a whole.[9] Additionally, while the strategies implemented in LHASA have been refined since their initial publication, they form the basis of high-level logic approaches. LHASA is no longer available. However, it serves as an important foundation in the field. For this reason, our first case study is the application of LHASA's chiral starting material program to the synthesis of bicycle **1** (Figure 3). In this case, the mapping heuristic was able to identify a non-obvious starting material, citronellol. After the program identified the material, the chemist users interfaced with LHASA's detailed planner to arrive at a complete retrosynthesis. Independently, comparisons with published work[10] indicated this was a viable strategy that had been previously carried out successfully in the lab. This case exemplifies one goal of applying these programs in that they can occasionally find non-intuitive solutions that may not be obvious to the human observer, and can lead to efficient syntheses.

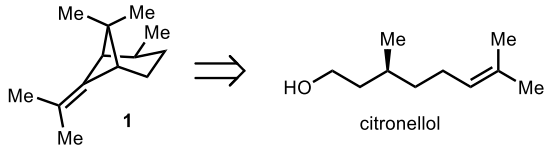

Figure 3. Identification of a non-obvious enantioenriched, abundant starting material citronellol by Logic and Heuristics Applied to Synthetic Analysis (LHASA).

3.3 Detailed Retrosynthetic Planners

An orthogonal strategy is the development of detailed synthetic planners that do not require human input in the planning process. In software such as these, chemists do not need to select a particular heuristic to apply, rather one can simply input the synthetic target and review the solution(s) provided (Figure 1b).

3.3.1 General Considerations for Developing Detailed Retrosynthetic Planners

Instead of merely identifying strategic elements, detailed retrosynthetic planners propose discrete intermediate compounds which can be used as stepping stones to reach the target. This process requires a module that disconnects the target compound into potential precursors and reports back a proposed structure to the user.[11] Internally, these modules typically apply either rule-based or rule-free methods to propose possible transforms.

Rule-based methods are conceptually akin to the process of an organic chemist selecting a known reaction type to apply to a particular synthetic target. It follows that one way to build the necessary reaction rules is to have expert organic chemists encode a transform defined by the substructures of the products and reactants as well as necessary molecular context (e.g., functional group compatibility, stereoselectivity, etc.). Indeed, this approach has been well implemented in state-of-the-art detailed synthesis planners;[12] however, building a library of expert-coded rules is both extremely laborious and inherently dependent on the expertise of the coders. As a result, a growing area of research is the automatic generation of the reaction rules from accessible reaction databases.[13] In this process, typically, a library of reaction templates is extracted from each reaction

within the database. In a rule-based approach, these templates are then clustered and processed with additional molecular context to automatically generate explicit reaction rules.[14] Other approaches apply templates directly to the target; in these cases, filters (e.g., similarity-based neural networks) are often used to apply only a chemically relevant subset of the template library to reduce the required computational power.[15] While these methods are common in state-of-the-art detailed synthesis planners, it is worth noting that there is significant computational cost in automatically extracting rule or template libraries; additionally, such libraries inherently exclude rare reactions with sparse literature examples.

In contrast, rule-free methods bypass the need to build a library of reaction rules by directly mapping products to potential starting materials. Early examples in this field recognized that by representing molecules as text (e.g., SMILES strings), retrosynthesis could be treated like a natural language processing problem in which the target molecule (one language) is translated to reactants (another language).[16] Implementation of sequence-to-sequence neural networks was able to effectively generate single-step retrosyntheses.[17] One inherent challenge to this approach is that not all generated SMILES strings lead to a valid chemical structure.[18] Subsequent research built upon this work by applying the newly developed transformer neural networks which have been able to more accurately produce valid SMILES strings.[19] Recently, rule-free approaches have also been developed which represent the molecules as information-rich subgraphs rather than as a string of text.[20] Compared to rule-based approaches, rule-free methods are more generalizable and have a lower associated computational cost; however, they lack comparative interpretability. Today, rule-based or template-based methods are more common in detailed retrosynthetic planners but multi-step rule-free planners are emerging[19a] and remain an important area of development.

As one considers multi-step syntheses, applying these approaches to generate simplifying transformations will lead to an exponential increase in the number of precursor compounds analyzed.[3b] To prioritize among this amalgam of possibilities, a program must rank the most promising disconnections to navigate the synthetic tree; this navigation strategy will significantly impact the output synthetic route. One example is the use of a Monte Carlo tree search with reinforcement learning to balance exploration against exploitation in navigating the synthesis search space.[21] Additionally, while promising disconnections typically reduce complexity, developing an objective measure for ranking synthetic transformations can be particularly difficult as an ideal synthesis is concerned only with target relevant synthetic complexity which cannot be locally determined. Moreover, there is no guarantee that an ideal synthesis for a given target can be achieved with currently available methods or that application of a particular transform will be feasible in the forward synthetic sense. For this reason, many measures of structural complexity[22] have been applied,[3b] however recent efforts have focused toward implementing measures of synthetic complexity.[23] Other programs have eliminated this issue by incorporating human interaction at each step to determine the feasibility of a proposed strategy, albeit in a less automated way.[7d, 24] Considerations for generating and prioritizing disconnections are vital when building, evaluating, or applying a retrosynthetic program.

3.3.2 Results from Detailed Retrosynthetic Planners

The output of retrosynthetic planners is relatively uniform, as each planner generally proposes a synthetic route through several intermediates (Figure 4).[21a, 25] Additional rigor can be

added to a program through the use of reaction prediction software,[15a, 20b, 26] either as a part of the algorithm or through post-processing, to indicate how likely the corresponding forward synthesis is to proceed. As each molecule will generate multiple solutions, another necessary feature is the ability to rank and highlight the most promising of several possible routes that returned a "successful" synthesis. Typically, metrics such as anticipated selectivity and expected yield based on literature precedent, as well as step count, are prioritized in ranking syntheses as these are likely to correlate with whether the synthesis will be viable and economical – in terms of cost, steps, time, and waste – in the laboratory.

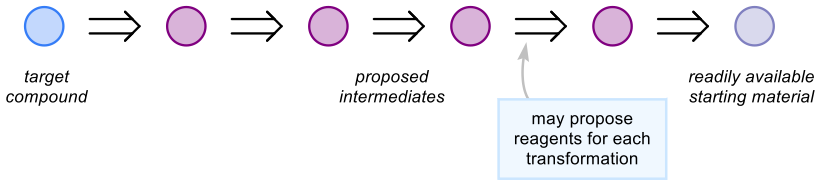

Figure 4. Cartoon depiction of results from a detailed retrosynthetic planner that proposes discreet intermediates *en route* to a target compound. Each node represents an intermediate and each arrow represents a reaction. Depending on the program this may include proposed conditions for each transformation.

To determine if a program has successfully identified a viable route, synthetic validation of the proposal is preferable, but this requires significant investment of resources. Nonetheless, several computer-generated syntheses have been successfully carried out in the laboratory.[12, 25] Other methods of validation include comparisons of the proposed route to existing literature that was not in the program's data set,[15a, 15b] or double-blind surveys with trained chemists[21a] that can be used to probe the perceived effectiveness, as well as the elegance, of a route.

In order to minimize computational cost, each aspect of retrosynthesis programs, such as the development of the module to generate disconnections, the prioritization of different routes, and the maximum allowed search depth, are designed to balance performance and computational power to maximize success within the intended application. The computational cost associated with successfully identifying a synthetic route to a target varies widely depending on the complexity of the molecule, and the algorithms used. State-of-the-art programs perform well on reasonably complex targets and can identify many well precedented reactions such as cycloadditions as well as myriad ways to modularly synthesize molecules with reactions such as Suzuki and amide couplings. The synthesis of topologically complex targets remains at the forefront of the field, with a recent synthesis of the fused-ring alkaloid (*R*,*R*,*S*)-tacamonidine representing one of the most complex molecules to date where a computationally-predicted retrosynthesis has been experimentally vetted.[27]

3.3.3 Case Studies for Detailed Retrosynthetic Planners

Computer-assisted retrosynthesis has been an active area of research for more than half a century that has seen renewed interest because of the significant opportunities offered by the revolution in data science and new machine learning techniques. This renaissance has culminated in both excellent software to inspire chemists through logic-based programs and fully automated generation of retrosyntheses that have been experimentally validated in the laboratory. In the past

decade, this has led to numerous reports on the implementation of detailed retrosynthetic planners and various components of the software. In particular, we will review two retrosynthesis programs and their approach and successes in identifying routes to complex molecules. The reader is also referred to other literature detailing synthesis planners that highlight developments in this area.[14a, 21a, 28]

Expert-coded retrosynthetic planning

Synthia™, formerly known as Chematica, has been developed over the past decade and has recently been commercialized by MilliporeSigma. This software boasts a collection of more than 100,000 expert-coded rules that are recursively applied to synthetic targets. In each hand-coded rule, there also exists general reaction conditions and identification of potential functional group conflicts, which provides insight into whether protecting groups are necessary.[29] Two important components in multi-step synthetic planning are the way in which the algorithm selects which branches of the synthetic tree to pursue, that is, how it selects which disconnections are valuable, and the way in which the algorithm selects the "best" of many syntheses. In Synthia™ these functions are called the chemical scoring function and reaction scoring function, respectively, and are editable by the user to allow prioritization based on factors such as overall step count, starting material cost, and use of protecting groups.

In a recent example, several molecules of interest to MilliporeSigma were analyzed by Synthia™ (Figure 5a), and the routes were vetted experimentally (Figure 5b).[12] In these cases, for drug-like molecules, average computation time was around 15–20 minutes per molecule and the first or second top-rated route was chosen to vet without allowing significant changes from the proposed reagents. A restriction was implemented that only 70 hours of bench work would be allowed to develop the experimental execution of predicted routes. In particular, for a quinoline-appended lactam (**2**) selected for its biological activity, Synthia™'s proposed route was not only successful when vetted by organic chemists, but also led to an overall yield improvement of more than six-fold over what was previously reported and decreased the required column chromatography steps from five to three. Seven additional targets were also synthesized using the output from Synthia™ and each included some benefit over the previous route including obtaining higher yields, shorter step counts, higher purity, or more facile separation.

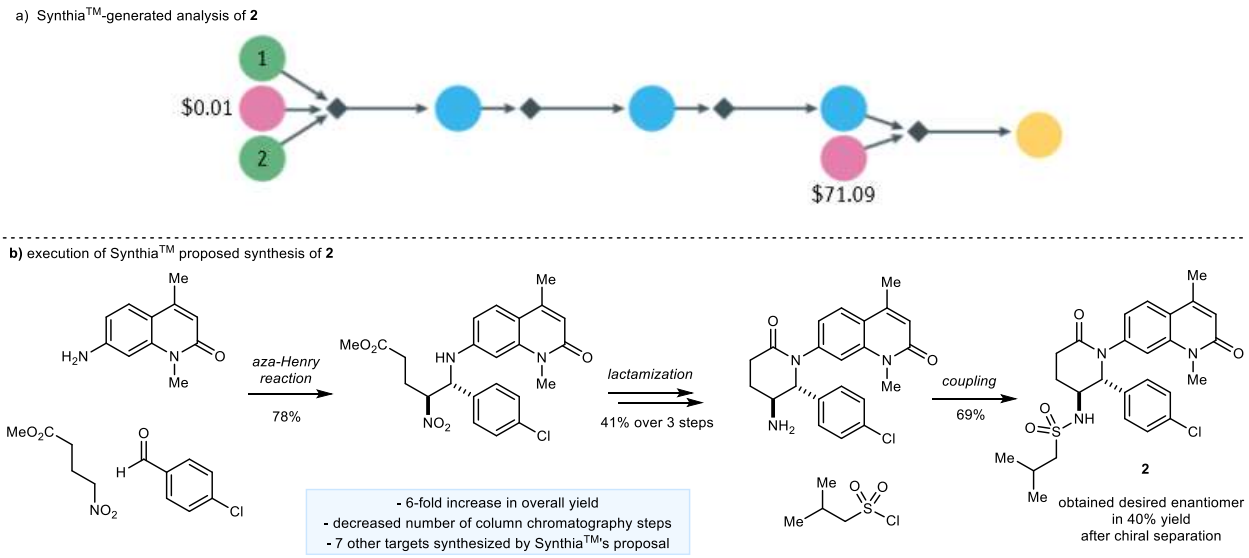

Figure 5. Applications of retrosynthetic planning validated by laboratory efforts. a) Synthia™-generated results for lactam **2**. Each diamond represents a reaction step, showing the map of known starting materials (green) and commercial starting materials (pink) through intermediates (blue) to the product (yellow). **b**) Laboratory validated forward synthesis of lactam **2** with only minor variations from Synthia™-generated results.

Retrosynthesis planning toward fully automated syntheses

Another well-known package is the ASKCOS suite, an open-source software package meant to aid in many aspects of computer-assisted synthesis including reaction planning and one-step retrosynthesis.[11, 15b, 20a, 23b, 26c, 30] Several of these tools individually fit into either a logic-based approach or an iterative automated setup which has recently been applied to retrosynthetic planning for the synthesis of fifteen drug molecules.[25]

Building on earlier developments in detailed retrosynthetic planning,[21a] ASKCOS was trained to automatically extract reaction templates from the U.S. Patent and trademark office as well as the Reaxys database, arriving at a library of 163,723 transforms. Within the algorithm, the templates extracted from similar molecules, and thus predicted to work well on the target molecule, are applied to identify possible disconnections (Figure 6a).[15a] At this stage, another module of the software tests a forward reaction prediction software to ascertain if reaction conditions that are expected to furnish the desired product from the proposed starting material exist. Additionally, another module that predicts the major product is used to determine if there are likely to be side products or other considerations that affect the feasibility of a given transformation (Figure 6b). Limits are set on the maximum search depth to explore the synthetic tree and it is explored through a Monte Carlo tree search to balance exploration of "promising" routes as well as the exploration of less frequently visited branches. Notably, the program successfully developed routes to targets it had not been exposed to previously, as well as useful active pharmaceutical ingredients.

The proposed syntheses of safinamide, as well as fourteen other medicinal compounds, were completed from inexpensive, commercially available reagents using a fully automated system.

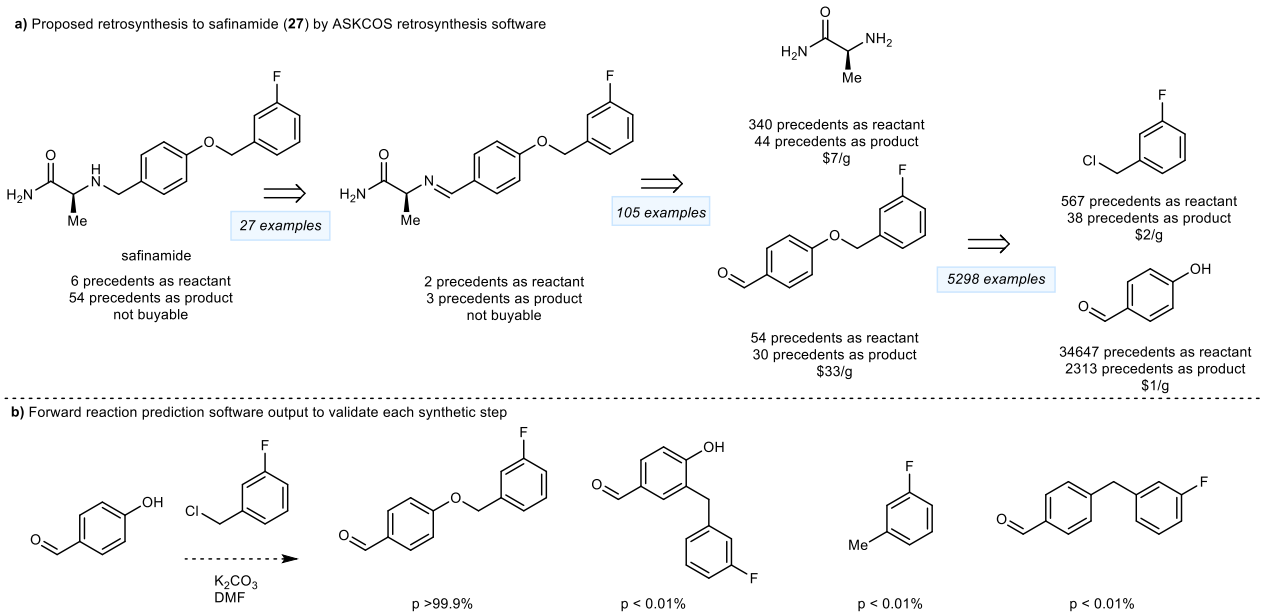

Figure 6. Retrosynthetic planning directed by ASKCOS. a. Proposed retrosynthesis of safinamide by automated retrosynthesis software **b.** Example forward reaction prediction for the base-mediated coupling of phenol and arene. This validation was performed for each reaction in the proposed retrosynthesis.

Ultimately, these examples showcase the capabilities of retrosynthetic planning software to arrive at new syntheses of useful molecules in a quick and efficient manner.

3.4 Data and Reproducibility

High-quality datasets are essential to build quality retrosynthesis planning software. While proprietary databases, such as Reaxys and Scifinder®, can yield large amounts of reaction data, these entries can be incomplete or missing key information such as stereochemistry or yields. Mining data from the chemical literature can be a time-intensive process, often requiring the manual extraction of data from supplemental text. Moreover, consistency of data can be uncertain and unsuccessful reactions are often underrepresented. Specifically, this plays into the quality of the reaction templates used in retrosynthesis planners. A retrosynthetic software built on incorrect or incomplete templates may miss obvious disconnections. The development of robust models trained on large datasets, if available, can overcome a few aberrant data points. In short, ideal data is complete, covers a wide chemical space, and is reproducible. Ensuring abundant, high quality data is available is an on-going challenge.

While reproducibility of reaction data itself is vital, it is worth noting that even data-driven methods of retrosynthetic planning are not fully translatable. In many workflows, decisions may be made by the user that factor in so-called “chemical intuition” in the construction of the model—for example, the selection of a particular retrosynthetic disconnection. Furthermore, retrosynthetic planning programs often contain a randomized element, such as a randomized initialization in the set of reaction templates, leading to slightly different results. For these reasons, duplicating an exact synthetic proposal using step-by-step algorithms can be challenging. However, in cases where a retrosynthesis program can identify a particularly efficient reaction sequence, it is likely to converge on that route, regardless of randomized elements, if given enough search time.

Successful implementation of these methods in synthetic chemistry requires an understanding of their inherent limitations. By keeping in mind the challenges incurred in their use, one can avoid common pitfalls and better understand the utility of these techniques.

3.5 Limitations

While many programs have successfully designed routes to a target compound, there is wide variability in the complexity of the target molecules. For example, natural product synthesis often focuses on complex sp^3-rich molecules as targets, which often have additional stereoelectronic challenges associated with building their framework. On the other hand, a program designed to identify pathways to drug-like molecules is often trained on data specific to sp^2-rich molecules. Furthermore, by virtue of close literature precedent being intimately tied to a program's perceived likelihood of success for a particular reaction, detailed retrosynthesis programs are generally unable to propose novel disconnections which, if proposed, would be viewed skeptically by the user. As the adoption of these methods continues, we anticipate the need for studies that demonstrate the capabilities of these softwares for natural product synthesis.

Historically, retrosynthetic planners were only accessible to a handful of groups. Today, accessibility is increasing as many platforms have been made open source (e.g., AiZynthFinder,[31] ASKCOS,[32] IBM RXN for Chemistry[33]) while many others have been developed commercially (e.g. SciFinder-^{n},[34] Synthia™,[29] Molecule.One,[35] Reaxys,[36] ICSynth,[37] Chemical.AI,[38] Iktos spaya.ai[39]).

3.6 Summary and Outlook

As the field of synthetic chemistry works to incorporate emerging methods for retrosynthesis into the synthetic chemist's toolkit, it is necessary to take stock of what has been accomplished. Although the work highlighted in this chapter represents a limited cross-section of achievements in the field, new developments are continually emerging. These solutions should not be viewed or implemented as a replacement for the chemist; rather, these methods enable chemists to streamline the tedious steps of synthesis and focus on creativity.

With regards to retrosynthesis planners, many of these detailed planners will allow for synthesis applications focused on building moderately complex compounds. We envision these planners can augment the way we search the literature, much in the same way that database searching such as Reaxys® or Scifinder® facilitates data access. In this way, we can accelerate the process of navigating many potential routes and enable practitioners to focus on bigger overall questions in their research.

While it can be difficult to reconcile the use of these retrosynthetic planning programs which rely on known, well-precedented reactions, it's worth noting that computer-assisted synthesis also fosters innovation. The use of heuristic-based programs often invites and necessitates creativity from chemists to arrive at a more ideal route. Additionally, step-by-step retrosynthesis programs rely on definitions of synthetic complexity and reduction in complexity where there is still considerable room for improvement.

Ultimately, information-rich techniques will become a part of the practicing synthetic chemist's toolkit toward the dream of realizing the synthesis of any given molecule from route prediction to execution to prepare target compounds in high yield with minimal human effort. In reality we are far from this, and it's unlikely to ever be the case for all molecules. Incrementally,

we will continue to work towards this goal by developing new tools, standardizing those that are currently available, and streamlining the inefficiencies of synthesis to allow chemists to focus on new and creative aspects of synthesis.

3.7 Contributors

A majority of this chapter is reproduced with permission from Shen, Y.;* Borowski, J. E.;* Hardy, M. A.;* Sarpong, R.; Doyle, A. G.; Cernak, T. Automation and Computer-Assisted Planning for Chemical Synthesis. Nat Rev Methods Primers. 1, Article number: 23 (2021).

3.8 References

1. (a) Corey, E. J.; Wipke, W. T. *Science* **1969**, *166*, 178; (b) Vléduts, G. É. *Inform. Stor. Retr.* **1963**, *1*, 117–146; (c) Ugi, I.; Bauer, J.; Blomberger, C.; Brandt, J.; Dietz, A.; Fontain, E.; Gruber, B.; v. Scholley-Pfab, A.; Senff, A.; Stein, N. *J. Chem. Inf. Comput. Sci.* **1994**, *34*, 3–16; (d) Ugi, I.; Bauer, J.; Bley, K.; Dengler, A.; Dietz, A.; Fontain, E.; Gruber, B.; Herges, R.; Knauer, M.; Reitsam, K.; Stein, N. *Angew. Chem. Int. Ed.* **1993**, *32*, 201–227.
2. Corey, E. J., *The logic of chemical synthesis*. Nobel foundation, [Nobelstiftelsen]: 1991.
3. (a) Todd, M. H. *Chem. Soc. Rev.* **2005**, *34*, 247–266; (b) Szymkuć, S.; Gajewska, E. P.; Klucznik, T.; Molga, K.; Dittwald, P.; Startek, M.; Bajczyk, M.; Grzybowski, B. A. *Angew. Chem. Int. Ed.* **2016**, *55*, 5904–5937.
4. Pensak, D. A.; Corey, E. J., LHASA—Logic and Heuristics Applied to Synthetic Analysis. In *Computer-Assisted Organic Synthesis*, AMERICAN CHEMICAL SOCIETY: 1977; Vol. 61, pp 1–32.
5. Campbell, M.; Hoane, A. J.; Hsu, F.-h. *Artificial Intelligence* **2002**, *134*, 57-83.
6. Silver, D.; Huang, A.; Maddison, C. J.; Guez, A.; Sifre, L.; van den Driessche, G.; Schrittwieser, J.; Antonoglou, I.; Panneershelvam, V.; Lanctot, M.; Dieleman, S.; Grewe, D.; Nham, J.; Kalchbrenner, N.; Sutskever, I.; Lillicrap, T.; Leach, M.; Kavukcuoglu, K.; Graepel, T.; Hassabis, D. *Nature* **2016**, *529*, 484–489.
7. (a) Hanessian, S.; Franco, J.; Larouche, B. *Pure Appl. Chem.* **1990**, *62*, 1887-1910; (b) Wipke, W. T.; Rogers, D. *J. Chem. Inf. Comput. Sci.* **1984**, *24*, 71–81; (c) Mehta, G.; Barone, R.; Chanon, M. *Eur. J. Org. Chem.* **1998**, *1998*, 1409–1412; (d) Corey, E. J.; Long, A. K.; Rubenstein, S. D. *Science* **1985**, *228*, 408.
8. Marth, C. J.; Gallego, G. M.; Lee, J. C.; Lebold, T. P.; Kulyk, S.; Kou, K. G. M.; Qin, J.; Lilien, R.; Sarpong, R. *Nature* **2015**, *528*, 493.
9. Johnson, A. P.; Marshall, C.; Judson, P. N. *Recl. Trav. Chim. Pays Bas* **1992**, *111*, 310-316.
10. Snider, B. B.; Kulkarni, Y. S. *J. Org. Chem.* **1987**, *52*, 307–310.
11. Coley, C. W.; Green, W. H.; Jensen, K. F. *Acc. Chem. Res.* **2018**, *51*, 1281–1289.
12. Klucznik, T.; Mikulak-Klucznik, B.; McCormack, M. P.; Lima, H.; Szymkuć, S.; Bhowmick, M.; Molga, K.; Zhou, Y.; Rickershauser, L.; Gajewska, E. P.; Toutchkine, A.; Dittwald, P.; Startek, M. P.; Kirkovits, G. J.; Roszak, R.; Adamski, A.; Sieredzińska, B.; Mrksich, M.; Trice, S. L. J.; Grzybowski, B. A. *Chem* **2018**, *4*, 522–532.
13. Ravitz, O. *Drug Discovery Today: Technologies* **2013**, *10*, e443-e449.
14. (a) Law, J.; Zsoldos, Z.; Simon, A.; Reid, D.; Liu, Y.; Khew, S. Y.; Johnson, A. P.; Major, S.; Wade, R. A.; Ando, H. Y. *J. Chem. Inf. Model.* **2009**, *49*, 593–602; (b) Christ, C. D.; Zentgraf, M.; Kriegl, J. M. *J. Chem. Inf. Model.* **2012**, *52*, 1745–1756.

15. (a) Segler, M. H. S.; Waller, M. P. *Chem. Eur. J.* **2017**, *23*, 5966–5971; (b) Coley, C. W.; Rogers, L.; Green, W. H.; Jensen, K. F. *ACS Cent. Sci.* **2017**, *3*, 1237–1245; (c) Segler, M. H. S.; Waller, M. P. *Chem. Eur. J.* **2017**, *23*, 6118–6128; (d) Baylon, J. L.; Cilfone, N. A.; Gulcher, J. R.; Chittenden, T. W. *J. Chem. Inf. Model.* **2019**, *59*, 673–688.
16. (a) Gómez-Bombarelli, R.; Wei, J. N.; Duvenaud, D.; Hernández-Lobato, J. M.; Sánchez-Lengeling, B.; Sheberla, D.; Aguilera-Iparraguirre, J.; Hirzel, T. D.; Adams, R. P.; Aspuru-Guzik, A. *ACS Central Science* **2018**, *4*, 268-276; (b) Segler, M. H. S.; Kogej, T.; Tyrchan, C.; Waller, M. P. *ACS Cent. Sci.* **2018**, *4*, 120–131.
17. Liu, B.; Ramsundar, B.; Kawthekar, P.; Shi, J.; Gomes, J.; Luu Nguyen, Q.; Ho, S.; Sloane, J.; Wender, P.; Pande, V. *ACS Cent. Sci.* **2017**, *3*, 1103–1113.
18. Krenn, M.; Häse, F.; Nigam, A.; Friederich, P.; Aspuru-Guzik, A. *Machine Learning: Science and Technology* **2020**, *1*, 045024.
19. (a) Lin, K.; Xu, Y.; Pei, J.; Lai, L. *Chem. Sci.* **2020**, *11*, 3355–3364; (b) Karpov, P.; Godin, G.; Tetko, I. V. In *A Transformer Model for Retrosynthesis*, Cham, Springer International Publishing: Cham, 2019; pp 817–830; (c) Schwaller, P.; Laino, T.; Gaudin, T.; Bolgar, P.; Hunter, C. A.; Bekas, C.; Lee, A. A. *ACS Cent. Sci.* **2019**, *5*, 1572–1583.
20. (a) Vignesh Ram Somnath, C. B., Connor W. Coley, Andreas Krause, Regina Barzilay *arXiv* **2020**; (b) Mikołaj Sacha, M. B., Piotr Byrski, Paweł Włodarczyk-Pruszyński, Stanisław Jastrzębski *arXiv* **2020**.
21. (a) Segler, M. H. S.; Preuss, M.; Waller, M. P. *Nature* **2018**, *555*, 604; (b) Marwin Segler, M. P., Mark P. Waller *arXiv* **2017**.
22. Bertz, S. H. *J. Am. Chem. Soc.* **1981**, *103*, 3599–3601.
23. (a) Huang, Q.; Li, L.-L.; Yang, S.-Y. *J. Chem. Inf. Model.* **2011**, *51*, 2768–2777; (b) Coley, C. W.; Rogers, L.; Green, W. H.; Jensen, K. F. *J. Chem. Inf. Model.* **2018**, *58*, 252–261.
24. Gasteiger, J.; Pförtner, M.; Sitzmann, M.; Höllering, R.; Sacher, O.; Kostka, T.; Karg, N. *Perspect. Drug Discov. Des.* **2000**, *20*, 245-264.
25. Coley, C. W.; Thomas, D. A.; Lummiss, J. A. M.; Jaworski, J. N.; Breen, C. P.; Schultz, V.; Hart, T.; Fishman, J. S.; Rogers, L.; Gao, H.; Hicklin, R. W.; Plehiers, P. P.; Byington, J.; Piotti, J. S.; Green, W. H.; Hart, A. J.; Jamison, T. F.; Jensen, K. F. *Science* **2019**, *365*.
26. (a) Coley, C. W.; Barzilay, R.; Jaakkola, T. S.; Green, W. H.; Jensen, K. F. *ACS Cent. Sci.* **2017**, *3*, 434–443; (b) Schwaller, P.; Gaudin, T.; Lányi, D.; Bekas, C.; Laino, T. *Chem. Sci.* **2018**, *9*, 6091–6098; (c) Coley, Connor W.; Jin, W.; Rogers, L.; Jamison, T. F.; Jaakkola, T. S.; Green, W. H.; Barzilay, R.; Jensen, K. F. *Chem. Sci.* **2019**, *10*, 370–377.
27. Mikulak-Klucznik, B.; Gołębiowska, P.; Bayly, A. A.; Popik, O.; Klucznik, T.; Szymkuć, S.; Gajewska, E. P.; Dittwald, P.; Staszewska-Krajewska, O.; Beker, W.; Badowski, T.; Scheidt, K. A.; Molga, K.; Młynarski, J.; Mrksich, M.; Grzybowski, B. A. *Nature* **2020**.
28. (a) Philippe Schwaller, R. P., Valerio Zullo, Vishnu H Nair, Rico Andreas Haeuselmann, Riccardo Pisoni, Costas Bekas, Anna Iuliano, Teodoro Laino *arXiv* **2019**; (b) Genheden, S.; Thakkar, A.; Chadimová, V.; Reymond, J.-L.; Engkvist, O.; Bjerrum, E. *J. Cheminformatics* **2020**, *12*, 70; (c) Nicolaou, C. A.; Watson, I. A.; LeMasters, M.; Masquelin, T.; Wang, J. *J. Chem. Inf. Model.* **2020**, *60*, 2728–2738; (d) Bøgevig, A.; Federsel, H.-J.; Huerta, F.; Hutchings, M. G.; Kraut, H.; Langer, T.; Löw, P.; Oppawsky, C.; Rein, T.; Saller, H. *Organic Process Research & Development* **2015**, *19*, 357-368.
29. Synthia™ Organic Retrosynthesis Software | Sigma-Aldrich. https://www.sigmaaldrich.com/chemistry/chemical-synthesis/synthesis-software.html (accessed January 7, 2021).

30. (a) Coley, C. W.; Barzilay, R.; Jaakkola, T. S.; Green, W. H.; Jensen, K. F. *ACS Cent Sci* **2017**, *3*, 434-443; (b) Gao, H.; Struble, T. J.; Coley, C. W.; Wang, Y.; Green, W. H.; Jensen, K. F. *ACS Cent Sci* **2018**, *4*, 1465-1476.
31. MolecularAI/aizynthfinder. https://github.com/MolecularAI/aizynthfinder (accessed January 7, 2021).
32. connorcoley/ASKCOS. https://github.com/connorcoley/ASKCOS (accessed January 7, 2021).
33. IBM RXN for Chemistry. https://rxn.res.ibm.com/ (accessed January 7, 2021).
34. Chemical Abstracts Service - Scifinder^{n}. https://www.cas.org/products/scifinder (accessed October 28, 2020).
35. Molecule.one. https://molecule.one/ (accessed January 7, 2021).
36. Automating the underlying processes in synthetic route creation - Reaxys Chemical Data | Elsevier Solutions. https://www.elsevier.com/solutions/reaxys/features-and-capabilities/synthesis-planner (accessed January 7, 2021).
37. ICSYNTH. https://www.deepmatter.io/products/icsynth/ (accessed January 7, 2021).
38. Chemical.AI | An Artificial Intelligence Company | Shape the future of Chemistry. https://Chemical.AI (accessed January 7, 2021).
39. Spaya AI. https://beta.spaya.ai/ (accessed January 7, 2021).

Chapter 4. Applications of Synthia™ to the Synthesis of Natural Products in the Pupukeanane Family

4.1 Computer-Assisted Synthesis in the 2020s

Nearly half a century after Corey's influential paper outlining an approach for computer-assisted synthesis,[1] recent advancements in machine learning (ML), accessibility of data, and fast calculations have renewed interest in computer-assisted synthesis. In the last decade, increasingly advanced algorithms to navigate synthetic pathways,[2] predict reaction products,[3] and determine optimal reaction conditions[4] have been developed.

A well-known challenge in the synthesis of complex molecules is the extension of methods for the preparation of relatively flat, sp^2-rich molecules to more topologically complex, sp^3-rich, caged structures.[5] It is these structurally complex sp^3-rich scaffolds that often imbues natural products with important biological function and generates interest in strategies, tactics, and methods for their synthesis. In addition to recent advances that enable retrosynthetic planning programs to accurately predict routes and conditions for the synthesis of drug-like molecules,[6] the program Synthia™ has recently been deployed to plan the synthesis of sp^3-rich, complex targets by using enhanced searching strategies. Notably, Synthia™-planned syntheses of multiple natural products have now been validated in the laboratory.[7]

In this Chapter, we will examine synthetic strategies that Synthia™ applies toward the pupukeanane natural products. In particular, we will consider these Synthia™-proposed routes in comparison with previously published syntheses (detailed in Chapter 1), focusing on the formation of the key C–C bonds that forge their tricyclic skeletons. The goal of this analysis is to elucidate the capabilities of Synthia™ as well as some of its limitations in tackling the total synthesis of small, moderately complex natural products. While several metrics exist to compare syntheses (i.e., step count, yield, cost of materials, etc.,) we aim to evaluate the ability of these proposed routes to advance the science of synthesis by bringing new perspectives on the available strategies to access the complex, tricyclic core of the pupukeanane family of natural products.

4.2 The Inner Workings of Synthia™

Synthia™, formerly known as Chematica, has been developed over the past decade and has recently been commercialized by MilliporeSigma. The program includes a detailed set of more than 100,000 expert-coded reaction rules. Each rule details the outcome of the transform (i.e., the affected functional groups necessary to make that disconnection) as well as illustrative references, sample conditions, and additional reaction metadata that indicates functional group compatibility and expected selectivity outcomes.[8] Synthia™ applies these by a workflow that is analogous to how a chemist may analyze a synthetic target (Figure 1).

From a given synthetic target, a chemist would likely consider many possible disconnections, explicitly or subconsciously, that may simplify a given target using their learning knowledge (Step 1); the chemist would then select a promising transform on the basis of how

simplifying it would be as well as its compatibility with the target in question (Step 2). Synthia™ mimics this by applying these reaction rules to generate potential substrates that would enable the synthesis of the desired target. It then evaluates how effective the application of any given rule might be based on the structural complexity of the precursor compounds using a Chemical Scoring Function (CSF). This scoring function is user editable but typically prioritizes the reduction of structural complexity at each step as measured by metrics such as the number of rings, stereocenters, and atoms present in the precursor compounds.

At this stage, either a chemist or the software would identify whether the substrates are readily available (Step 3) by searching a chemical database. If the compounds are not readily available, the process is repeated (Step 4) until suitable starting materials have been identified. At this time, a synthetic chemist may write down the route to consider and iterate the process until several possible routes have been identified (Step 5). With several possible routes to consider, a chemist would need to choose the "best" synthetic strategy, which may rely on the prediction of metrics such as step count, expected yield, the use of hazardous reagents, cost of starting materials or less quantifiable elements such as elegance, creativity, or the perceived ability to access other analogues of the target compound. Synthia™ will select the best scoring route through a Reaction Scoring Function (RSF) which typically takes into account factors such as the use of protecting groups, the number of steps, and the presence of possible reactivity conflicts.

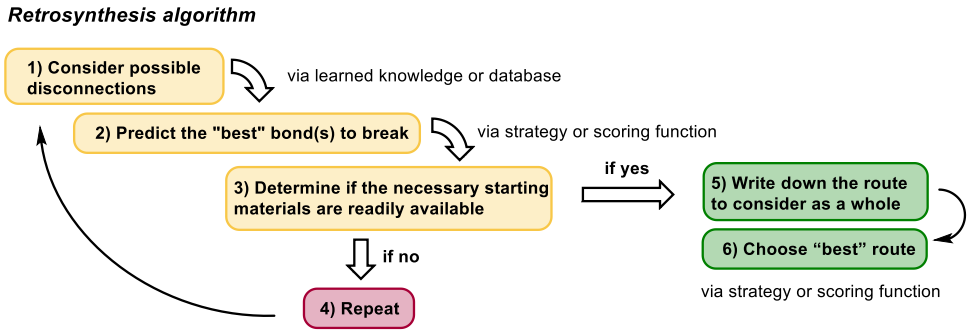

Figure 1. A general scheme for understanding computer-assisted retrosynthesis decision making.

This simplistic picture does not detail all the functions of Synthia™, but is meant to provide an overview of important components for the program and how a user can modify them. Another key consideration is that natural products synthesis often requires farsighted, multi-step strategies that may not be favored by an algorithm which prioritizes the reduction of complexity of the target compound. One approach to incorporate this into Synthia™ included the development of a database of tactical combinations that consisted of more than 100,000 two-step sequences that could be applied.[9] More recently, identification of causal relationships that led to improved treatment of certain classes of reactions (i.e., allowing multiple functional group interconversions without deprioritizing the route) have been implemented to assist in multi-step strategizing. These advancements were key to enhancing Synthia™'s capabilities to enable the synthetic proposals of multiple natural product syntheses that have been validated in the laboratory.[7]

4.3 Unique Scaffolds in the Pupukeanane Family

To conduct our survey, we analyzed one of each scaffold type in the pupukeanane family (Figure 2) through a Synthia™-generated pathway. Often within only a few minutes of searching, Synthia™ was able to propose numerous routes. In each case, after completion of the search the best scoring pathway was analyzed. One potential roadblock in the integration of computer-assisted synthesis in the laboratory by organic chemists is the learning curve required to begin understanding and using the software, for this reason we opted to show routes that could be produced with near default parameters, selecting the recommended setting for natural products by the Synthia™ program.

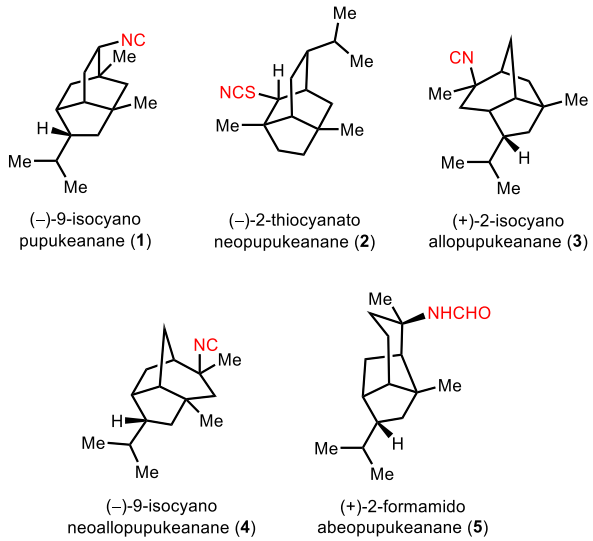

Figure 2. Selected natural products for each unique skeleton of the pupukeanane family.

4.4 The Pupukeanane Skeleton

We began our survey by using the Synthia™ software to plan routes to the isotwistane containing pupukeanane. Given its popularity as a synthetic target, we first analyzed 9-pupukeanone (**6**, Scheme 1), a known degradation product of **1** which has previously been elaborated to **1** in a four-step sequence.[10]

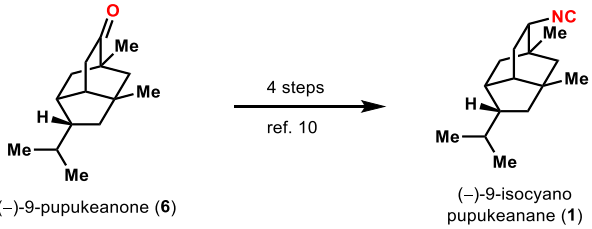

Scheme 1. Elaboration of 9-pupukeanone (**6**) to 9-isocyanopupukeanane (**1**).

4.4.1 Synthia™'s Proposed Route to 9-Pupukeanone

Synthia™'s proposed route to 9-pupukeanone (**6**) proceeds through a key Diels–Alder [4 +2] cycloaddition (see **16** to **6**, Scheme 2) to build the pupukeanane tricyclic core. In the forward direction, the proposed synthesis begins with an organocatalytic desymmetrization of prochiral

cyclohexanone **7**. This type of selective deprotonation with a chiral phase-transfer catalyst has been previously used to access enantiomerically enriched silyl enol ethers which can be oxidized under Pd conditions to the corresponding enone (**8**). At this stage, the software proposed a sequential *α*-methylation and *O*-methylation of the enone to arrive at diene **11**. Interestingly, Synthia™'s raw output explicitly proceeds through the enol tautomer (**10**), which, if implemented, would likely be only generated *in situ*. Subsequent reduction of the ester and Appel type substitution would lead to alkyl halide **13**. To append the isopropyl group, an Ender's RAMP/SAMP alkylation of 3-methyl butanal (**14**) is proposed to give aldehyde **15**. Tebbe olefination of **15** would give cycloaddition precursor **16**. The [4 + 2] cycloaddition of this precursor is expected to give the desired 9-pupukeanone (**6**) after an acidic workup.

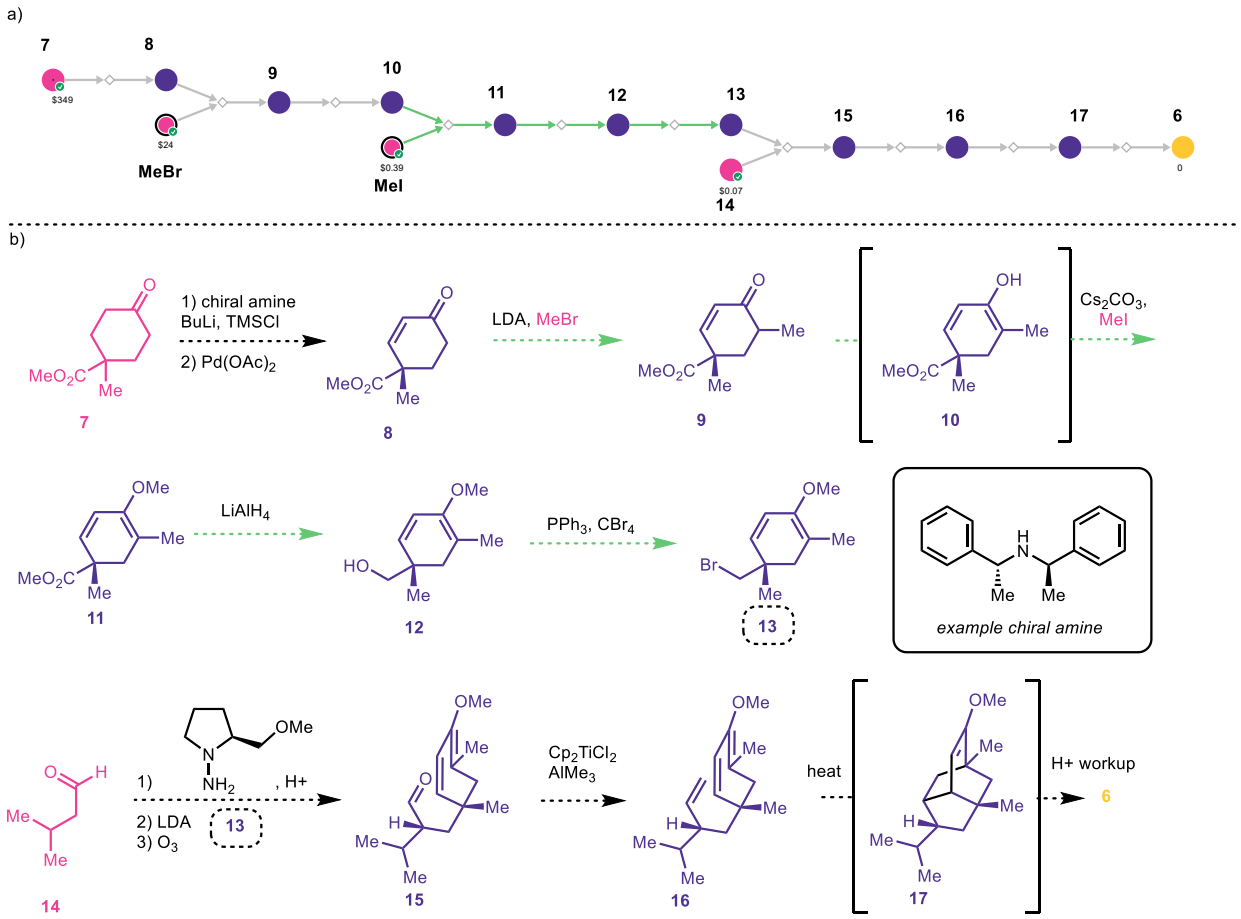

Scheme 2. Synthia™'s proposed forward synthesis for 9-pupukeanone (**6**) as a a) summary graphic and b) detailed scheme. Each diamond represents a reaction step, showing the map of known starting materials (teal) and commercial starting materials (pink) through intermediates (purple) to the product (yellow). Green reaction arrows indicate that the transform was identified through a multi-step strategy. Red reaction arrows indicate that the transformation is either not selective or only diastereoselective.

Notably, disconnection across this tricyclic core has been previously proposed and synthetically validated by the Yamamoto,[10a] White,[11] and Piers[12] groups in their syntheses of 9-pupukeanone (**6**, Scheme 3a). Each of these three previous syntheses that employ a Diels–Alder

cycloaddition proceed to give a single isomer of the desired tricycle (i.e., **19**). However, a primary difference in the route proposed by Synthia™ when compared to previous syntheses is that in Synthia™'s route, the isopropyl group is installed prior to the cycloaddition.

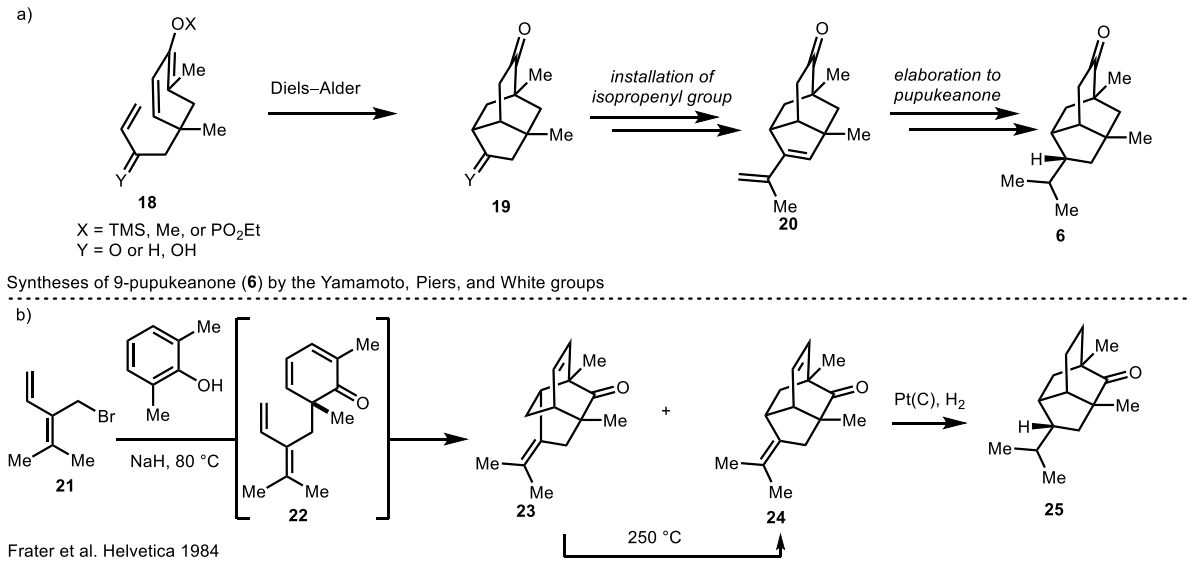

Scheme 3. a) General strategy applied by the Yamamoto, White, and Piers groups in their synthesis of 9-pupukeanaone (**6**) and b) synthesis of 2-pupukeanone (**26)** by Frater's Diels-Alder transformation.

In Frater's synthesis of 2-pupukeanone (Scheme 3b) which employed the same Diels-Alder transformation to build the isotwistane core (**24**) from a monocyclic precursor (**22**) the carbons of the isopropyl group were pre-installed. In this cycloaddition, two isomers were observed following the Diels-Alder cycloaddition step, which were a mixture of the desired isotwistane **24** and undesired twistane **23** in a 3:1 ratio. In a subsequent step, twistane **23** could be converted to the more thermodynamically stable isomer (**24**) by heating at 250 °C for 5 min to presumably effect a retro-Diels–Alder/Diels–Alder. These previous studies support the proposal by Synthia™ that in the case of a mono-cyclic precursor bearing all the carbons of the skeleton, the Diels-Alder reaction will be able to be effected.

Ultimately, without being explicitly trained on the existing syntheses, Synthia™ was able to identify strategic disconnections to propose routes that were comparable, but distinct from previously published routes. In the case of 9-pupukeanone (**6**), the route proposed would be the shortest synthetic sequence to access **6** to date and has the potential to provide access to enantioenriched material. This speaks to the robustness of the proposals Synthia™ produces, which are designed to prioritize selective reactions with good precedent in its default search parameters.

4.5 The Neopupukeanane Natural Products

The related neopupukeanane skeleton also contains an isotwistane scaffold that is proposed to arise through a series of carbocation rearrangements in the biosynthesis of these natural products.[13] This results in unique alkyl substitution pattens compared to the pupukeananes. To

date, three unique neopupukeananes have been isolated including two rare thiocyanate-containing natural products: 2-thiocyanatoneopupukeanane (**2**) and 4-thiocyanatoneopupukeanane (**27**).[14] In applying Synthia™ searches to identifying routes for the synthesis of the neopupukeananes, we first observed that searches with the natural products bearing the thiocyanate group (**2** and **27**) as the target were not productive. Instead, a search for precursor ketones (i.e., **26** and **28**), which have been previously synthesized and carried forward to the thiocyanate natural products,[15] were more promising in identifying routes to the neopupukeanyl isotwistane scaffold. This modification of the search away from the thiocyanate group was critical and highlights the limited examples of this functional group in the Synthia™ rule library — thus, requiring an adjustment by the synthetic chemist to accommodate this limitation.

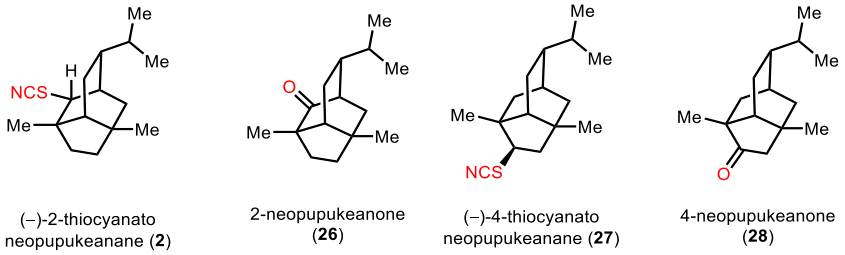

Figure 3. Selected neopupukeanane targets.

4.5.1 Synthia™'s Proposed Route to 2-Neopupukeanone

Synthia™ proposed building 2-neopupukeanone (**26**, Scheme 4a and b) using a radical cyclization similar to those employed by Subba Rao[16] and by Srikrishna[17] in their previous syntheses of the 2-pupukeananes (see Chapter 1). The proposed forward synthesis begins from known dehydrocarvone (**29**) to access α-phellandrene (**30**). Introduction of a ketene equivalent would lead to the corresponding [2.2.2]-bicycle, notably Synthia™ correctly marks this step as "not selective" as it would likely give a mixture of epimers. However, this is expected to be inconsequential as these epimers would ultimately converge to a single product after subsequent manipulation. This dithiane (**32**) could be cleaved to give norbornenone **33**, which sets the stage to install the southern bridge of the tricycle.

In this proposal, the α-alkylation could occur through treatment of **33** with LDA followed by introduction of an electrophile such as bromo ethanol **34**. Notably, Synthia™ flags that bromo-ethanol (**34**) would need to be protected to prevent deprotonation of the alcohol. One simple (human-proposed) solution would be the use of the THP-protected alcohol (**37**) as has been used in previous syntheses of these molecules[12] that would allow seamless integration into the existing route and could likely be cleaved in an acidic workup without increasing the longest linear step count. This would provide bicycle **35** which would be primed for the key radical cyclization after an Appel-type substitution of the hydroxyl for bromine to give **36**. Alternatively, we propose the use of dibromoethane could be a suitable alternative and obviate the need to substitute the alcohol for a bromine (Scheme 4c).

From bicycle **36**, a 5-exo-trig radical cyclization is proposed to give 2-neopupukeanone (**26**), which would complete a formal synthesis of (–)-**2** by Uyehara's method.[15b] Synthia™ suggests that a protection of the ketone may be necessary, however previous syntheses of the

pupukeananes have accomplished similar transformations with unmasked ketones in similar enviroments.[17b, 18]

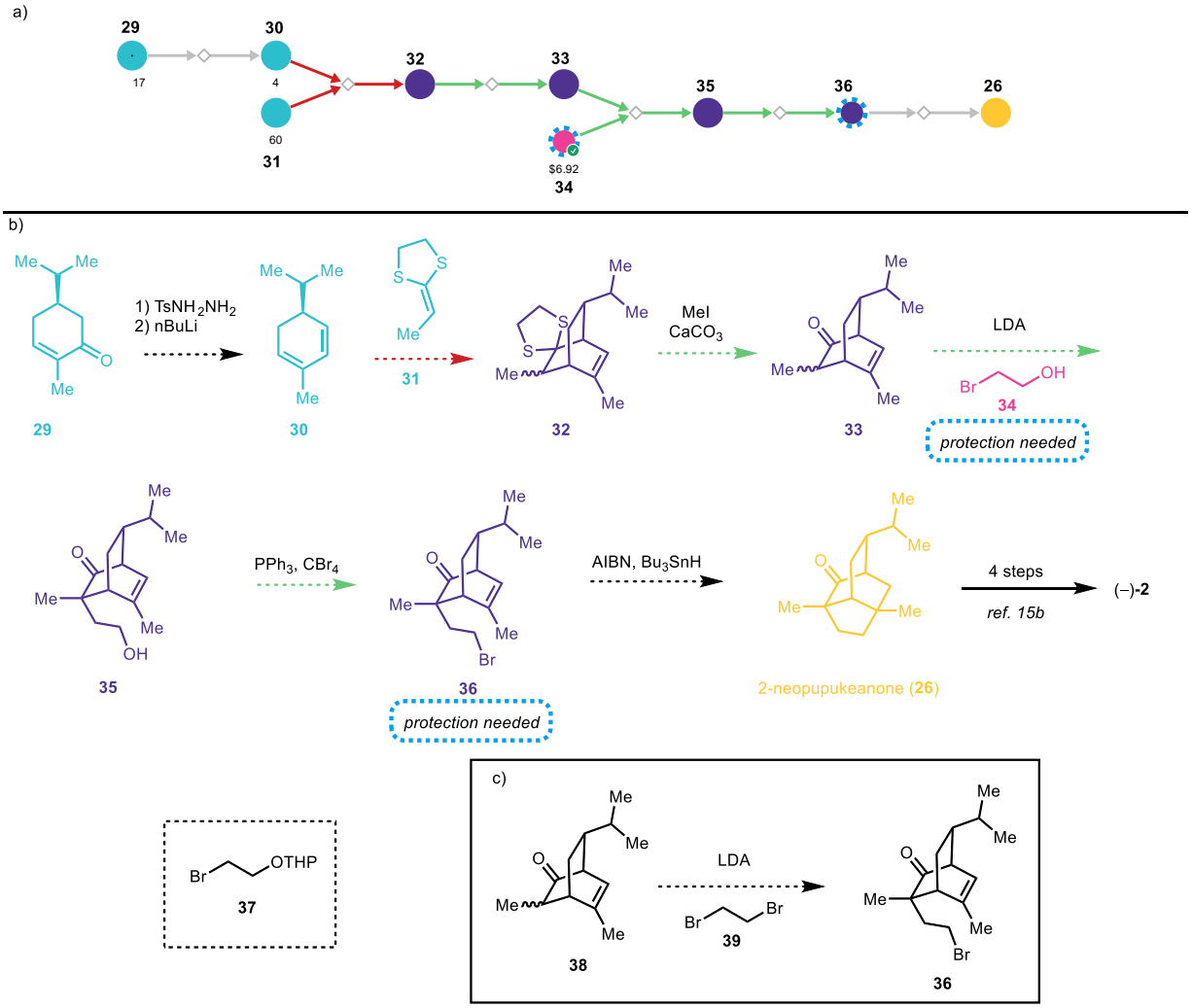

Scheme 4. Synthia™'s proposed forward synthesis for 2-neopupukeanone (**6**) as a a) summary graphic and b) detailed scheme. c) Human-proposed modifications to Synthia™'s route. Each diamond represents a reaction step, showing the map of known starting materials (teal) and commercial starting materials (pink) through intermediates (purple) to the product (yellow). Green reaction arrows indicate that the transform was identified through a multi-step strategy. Red reaction arrows indicate that the transformation is either not selective or only diastereoselective.

Overall, this Synthia™-proposed synthesis of **26** uses relatively robust chemistry that bears similarity to tactics previously applied to the syntheses of related molecules to arrive at a relatively short synthesis. Additionally, this case study highlights the ability of human design to provide improvements in these modular routes. We posit that tools such as Synthia™ are most powerful when used in tandem with human knowledge.

4.5.2 Synthia™'s Proposed Route for 4-Neopupukeanone

Interestingly, in the case of the related 4-neopupukeanone (**28**) which bears the same skeleton as 2-neopupukeanone (**26**), the Synthia™-generated route is a very distinct strategy which

involves building the isotwistane core through a ring expansion of cyclobutanone **49** (Scheme 5a and b). This strained intermediate (**49**) is proposed to arise from a [2+2] photocycloaddition from masked ketene **47**. Notably, two steps of this pathway are flagged by Synthia™ as "not selective" because they are likely to furnish isomeric mixtures.

In considering this route, an experienced organic chemist would likely realize that intermediates such as **45** are notably similar to (*R*)-carvone (**50**) whereas Synthia™ identified a route from vinyl iodide **40**. Given the advantages inherent in starting from cheap, commercially available enantioenriched materials such as carvone, this situation represents an opportunity for a hybrid human-designed/Synthia™-inspired approach in which a route could be independently designed to access **45** to allow enantiospecific entry into a proposed route.

While the Synthia™ proposed synthesis of **28** has some selectivity challenges, it inspired us to consider the development of selective methods to address these challenges. One can envision that from compound **51** (Scheme 5c), inspired by Synthia™'s use of **49**, there would be opportunities to desymmetrize this prochiral compound at a late-stage, which would lead to an elegant approach to these molecules. For example, using a desymmetrizing Tiffeneau-Demjanov reaction[19] could lead to a compound such as **52**, after which the isopropyl group could likely be installed diastereoselectively at a late-stage. If effected, these creative tactics would undoubtedly be of interest to the synthesis community. In this way, Synthia™'s proposals can be aspirational and, in the cases where certain proposed steps may seem improbable, push chemists to look beyond precedent in order to effect the desired transformation.

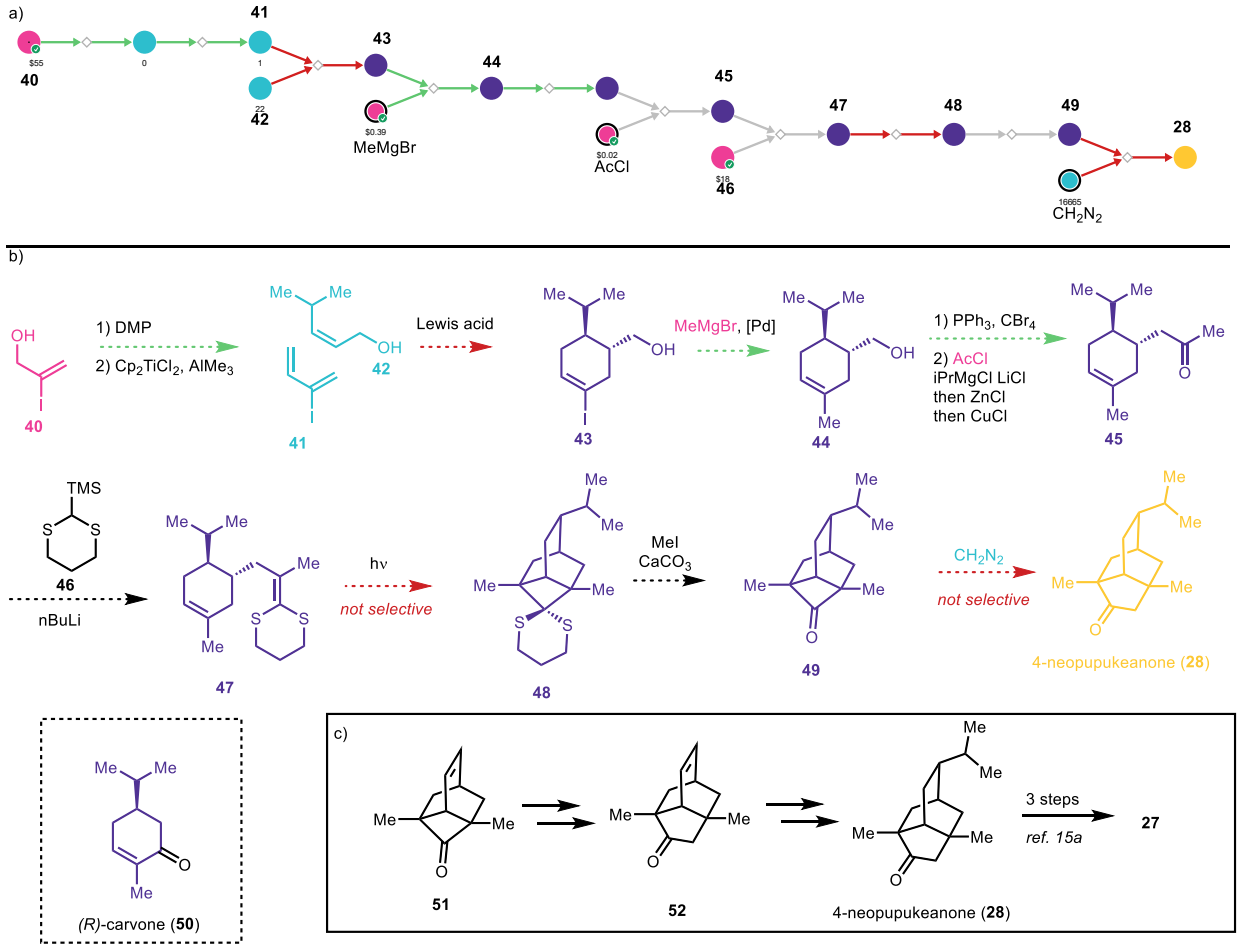

Scheme 5. Synthia™'s proposed forward synthesis for 4-neopupukeanone (**6**) as a a) summary graphic and b) detailed scheme. c) Human-proposed modifications to Synthia™'s route. Each diamond represents a reaction step, showing the map of known starting materials (teal) and commercial starting materials (pink) through intermediates (purple) to the product (yellow). Green reaction arrows indicate that the transform was identified through a multi-step strategy. Red reaction arrows indicate that the transformation is either not selective or only diastereoselective.

Ultimately these examples showcase that Synthia™'s routes can engender meaningful strategic elements that serve as a starting point in identifying the synthetic routes an organic synthetic chemist may want to pursue.

4.6 Pupukeananes Bearing the [5.2.1.0^{4,8}]Decane Core

While several syntheses of the isotwistane core, the most well-studied of the pupukeanane family, have been reported, there are relatively fewer studies toward the synthesis of the rearranged [5.2.1.0^{4,8}]decane core: 2-isocyanoallopupukeanane (**3**, Scheme 6) and 9-isocyanoneoallopupukeanane (**4**). The synthesis of natural products with these scaffolds are relatively underexplored. Prior to our synthesis of 2-isocyanoallopupukeanane (**3**) (described in Chapter 2), there was only a single published route to access 2-isocyanoallopupukeanane while no synthetic studies toward the recently isolated neoallopupukeananes have been reported thus far.

4.6.1 Synthia™'s Proposed Route to 2-Isocyanoallopupukeanane

Synthia™ proposes a direct disconnection of the allopupukeanyl core back to a fused bicycle. Interestingly, in all of our analyses of synthesis routes to the pupukeananes using Synthia™, this was the first time that the top scoring route proposed a disconnection of these highly bridged tricycles (i.e., **63**) to an all-fused system, specifically [4.3.0]-bicycle **62**. As first described by Corey[20] and in subsequent work from Wender,[21] Hoffmann,[22] and others, disconnections of the maximally bridged ring can lead to a rapid simplification in the retrosynthetic direction. In the forward sense, Synthia™ proposed a radical cyclization to forge this bridged tricycle. However, the syntheses of this precursor compound (**62**) as proposed by Synthia™ are extremely lengthy due to the complexity of installing multiple contiguous stereocenters to build these densely functionalized cores and proceed through intermediates that may be challenging to access in the laboratory (i.e., **56**). Nonetheless, the identification of this key disconnection could serve as a platform to inspire new methods development from a keen organic chemist.

Notably, this general strategy has been applied in the synthesis of a related compound, 2-pupukeanone.[16a, 17a] However, in the existing syntheses of 2-isocyanoallopupukeanane (**3**),[23] this disconnection has not been reported.

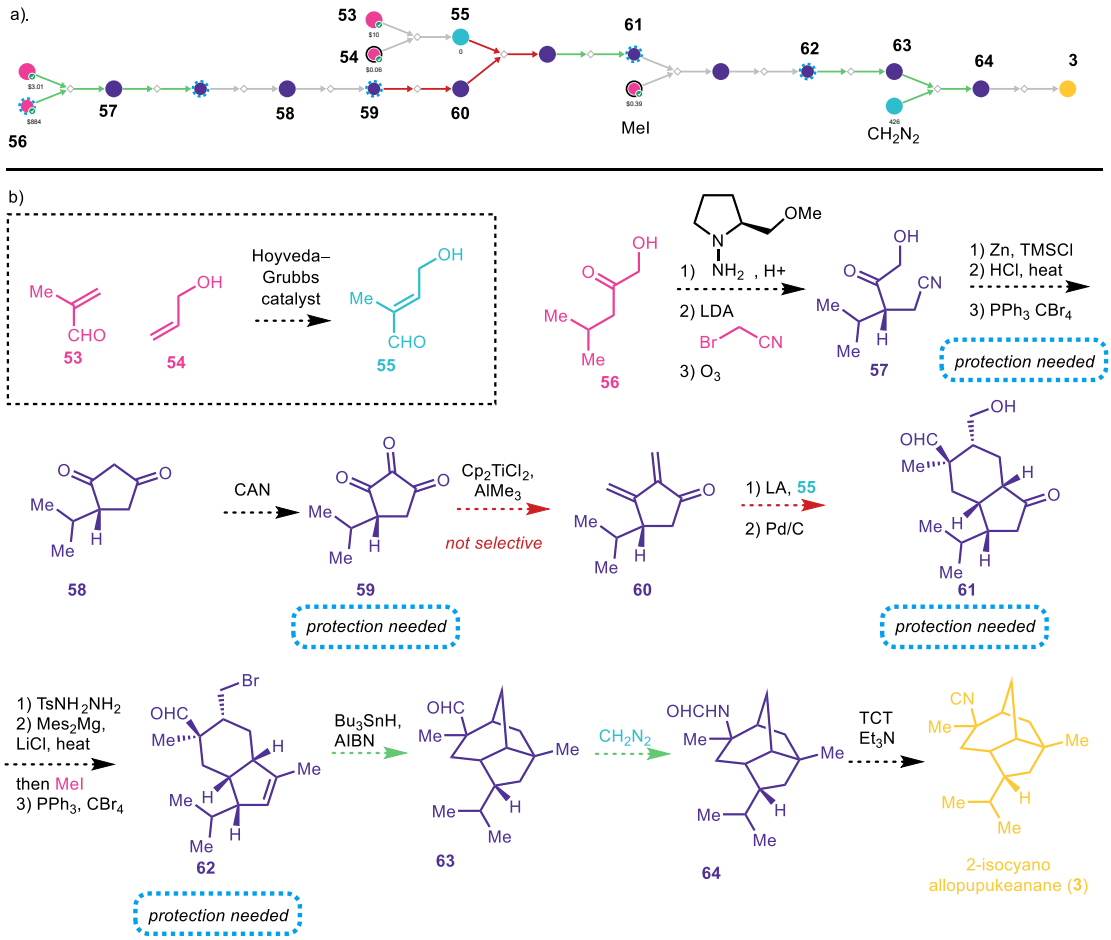

Scheme 6. Synthia™'s proposed forward synthesis for 2-isocyanoallopupukeanane (**3**) as a a) summary graphic and b) detailed scheme. Each diamond represents a reaction step, showing the map of known starting materials (teal) and

commercial starting materials (pink) through intermediates (purple) to the product (yellow). Green reaction arrows indicate that the transform was identified through a multi-step strategy. Red reaction arrows indicate that the transformation is either not selective or only diastereoselective.

4.6.2 Synthia™'s Proposed Route to 9-Isocyanoneoallopupukeanane

Unsurprisingly, for the related neoallopupukeanane skeleton (**4**, Scheme 7), Synthia™ proposes the same key disconnection (see **65** to **66**).

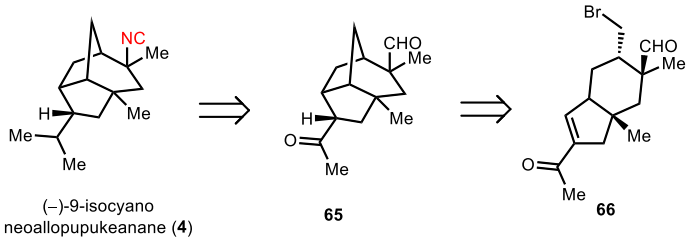

Scheme 7. Synthia™'s proposed retrosynthesis of 9-isocyanoneoallopupukeanane.

Ultimately, Synthia™'s proposals to build natural products bearing this scaffold highlight the ability of the program to recognize the value of topologically simplifying disconnections. While the route proposed to 2-isocyanoallopupukeanane (**3**) is lengthy, it is comparable in overall step count to the first published synthesis of this molecule.[23] The ability to rapidly generate these routes, which capture important elements of strategy, could enhance the route planning process for organic chemists by providing a unique starting place.

4.7 Considering 2-Formamidobeopupukeanane

Only a single natural product has been isolated bearing the abeopupukeanane skeleton, 2-formamidoabeopupukeanane (**5**, Scheme 8). To date, no synthetic studies toward this natural product have been reported. For this reason, we were particularly interested in the strategies Synthia™ would propose for its synthesis.

A Synthia™ analysis of 2-formamidoabeopupukeanane led to a proposed route that proceeds through a key Diels–Alder cycloaddition to close the tricyclic core from a monocyclic precursor (**72**). In the forward sense, the synthesis commences with the diastereoselective [4+2] cycloaddition of commercially available dienophile **67** and diene **68** to yield cyclohexene **69**. Wittig-Schlosser type homologation using a protected 4-bromobutan-2-one (**70**) could then lead to homologated cyclohexene **71.** Trapping this compound in the enamine form (**72**) would set the stage for the key cycloaddition to build the abeopupukeanane skeleton (**73**). At this stage, heterogenous hydrogenation of the bridging olefin would give **74**, followed by formylation of the amine to furnish 2-formamidoabeopupukeanane (**5**).

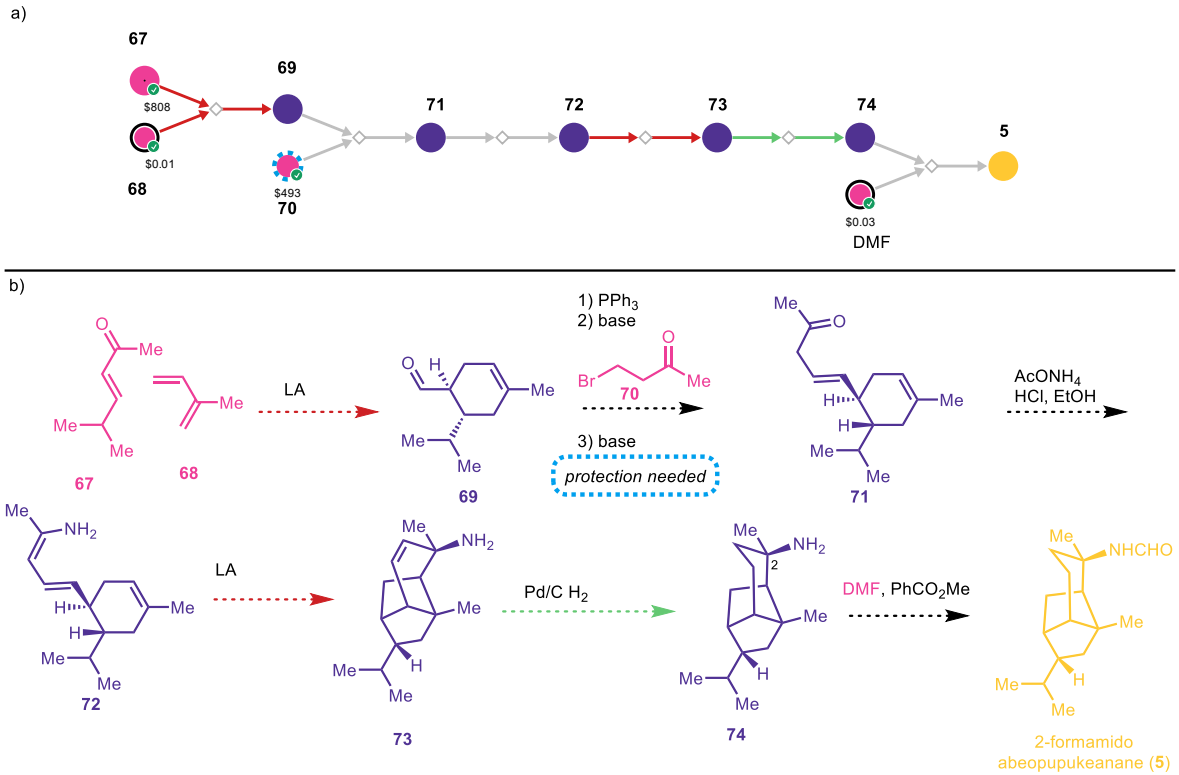

Scheme 8. Synthia™'s proposed forward synthesis for 2-formamidoabeopupukeanane (**5**) as a a) summary graphic and b) detailed scheme. Each diamond represents a reaction step, showing the map of known starting materials (teal) and commercial starting materials (pink) through intermediates (purple) to the product (yellow). Green reaction arrows indicate that the transform was identified through a multi-step strategy. Red reaction arrows indicate that the transformation is either not selective or only diastereoselective.

One key challenge in the Synthia™-proposed cycloaddition to form **72** is the potential for a competing *E/Z* isomerization of the enamine prior to the cycloaddition, which may lead to a mixture of diastereomers at the amino group-bearing C_2 position of **74**. Additionally, to the best of our knowledge, cycloadditions to build [2.2.1]-bicycles in this manner are not known and may prove challenging. While further studies are necessary to understand the feasibility of this transformation, this strategy, if realized, would provide efficient to this natural product scaffold. The example described here represents a disconnection that we may not have otherwise considered. In this way, Synthia™ forces the synthetic chemist to combat inherent bias in the selection of routes for synthesis.

4.8 Summary and Outlook

In this Chapter, we have detailed syntheses proposed by the retrosynthesis software Synthia™ to access members of the pupukeanane family. Complete routes to several compounds were proposed by Synthia™, including routes to three unique carbon skeletons that comprise the frameworks of five natural products with novel scaffolds. Overall, we observed that several of the routes to the topologically complex structures of the pupukeananes proposed by Synthia™ possess a high level of creativity by recognizing unusual disconnections that appear attractive and feasible. In addition, we have demonstrated how human-design can enhance the computer-generated

proposals. Specifically, this can occur through strategic searches for routes to earlier stage intermediates, through the development of new synthetic proposals based on a key step identified by Synthia™, or through modifications to steps that are proposed to shorten a synthesis or enhance selectivity.

As technologies increasingly advance, computational tools such as Synthia™ are likely to become integrated into the synthesis "toolbox". In our estimation, Synthia™'s interface is extremely user friendly, with default settings and searches able to be set up without any background in coding. Additionally, the software integrates with an easy-to-use structure editor, or targets can be readily inputted by copying the associated SMILES string from ChemDraw, a quintessential program that most organic chemists use frequently.

Relative to the effort inherent in synthesizing a molecule, the time it takes for Synthia™ to identify routes is extremely short. Importantly, Synthia™ effectively identifies a wealth of reactions with literature precedent that may be immediately tested and possesses an integrated Reaxys search function that assists in finding the most closely related literature examples. Even if the exact route proposed by Synthia™ is not carried out in the laboratory, this information can greatly accelerate synthesis planning. Additionally, Synthia™ has already integrated several easy-to-use methods for chemists to accomplish these goals including integrated molecular mechanics level calculations to estimate the strain energy of various intermediates.

Cases where target structures bear certain rare functional groups, specifically thiocyanates in the case of the pupukeananes, present challenges for the program. In these instances, we propose that a combination of human-generated disconnections and strategic Synthia™ searches can allow for the design of hybrid routes. Additionally, the reaction rules and searching algorithms are continually being updated. In cases such as these where one can identify a likely cause for the program failing, the program offers a direct communication button with engineers at MilliporeSigma who immediately begin to work to address the problem — for example by adding additional reaction rules to address these cases. This feedback loop between the creators and the users of the program is key to keeping up with the ever-expanding breadth of chemical space and literature.

Although education is not the express purpose of a retrosynthesis tool such as Synthia™, it's worth noting that the vast database of reactions that are readily applied to these targets make the use of these tools extremely valuable, especially for early-stage career scientists as well as those focused on identifying synthesis routes backed by precedent (e.g., in industry). Importantly, parsing through the synthesis of several different targets usually provides a wealth of different reactions, although some do appear quite frequently in cases where they build multiple bonds or stereocenters and may be prioritized for that reason. For example, in the case of the pupukeanane natural products, the Diels-Alder reaction was often invoked to build the bridged core of these molecules as the Diels-Alder transform is powerfully simplifying.

Ultimately, Synthia™ represents a powerful new computational tool that can augment the process of retrosynthetic planning. With recent modifications, it is well equipped to propose syntheses to complex natural products such as the pupukeananes. Depending on the target in question, the routes that are suggested by computer may serve as an aspirational goal that inspires creativity, as a starting point for synthetic chemists tackling these natural product targets, or even as a blueprint for the synthesis of the target compound.

4.9 Synthia™ Search Parameters

4.9.1 General Search Parameters

Each natural product or derivative was input as a SMILES string as a single enantiomer. The search details are included in the order they are selected in the commercial Synthia application. For each search, only the best scoring pathway was analyzed.

4.9.2 Pathways: Pupukeananes Default Search

Analysis type: Automatic Retrosynthesis

Rules: none selected

Filters: Multicut, Power Search, Legacy Strategies

Max. paths returned: 50

Max. iterations: 10000

Commercial: Max. molecular weight:1000 g/mol

Max. price: 1000 $/g

Published:

Max. molecular weight: 200 g/mol, Popularity: 5

Shorter paths: yes

Pathway linearity: CONVERGENT

Protecting groups: MORE

Reaction scoring formula:

100*(TUNNEL_COEF*FGI_COEF*20+1000000*(FILTERS+CONFLICT)+500*NON_SELEC

TIVITY+10*PROTECT)

Chemical scoring formula: 100*(SMALLER^3)

Min. search width: 500

Max. reactions per product: 60

4.10 References

1. Corey, E. J.; Wipke, W. T. *Science* **1969**, *166*, 178.
2. (a) S., S. M. H.; P., W. M. *Chem. Eur. J.* **2017**, *23*, 5966–5971; (b) Marwin Segler, M. P., Mark P. Waller *arXiv* **2017**; (c) Segler, M. H. S.; Preuss, M.; Waller, M. P. *Nature* **2018**, *555*, 604.
3. (a) Coley, C. W.; Barzilay, R.; Jaakkola, T. S.; Green, W. H.; Jensen, K. F. *ACS Cent. Sci.* **2017**, *3*, 434–443; (b) Wei, J. N.; Duvenaud, D.; Aspuru-Guzik, A. *ACS Cent. Sci.* **2016**, *2*, 725–732.
4. (a) Shields, B. J.; Stevens, J.; Li, J.; Parasram, M.; Damani, F.; Alvarado, J. I. M.; Janey, J. M.; Adams, R. P.; Doyle, A. G. *Nature* **2021**, *590*, 89–96; (b) Reid, J. P.; Sigman, M. S. *Nature* **2019**, *571*, 343–348.

5. Lovering, F.; Bikker, J.; Humblet, C. *J. Med. Chem.* **2009**, *52*, 6752–6756.
6. (a) Klucznik, T.; Mikulak-Klucznik, B.; McCormack, M. P.; Lima, H.; Szymkuć, S.; Bhowmick, M.; Molga, K.; Zhou, Y.; Rickershauser, L.; Gajewska, E. P.; Toutchkine, A.; Dittwald, P.; Startek, M. P.; Kirkovits, G. J.; Roszak, R.; Adamski, A.; Sieredzińska, B.; Mrksich, M.; Trice, S. L. J.; Grzybowski, B. A. *Chem* **2018**, *4*, 522–532; (b) Coley, C. W.; Thomas, D. A.; Lummiss, J. A. M.; Jaworski, J. N.; Breen, C. P.; Schultz, V.; Hart, T.; Fishman, J. S.; Rogers, L.; Gao, H.; Hicklin, R. W.; Plehiers, P. P.; Byington, J.; Piotti, J. S.; Green, W. H.; Hart, A. J.; Jamison, T. F.; Jensen, K. F. *Science* **2019**, *365*, eaax1566.
7. Mikulak-Klucznik, B.; Gołębiowska, P.; Bayly, A. A.; Popik, O.; Klucznik, T.; Szymkuć, S.; Gajewska, E. P.; Dittwald, P.; Staszewska-Krajewska, O.; Beker, W.; Badowski, T.; Scheidt, K. A.; Molga, K.; Mlynarski, J.; Mrksich, M.; Grzybowski, B. A. *Nature* **2020**, *588*, 83–88.
8. Szymkuć, S.; Gajewska, E. P.; Klucznik, T.; Molga, K.; Dittwald, P.; Startek, M.; Bajczyk, M.; Grzybowski, B. A. *Angew. Chem. Int. Ed.* **2016**, *55*, 5904–5937.
9. Gajewska, E. P.; Szymkuć, S.; Dittwald, P.; Startek, M.; Popik, O.; Mlynarski, J.; Grzybowski, B. A. *Chem* **2020**, *6*, 280–293.
10. (a) Yamamoto, H.; Sham, H. L. *J. Am. Chem. Soc.* **1979**, *101*, 1609–1611; (b) Corey, E. J.; Ishiguro, M. *Tetrahedron Lett.* **1979**, *20*, 2745–2748.
11. Schiehser, G. A.; White, J. D. *J. Org. Chem.* **1980**, *45*, 1864–1868.
12. Piers, E.; Winter, M. *Liebigs Ann. Chem.* **1982**, *1982*, 973–984.
13. McCulley, C. H.; Tantillo, D. J. *J. Phys. Chem. A* **2018**, *122*, 8058–8061.
14. (a) Pham, A. T.; Ichiba, T.; Yoshida, W. Y.; Scheuer, P. J.; Uchida, T.; Tanaka, J.-i.; Higa, T. *Tetrahedron Lett.* **1991**, *32*, 4843–4846; (b) He, H. Y.; Salva, J.; Catalos, R. F.; Faulkner, D. J. *J. Org. Chem.* **1992**, *57*, 3191–3194.
15. (a) Srikrishna, A.; Gharpure, S. J. *Tetrahedron Lett.* **1999**, *40*, 1035–1038; (b) Uyehara, T.; Onda, K.; Nozaki, N.; Karikomi, M.; Ueno, M.; Sato, T. *Tetrahedron Lett.* **2001**, *42*, 699–702.
16. (a) Kaliappan, K.; Rao, G. S. R. S. *Tetrahedron Lett.* **1997**, *38*, 2185–2186; (b) Kaliappan, K.; S. R. Subba Rao, G. *J. Chem. Soc. Perkin Trans. I* **1997**, 3387–3392; (c) Kaliappan, K.; Subba Rao, G. S. R. *J. Chem. Soc. Perkin Trans. I* **1997**, 3393–3400.
17. (a) Srikrishna, A.; Jagadeeswar Reddy, T. *J. Chem. Soc. Perkin Trans. I* **1997**, 3293–3294; (b) Srikrishna, A.; Vijaykumar, D.; Sharma, G. V. R. *Tetrahedron Lett.* **1997**, *38*, 2003–2004; (c) Srikrishna, A.; Reddy, T. J. *J. Chem. Soc. Perkin Trans. I* **1998**, 2137–2144; (d) Srikrishna, A.; Vijaykumar, D.; Sharma, G. V. R. *Indian J. Chem., Sect. B* **1999**, *38*, 766–770.
18. Kaliappan, K.; Rao, G. S. R. S. *Tetrahedron Lett.* **1997**, *38*, 2185-2186.
19. Hashimoto, T.; Naganawa, Y.; Maruoka, K. *J. Am. Chem. Soc.* **2009**, *131*, 6614–6617.
20. Corey, E. J.; Howe, W. J.; Orf, H. W.; Pensak, D. A.; Petersson, G. *J. Am. Chem. Soc.* **1975**, *97*, 6116–6124.
21. Wender, P. A. M., B. L., *Toward the Ideal Synthesis: Connectivity Analysis and Multibond-Forming Processes*. JAI Press: Greenwich, CT, 1993; Vol. 2.
22. Hoffmann, R. W., *Elements of Synthesis Planning*. Springer-Verlag: Berlin, Germany, 2009.
23. Ho, T.-L.; Kung, L.-R. *Org. Lett.* **1999**, *1*, 1051–1052.